LINKING FIBROSIS AND CANCER THROUGH THE DIFFERENTIATION OF FIBROCYTES

A Dissertation

By

MICHAEL JOHN VICTOR WHITE

Submitted to the Office of Graduate and Professional Studies of
Texas A&M University
in partial fulfillment of the requirements for the degree of

DOCTOR OF PHILOSOPHY

Chair of Committee,	Richard Gomer
Committee Members,	Robert Chapkin
	Xiaorong Lin
	Arne Lekven
Head of Department,	Tom McKnight

May 2015

Major Subject: Biology

ABSTRACT

Fibrosis is a disease in which scar tissue invades healthy organs and reduces their function. Fibrosis is involved in 45% of deaths in the United States, yet little is known about the signaling that underlies the early formation of a fibrotic lesion. Fibrocytes are fibroblast-like monocyte-derived cells, and are a key component of scar tissue. Monocytes can also differentiate into macrophages, and pro-fibrotic macrophages are an important component of scar tissue.

Scar tissue is also essential for healing wounds. Chronic, non-healing wounds cost $25 billion annually to treat in the United States.

How scar tissue starts to form in both healing wounds and fibrosis is poorly understood. A key question is what mechanism overrides the inhibitory signals present in wounds and at the site of fibrosis to trigger the differentiation of monocytes into fibrocytes.

In this dissertation, I present evidence that proteases present in the early wound and scar tissue environment appear to be potent signals for fibrocyte, and pro-fibrotic macrophage, differentiation. Transient exposure of trypsin, tryptase, and thrombin to monocytes potentiates fibrocyte differentiation, even in the presence of fibrocyte inhibitors serum amyloid P (SAP) or interferon-gamma (IFN-γ), suggesting that proteases may be an early stage pro-fibrotic signal.

Cancer is involved in 25% of deaths in the United States. The majority of these deaths are not caused by the primary tumor, but rather by metastases. Metastasis is a process whereby cancer cells migrate from a primary tumor to distant tissues. The tumor

environment is heterogeneous, and contains cancer-associated macrophages and fibroblasts in addition to cancer cells. Tumors are frequently surrounded by scar tissue, and in order to metastasize, cancer cells must pass through this scar tissue. Little is known about the molecular mechanisms cancer cells use to disrupt the scar tissue and escape the surrounded tumor.

In this dissertation, I present evidence that galectin-3 binding protein (LGALS3BP) is secreted by metastatic cancer cells, inhibits fibrocyte differentiation, and acts through the CD209/DCSIGN receptor. LGALS3BP is upregulated at the leading edge of tumors metastasizing into surrounding scar tissue. This data suggests a role for LGALS3BP in metastasis.

This dissertation is focused on why fibrocytes differentiate and discovering novel methods for potentiating and inhibiting this differentiation, with an eye towards developing novel therapeutics for fibrosing diseases, chronic wounds, and cancer.

DEDICATION

I'd like to dedicate this dissertation to my family and friends, especially my mother Vicki Quade, my dad Charlie White, my brother David, and my sister Catherine. I'd also like to thank my friends in College Station, without whose support I would not have been able to complete this dissertation. Thank you.

ACKNOWLEDGEMENTS

I would like to thank my committee chair, Dr. Gomer, and my committee members, Dr. Chapkin, Dr. Lin, and Dr. Lekven, for their guidance and support throughout the course of this research.

I'd like to thank my collaborator, David Roife, for his images of human biopsies. I'd also like to specially thank Dr. Porter, Dr. Chapkin, and Dr. Wallis for their kind gift of cell lines used in this dissertation.

I'd like to thank the nurses at the Beutel health center who performed every blood draw for the experiments in this dissertation.

Finally, thanks to my family for their encouragement and patience.

NOMENCLATURE

LGALS3BP	Galectin-3 binding protein
CM	Conditioned Media
PAR-1	Protease activated receptor-1
PAR-2	Protease activated receptor-2
M1	Classically activated macrophage
M2	Alternatively activated macrophage
M2a	Wound healing macrophage
DCIS.COM	Non-metastatic breast cancer cell line
MCF-7	Non-metastatic breast cancer cell line
MDA-MB 231	Metastatic breast cancer cell line
MDA-MB 435	Metastatic melanoma cell line
MONO MAC-1	Leukemia cell line
MONO MAC-6	Leukemia cell line
U937	Leukemia cell line
HL-60	Leukemia cell line
THP-1	Leukemia cell line
K562	Leukemia cell line
HT-29	Colon cancer cell line
HCT 15	Colon cancer cell line
SW480	Colon cancer cell line

DKOB8	Colon cancer cell line
HCT (P21+/P53+)	Colon cancer cell line
HCT (P21-/P53+)	Colon cancer cell line
HCT (P21+/P53-)	Colon cancer cell line
HCT (P21-/P53-)	Colon cancer cell line
HEK-293	Embryonic kidney cell line
ADR-RES	Ovarian cancer cell line
OVCAR-8	Ovarian cancer cell line
SNU 398	Liver cancer cell line
HEP-G2	Liver cancer cell line
SW-1088	Brain cancer cell line
U-87 MG	Brain cancer cell line
PANC-1	Pancreatic cancer cell line

TABLE OF CONTENTS

LIST OF FIGURES

Page

LIST OF MODELS

Page

CHAPTER I

INTRODUCTION AND LITERATURE REVIEW

Cancer, chronic wounds, fibrosis

Cancer is involved in 25% of deaths in the United States, affects more than 1.5 million new patients each year, and has an economic cost of $216 billion annually (1, 2). Metastasis is the primary cause of the 500,000 cancer related fatalities in the United States, and in breast cancer metastasis causes a drop in survival rate of 74% (1, 3). In certain solid tumors, the immune system may participate in a desmoplastic response, encapsulating the tumor with scar tissue before it can metastasize (4). Far from being a static shell surrounding a tumor, this desmoplastic sheath is a dynamic, responsive tissue that adjusts to changing tumor conditions (5, 6). In these cases, the tumor cells must pass through this sheath of fibrotic tissue in order to metastasize (4-11).

The treatment of acute and chronic wounds is a major medical concern, with both acute and chronic wounds consuming treatment time and resources. Approximately 1 in 250 people will require medical treatment for an acute wound in a given year, and between 25-40% of hospital patients receive treatment for either an acute or chronic wound (12-16). Chronic, non-healing wounds affect more than 6.5 million US patients per year, which is approximately 2% of the population, and cost more than $25 billion to treat (17). Chronic wounds also resist conventional healing treatments and often occur in at-risk populations, including the elderly, obese, immuno-compromised, or diabetic patients (17, 18).

The opposite of a chronic wound is a fibrosing disease, in which inappropriate scar tissue is excessively formed. In fibrosing diseases, this scar tissue forms on a healthy organ, reducing its function (19). Fibrosing diseases include pulmonary fibrosis, congestive heart failure, liver cirrhosis, kidney fibrosis, and are involved in 45% of deaths in the United States (20). There are currently few FDA approved treatments for fibrosis (20, 21). Cancer, wound healing, and fibrosis all involve scar tissue formation, and a key component of scar tissue is the fibrocyte (22, 23).

Fibrocytes

Fibrocytes are monocyte-derived, fibroblast-like cells, first discovered by James Paget in the 1850s (24). Monocytes are circulating, innate-immune system cells that are recruited to wounds or fibrotic lesions by chemokines (25, 26), and in response to unknown wound signals differentiate into fibrocytes (27, 28). Fibrocytes express collagen and other extracellular matrix proteins, secrete pro-angiogenic factors, and activate nearby fibroblasts to proliferate and secrete collagen (22, 23, 27, 29-31), forming a scar.

Fibrocytes are CD45 positive, and are a key component of both wound healing and fibrosing diseases (22, 27, 29, 30) and the development of the body's desmoplastic response to foreign or invasive bodies (9, 22). Within a wound, increasing fibrocyte differentiation potentiates wound healing, while decreasing fibrocyte differentiation leads to slower wound healing (32).

Monocytes isolated from peripheral blood mononuclear cells differentiate into fibrocytes *in vitro* in defined media (33). The differentiation can be modulated by factors such as the

serum protein Serum Amyloid P (SAP), NaCl, cytokines such as interleukins-4, -12, and -13, interferon-γ, or hyaluronic acid (34-37). The presence of as little as 0.01% serum inhibits fibrocyte differentiation (33, 36). The SAP concentration in plasma is ~30 μg/ml (38). The IC50 for SAP inhibition of fibrocyte differentiation is 0.2 μg/ml (36, 39), and ~1 μg/ml SAP completely inhibits fibrocyte differentiation (36). In humans, in addition to being present in plasma, a considerable amount of SAP is present in the interstitial space between cells within tissues (40). Normal tissues contain very few fibrocytes (31), but local increases in fibrocyte differentiation correlate with increased fibrosis and wound healing in animal models (32, 41). *In vivo*, SAP slows wound healing, while removing SAP from a wound promotes healing (32, 42). Conversely, SAP injections that double the serum SAP concentration inhibit fibrosis in a variety of animal models (41, 43-45).

Wound healing macrophages

In addition to differentiating in fibrocytes, monocytes also differentiate into both classically-activated M1 macrophages and alternatively-activated M2 macrophages (46). M1 macrophages are involved with the immune system's response to pathogens like viruses and bacteria, and M2 macrophages are involved with immuno-regulation and tissue repair (47, 48). There are several subpopulations of M2 macrophages, including the M2a and Mreg subtypes (46). M2a macrophages are involved in scar tissue formation in both wound healing and fibrosis (49-52), while Mreg macrophages have an anti-inflammatory phenotype (46). Unpolarized monocytes are cells that have not been exposed to factors that potentiate either M1 or M2 macrophage differentiation (53).

M1, M2a, and Mreg macrophages, while morphologically similar, display different surface markers and secrete different cytokines (46). CD163 is a marker of Mreg macrophage differentiation (47, 54). Fibronectin is a marker of M2a macrophage differentiation (55). CD206 is sometimes classed as an Mreg marker, and sometimes as an M2a marker (47, 54). CCR7 is a commonly used marker for M1 classical macrophage activation (47). Macrophage subtypes also have different secretion profiles, with M1 macrophages secreting higher levels of the cytokine IL-12 compared to M2 macrophages (46). M2 regulatory macrophages secrete increased levels of the anti-inflammatory cytokine IL-10 (46). M2a macrophages secrete intermediate amounts of IL-12 and IL-10, and high amounts of IL-4 (46).

Proteases and PAR

Proteases are proteolytic enzymes that cleave proteins at specific amino acid sequences. One family of proteases is defined by a serine at the enzyme's active site. These serine proteases are commonly found in the digestive system, as well as in immune responses to pathogens, inflammation, and wounding.

Trypsin, chymotrypsin, and pepsin are the primary mammalian serine proteases used in digestion. Each is secreted as a zymogen, and later cleaved to an active form. Each also cuts at a different amino acid pattern. Trypsin is a proteolytic enzyme that cuts at lysine or arginine residues, except when the following amino acid is proline (56). Chymotrypsin preferentially cleaves following the aromatic amino acids tyrosine, tryptophan, or phenylalanine (57). Pepsin cuts preferentially between hydrophobic and

aromatic amino acids (58). Endoproteinase Glu-C is a protease isolated from *Staphylococcus aureus* which cleaves at glutamic or aspartic acid (59, 60).

Proteases also participate in wound healing. One of the events preceding scar tissue formation in a wound is the clotting cascade, in which the zymogen prothrombin is cleaved to thrombin, which in turn cleaves fibrinogen to fibrin. In addition to being upregulated during wound healing, thrombin activity is also upregulated in fibrotic lesions (61, 62). Thrombin causes inflammation when added to the lungs of mice, and increased concentrations of thrombin within lungs exacerbate fibrosis, while inhibition of thrombin attenuates fibrosis (63-66). Thrombin cleaves a six amino acid recognition site which is found on protease activated receptor-1 (PAR-1) (67, 68). This receptor is found on a variety of cell types including monocytes (69), and mediates the ability of thrombin to induce platelet aggregation (70).

Proteases also participate in the immune system's response to inflammation and foreign pathogens. Mast cells are found in both internal fibrotic lesions and sites of wound healing (71-73). Mast cells degranulate in response to objects the immune system recognizes as foreign, including certain tumors and pathogens like schistosomes, which are too large to be effectively engulfed by a single cell (73). In these cases, mast cells encourage the deposition of fibrocytes and fibroblasts to form a sheath of fibrotic tissue around the foreign object (74-77). Mast cell degranulation products include the protease tryptase, a protease similar to trypsin but which must be stabilized by heparin in order to be enzymatically active (73, 78, 79). Tryptase is upregulated in areas of increased mast cell degranulation, including wounds and especially in fibrotic lung tissue (71, 72, 78-80).

Elevated extracellular tryptase levels are also associated with collagen deposition in idiopathic pulmonary fibrosis (80). Tryptase cleaves at lysine and arginine residues, except when the following amino acid is proline (56). Tryptase activates protease activated receptor-2 (PAR-2) (73, 81). This receptor is found on a variety of cells including monocytes (69), and mediates the ability of tryptase to increase the proliferation of, and collagen production by, fibroblasts (73). Intratracheal administration of tryptase causes inflammation, and inhibition of tryptase attenuates this inflammation (82-85). Inhibition of PAR-2 receptors attenuates collagen deposition in a heart disease model (86).

Trypsin, tryptase, and thrombin influence wound healing and scar tissue formation by causing fibroblast proliferation and collagen secretion (73, 87-89), and by causing platelet aggregation (70).

Cancer mutation and progression

Cancers are highly variable, and display different phenotypes depending on their tissue of origin, the mutations to their genomes, the types of heterogeneous cells present in the tumor, and whether the cancer has metastasized or not. Due to this variation, some cancers are more dangerous than others. Some cancers are slow growing, others are fast growing, some are benign, others are metastatic (90). These stages of cancer can represent different cancers from different tissues, or represent different stages within one tumor over time. If left untreated (or undiscovered), some types of cancer will progress from benign stages to metastatic stages (10).

The multi-hit model of cancer progression proposes that as cancers undergo

additional mutations they progressively lose control over cell-cycle regulation and basic cellular control functions (91). As cancer progresses and cancer cells undergo more mutations they change their phenotype by changing their protein expression profile. These expression changes have the effect of changing the cancer cell from a more epithelial phenotype (terminally differentiated cells which display tissue specific markers) to a more mesenchymal phenotype (stem-like cells which do not display tissue specific markers) (92, 93).

Cancer cells that undergo this epithelial-to-mesenchymal transition (EMT) may be more able to resist cell death, evade the immune system, and activate invasion and metastasis, or commandeer nearby macrophages, epithelial cells, and fibroblasts to perform these functions (94). Mesenchymal cancer cells display fewer markers from their tissue of origin, and cancer cells that have metastasized differ further in their protein expression profile from their benign precursors (95-97). As cancer progresses a mesenchymal phenotype, it interacts with the immune system in different ways. Some tumors attempt to evade the immune system, and others act to suppress the immune system (98-102).

Cancer cell lines

The MDA-MB-231 breast cancer line was isolated from metastases of a patient in the 1970s by the MD Anderson Cancer Center (103). MDA-MB-231 cells proliferate rapidly in culture and rapidly metastasize in murine models, indicating that these cells

retain the protein expression profile which allowed them to metastasize in the original patient (104).

MDA-MB 435 has an uncertain origin: at the initiation of this project, the cell line was listed as a breast cancer line by the ATCC (105). Currently, the cell line is listed as a melanoma cell line (106).

OVCAR-8 is an ovarian cancer cell line derived from a metastatic site (107, 108). U87-mg is derived from a glioblastoma (109). MCF-7 is a breast cancer cell line derived from a pleural effusion (110). DCIS.com is derived from a normal breast tissue cell line (MCF10A) passaged through a mouse, which forms a non-metastatic ductal carcinoma in-situ when injected into mice (111). HT-29 (112), SW480 (113), DKOB8 (114), and HCT (115) are derived from non-metastatic colon cancers. ADR-RES (116) is derived from a non-metastatic ovarian cancer. SNU 398 (117) and HEP-G2 (118) are derived from non-metastatic liver cancers. SW 1088 (119) and U87 MG (109) are derived from non-metastatic brain cancers. PANC-1 (120) is derived from a non-metastatic pancreatic cancer. Mono Mac 1 (121), Mono Mac-6 (122), U-937 (123), HL-60 (124), and THP-1 (125) are derived from leukemias.

Galectin-3 binding protein and galectin-3

Galectin-3 binding protein (LGALS3BP) is a 60 kDa heavily glycosylated protein that was originally identified as a biomarker for metastatic melanoma (126). LGALS3BP was initially called antigen 90K because the protein isolated from human serum ran at 90

kDa on an SDS-page gel (127). LGALS3BP binds to galectins -1, -3, and -7, laminin, fibronectin, and collagen (127-129). LGALS3BP is a member of the scavenger receptor cysteine-rich domain (SRCR) family of proteins (130).

LGALS3BP is ubiquitously expressed in bodily secretions, including milk, tears, semen and serum, usually in the range of 10 μg/ml (131). This value can change greatly, however, depending on the individual or upon the different factors affecting the individual. In blood serum, for instance, LGALS3BP concentration in patients with breast cancer or melanoma can be an order of magnitude higher than normal serum levels (132). In breast milk, LGALS3BP concentration can rise and fall over the same range (approximately 10 μg/ml to 100 μg/ml) depending on the length of time after the pregnancy (131). LGALS3BP mRNA transcripts are found in normal tissues throughout the body, predominately in lung and colon tissue (128). LGALS3BP is also elevated in the serum of HIV patients, suggesting that LGALS3BP is upregulated in response to HIV infection (133, 134). LGALS3BP has been suggested to be involved in resistance to infant respiratory infections (135).

LGALS3BP has been primarily studied in the fields of immunology and cancer (128, 130). In cancer research, LGALS3BP is upregulated in the serum of patients with aggressive hormone-regulated cancers, including breast and ovarian cancer (136, 137). Higher levels of LGALS3BP correlate with worse outcomes in breast cancer patients (138, 139), while increased serum concentrations of galectin-3 correlate's with increased survival (140). LGALS3BP has also been found to promote VEGF secretion by breast cancer cells, including MDA-MB 231 cells (128, 141). Mouse knockouts of LGALS3BP

show higher circulating levels of TNF-alpha, IL-12, and interferon-gamma, suggesting a role in regulating the immune system (142).

Galectin-3 is a ~30 kDa protein expressed nearly ubiquitously throughout the body, and can be found in and secreted by different cell types (140). Galectin-3 is a biomarker of fibrosing diseases such as heart disease and pulmonary fibrosis (143, 144). As the severity of the fibrosing disease increases, galectin-3 concentration in the serum increases. Galectin-3 is also secreted as an immunomodulator by macrophages (145).

Galectin-3 interacts promiscuously with a number of intercellular and intracellular receptors and ligands, and is theorized to have roles in inflammation, host response to a virus, and wound healing (145, 146). Galectin-3 is a biomarker of fibrosing diseases such as heart disease and pulmonary fibrosis (143, 144). Galectin-3 can be secreted from cells, associated with membrane bound carbohydrates, or located in the cytoplasm (147). Galectin-3 is expressed by innate immune system cells such as macrophages, eosinophils, neutrophils, and mast cells (148). Further, galectin-3 is upregulated in colon, thyroid, and pancreatic cancers. Galectin-3 is also expressed in the kidneys and the gastro-intestinal tract (149, 150).

Galectin-3 knockout mice have decreased granulocyte number, increased susceptibility to *S. pneumonaie* infection, and lack macrophage activation and chemotaxis under stimulation by IL-4 and IL-13, and have fewer atherosclerotic lesions of the heart (151). Additionally, knockout mice have lower numbers of leukocytes and monocytes after thioglycollate broth administration than do control mice (151).

Summary

A key question in wound healing and fibrosis is thus the mechanism that overrides the inhibitory effect of SAP (and other fibrocyte differentiation inhibitors) to induce fibrocyte differentiation.

The methods which cancer cells use to evade the immune system are incompletely understood. This is especially true for cancer's evasion of the innate immune system's inflammatory desmoplastic response to tumors. A longstanding question in metastasis is how tumor cells are able to disrupt the fibrotic cover to escape the surrounded tumor. It is unknown what role increased galectin-3 binding protein (LGALS3BP) concentration plays in metastatic cancers, or the role of increased galectin-3 concentration in scar tissue.

CHAPTER II

TRYPSIN POTENTIATES HUMAN FIBROCYTE DIFFERENTIATION*

Summary

Trypsin-containing topical treatments can be used to speed wound healing, although the mechanism of action is unknown. To help form granulation tissue and heal wounds, monocytes leave the circulation, enter the wound tissue, and differentiate into fibroblast-like cells called fibrocytes. We find that 20 to 200 ng/ml trypsin (concentrations similar to those used in wound dressings) potentiates the differentiation of human monocytes to fibrocytes in cell culture. Adding trypsin inhibitors increases the amount of trypsin needed to potentiate fibrocyte differentiation, suggesting that the potentiating effect is dependent on trypsin proteolytic activity. Proteases with other site specificities such as pepsin, endoprotease GluC, and chymotrypsin do not potentiate fibrocyte differentiation. This potentiation requires the presence of albumin in the culture medium, and tryptic fragments of human or bovine albumin may also potentiate fibrocyte differentiation. These results suggest that topical trypsin speeds wound healing by generating tryptic fragments of albumin, which in turn potentiate fibrocyte differentiation.

Hypotheses: Trypsin potentiate fibrocyte differentiation, and increases collagen secretion by monocyte derived cells, making trypsin potentially pro-fibrotic.

---

* Reprinted with permission. Originally published in PLoS ONE. White MJ, Glenn M, Gomer RH. Trypsin potentiates human fibrocyte differentiation. PLoS One. 2013 Aug 7;8.

Introduction

The failure of wounds to heal properly constitutes a major medical problem, with both acute and chronic wounds consuming treatment time and resources. Between 25-40% of hospital patients receive treatment for either an acute or chronic wound (12-16). Poorly-healing chronic wounds affect more than 6.5 million US patients per year, and cost more than $25 billion to treat (17). Chronic wounds resist conventional wound-dressing treatments and often occur in elderly, obese, immuno-compromised, or diabetic patients (17, 18).

Monocytes are circulating cells that are recruited to wounds and sites of tissue injury by chemokines (25, 26). To help heal wounds, monocytes enter the wounded tissue and differentiate into fibroblast-like cells called fibrocytes (27, 28). Fibrocytes are collagen-expressing CD45+ cells which assist in scar tissue formation, a key component of both wound healing and fibrosing diseases (22, 27, 29, 30) and the development of the body's desmoplastic response to foreign or invasive bodies (9, 22). Increasing fibrocyte differentiation within a wound healing environment potentiates wound healing, and decreasing fibrocyte differentiation leads to slower wound healing (32). Monocytes isolated from peripheral blood mononuclear cells differentiate *in vitro* in a defined media into fibrocytes (33). The differentiation can be modulated by factors such as the serum protein Serum Amyloid P (SAP), salt concentration, cytokines such as interleukins 4, 12, and 13 and interferon, or hyaluronic acid (34-37). Increased fibrocyte differentiation correlates with increased fibrosis and wound healing in animal models (32, 41).

After wounding, the blood clots, leaving serum on the wound. Albumin is the most common protein in serum, with levels between 35-50 g/L and accounting for ~50% of the total protein in blood (152). Albumin is produced in the liver and maintains blood homeostasis (152). Increased albumin levels are associated with increased wound healing in both acute (153) and chronic wounds (154-156).

Trypsin, chymotrypsin, and pepsin are mammalian proteolytic enzymes. Each is secreted as a zymogen, and later cleaved to an active form. Each also cuts at a different amino acid pattern. Trypsin is a proteolytic enzyme that cuts at lysine or arginine residues, except when the following amino acid is proline (56). Chymotrypsin preferentially cleaves following the aromatic amino acids tyrosine, tryptophan, or phenylalanine (57). Pepsin cuts preferentially between hydrophobic and aromatic amino acids (58). Endoproteinase Glu-C is a protease isolated from *Staphylococcus aureus* which cleaves at glutamic or aspartic acid (59, 60).

Although trypsin is generally thought of as a digestive enzyme, trypsin is also active in multiple cellular processes, including development and tumor invasion (157-166). Trypsin is involved in gastric inflammation through cleavage of the proteinase-activated receptors (PAR1-4) (67, 167, 168), and PAR1 and PAR2 digestion has also been implicated in cancer signaling (169, 170). Topical application of trypsin has been used to potentiate healing of both conventional and chronic wounds for more than 50 years after having been initially tested as a burn debridement treatment (171-177). In this report, we show that when trypsin potentiates fibrocyte differentiation, suggesting a mechanism of action for the effect of trypsin on wound healing.

Materials and methods

Cell isolation and exposure of PBMCs to proteases and inhibitors

Human blood was collected from adult volunteers who gave written consent and with specific approval from the Texas A&M University human subjects Institutional Review Board. Peripheral blood mononuclear cells (PBMC) and monocytes were isolated as previously described (34), and monocytes were checked for enrichment by flow cytometry in comparison to the un-enriched PBMC population (178). Cells were cultured in Fibrolife basal media as previously described (33), in either protein-free media (PFM) or serum-free media (SFM). PFM is composed of Fibrolife basal media (Lifeline Cell Technology, Walkersville, MD) supplemented with 10 mM HEPES (Sigma), 1× non-essential amino acids (Sigma), 1 mM sodium pyruvate (Sigma), 2 mM glutamine (Lonza), 100 U/ml penicillin and 100 μg/ml streptomycin (Lonza). SFM is composed of PFM supplemented with 1× ITS-3 (500 μg/ml bovine serum albumin, 10 μg/ml insulin, 5 μg/ml transferrin, 5 ng/ml sodium selenite, 5 μg/ml linoleic acid, and 5 μg/ml oleic acid, (Sigma). Where indicated, PFM was supplemented with recombinant insulin suitable for cell culture (Sigma), transferrin suitable for cell culture (Sigma), or human or bovine albumin to the above concentrations, or 12.5% human serum. TPCK is an irreversible inhibitor of chymotrypsin, and TLCK is an irreversible inhibitor of trypsin. TPCK-treated trypsin (Sigma), TLCK-treated chymotrypsin (Sigma), pepsin from porcine stomach mucosal lining (EMD), or endoproteinase Glu-C from *S. aureus* (Sigma) were all resuspended to 10 mg/ml following the manufacturer's instructions. Complete protease inhibitor cocktail (Roche, Indianapolis, IN) was resuspended to 40 mg/ml in water, and soybean trypsin

inhibitor (Sigma) was resuspended to 10 mg/ml in water. Fibrocytes were stained, identified and counted as previously described (179).

Purification of albumin

Albumin was purified from sterile filtered non-blood type specific human serum, tested negative for hepatitis A and B and HIV I and II (Lonza, Basel, Switzerland and Gemini Bio-products, West Sacramento, California) or from triple filtered US origin fetal calf serum, tested for sterility and mycoplasma (Thermo Fisher Scientific, Milwaukee, WI) by affi-gel bead affinity elution (Bio-Rad, Hercules, California). 4 ml of beads were washed three times in 25 ml PBS, and were added to 40 ml of serum with gentle mixing at room temperature for 2 hours. The beads were collected by centrifugation at 300 x g for 5 minutes and washed three times with 25 ml of filter-sterilized buffer (20 mM Tris, 140 mM NaCl, 2 mM $CaCl_2$ pH 8.0) and eluted overnight with gentle mixing in 25 ml of 0.5 M NaCl. The beads were then removed by centrifugation at 300 x g for 5 minutes. The 0.5 M NaCl solution containing the eluted albumin was then buffer exchanged three times through a 10 kDa filter (EMD Millipore, Billerica, MD) using 15 ml Earle's balanced salt solution (EBSS buffer) (Sigma, St. Louis, MO), tested for concentration using by absorbance at 280 nm, and diluted to a final concentration of 25 mg/ml in EBSS and stored at 4° C. Samples were diluted 1:10 in 20 mM sodium phosphate buffer, pH 7.2, and run on 4-20% SDS gels (Bio-Rad, Hercules, California), which were silver stained to check for albumin purity.

Depletion of albumin

Albumin was depleted from human serum by affi-gel bead affinity elution (Bio-Rad). 500 µl of beads were washed three times in 2 ml PBS, and were added to 2 ml of serum with gentle mixing at room temperature for 2 hours. The beads were removed by centrifugation at 300 x g for 5 minutes and the albumin depletion was repeated as above twice more. Samples were diluted 1:10 in 20 mM phosphate buffer and run on 4-20% SDS gels which were silver stained to show differences in protein concentrations. Serum and depleted serum were diluted to 1:100 and 1:10 concentrations, respectively, and western blots were stained with mouse monoclonal anti human-albumin antibody, clone HSA-11, following the manufacturer's instructions (Sigma).

Trypsin digest products added to culture

TPCK-treated trypsin-coated agarose beads (Sigma) were washed according to the manufacturer's instructions. To digest serum or albumin, 12.5 µl of beads was mixed with 250 µl of serum, 25 mg/ml albumin, 250 µl SFM containing 500 µg/ml human albumin or bovine albumin, or 250 µl serum-free medium containing 10 µg/ml insulin or 5 µg/ml transferrin. Beads were incubated with gentle rotation at 37 ˚C for 2 hours, and were removed by centrifugation at 300 x g for 5 minutes. The digested media and undigested controls were mixed with PFM or SFM supplemented with bovine albumin. In experiments where human albumin was digested, the trypsinized human albumin and untrypsinized human albumin controls were, if indicated, mixed with SFM supplemented with human albumin.

Collagen staining by flow cytometry

24-well tissue culture treated plates (BD Bioscience, San Jose, CA) were coated for 1 hour at 37° C with 20 µg/ml human cellular fibronectin from fibroblasts (Sigma) in PBS and gently rinsed twice with sterile PBS. 500 µl of PBMC at $1x10^6$ cells/ml in SFM was added to each well. Control wells were supplemented with 250 µl SFM containing 500 µg/ml human albumin, while sample wells were supplemented with SFM digested by TPCK-treated trypsin-coated agarose beads as described above. After 5 days, cells were washed with warm PBS and exposed to 125 µl accutase (Innovative Cell Technologies, San Diego, CA) for 20 minutes at 37 °C. Cells were resuspended via gentle pipetting, and washed by suspension in 1 ml ice cold PBS, collected by centrifugation at 300 x g for 5 minutes, then washed once more. Cells were resuspended in 1% paraformaldehyde/ 0.2% saponin/ PBS for 15 minutes on ice, washed twice as above, and resuspended in 2% BSA/ 0.2% saponin/ PBS for 15 minutes of blocking. Anti-collagen type I rabbit (Rockland, Gilbertsville, PA) and control rabbit IgG (Jackson Immunoresearch, West Grove, PA) antibodies were added to the cell suspensions at 1 µg/ml and incubated on ice for 30 minutes. Cells were washed twice with ice cold PBS and resuspended in 4 µg/ml goat anti-rabbit alexa-fluor 488 secondary antibody (Molecular Probes, Eugene, OR) for 30 minutes on ice. Cells were washed twice and resuspended in ice cold PBS and analyzed with an Accuri C6 flow cytometer for fluorescence. Negative controls were used to set gates.

Statistical analysis

Statistics were performed using Prism (Graphpad software, San Diego, CA). Differences among multiple groups were assessed by 1-way ANOVA (with Dunnett's post test), and between two groups by a two-tailed Mann-Whitney t-test. Significance was defined by $p < 0.05$.

Results

Trypsin treatment increases fibrocyte number

Topical treatment with trypsin improves wound healing, although the mechanism is unknown (171-177). The differentiation of monocytes into fibrocytes plays a role in wound healing (22, 27, 28, 30). To test the hypothesis that trypsin increases wound healing by potentiating fibrocyte differentiation, we examined the effect of trypsin on fibrocyte differentiation in culture. Human peripheral blood mononuclear cells (PBMC) were incubated with trypsin for 5 days in a defined serum-free medium. The cells were then stained and scored for fibrocyte formation. Fibrocyte numbers were normalized to trypsin-free controls due to variability in donors as we previously observed (33-36, 179). Trypsin concentrations between 20 and 150 ng/ml significantly increased the number of fibrocytes (Figure 1A), and this effect was observed for all donors tested. Trypsin concentrations above 1000 ng/ml decreased the number of fibrocytes. The number of adherent cells following fixing and staining was not significantly affected by trypsin (Figure 1B), suggesting that trypsin specifically increases the number of differentiated fibrocytes, rather than increasing the general cell viability or adhesion. This suggests that trypsin can potentiate fibrocyte differentiation.

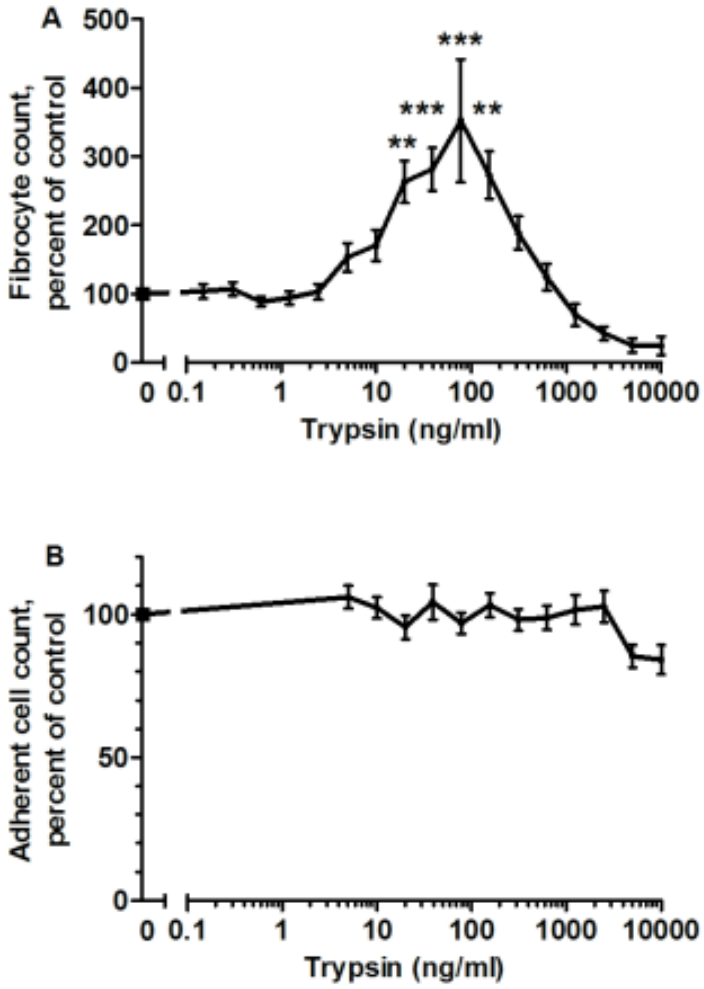

Figure 1. Trypsin potentiates fibrocyte differentiation.
(A) PBMC were cultured in serum free media in the presence of the indicated concentrations of trypsin for 5 days, after which the PBMC were air-dried, stained, counted for fibrocyte differentiation, and normalized for each donor to the no-trypsin control. The no-trpysin controls developed 41.8 ± 5.4 fibrocytes per 10^5 PBMC. (B) The same PBMC populations were then counted for the total number of PBMC adhered to the plate following fixing and staining and normalized for each donor to the no-trypsin control. There were no significant differences in the numbers of adhered PBMC following fixing and staining. Values in A and B are mean ± SEM, n=9. ** indicates $p < .01$ and *** indicates $p < .001$ compared to the no-trypsin control by 1- way ANOVA, Dunnett's test.
Other proteases do not increase fibrocyte number

To determine if other proteases also potentiate fibrocyte differentiation, we examined the effect of three other proteases. Pepsin and endoproteinase Glu-C had no

significant effect on fibrocyte differentiation or the number of adhered PBMC (Figure 2A and B). Chymotrypsin at 5000 ng/ml and above caused lower fibrocyte numbers and lower numbers of adhered PBMC (Figure 2A and 2B). These results suggest that not all proteases potentiate fibrocyte differentiation, and that a specific aspect of the protein structure or activity of trypsin is responsible for trypsin potentiating fibrocyte formation.

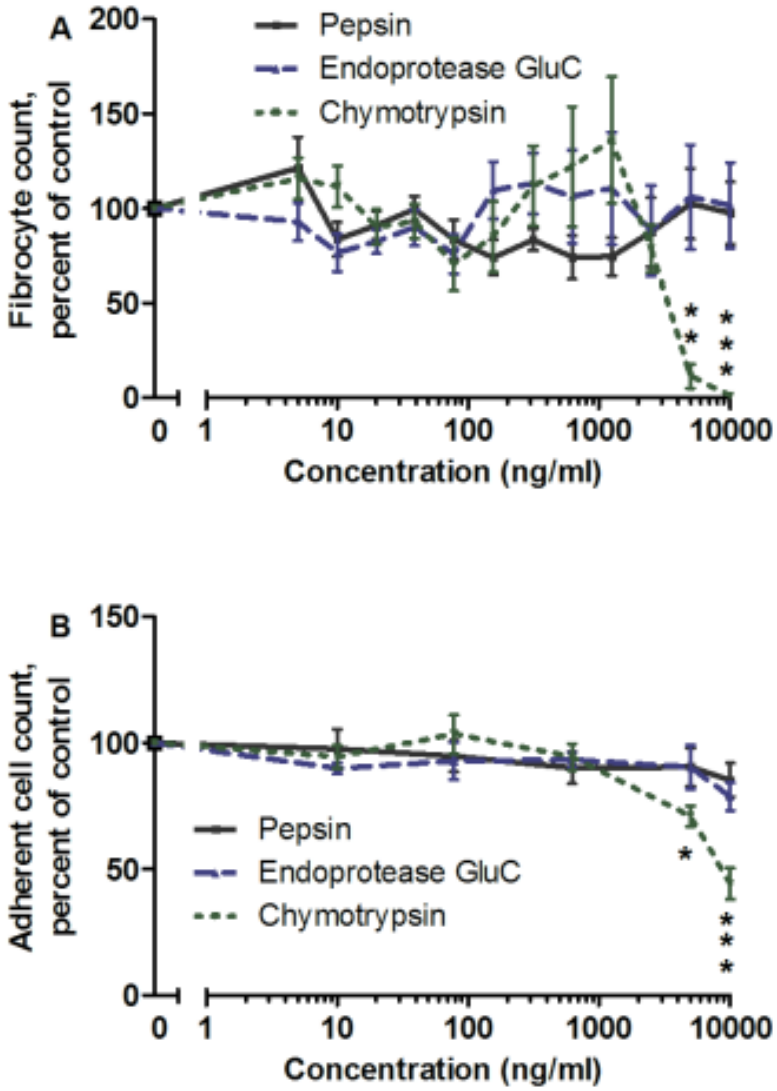

Figure 2. Chymotrypsin, pepsin, and endoproteinase GluC do not potentiate fibrocyte differentiation.

(A) PBMC were cultured with the indicated concentrations of protease for 5 days, and fibrocytes were counted as in figure 1. (B) The same PBMC populations were then counted for the total number of PBMC adhered to the plate following fixing and staining, and normalized to the no-protease control. At high concentrations, chymotrypsin significantly lowered the numbers of fibrocytes and adhered PBMC. Values are mean ± SEM, n=9 for pepsin and endoproteinase GluC, and n=7 for chymotrypsin. * indicates $p < .05$, ** indicates $p < .01$, and *** indicates $p < .001$ compared to the no-protease control by 1-way ANOVA, Dunnett's test.

Trypsin's enzymatic activity causes fibrocyte potentiation

To determine whether trypsin's enzymatic activity is necessary to potentiate fibrocyte formation, we examined the effect of two trypsin inhibitors on the ability of trypsin to potentiate fibrocyte differentiation. Adding trypsin inhibitors alone to cultures of PBMC had no significant effect on fibrocyte differentiation, with the exception of 4 µl/ml protease inhibitor cocktail, which decreased overall fibrocyte formation (Figure 3A). The addition of soybean trypsin inhibitor (Figure 3B) or protease inhibitor cocktail (Figure 3C) increased the amount of trypsin needed to potentiate fibrocyte differentiation. Increasing the inhibitor concentration increased the concentration of trypsin necessary to double fibrocyte differentiation compared to the controls (Arrows, Figures 3B and 3C). Pre-incubating trypsin and inhibitor completely abrogated trypsin's potentiation of fibrocyte differentiation (data not shown). Together, these results suggest that the protease activity of trypsin affects its ability to potentiate fibrocyte differentiation.

Figure 3. Trypsin inhibitors increase the amount of trypsin needed to potentiate fibrocyte potentiation.

Trypsin inhibitors were added to PBMC cultures at the beginning of the 5-day incubation period at the indicated concentrations, with and without trypsin present. PBMC were then air dried, stained, counted for fibrocyte differentiation, and normalized to the no-trypsin control. (A) Trypsin inhibitors did not significantly affect fibrocyte differentiation with the exception of 4 µl/ml Roche inhibitor, which decreased fibrocyte formation. ** indicates $p < .01$ compared to the inhibitor-free control. (B) Soybean trypsin inhibitor inhibited trypsin-induced fibrocyte potentiation. No-inhibitor data is the same as figure 1A. Fibrocyte counts were normalized to the inhibitor-containing trypsin-free control. Arrows indicate the lowest trypsin concentrations that doubled the fibrocyte number. Compared to the no-trypsin control, there was a significant increase in the number of fibrocytes with $p < .05$ for 4 µl/ml inhibitor for 10,000 ng/ml and at 1 µl/ml inhibitor for 5,000 ng/ml, and $p < .001$ at 1 µl/ml inhibitor for 2,500 and 10,000 ng/ml and at 0.1 µl/ml inhibitor for 2500 and 5,000 ng/ml (1-way ANOVA, Dunnett's test). (C) Roche complete protease inhibitor cocktail inhibitor in the cell culture medium also inhibited trypsin-induced fibrocyte potentiation. No-inhibitor data is the same as figure 1A. Arrows indicate the lowest trypsin concentrations that doubled the fibrocyte number. Compared to the no-trypsin control, there was a significant increase in the number of fibrocytes with $p < .05$ at 4 µl/ml inhibitor for 1250 ng/ml and 0.1 µl/ml inhibitor for 1250 and 2500 ng/ml, $p < .01$ at 1 µl/ml inhibitor for 10,000 ng/ml and at 0.1 µl/ml inhibitor for 10,000 ng/ml, and $p < .001$ at 4 µl/ml inhibitor for 2500, 5000, and 10,000 ng/ml (1-way ANOVA, Dunnett's test). Values are mean ± SEM, n=7.

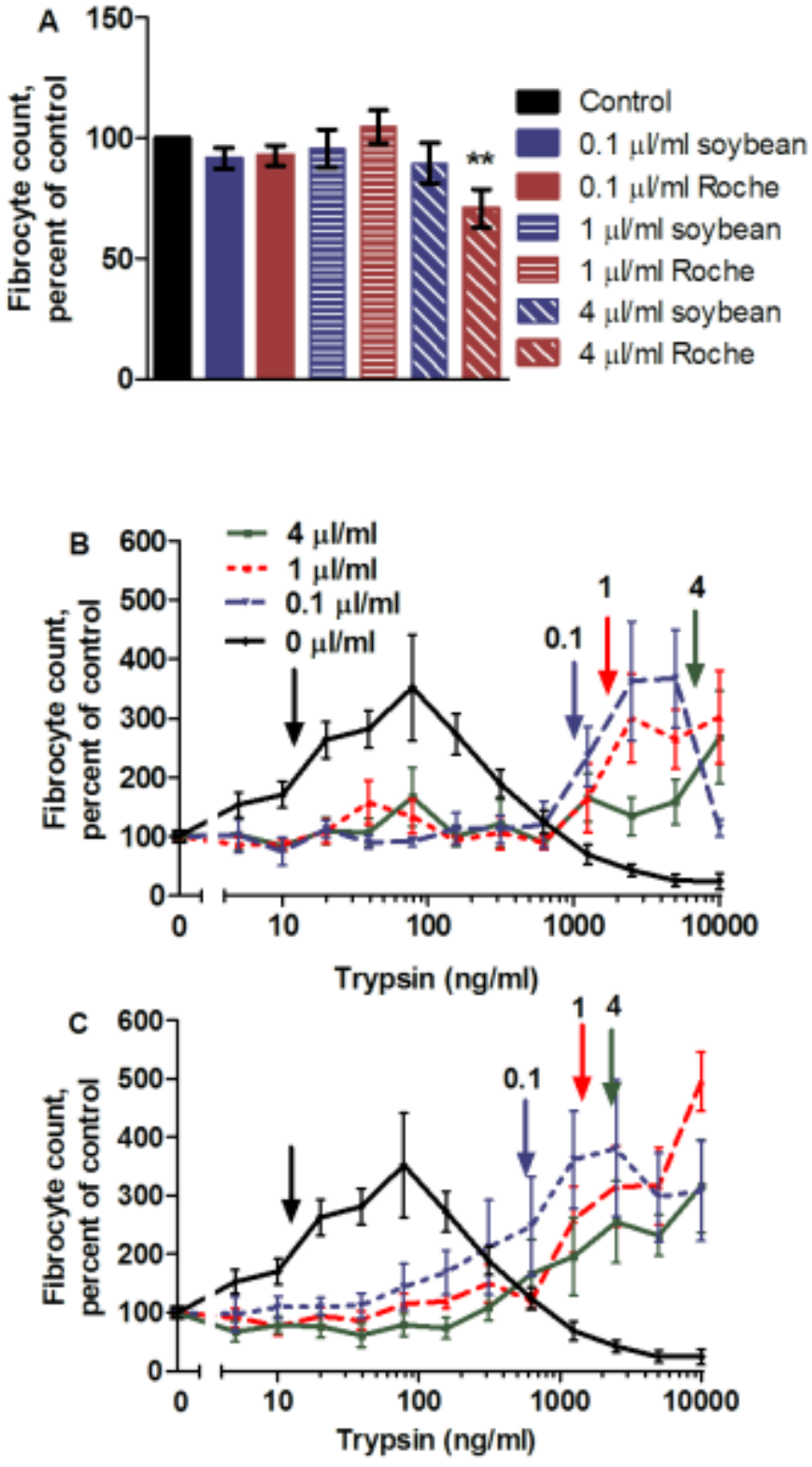
A
Fibrocyte count, percent of control
150
100
50
0
**
Control
0.1 µl/ml soybean
0.1 µl/ml Roche
1 µl/ml soybean
1 µl/ml Roche
4 µl/ml soybean
4 µl/ml Roche
B
4 µl/ml
1 µl/ml
0.1 µl/ml
0 µl/ml
0.1
1
4
600
500
400
300
200
100
0
10
100
1000
10000
Trypsin (ng/ml)
C
0.1
1
4
Trypsin (ng/ml)

Albumin is necessary for trypsin to potentiate fibrocyte differentiation

To test the hypothesis that trypsin acts on a protein supplement in the media to potentiate fibrocyte differentiation, we removed the protein supplements from our defined medium and added trypsin to this protein-free media. According to the manufacturer, Fibrolife medium is protein-free. Trypsin added to Fibrolife media lacking all three protein supplements (albumin, insulin and transferrin) did not potentiate fibrocyte differentiation (Figure 4A). At concentrations of 5 µg/ ml and higher, trypsin significantly decreased both fibrocyte numbers and the number of adhered cells (Figures 4A and 4B), presumably by decreasing cell adhesion. These results suggest that trypsin acts on or with a protein supplement to potentiate fibrocyte differentiation.

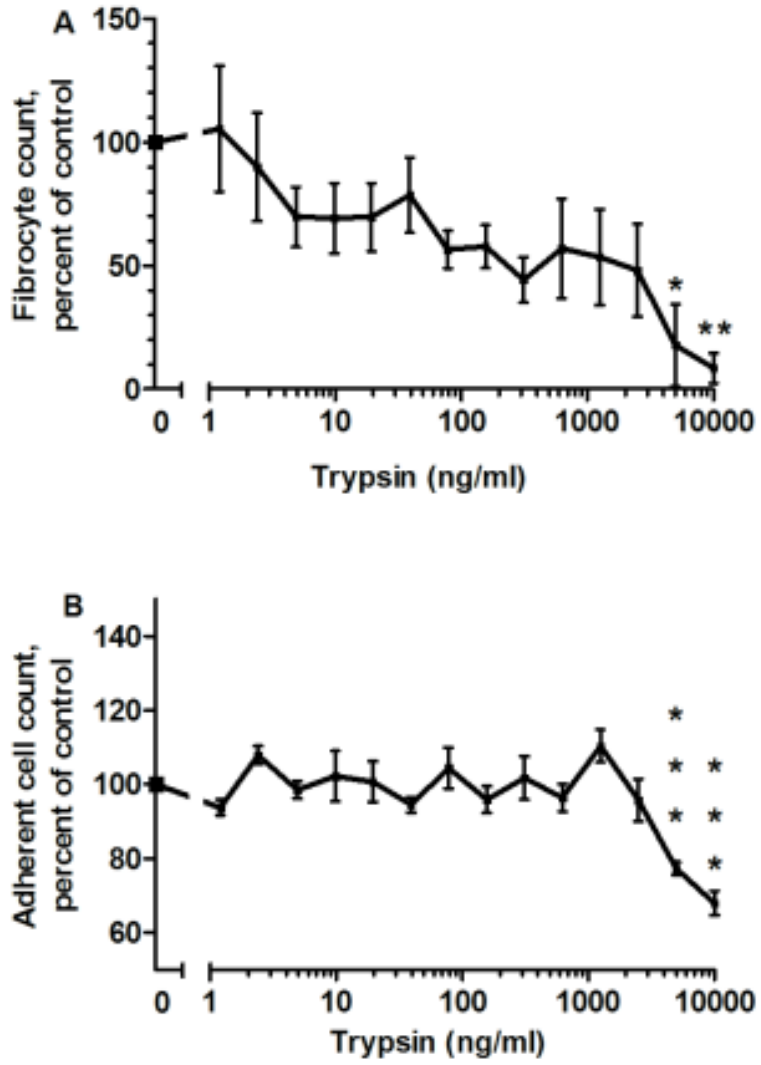

Figure 4. Trypsin does not potentiate fibrocyte differentiation in medium lacking protein supplements.

(A) PBMC were cultured with the indicated concentrations of trypsin for 5 days in protein-free medium, after which the PBMC were air-dried, stained, counted for fibrocyte differentiation, and normalized to the no-trypsin control. The no-trypsin controls developed 39 ± 7.2 fibrocytes per 10^5 PBMC. (B) The same PBMC populations were then counted for the total number of PBMC adhered to the plate following fixing and staining. Values are mean ± SEM, n=7. * indicates $p < .05$, ** indicates $p < .01$, and *** indicates $p < .001$ compared to the no-trypsin control by 1-way ANOVA, Dunnett's test.

Serum-free media contains three proteins: insulin, transferrin, and albumin. To determine whether insulin, transferrin or albumin potentiates fibrocyte differentiation when exposed to trypsin, we purified human and bovine albumin and made media containing only insulin, transferrin, or albumin. When TPCK-treated trypsin-coated agarose beads were used to trypsinize culture media containing purified human or bovine albumin, the trypsinized media potentiated fibrocyte formation following the removal of the beads and addition to PBMC (Figure 5A). Fibrocyte potentiation did not occur after the addition of protein-free, insulin-containing, or transferrin-containing media trypsinized in the same fashion (Figure 5A). To verify that TPCK did not influence fibrocyte differentiation, we digested human-albumin containing SFM with non TPCK-treated trypsin beads. Media containing human albumin digested by non TPCK-treated trypsin-beads also potentiated fibrocyte differentiation (Figure 5B). Using trypsin-coated beads to directly digest bovine and human albumin into fragments, and then adding those fragments to protein-free medium also potentiated fibrocyte differentiation compared to undigested controls (Figure 6A). SDS-PAGE gels indicated that the protease treatment of albumin caused the formation of digestion products (Figure 6B). These results suggest that a trypsin fragment of albumin may potentiate fibrocyte differentiation.

Figure 5. Serum-free medium containing albumin potentiates fibrocyte differentiation after temporary mixing with trypsin-coated agarose beads.
TPCK-treated trypsin-coated agarose beads were used to digest protein-free culture media (PFM) and PFM containing bovine albumin, human albumin, transferrin, or insulin, after which the beads were removed. Digested media and controls were mixed with SFM at the indicated percentages and added to PBMC at the beginning of a 5 day incubation, after which the PBMC were air-dried, stained, counted for fibrocyte differentiation, and normalized to the control media containing the same amount of undigested protein. (A) After removal of the beads, only medium containing albumin fragments potentiated fibrocyte differentiation. Values are mean ± SEM, n=3 for protein-free medium (PFM), insulin, and transferrin, n=4 for bovine albumin, and n=7 for human albumin. Compared to the human albumin control, digested human albumin significantly increased the number of fibrocytes with $p < .05$ at 62 µg/ml, $p < .01$ at 250 µg/ml, and $p < .001$ at 500 µg/ml. Compared to the bovine albumin control, digested bovine albumin increased the number of fibrocytes with $p < .05$ at 31 µg/ml, $p < .01$ at 250 µg/ml, and $p < .001$ at 500 µg/ml (1-way ANOVA, Dunnett's test). (B) Human albumin-containing media potentiated fibrocyte differentiation when digested by non-TPCK treated trypsin-coated agarose beads. Values are mean ± SEM, n=3. * indicates $p < .05$ and ** indicates $p < .01$ compared to the human albumin control by 1-way ANOVA, Dunnett's test.

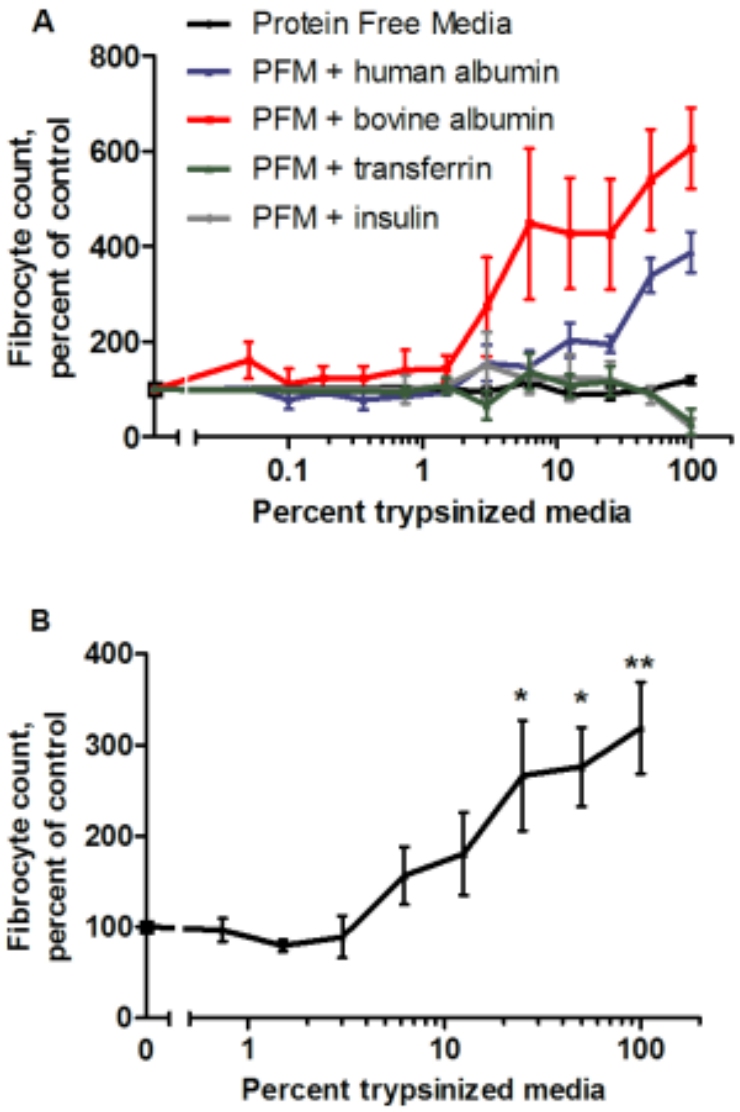
A
Protein Free Media
PFM + human albumin
PFM + bovine albumin
PFM + transferrin
PFM + insulin
Fibrocyte count, percent of control
800
600
400
200
0
0.1
1
10
100
Percent trypsinized media
B
Fibrocyte count, percent of control
400
300
200
100
0
*
*
**
0
1
10
100
Percent trypsinized media

Figure 6. Albumin potentiates fibrocyte differentiation after temporary mixing with trypsin-coated agarose beads.
TPCK-treated trypsin-coated agarose beads were used to digest bovine or human albumin. After the beads were removed, the digested albumin was added to PBMC cultures in SFM at the indicated concentrations for 5 days, after which the PBMC were air-dried, stained, counted for fibrocyte differentiation, and normalized to the bovine or human albumin controls. Values are mean ± SEM, n=4, ** indicates $p < .01$ and *** indicates $p < .001$ for both bovine and human albumin compared to the no-albumin control (1-way ANOVA, Dunnett's test). (B) 250 µl of protein-free media supplemented with human albumin was digested for two hours with gentle rotation at 37°C with 1 µg/ml protease, 0.1 µg/ml protease, or with 12.5 µg/ml TPCK-treated trypsin-coated agarose beads. Samples were then run on a 7.5% SDS-PAGE gel and silver stained. PFM indicates protein free medium, CT indicates chymtotrypsin, and Glu-C indicates endoprotease Glu-C. Alternative prep indicates samples from a repeat of this experiment that happened to be included in this gel. This gel is a digestion of human albumin, and is representative of similar gels of digestions of medium containing bovine albumin or ITS-3.

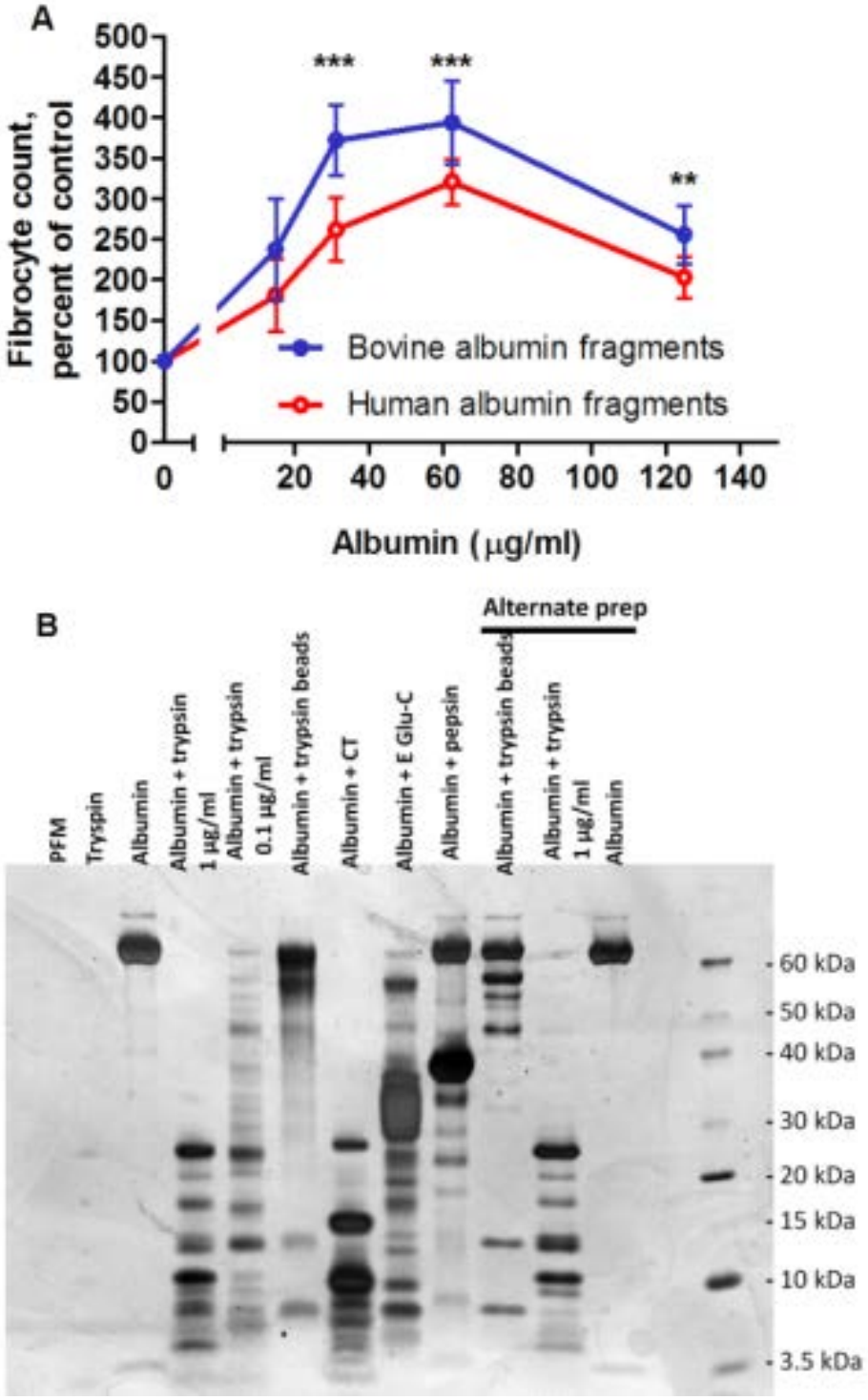
A
Fibrocyte count, percent of control
500
450
400
350
300
250
200
150
100
50
0
***
***
**
Bovine albumin fragments
Human albumin fragments
0
20
40
60
80
100
120
140
Albumin (μg/ml)
B
Alternate prep
PFM
Trypsin
Albumin
Albumin + trypsin 1 μg/ml
Albumin + trypsin 0.1 μg/ml
Albumin + trypsin beads
Albumin + CT
Albumin + E Glu-C
Albumin + pepsin
Albumin + trypsin beads
Albumin + trypsin 1 μg/ml
Albumin
60 kDa
50 kDa
40 kDa
30 kDa
20 kDa
15 kDa
10 kDa
3.5 kDa

Increased fibrocyte numbers are associated with increased collagen expression

Increased collagen expression in a PBMC culture is a marker for increased fibrocyte differentiation (27, 28, 178). To determine whether trypsinized human albumin increases collagen-positive cells, we resuspended and stained PBMC with an anti-collagen antibody following our 5-day differentiation assay. Increased collagen expression was detected by flow cytometry in PBMC cultures incubated with trypsinized human albumin (Figures 7A). A representative flow plot can be seen in Figure 7B. This suggests that the albumin fragment-induced increase in fibrocyte number is accompanied by an increase in collagen expression.

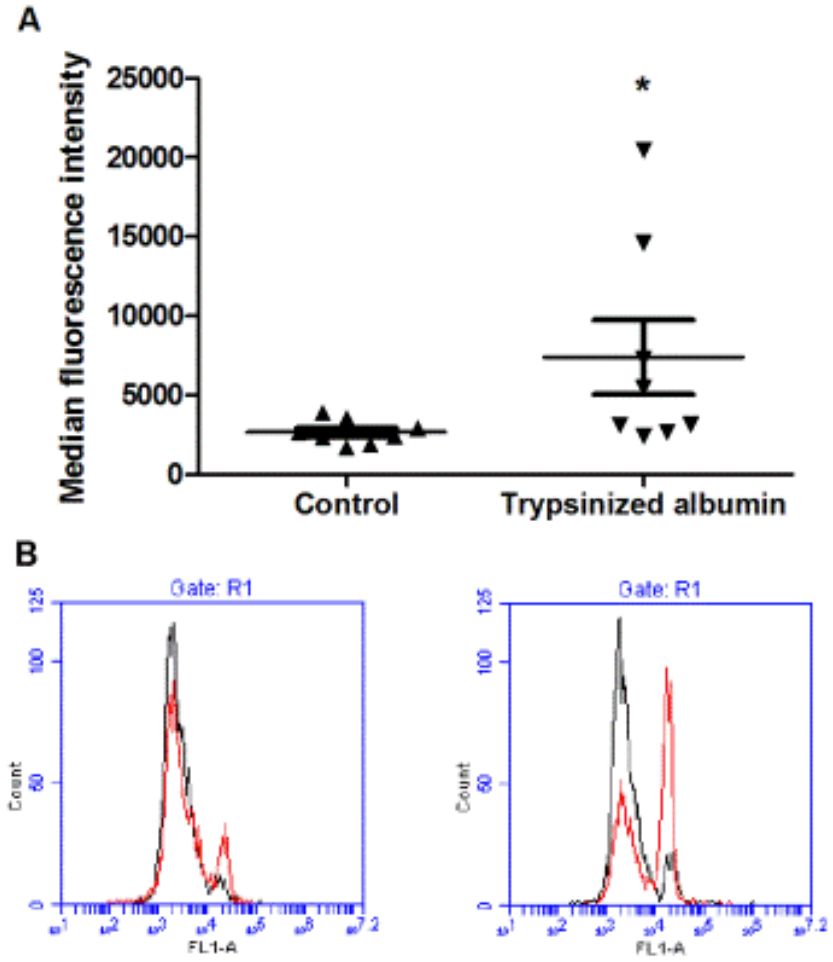

Figure 7. Collagen production is increased in PBMC exposed to trypsinized albumin. (A) TPCK-treated trypsin-coated agarose beads were used to digest protein-free media and media containing human albumin. After the beads were removed, the media was added to PBMC cultures in serum-free medium at a 33% concentration. Cells were exposed to trypsinized human albumin for 5 days, then resuspended, stained with anti-collagen and alexa-fluor secondary antibodies, and measured for fluorescence by flow cytometry. Values are mean ± SEM, n=9, * indicates $p < .05$ by two tailed Mann-Whitney's t-test. (B) Representative fluorescence overlay for collagen staining. The cells in the left plot were stained with isotype control primary antibodies, while the cells in the right plot were stained with anti-collagen primary antibodies. Red indicates trypsin-treated cells, while black indicates no trypsin treatment of the cells.

Trypsinized albumin increases fibrocyte formation in an enriched monocyte population

Fibrocytes differentiate from monocytes (22, 27, 33). Cells in a PBMC population can include T-cells, B-cells, or NK cells (36). To determine whether trysinized albumin acts directly on monocytes to potentiate fibrocyte differentiation, as opposed to an indirect action through other cells in the PBMC population, we isolated monocytes by negative selection from an average of 16% to an average of 83% purity. When added to the monocyte-enriched cells, 70 μg/ml trypsinized albumin potentiated fibrocyte differentiation by 223% ± 9% ($n=3$; $p < 0.01$, t-test). This suggests that tryptic fragments of albumin act directly on monocytes to potentiate fibrocyte differentiation.

Trypsinizing albumin-containing serum promotes fibrocyte differentiation

In a wound environment, monocytes and exogenous trypsin would be exposed to serum. Human serum contains more than 500-1200 proteins, of which the primary component is albumin (180, 181). To determine whether trypsin potentiates fibrocyte differentiation when mixed with human serum, we digested human serum with trypsin, and then added these digestion products to PBMCs. As previously observed (36), human serum inhibited fibrocyte differentiation, presumably due to the presence of serum amyloid P (SAP) in the serum (Figure 8A). Compared to no trypsin, trypsin-treated serum increased fibrocyte differentiation.

When the serum was depleted of albumin (Figures 8B and 8C), the serum also inhibited fibrocyte differentiation, and compared to no trypsin, trypsin treatment did not

cause an increase in the number of fibrocytes (Figure 8A). Compared to the no-trypsin control, in media containing 12.5% human serum, trypsin concentrations between 5 and 20 µg/ml increased fibrocyte differentiation, while the same concentrations of trypsin in albumin-depleted serum media did not increase fibrocyte differentiation (Figure 8D). These results indicate that trypsin's potentiation of fibrocyte differentiation in serum requires albumin.

Figure 8. Trypsinized human serum containing albumin potentiates fibrocyte differentiation.

(A) TPCK-treated trypsin-coated agarose beads were used to digest human serum and albumin-depleted human serum, which were then added to PBMC in protein-free media at the indicated concentrations for 5 days, after which the cells were air-dried, stained, counted for fibrocyte differentiation. Values are mean ± SEM, n=7 for serum, n=4 for depleted serum. Compared to the trypsinized depleted serum, trypsinized serum significantly increased the number of fibrocytes: * indicates $p < .05$ by a two-tailed Mann-Whitney's t-test. Compared to depleted serum, trypsinized depleted serum did not significantly increase fibrocyte number by a two-tailed Mann-Whitney's t-test. (B) Albumin-depleted serum shows less albumin, but a similar protein pattern to human serum, when both are run at 1:10 dilutions on a silver stained 4-20% SDS-PAGE gel. (C) A Western blot of serum and albumin-depleted serum stained with anti human-albumin antibodies. (D) Trypsin was added to PBMC in a 12.5% serum containing medium, and a 12.5% albumin-depleted serum containing medium, at the indicated concentrations for 5 days, after which the cells were air-dried, stained, counted for fibrocyte differentiation. Values are mean ± SEM, n=7 for serum, n=4 for depleted serum. Compared to the trypsinized depleted serum, trypsinized serum significantly increased the number of fibrocytes: * indicates $p < .05$ by a two-tailed Mann-Whitney's t-test.

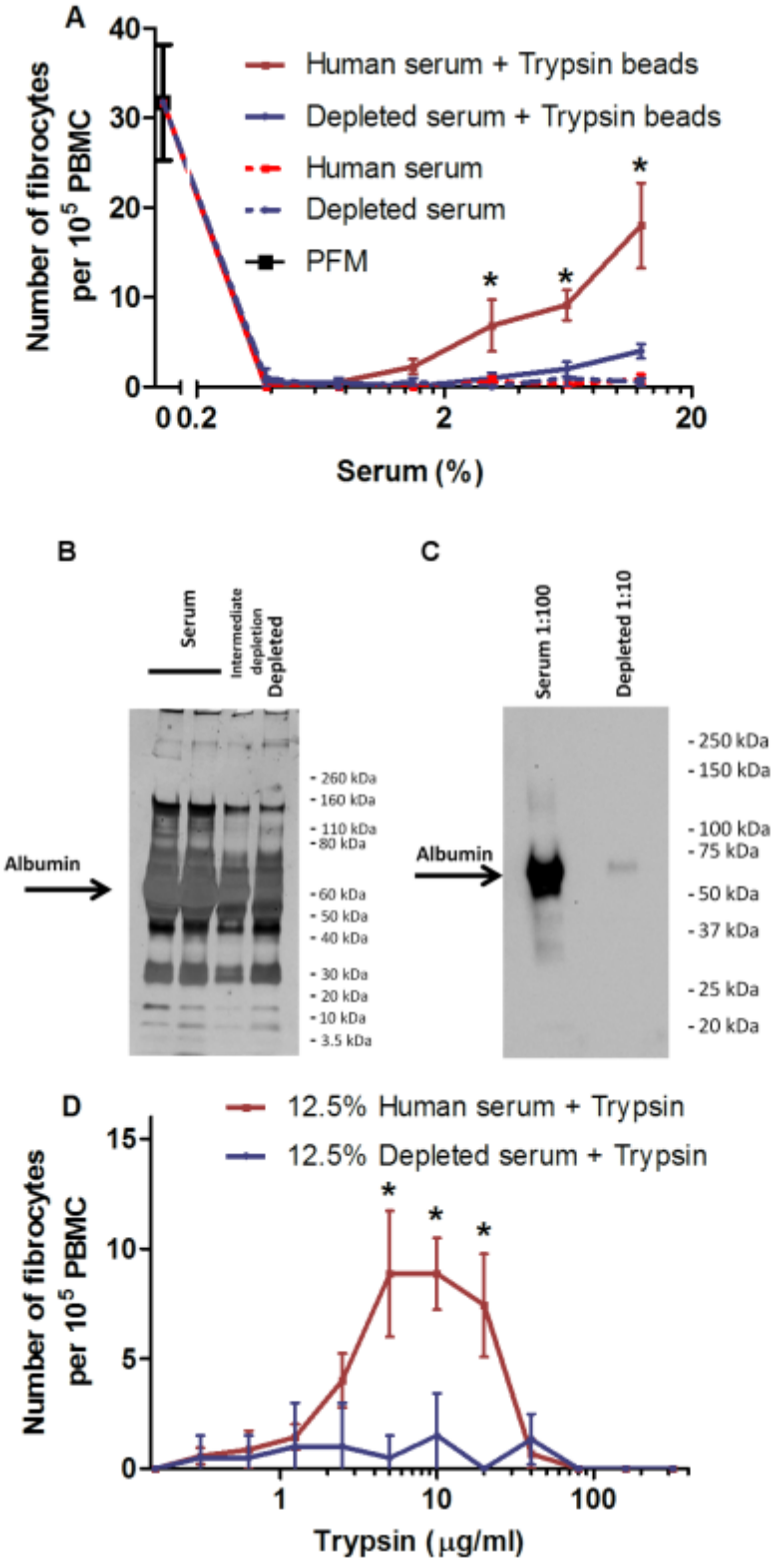
A
Number of fibrocytes per 10^5 PBMC
Human serum + Trypsin beads
Depleted serum + Trypsin beads
Human serum
Depleted serum
PFM
Serum (%)
B
Serum
Intermediate depletion
Depleted
Albumin
260 kDa
160 kDa
110 kDa
80 kDa
60 kDa
50 kDa
40 kDa
30 kDa
20 kDa
10 kDa
3.5 kDa
C
Serum 1:100
Depleted 1:10
Albumin
250 kDa
150 kDa
100 kDa
75 kDa
50 kDa
37 kDa
25 kDa
20 kDa
D
12.5% Human serum + Trypsin
12.5% Depleted serum + Trypsin
Number of fibrocytes per 10^5 PBMC
Trypsin (μg/ml)

Discussion

Trypsin speeds the healing of dermal wounds (171-177). Albumin is a major component of serum, and a trypsin-treated extract of serum potentiates wound healing (172). In this report, we showed that trypsin indirectly potentiates monocyte differentiation into fibrocytes in culture while albumin was necessary for this potentiation to occur. This then suggests that topical trypsin and trypsin-treated serum potentiates wound healing by tryptic fragments of albumin potentiating fibrocyte differentiation.

Trypsin inhibitors in the culture medium of PBMC caused more trypsin to be necessary to potentiate fibrocyte differentiation, indicating that trypsin's enzymatic activity is the key factor in albumin digestion and fibrocyte potentiation. Soybean trypsin inhibitor is a slow-binding but nearly irreversible inhibitor of trypsin's enzymatic activity (182). Soybean trypsin inhibitor stoichiometrically binds trypsin, and the amount of soybean-trypsin inhibitor added to the trypsin-containing PBMC cultures at higher concentrations was in excess of the total amount of trypsin added. Human serum also contains reversible protease inhibitors with less binding efficacy for trypsin than soybean inhibitor (183, 184). When mixed and immediately added to albumin-containing medium, not even the highest concentration of soybean inhibitor or serum (Figures 3B and 8D) completely abrogated trypsin's albumin-induced fibrocyte potentiation, suggesting that transient trypsinization is enough to digest albumin and induce fibrocyte differentiation.

Increased fibrocyte formation correlates with increased fibrosis (185) and faster wound healing (32), and protein additives to wound dressings can improve the wound healing response (32). Chronic non-healing wounds are often resistant to more usual

treatment dressings (17, 18). Chronic wounds are associated not only with infection, age, and diabetes, but also with decreased albumin concentrations in the wound area (153-156). An intriguing possibility is that if albumin degradation products in wounds potentiate fibrocyte differentiation, the decreased albumin concentrations in the chronic wounds might result in lower levels of the albumin degradation products in the chronic wounds, resulting in lower levels of fibrocyte differentiation.

Trypsin at ~50 mg/L (50 µg/ml) has been used to produce a lyophilized, trypsinized serum for wound treatment (172). We observed that 5-20 µg/ml trypsin added to 12.5% serum potentiates fibrocyte differentiation (Figure 8D). This would then correspond to 40-160 µg/ ml trypsin in 100% serum, which corresponds to the trypsin concentration used for the wound-healing product.

Proteinases have previously been implicated in interactions with proteinase-activated receptors (PARs) (67). PARs are activated by cleavage of a small peptide from the surface of the receptor by a serine protease, usually trypsin or chymotrypsin (67). Research on PARs has been primarily confined to mesenchymal cells, usually in the digestive tract where trypsin is a common enzyme (186-189). Since cells treated with trypsin in protein-free media do not have increased fibrocyte formation, and chymotrypsin does not potentiate fibrocyte differentiation, trypsin's effect on fibrocyte differentiation does not appear to be mediated by proteinase activated receptors.

Monocyte-derived fibrocytes are found in wound healing environments (22, 27, 28) and at tissue near a tumor edge (7, 8, 11), both areas of increased serine proteinase activity (162, 190-193). For instance, marapsin, a protease that also cleaves at arginine, is

up-regulated in wound healing environments (190). An intriguing possibility is that endogenous proteases, by generating tryptic fragments of albumin, help to potentiate fibrocyte differentiation in wounds and tissues near a tumor edge.

Taken together, our results suggest that topical trypsin and trypsinized albumin potentiate wound healing at least in part by potentiating fibrocyte differentiation. While trypsin has been used in the treatment of burns and in wound dressings for more than 50 years, a mixture of albumin and trypsin may further speed wound healing, especially when applied to chronic wounds deficient in albumin (153-156).

CHAPTER III

A BRIEF EXPOSURE TO TRYPTASE OR THROMBIN POTENTIATES FIBROCYTE DIFFERENTIATION IN THE PRESENCE OF SERUM OR SAP*

Summary

A key question in both wound healing and fibrosis is the trigger for the initial formation of scar tissue. To help form scar tissue, circulating monocytes enter the tissue and differentiate into fibroblast-like cells called fibrocytes, but fibrocyte differentiation is strongly inhibited by the plasma protein Serum Amyloid P (SAP), and healthy tissues contain very few fibrocytes. In wounds and fibrotic lesions, mast cells degranulate to release tryptase, and in early wounds thrombin mediates blood clotting. Tryptase and thrombin are upregulated in wound healing and fibrotic lesions, and inhibition of these proteases attenuates fibrosis.

* Reprinted with permission. Originally published in the Journal of Immunology. White MJ, Glenn M, Gomer RH. A brief exposure to tryptase or thrombin potentiates fibrocyte differentiation in the presence of serum or serum amyloid p. Journal of Immunology. 2015 Jan 1;194(1):142-50.

Here we report that tryptase and thrombin potentiate human fibrocyte differentiation at biologically relevant concentrations and exposure times, even in the presence of concentrations of serum and SAP that normally completely inhibit fibrocyte differentiation. The fibrocyte potentiation by thrombin and tryptase is mediated by protease-activated receptors 1 and 2, respectively. Together, these results suggest that tryptase and thrombin may be an initial trigger to override SAP inhibition of fibrocyte differentiation to initiate scar tissue formation.

Hypothesis: Tryptase and thrombin, two proteases involved with scar tissue formation, will promote fibrocyte differentiation at a physiological concentration

Introduction

Poorly-healing chronic wounds affect more than 6.5 million US patients per year (17). The opposite of poorly healing wounds is fibrosing diseases, where inappropriate scar tissue forms in an organ (19). Fibrosing diseases such as pulmonary fibrosis, congestive heart failure, liver cirrhosis, and kidney fibrosis are involved in 45% of deaths in the United States (20). Both wound healing and fibrosis involve scar tissue formation. A key component of scar tissue is the fibrocyte (22, 23). Monocytes are recruited to wounds or fibrotic lesions, and in response to unknown wound signals differentiate into fibrocytes (27, 28). Fibrocytes express collagen and other extracellular matrix proteins, secrete pro-angiogenic factors, and activate nearby fibroblasts to proliferate and secrete collagen (22, 23, 27, 29-31).

In serum-free cultures, monocytes differentiate into fibrocytes, but the presence of as little as 0.01% serum inhibits fibrocyte differentiation (33, 36). Fibrocyte differentiation can be inhibited by the plasma protein Serum Amyloid P (SAP), interferon-γ, and IL-12 (34-37). The SAP concentration in plasma is ~30 μg/ml (38). The IC50 for SAP inhibition of fibrocyte differentiation is 0.2 μg/ml (36, 39), and ~1 μg/ml SAP completely inhibits fibrocyte differentiation (36). *In vivo*, SAP slows wound healing, while removing SAP from a wound promotes healing (32, 42). Conversely, SAP injections that double the serum SAP concentration inhibit fibrosis in a variety of animal models (41, 43-45).

Normal tissues contain very few fibrocytes (31). In humans, in addition to being present in plasma, a considerable amount of SAP appears to be present in the interstitial space (40). A key question in wound healing and fibrosis is thus the mechanism that

overrides the inhibitory effect of SAP (and other fibrocyte differentiation inhibitors) to induce fibrocyte differentiation. One of the events preceding scar tissue formation in a healing wound is the clotting cascade, in which the protease thrombin cleaves fibrinogen to fibrin. Thrombin activity is upregulated in fibrotic lesions (61) and immediately after wounding (62). Thrombin causes inflammation when added to mouse lungs, increased concentrations of thrombin within lungs exacerbate fibrosis, and inhibition of thrombin attenuates fibrosis (63-66). Thrombin cleaves a six amino acid recognition site which is found on protease activated receptor-1 (PAR-1) (67, 68). This receptor is found on a variety of cell types including monocytes (69), and mediates the ability of thrombin to induce platelet aggregation (70).

Mast cells are found in both internal fibrotic lesions and sites of wound healing (71-73). Mast cells degranulate in response to external stimuli (73) to release, among other things, the protease tryptase (73, 78, 79). Tryptase is upregulated in areas of increased mast cell degranulation, including wounds and especially in fibrotic lung tissue (71, 72, 78-80). Extracellular tryptase is upregulated and associates with collagen increases in scar tissue in idiopathic pulmonary fibrosis (80). Tryptase cleaves at lysine and arginine residues, except when the following amino acid is proline (56). Tryptase activates protease activated receptor-2 (PAR-2) (73, 81). This receptor is found on a variety of cells including monocytes (69), and mediates the ability of tryptase to increase the proliferation of, and collagen production by, fibroblasts (73). Intratracheal administration of tryptase causes inflammation, and inhibition of tryptase attenuates this inflammation (82-85). Inhibition of PAR-2 receptors attenuates collagen deposition in a heart disease model (86).

In this report we show that relatively brief exposures of human mononuclear cells to levels of thrombin and tryptase that would be found in a wound potentiate human fibrocyte differentiation, overriding the SAP and serum inhibition, and could be a triggering mechanism for fibrocyte-mediated wound healing and fibrotic lesions.

Materials and methods

Cell isolation and culture

Human blood was collected from volunteers who gave written consent and with specific approval from the Texas A&M University human subjects Institutional Review Board. Peripheral blood mononuclear cells (PBMC) and monocytes were isolated as previously described (34), and cultured as previously described (194), in either serum-free or protein-free media. Protein-free media (PFM) was Fibrolife basal media (Lifeline Cell Technology, Walkersville, MD) supplemented with 10 mM HEPES (Sigma, St. Louis, MO), 1× non-essential amino acids (Sigma), 1 mM sodium pyruvate (Sigma), 2 mM glutamine (Lonza, Basel, Switzerland), 100 U/ml penicillin and 100 μg/ml streptomycin (Lonza). Serum-free media (SFM) was PFM further supplemented with 10 μg/ml recombinant human insulin (Sigma), 5 μg/ml recombinant human transferrin (Sigma), and 550 μg/ml filter-sterilized human albumin (isolated and checked for purity as previously described (194)), fish skin gelatin (Sigma), or skim milk powder (EMD Millipore, Billerica, MD). Protein supplements were checked for concentration using absorbance at 280 nm. SFM made with each supplement was mixed with 500 ng/ml TPCK-treated bovine trypsin (Sigma) for 24 hours at 37˚C, and assayed on 4-20% SDS gels (Bio-Rad,

Hercules, California), which were silver stained to check for purity and the presence of breakdown products. Where indicated, PFM was supplemented to 2.5% (v/v) with sterile filtered non-blood type specific human serum, tested negative for hepatitis A and B and HIV I and II (Lonza and Gemini Bio-products, West Sacramento, California). Monocytes were purified, tested for purity, and cultured as previously described (194, 195). Fibrocyte counts, total cell counts, and collagen staining were performed as previously described (194).

Proteases, PAR agonists, and PAR inhibitors

PAR-1 agonists SFLLRN-NH2 (American Peptide Company, Sunnyvale, CA) and SFLLRNPNDKYEPF (Tocris, Minneapolis, MN), PAR-2 agonists 2f-LIGRL-NH2 (EMD Millipore, Billerica, MD) and AC 55541 (Tocris), TPCK-treated bovine trypsin (10,000 BAEE units/mg, Sigma) and human thrombin (1000 NIH units/mg, Sigma) were resuspended following the manufacturer's instructions. Tryptase purified from human mast cells (70 BPVANA units/mg, Fitzgerald, Acton, MA) was mixed with 15 kDa heparin from porcine stomach (Sigma) in a 1:10 molar ratio of tryptase to heparin immediately after thawing (196). Trypsin, tryptase, thrombin, PAR-1 agonist, and PAR-2 agonist were incubated with PBMC as described previously (194). For timecourse experiments, protease-containing SFM was completely removed from PBMC after the indicated times (4, 12, or 24 hours), then replaced with fresh SFM, or SFM containing SAP or serum, as indicated.

PAR-1 inhibitors SCH 79797 hydrochloride (Axon Medchem, Reston, VA, added to cells at 5 µg/ml (197)) and vorapaxar (Axon Mechem, 25 µg/ml (198)), and PAR-2 inhibitors ENMD-1068 (Enzo Life Sciences, Farmingdale, NY, 50 µg/ml (73)) and FSLLRY (Tocris, 1 µg/ml (86)) were resuspended following the manufacturer's instructions. After a 1-hour incubation on ice in PFM, PBMC were collected by centrifugation at 300 x g for 10 minutes, resuspended in ice-cold PBS, and washed at 300 x g for 10 minutes, twice. PBMC were then plated and allowed to differentiate under the indicated conditions as described previously (194).

SAP and interferon-γ

Human SAP was purified as previously described (36) with the following modifications. Human serum from blood donors was mixed 1:1 with PBS. This was mixed with gentle rolling in a 10:1 ratio with SP sepharose beads (GE Healthcare, Piscataway, NJ) in 20 mM Tris, 140 mM NaCl, 2 mM $CaCl_2$ pH 8.0 and eluted as previously described (36). The SAP purity was checked by silver stain on an SDS-PAGE gel, and concentration was assessed by absorbance at 280 nm. Proteases at 40 ng/ml were co-incubated with purified SAP, and the reactions were analyzed by PAGE with 4-20% SDS gels and silver stained to assess cleavage of SAP. Recombinant human interferon-γ (IFN-γ, Peprotech, Rocky Hill, NJ) was resuspended according to the manufacturer's instructions. SAP and IFN-γ were then added to SFM at the indicated concentrations.

Transwell migration

Transwell migration of monocytes was performed as previously described (199), with the following modifications: The filter size was 8 μm, SFM was used as media, cells were allowed to pass through the filter for 12 hours, and adherent cells that passed through the filter were imaged with an InCell 2000 microscope (GE Healthcare) and then counted by CellProfiler (200).

Statistics

Statistics were performed using Prism (Graphpad Software, San Diego, CA). Differences were assessed by two-tailed t-tests or Mann-Whitney tests. Significance was defined by $p<0.05$.

Results

Tryptase and thrombin potentiate fibrocyte differentiation

We previously observed that trypsin, but not chymotrypsin, pepsin, or endoprotease GluC, potentiates fibrocyte differentiation (194). Fibrocytes are involved in wound healing, and trypsin is used topically to speed wound healing (171-176). The extracellular levels of both tryptase and thrombin increase during the formation of scar tissue (62, 71). To determine whether tryptase and thrombin also potentiate fibrocyte differentiation, we examined the effect of these proteases on fibrocyte differentiation in culture. Our previous assays had been done in media with a supplement called ITS-3; due to difficulties in obtaining this, we substituted human albumin for ITS-3 (194). Human peripheral blood mononuclear cells (PBMC) were incubated with trypsin, tryptase or

thrombin for 5 days in serum-free medium containing human albumin. The cells were then stained and scored for fibrocyte formation. In the absence of added proteases, we observed 388 to 1120 fibrocytes per 10^5 PBMCs from the different donors, similar to what we have previously observed (33-35, 194). Because of this variability, fibrocyte numbers were thus normalized to protease- free controls. In media with albumin as the supplement, 0.2 to 445 ng/ml trypsin potentiated fibrocyte differentiation (Figure 9A and D), encompassing the 20 to 200 ng/ml trypsin concentrations that we previously observed to increase fibrocyte differentiation in media with ITS-3 (194). Tryptase concentrations between 4 and 56 ng/ml and thrombin concentrations between 3 and 50 ng/ml also significantly increased the number of fibrocytes (Figure 9B-D). Tryptase concentrations above 100 ng/ml and thrombin concentrations above 400 ng/ml decreased the number of fibrocytes (Figures 9B and 9C). These effects were observed for all donors tested. In addition to having a unique morphology, fibrocytes express collagen, and the protease-induced increase in the number of visible fibrocytes was accompanied by an increase in the number of collagen-positive cells (Figure 10). The number of adherent cells following fixing and staining were not significantly affected by tryptase or thrombin (Figure 11), suggesting that tryptase and thrombin specifically increase the number of differentiated fibrocytes, rather than increasing general cell viability or adhesion.

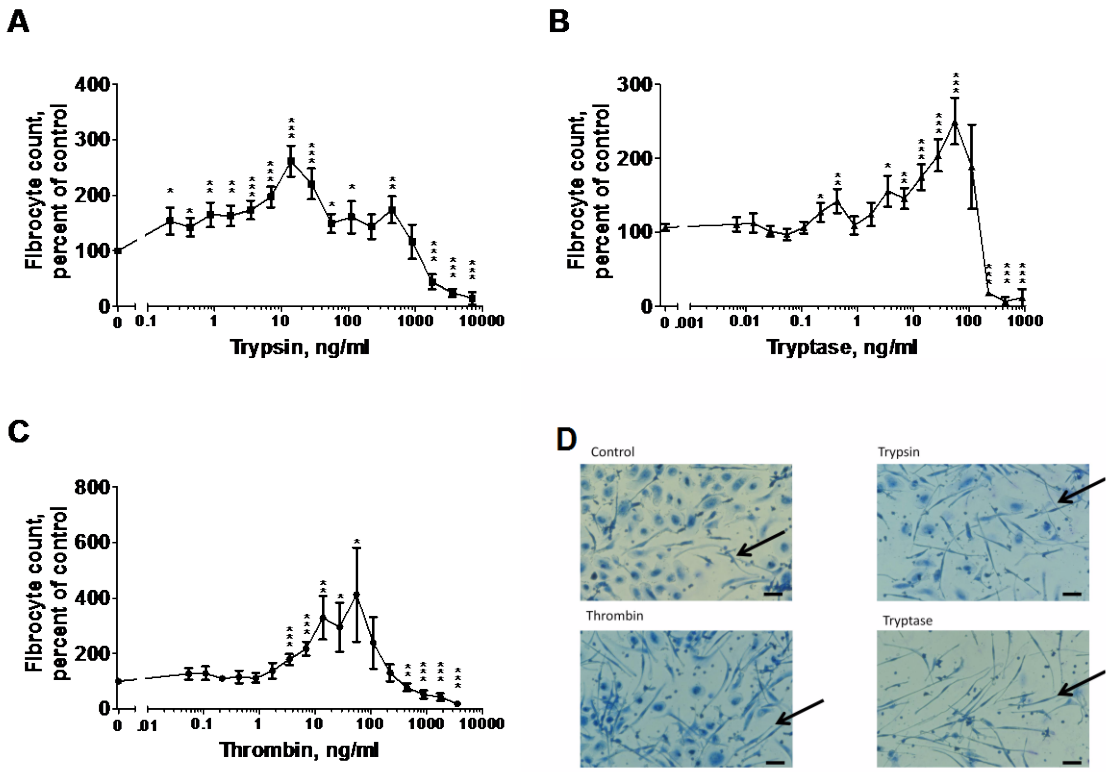

Figure 9. Trypsin, tryptase and thrombin potentiate fibrocyte differentiation. PBMC were cultured in serum free media in the presence of the indicated concentrations of (A) trypsin (n=13), (B) tryptase (n=15), or (C) thrombin (n=14) for 5 days. Fibrocyte counts were normalized for each donor to the no-protease control. The no-protease controls developed 767 ± 90 fibrocytes per 10^5 PBMC. Values in A through C are mean ± SEM; the absence of error bars indicates that the error was smaller than the plot symbol. * indicates $p < .05$, ** $p < .01$, and *** $p < .001$ compared to the no-protease control (t-test). (D) Images of PBMC after 5 days with no protease (control), 12.5 ng/ml trypsin, 12.5 ng/ml thrombin, or 55 ng/ml tryptase. Arrows indicate fibrocytes. Bar is 40 µm.

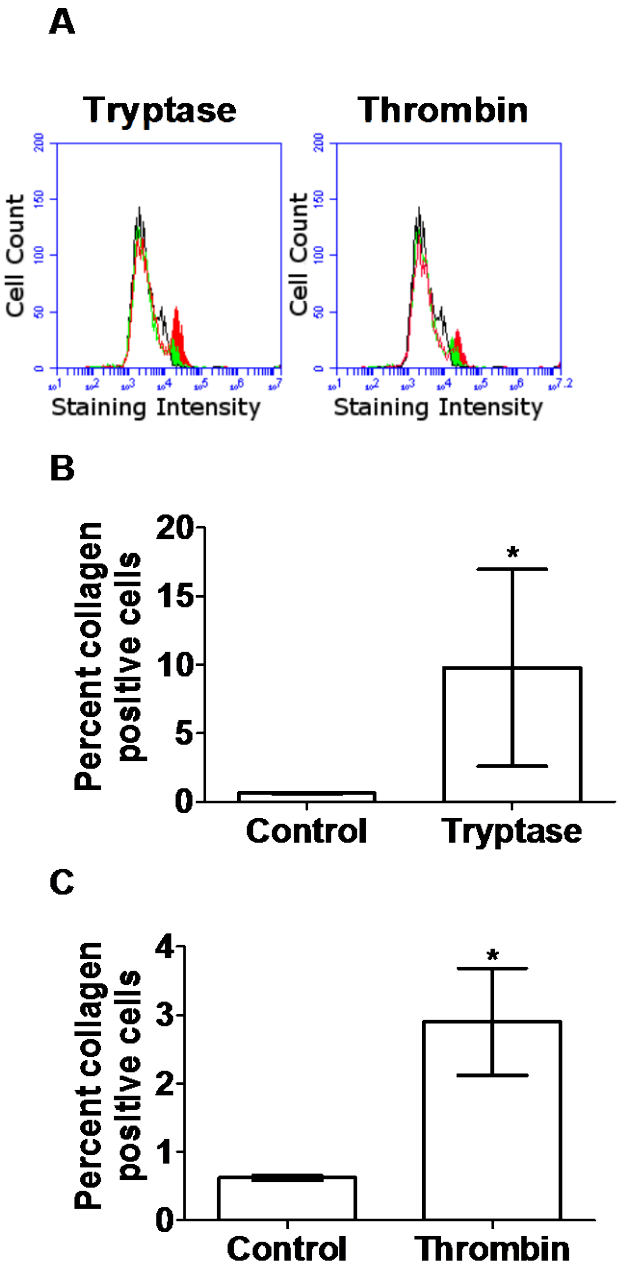

Figure 10. Tryptase and thrombin increase collagen secretion by PBMC.
(A) Representative flow plots of no-protease control PBMC stained with control rabbit IgG (black), and for collagen (green), and protease-treated PBMC stained for collagen (red). PBMC were exposed to 12.5 ng/ml (B) tryptase or (C) thrombin for 5 days, resuspended, stained for collagen, and assayed by flow cytometry. Values are mean ± SEM, n=5, * indicates $p < .05$ (t-test).

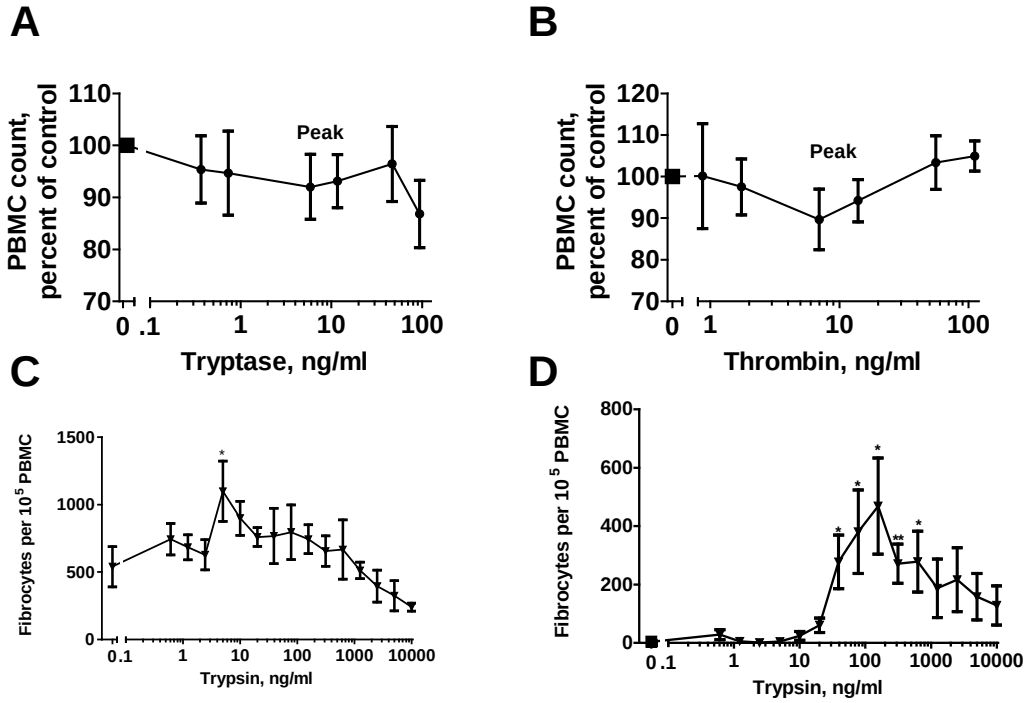

Figure 11. Tryptase and thrombin do not significantly affect the total number of adhered PBMC, and trypsin potentiates fibrocyte differentiation in the presence of fish gelatin or skim milk.
(A) The PBMC populations in Figure 9 were counted for the total number of PBMC adhered to the plate following fixing and staining for tryptase and (B) thrombin. Counts were normalized for each donor to the no-protease control. There were no significant differences in the numbers of adhered PBMC following fixing and staining. The protease concentrations causing peak fibrocyte counts are indicated. (C) PBMC were cultured in the presence of 500 µg/ml fish gelatin or (D) powdered skim milk in the presence of the indicated concentrations of trypsin. After 5 days, fibrocytes were counted as in Figure 9. Values are mean ± SEM, n=6. * indicates $p < .05$, ** $p < .01$ compared to the no-protease control (t-test).

The plasma thrombin concentration in a clotting wound is ~37 nM (62). The molecular mass of thrombin is ~36 kDa, so this thrombin concentration is ~1.3 x10^3 ng/ml. Far from a wound, the levels of active thrombin should be negligible, so assuming that a gradient of thrombin forms in the interstitial space, with the highest concentration in the clotting blood, at some point in the tissue near the wound the thrombin concentration

would be on the order of the 3-50 ng/ml that potentiates fibrocyte differentiation in vitro (Figure 9). Tryptase requires stabilization by heparin to be enzymatically active (196). Tryptase (~35 kDa) signaling thus must be measured by its activity. In wound fluid, tryptase activity is ~0.30 mU/mg wound fluid protein, where a unit is the cleavage of 1 µmol/min of Z-gly-pro-arg-pNA (201). In the assay conditions used by (201) tryptase activity is ~1.75 x 10^8 mU/g tryptase, and 35 nM tryptase cleaves 30 pmol/sec of 0.2 mM Z-gly-pro-arg-pNA (202). Wound fluid contains ~31 mg/ml protein (203), and combining these indicates that wound fluid contains ~63 ng/ml tryptase, within the range of tryptase concentrations that promote fibrocyte differentiation in vitro (Figure 9). Together, these results suggest that physiological concentrations of thrombin and tryptase can potentiate fibrocyte differentiation.

Fibrocytes differentiate from monocytes (22, 27, 33). Cells in the PBMC population include T cells, B cells, monocytes, and NK cells (36). To determine whether trypsin, tryptase, or thrombin act directly on monocytes to potentiate fibrocyte differentiation, we purified monocytes from PBMC by negative selection as previously described (194). Monocytes were 16% ± 9% (mean ± SEM, n=3) of the PBMCs and 92% ± 5% in the purified fraction. Trypsin, tryptase, and thrombin all potentiated the differentiation of fibrocytes from purified monocyte populations by a factor of ~2 (Figure 12), similar to the ~2-fold increase in fibrocyte these proteases caused in PBMC populations (Figure 9). Together, these results suggest that trypsin, tryptase, and thrombin directly affect monocytes to potentiate fibrocyte differentiation.

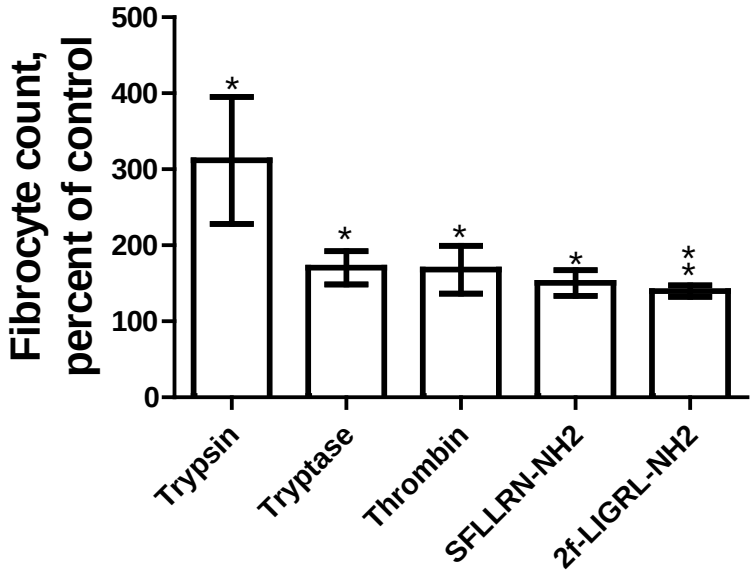

Figure 12. **Trypsin, tryptase, thrombin, PAR-1 agonist, and PAR-2 agonist potentiate fibrocyte differentiation from purified monocytes.**
Monocytes were cultured in SFM at 12.5 ng/ml protease or 10 μM agonist. After 5 days, fibrocytes were counted as in Figure 9. Values are mean ± SEM, n=3. * indicates $p < .05$, ** $p < .01$ compared to the SFM control (t-test).

Tryptase and thrombin potentiate fibrocyte differentiation in serum-containing media

We previously observed that trypsin potentiates fibrocyte differentiation in media supplemented with human serum (194). Serum is present in a wound after blood clots (204). To determine whether tryptase and thrombin can potentiate fibrocyte differentiation in an environment containing serum, we incubated PBMC in serum-containing media for five days with tryptase and thrombin. As previously observed (36), serum inhibited fibrocyte differentiation (Figure 13). In the presence of serum, 14 to 446 ng/ml tryptase and 28 to 224 ng/ml thrombin potentiated fibrocyte differentiation (Figure 13), indicating that levels of these proteases that would be observed in a wound can override the inhibitory effect of serum.

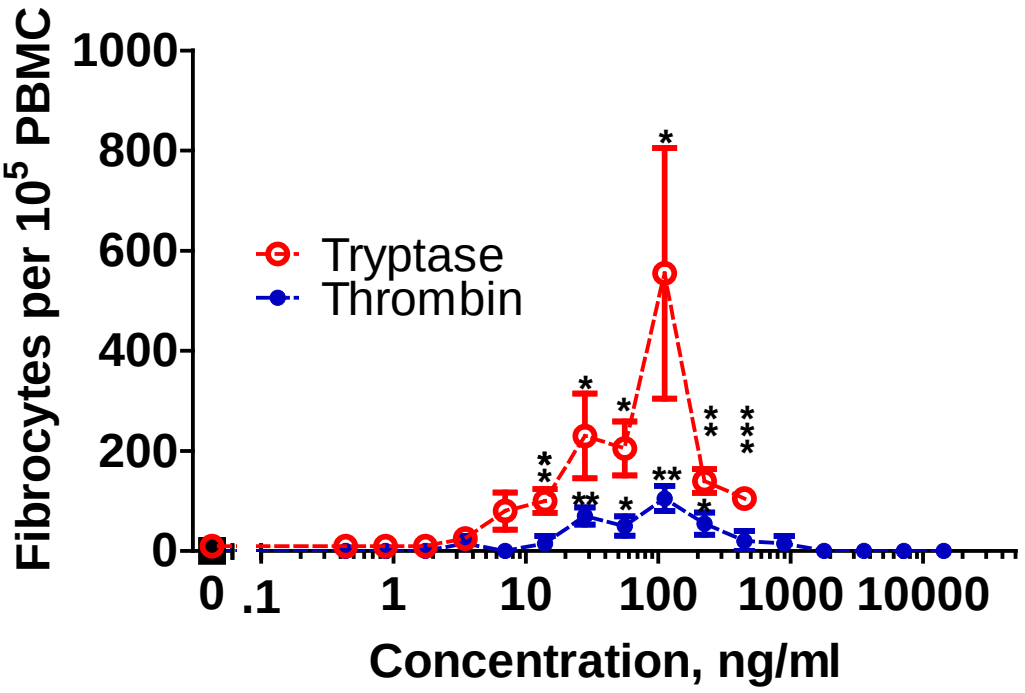

Figure 13. **Tryptase and thrombin potentiate fibrocyte differentiation in the presence of human serum.**
PBMC were cultured in medium containing serum in the presence of the indicated concentrations of tryptase or thrombin for 5 days, and fibrocytes were counted as in Figure 9. Serum-containing media complete inhibited fibrocyte differentiation in the no-protease control. Values are mean ± SEM, n = 4. * indicates $p < .05$, ** $p < .01$, and *** $p < .001$ compared to the no-protease control (t-test).

Trypsin potentiates fibrocyte differentiation in the absence of albumin

The observation that three different proteases, in the presence of albumin, potentiate fibrocyte differentiation suggests that either the proteases potentiate fibrocyte differentiation, or a proteolytic fragment of albumin potentiates fibrocyte differentiation. To determine if fibrocyte potentiation is dependent on the protein composition of the defined media, we co-incubated PBMC with trypsin and fish gelatin or skim milk powder. Trypsin caused fibrocyte potentiation when mixed with fish gelatin or skim milk powder

(Figure 9). There is only a 15% sequence similarity between human albumin and fish gelatin, and the largest identical sequence is 3 amino acids. This suggests that after proteolytic digestion of the two proteins, there is no common peptide produced that could activate fibrocyte differentiation. The observation that trypsin potentiates fibrocyte differentiation in the presence of fish gelatin, and the absence of albumin, suggests that albumin is not necessary for the trypsin effect, and thus that trypsin may directly potentiate fibrocyte differentiation.

Trypsin, tryptase, and thrombin signal through protease-activated receptors

Since trypsin, rather than a proteolytic fragment of albumin, appears to potentiate fibrocyte differentiation, we examined the possibility that trypsin activates a cell surface receptor. Proteases can act as extracellular signals by cleaving the extracellular domains of protease-activated receptors (PARs) (205). PAR-1 and PAR-2 are expressed on human monocytes (69). To determine if trypsin, tryptase, or thrombin potentiate fibrocyte differentiation through PAR-1 or PAR-2, we examined the effect of these proteases on PBMC differentiation after exposure to PAR-1 and PAR-2 inhibitors. ENMD-1068 and FSLLYR-NH2 are peptides which selectively block PAR-2 activation but do not interfere with the activities of PAR-1, 3, or 4 (73, 86). ENMD-1068 at 26 nM and FSLLRY-NH2 at 12 nM inhibit PAR-2 function as measured by proliferation and collagen production in fibroblasts (73, 86). 26 nM ENMD-1068 and FSLLRY-NH2 decreased trypsin and tryptase potentiation of fibrocyte differentiation (Figure 14A and B), but thrombin potentiation of fibrocyte differentiation was not significantly affected (Figure 14C).

SCH79797 and vorapaxar are inhibitors of PAR-1 that do not interfere with PAR-2 signaling (197, 198). SCH79797 at 70 nM and vorapaxar at 47 nM inhibit PAR-1 function in platelet aggregation assays (197, 198). SCH79797 and vorapaxar did not significantly affect trypsin's or tryptase's fibrocyte potentiation (Figure 14D and 14E), but blocked the ability of thrombin to potentiate fibrocyte differentiation (Figure 14F). Conversely, PAR-1 and PAR-2 agonists potentiated fibrocyte differentiation at concentrations similar to previously observed effective concentrations (206-209) when added to PBMCs (Figure 14G and 14H) or to purified monocytes (Figure 12). These data suggest that tryptase and trypsin signal through PAR-2, and thrombin signals through PAR-1, to potentiate fibrocyte differentiation.

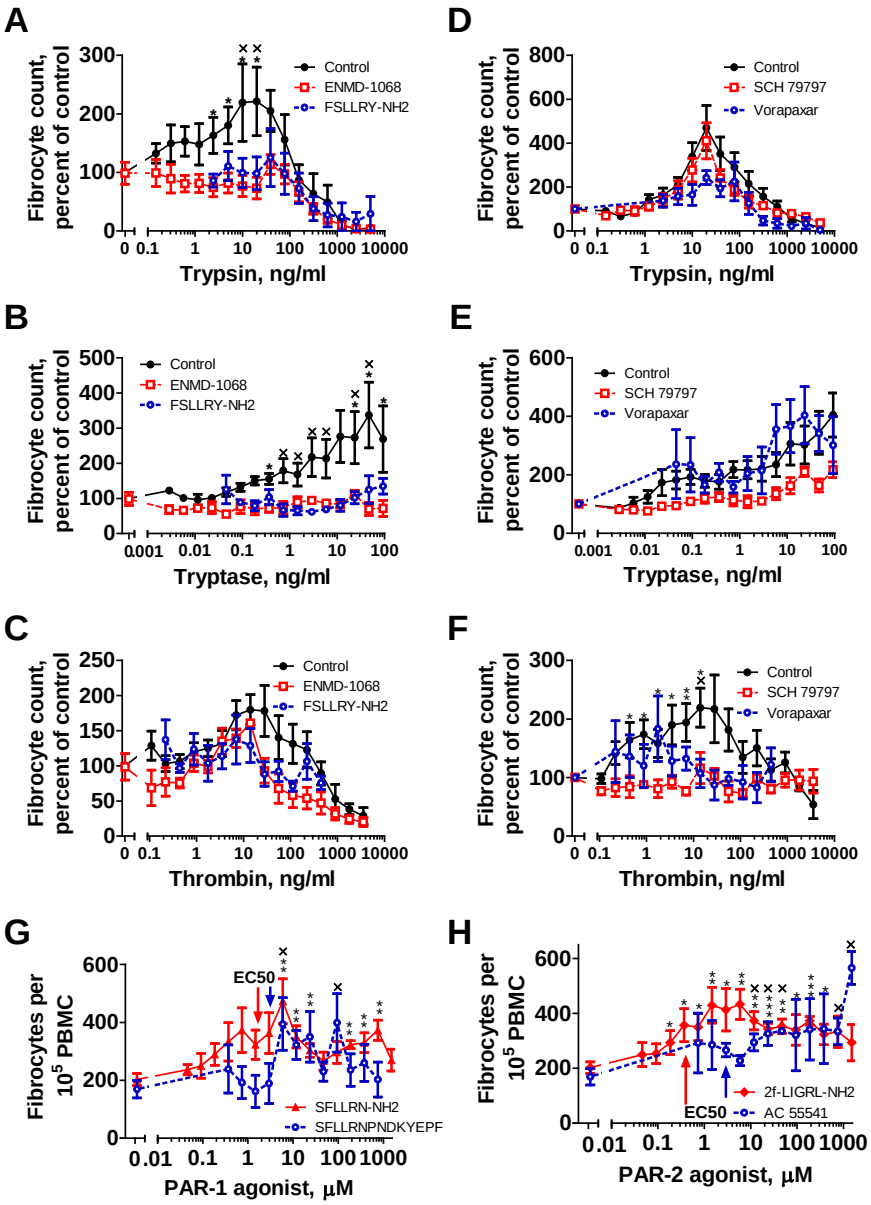

Figure 14. **PAR-1 and PAR-2 affect fibrocyte differentiation.**
PBMC were incubated with (A-C) inhibitors of protease activated receptor-2 (PAR-2) or (D-F) inhibitors of protease activated receptor-1 (PAR-1) before mixing with (A, D) trypsin, (B, E) tryptase, or (C, F) thrombin at the indicated concentrations. (G) PAR-1 agonists or (H) PAR-2 agonists were added to PBMC at the indicated concentrations. After 5 days, fibrocytes were counted as in Figure 9. Values are mean ± SEM, n=6. * indicates $p < .05$, ** $p < .01$, and *** $p < .001$ compared to the agonist-free or protease-free control (t-test) for ENMD-1068, SCH 79797, SFLLRN-NH2, and 2f-LIGRL-NH2. x indicates $p < .05$ for FSLLRY-NH2, Vorapaxar, SFLLRNDKYEPF, and AC 55541, each n=3. In G and H, arrows indicate the published EC50 concentrations.

Tryptase and thrombin compete with SAP to potentiate fibrocyte differentiation

SAP inhibits the differentiation of monocytes into fibrocytes, while trypsin, tryptase and thrombin potentiate this differentiation. Tryptase and thrombin are present in wounds along with SAP (62, 71). To determine how these signals might compete with each other, we co-incubated SAP with proteases. As previously observed (36), 10 µg/ml SAP completely inhibited fibrocyte differentiation (Figure 15 A-F). In the presence of 10 µg/ml SAP, trypsin showed no significant potentiation of fibrocytes from PBMC (Figure 15A) but did potentiate fibrocyte differentiation from monocytes (Figure 15F). Levels of tryptase and thrombin that would be observed in a wound, as well as PAR-1 and PAR-2 agonists, competed with 10 µg/ml SAP to potentiate fibrocyte differentiation from PBMC (Figure 15B-E) and purified monocytes (Figure 15F). This potentiation was not caused by protease digestion of SAP, as only trypsin caused any measurable cleavage of SAP (Figure 15G).

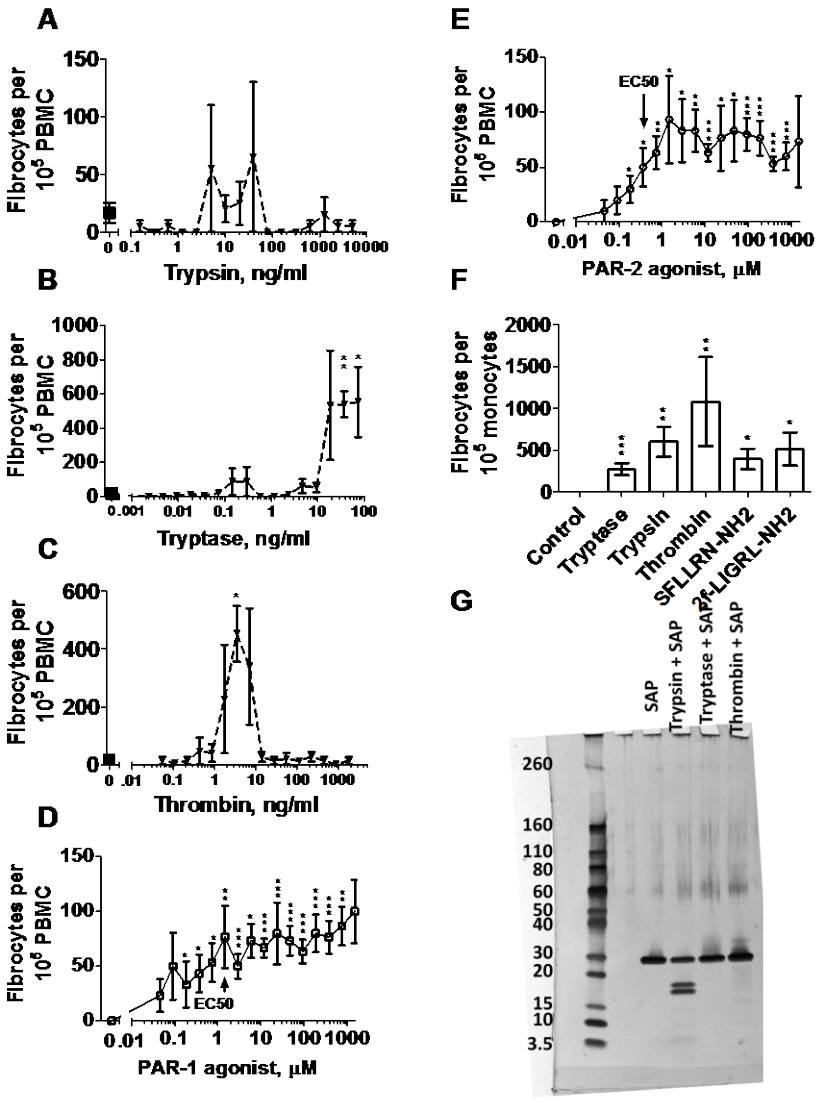

Figure 15. **Tryptase and thrombin compete with SAP to potentiate fibrocyte differentiation, but do not obviously digest SAP.**

PBMC mixed with SAP at 10 μg/ml were incubated with the indicated concentrations of (A) trypsin, (B) tryptase, (C) thrombin, (D) PAR-1 agonist SFLLRN-NH2, or (E) PAR-2 agonist 2f-LIGRL-NH2 for 5 days. Fibrocytes were then counted as in Figure 9. Values are mean ± SEM, n=4. * indicates $p < .05$ compared to SAP with no protease or no agonist (t-test). (F) Monocytes in SFM were co-incubated with 10 μg/ml SAP, in the absence (control) or presence of 12.5 ng/ml protease, or 10 μM PAR-1 or PAR-2 agonist. After 5 days, fibrocytes were counted as in Figure 12. Values are mean ± SEM, n=3. * indicates $p < .05$, ** $p < .01$, and *** $p < .001$ compared to the SAP control (t-test). (G) Purified SAP was incubated with proteases at 40 ng/ml for 24 hours at 37° C, run on a 4-20% SDS-PAGE gel and silver stained. Molecular masses in kDa are indicated at left.

To determine if trypsin, tryptase or thrombin change the IC50 of SAP's inhibition of fibrocyte differentiation, we co-incubated each protease with a series of SAP concentrations (Figure 16, Supplemental Figure 9E). Trypsin, tryptase, thrombin, PAR-1 agonist, and PAR-2 agonist significantly potentiated fibrocyte differentiation in the presence of SAP at some of the indicated SAP concentrations (Figure 16). SAP inhibited fibrocyte differentiation with an IC50 of 0.16 ± 0.05 μg/ml. SAP's IC50 with trypsin was 0.23 ± 0.13 μg/ml; with tryptase 0.39 ± 0.13 μg/ml; with thrombin 1.03 ± 0.46 μg/ml; with PAR-1 agonist 0.44 ± 0.31 μg/ml; and with PAR-2 agonist 1.59 ± 0.77 μg/ml. The tryptase, thrombin, and PAR-2 agonist effects on the IC50 were significant ($p<0.05$; Mann-Whitney test). Together, these results indicate that tryptase and thrombin can compete with SAP to potentiate fibrocyte differentiation.

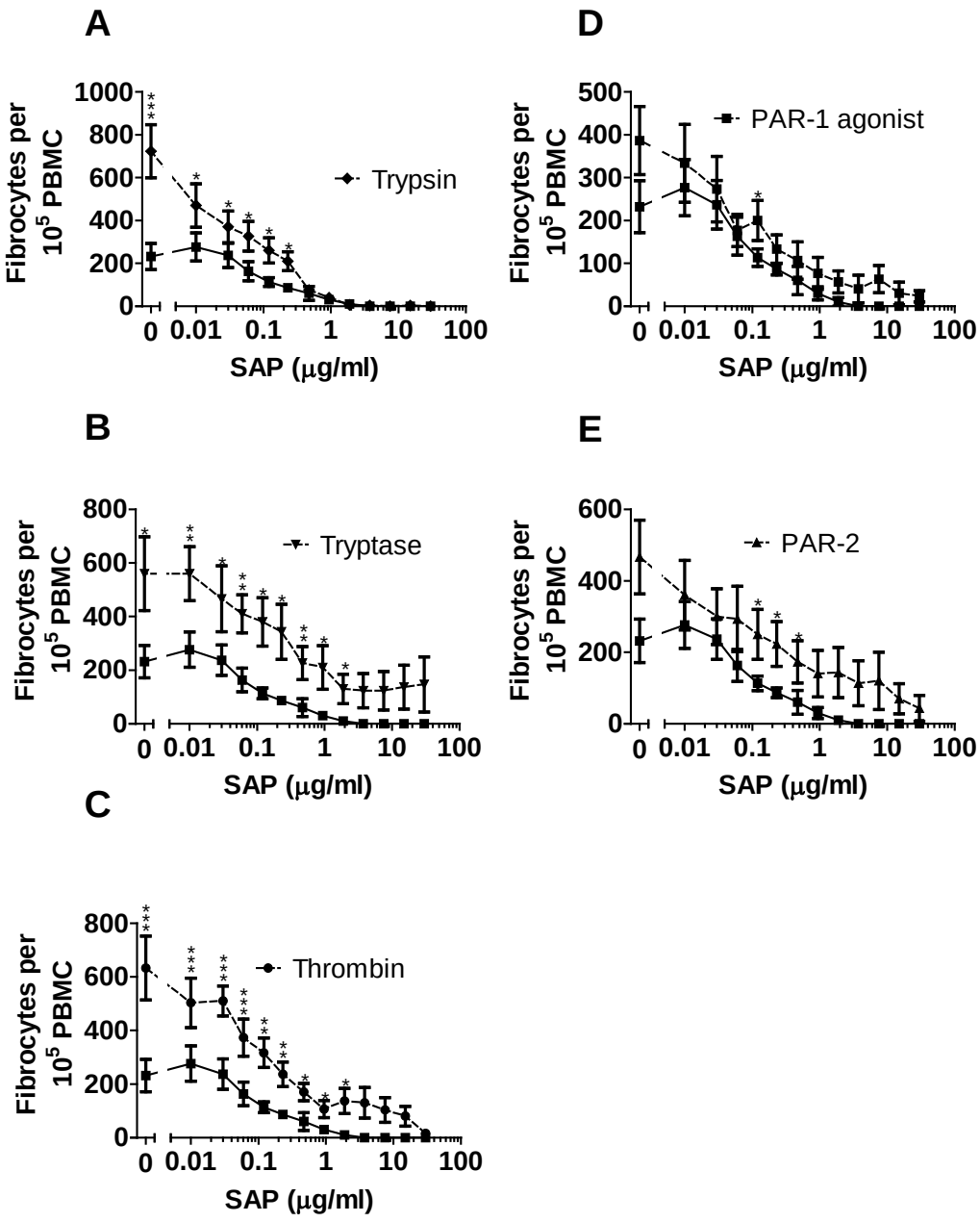

Figure 16. **Tryptase and thrombin alter SAP's IC50.**
PBMC were co-incubated with the indicated concentrations of SAP and 12.5 ng/ml (A) trypsin, (B) tryptase, (C) thrombin, or 10 μM (D) PAR-1 agonist or (E) PAR-2 agonist. After 5 days, fibrocytes were counted as in Figure 9. In A-E, the lower curve is SAP alone. Values are mean ± SEM, n=6. * indicates $p < .05$, ** $p < .01$, and *** $p < .001$ compared to the no-protease or no-agonist control (Mann-Whitney test).

Trypsin, tryptase, thrombin, PAR-1 and PAR-2 agonist compete with interferon-gamma (IFN-γ) to potentiate fibrocyte differentiation

Like SAP, interferon-gamma (IFN-γ) is present in wounds and scar tissue (210, 211) and inhibits the differentiation of monocytes into fibrocytes (37). To determine how these signals might compete with each other, we co-incubated proteases with IFN-γ. As previously observed, 10 ng/ml IFN-γ inhibited fibrocyte differentiation (37). Each protease and receptor agonist potentiated fibrocyte differentiation in the presence of 10 ng/ml IFN-γ (Figure 17).

To determine if proteases or PAR agonists act as monocyte chemoattractants or chemorepellents, we placed PBMC in the upper cup of a Boyden chamber and added each protease or agonist above, below, or on both sides of the filter. Each protease reduced PBMC migration through the filter, suggesting that these proteases may have a chemostatic effect on PBMC regardless of whether the protease was added above or below the filter (Figure 17). Each agonist acted as a chemoattractant whether added above or below the filter (Figure 17).

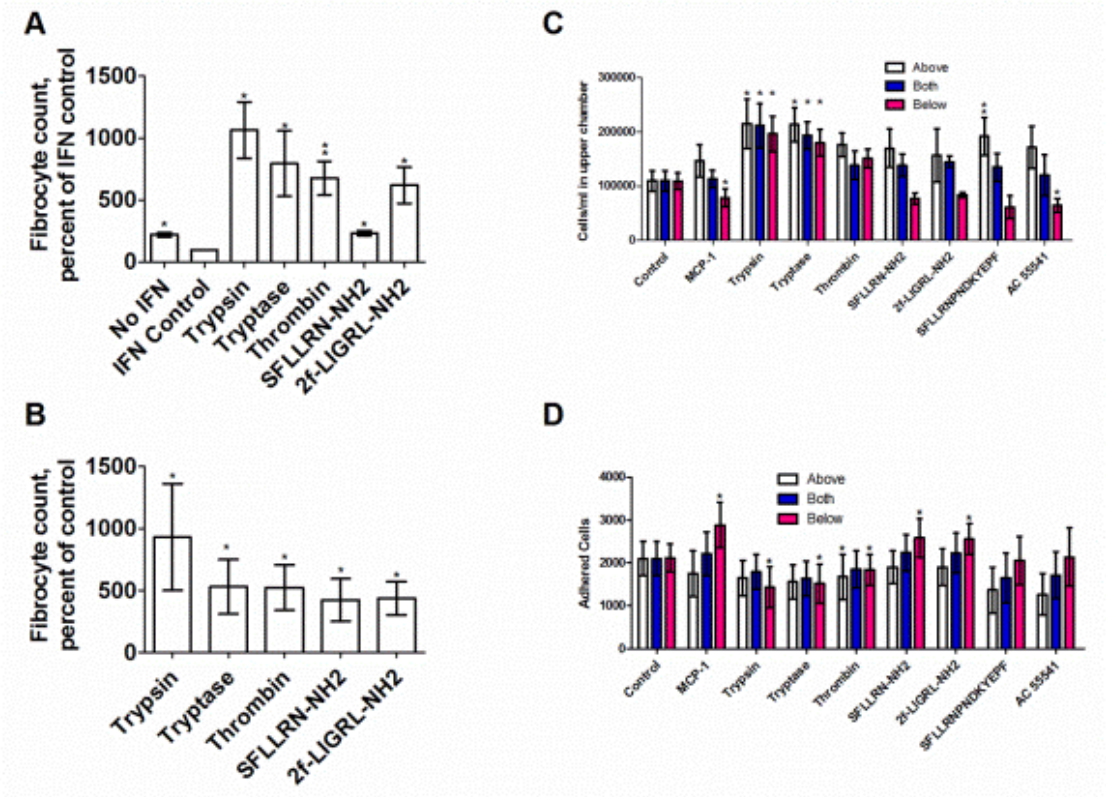

Figure 17. **Trypsin, tryptase, thrombin, PAR-1 agonist, and PAR-2 agonist potentiate fibrocyte differentiation in the presence of interferon-gamma (IFN-γ), and act as chemoattractants or chemostatic agents for monocytes.**
(A) PBMC were co-incubated with no IFN-γ or 10 ng/ml IFN-γ and either no protease or agonist (IFN-γ control), or 12.5 ng/ml trypsin, tryptase, or thrombin, or 0.1 μg/ml PAR-1 agonist (SFLLRN-NH2) or PAR-2 agonist (sf-LIGRL-NH2). After 5 days, fibrocytes were counted as in Figure 9, and counts were normalized to the IFN-γ control. Values are mean ± SEM, n=4. * indicates $p < .05$, ** $p < .01$, and *** $p < .001$ compared to the IFN-γ control (t-test). (B) Monocytes were co-incubated with 20 ng/ml IFN-γ and either no protease or agonist (IFN-γ control), or 12.5 ng/ml protease or 0.1 μg/ml PAR-1 or -2 agonist. Monocytes were incubated and counted as in Figure 12, and counts were normalized to the IFN control. Values are mean ± SEM, n=3. * indicates $p < .05$ compared to the IFN-γ control (t-test). (C) PAR-1 (SFLLRN-NH2 or SFLLRNPNDKYEPF) and PAR-2 (2f-LIGRL-NH2 or AC 55541) agonists were added at 10 μM, proteases were added at 12.5 ng/ml, and the monocyte chemoattractant MCP-1 (Peprotech) was added at 50 ng/ml, into SFM either above, below, or on both sides of an 8 μm pore size insert in a 24-well plate well. PBMC were added to the insert chamber and after 12 hours cells in the insert were counted. (D) PBMC that adhered to the plate were stained, imaged, and counted. Values are mean ± SEM, n=3. * indicates $p < .05$ and ** $p < .01$ compared to the SFM control (paired t-test).

A brief exposure to trypsin, tryptase, and thrombin potentiates fibrocyte differentiation

Tryptase and thrombin are proteolytically active over short time frames in wounds and in scar tissue (62, 196). To determine if a brief exposure to these proteases is sufficient to potentiate fibrocyte differentiation, we allowed PBMC to adhere to plates and exposed them to tryptase, trypsin, or thrombin for 4 (Figure 18), 12 (Figure 19), or 24 hours (Figure 20), then completely removed the media and added fresh, protease-free media to the PBMC for the rest of the 5 day assay. These conditions approximate the bursts of time proteases would be active in a fibrotic lesion or a healing wound environment.

At each timepoint, tryptase, trypsin, and thrombin were able to potentiate fibrocyte differentiation over a broader range than had been previously established in by exposing PBMC to proteases for 5 days (Figure 9). Similarly, proteases at each timepoint were able to significantly potentiate fibrocyte differentiation in the presence of 2.5 μg/ml SAP or 2.5% (v/v) human serum. These data suggest that even a brief exposure to tryptase, trypsin, or thrombin over biologically relevant concentrations is sufficient to induce fibrocyte differentiation.

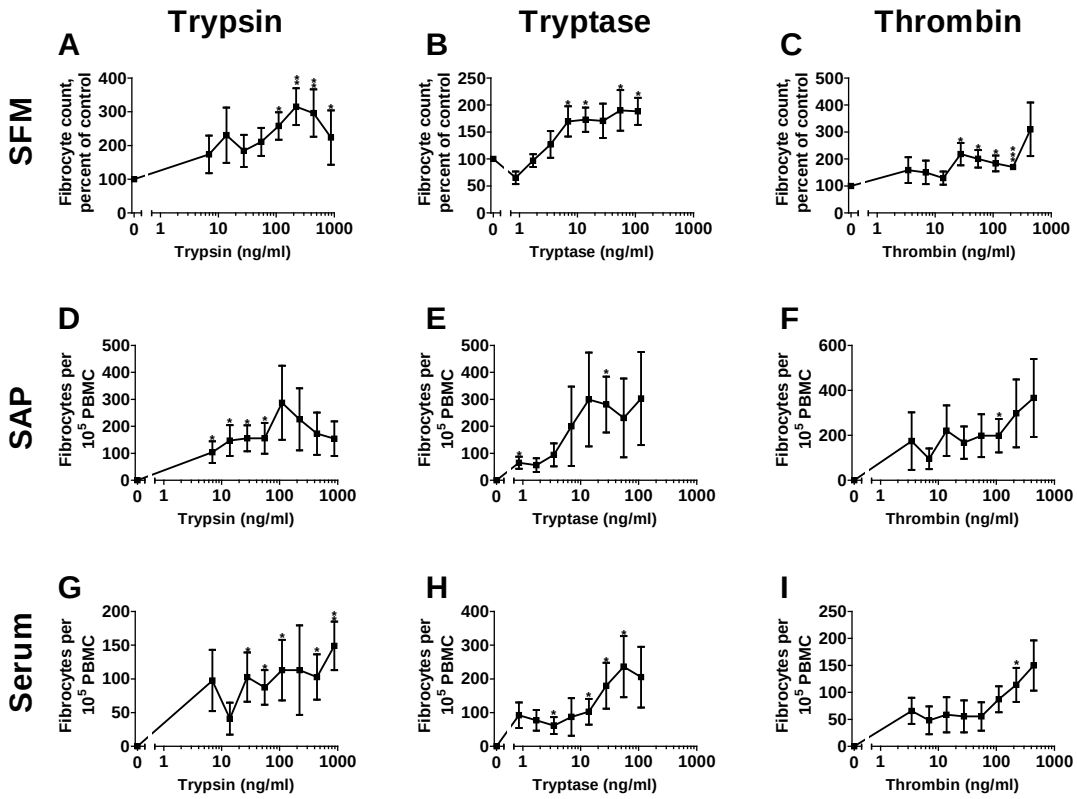

Figure 18. **A 4 hour exposure to tryptase, trypsin, and thrombin potentiates fibrocyte differentiation.**

PBMC were cultured in (A-C) SFM, (D-F) SFM with 2.5 µg/ml SAP, or (G-I) PFM with 2.5% (v/v) human serum in the presence of the indicated concentrations of (A,D,G) trypsin, (B,E,H) tryptase, or (C,F,I) thrombin for 4 hours, after which media was removed and replaced with (A-C) SFM , (D-F) SFM with 2.5 µg/ml SAP, or (G-I) PFM with 2.5% (v/v) human serum. Cells were then allowed to differentiate over the remainder of the five-day assay, and fibrocytes were counted as in Figure 9. Serum-containing and SAP-containing media completely inhibited fibrocyte differentiation in the protease-free control. Values are mean ± SEM, n = 5. * indicates $p < .05$, ** $p < .01$ and *** $p < .001$ compared to the protease-free control (t-test).

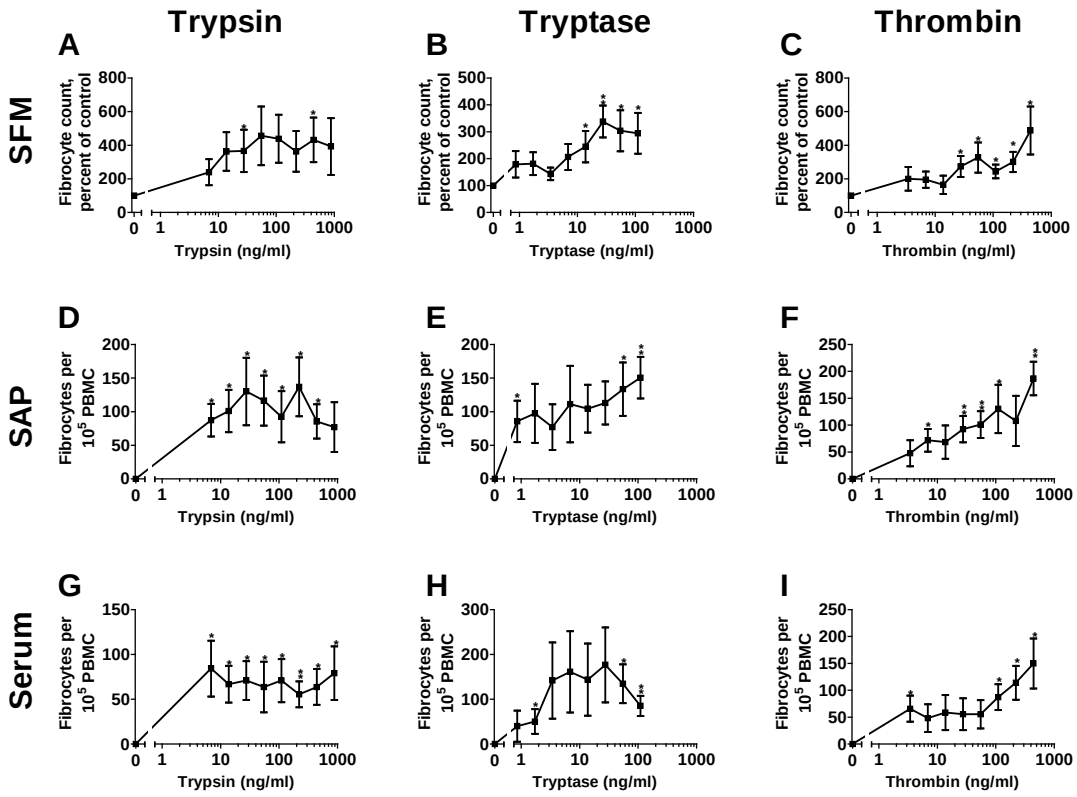

Figure 19. **A 12 hour exposure to tryptase, trypsin, and thrombin potentiates fibrocyte differentiation.**
Cells were incubated as in Figure 18, with the exception that media were changed at 12 hours instead of at 4 hours.

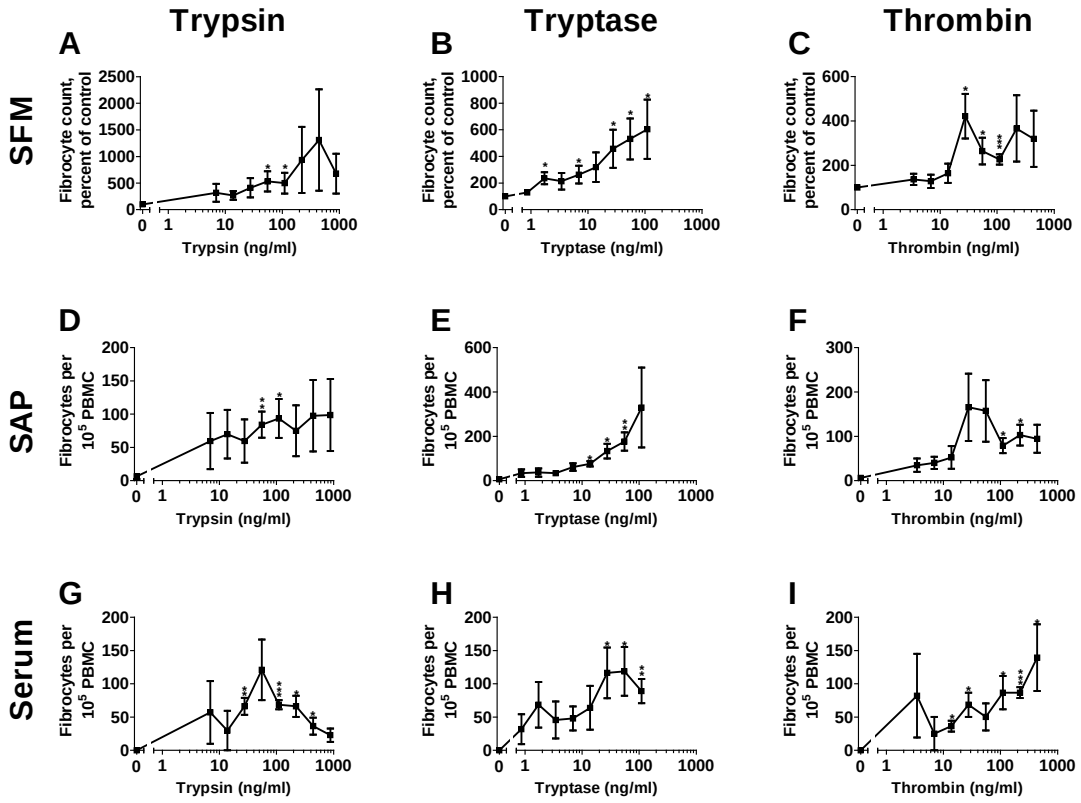

Figure 20. **A 24 hour exposure to tryptase, trypsin, and thrombin potentiates fibrocyte differentiation**.
Cells were incubated as in Figure 18, with the exception that media were changed at 24 hours instead of at 4 hours.

Discussion

In this report, we show that tryptase and thrombin potentiate fibrocyte differentiation and collagen production, and that this potentiation occurs even in the presence of levels of serum or SAP that completely inhibit fibrocyte differentiation. Tryptase and thrombin potentiation appears to act directly on monocytes, and is mediated by PAR-2 and PAR-1, respectively. Tryptase and thrombin potentiate fibrocyte differentiation at biologically relevant concentrations and exposure times. Not all proteases are pro-fibrotic, as pepsin and chymotrypsin do not activate PAR-1 or PAR-2

(212-214), and do not potentiate fibrocyte differentiation (194). These results suggest a triggering mechanism for fibrocyte-mediated wound healing and fibrotic lesions, where thrombin from clotting blood or tryptase from a sufficient amount of mast cell degranulation override SAP inhibition and initiate fibrocyte differentiation.

Tryptase, thrombin, PAR-1 signaling, and PAR-2 signaling have been implicated in the development of fibrosis through their effects on fibroblasts (61, 67, 68, 73, 80, 87-89, 215). Both PAR-1 and -2 have been implicated in liver fibrosis in mice (216, 217), and both PAR-1 knockout mice and PAR-2 knockout mice are less susceptible to both induced heart disease and inflammation (218-220). Intratracheal administration of trypsin, tryptase, and thrombin cause inflammation, and inhibition of tryptase and thrombin attenuate this inflammation (63, 66, 82, 84). Inhibitors of tryptase (221-223) and thrombin (224), and antagonists of both PAR-1 (225) and PAR-2 (226) are patented for the treatment of fibrosis. Both tryptase (227) and thrombin (228) inhibitors are currently in clinical trials for the treatment of fibrosis. However, while PAR-1 and PAR-2 antagonists have been suggested as therapeutics (229, 230), neither is currently in clinical trials. PAR-1 and PAR-2 thus mediate both fibroblast proliferation and fibrocyte differentiation, two major components of scar tissue (195, 231-233). Our work thus strongly supports and expands the idea that tryptase, thrombin, PAR-1 signaling, and PAR-2 signaling potentiate wound healing and fibrosis.

Systemic mastocytosis involves the degranulation of mast cells throughout the body (234), and is associated with serious local, and moderate systemic, fibrosis (235, 236). Mast cell degranulation causes the release of tryptase. Serum tryptase in healthy

patients is ~2 ng/ml, while mastocytosis patients have 20 to 100 ng/ml (237, 238). Our observation that 4 to 56 ng/ml tryptase potentiates fibrocyte differentiation suggests that the fibrosis seen in mastocytosis patients may be due to the released tryptase inducing fibrocyte differentiation.

That tryptase and thrombin compete with SAP suggests that the PAR-1 or PAR-2 pathway is capable of potentiating fibrocyte differentiation in the presence of SAP. Trypsin potentiates fibrocyte differentiation in the presence of SAP after a brief exposure (Figures 18-20), but not over the course of a 5-day differentiation (Figure 15A and 16A). Tryptase and thrombin potentiated fibrocyte differentiation under all timecourse, SAP, and serum conditions. Tryptase and trypsin appear to signal through the same receptor (73). Whether our results imply that different PAR-2 isoforms exist, or that PAR-2 can differentiate between trypsin and tryptase signaling, is unclear.

A protein additive was necessary for fibrocyte potentiation. While albumin mixed with protease was the most effective media treatment for potentiating fibrocyte differentiation, both fish gelatin and milk powder also increased fibrocyte differentiation when mixed with protease. This suggests that the fibrocyte potentiation caused by proteases relies on a suitable protein additive, not solely albumin. Albumin is increased in fibrotic lesions (61) and healing wounds (153), and is decreased in chronic, non-healing wounds (154-156), implying that albumin's presence may mediate the protease signaling that, by activating fibrocyte differentiation, may initiate key aspects of wound healing and fibrosis.

CHAPTER IV

TRYPSIN, TRYPTASE, AND THROMBIN BIAS MACROPHAGE DIFFERENTIATION TOWARDS A PRO-FIBROTIC M2A PHENOTYPE

Summary

For both wound healing and the formation of a fibrotic lesion, circulating monocytes enter the tissue and differentiate into fibroblast-like cells called fibrocytes and pro-fibrotic M2a macrophages, which together with fibroblasts form scar tissue. Monocytes can also differentiate into classically activated M1 macrophages and alternatively activated M2 macrophages. The proteases thrombin, which is activated during blood clotting, and tryptase, which is released by activated mast cells, potentiate fibroblast proliferation and fibrocyte differentiation, but their effect on macrophages is unknown. Here we report that thrombin, tryptase, and the protease trypsin bias macrophage differentiation towards a pro-fibrotic M2a phenotype from unpolarized monocytes, or from M1 and M2 macrophages. These results suggest that proteases can initiate scar tissue formation by affecting fibroblasts, fibrocytes, and macrophages.

Hypothesis: Trypsin, tryptase, and thrombin at physiological concentrations polarize macrophages towards a wound-healing phenotype

Introduction

The failure of wounds to heal properly constitutes a major medical problem, with both acute and chronic wounds consuming treatment time and resources (12, 14). The opposite of poorly healing wounds is fibrosing diseases, where unnecessary and inappropriate scar tissue forms in an organ (19). Fibrosing diseases include pulmonary fibrosis, congestive heart failure, liver cirrhosis, and kidney fibrosis, and are involved in 45% of deaths in the United States (20). A key question in wound healing and fibrosis is the triggering mechanism that induces scar tissue formation.

Extracellular levels of the proteases tryptase and thrombin are upregulated in both fibrotic scars and healing wounds (62, 71). One of the events preceding scar tissue formation in a healing wound is the clotting cascade, in which the protease thrombin cleaves fibrinogen to fibrin. Thrombin activity is upregulated immediately after wounding (62) and in fibrotic lesions (61). Mast cells are found in both internal fibrotic lesions and sites of wound healing (71-73). Mast cells degranulate to release tryptase, and tryptase is upregulated in wounds and fibrotic lung tissue (71-73, 78-80). Tryptase, and thrombin, as well as other proteases such as trypsin, potentiate wound healing and scar tissue formation by increasing fibroblast proliferation and collagen secretion (73, 87-89), inducing platelet aggregation (70), and by potentiating the differentiation of a subset of monocytes into fibroblast-like cells called fibrocytes (194, 239). Thrombin signals through protease-activated receptor-1 (PAR-1), trypsin and tryptase signal through protease-activated receptor-2 (PAR-2) (67, 68, 73, 81), and we found that agonists of PAR-1 and PAR-2 potentiate fibrocyte differentiation (239). Monocytes also differentiate into both

classically-activated M1 macrophages and alternatively-activated M2 macrophages (46). M1 macrophages are associated with pathogen responses, and M2 macrophages are associated with immuno-regulation and tissue restructuring (47, 48). There are at least two subpopulations of M2 macrophages. Mreg macrophages have an anti-inflammatory phenotype, and do not secrete matrix proteins. (46). M2a macrophages are involved in scar tissue formation in both wound healing and fibrosis (49-52). M2a macrophages become more prevalent as wound healing progresses and collagen deposition increases, and directly secrete the matrix protein fibronectin, a major component of scars (240-242). Macrophages are critical to wound healing (243). Removal of macrophages from a mouse wound by depletion or conditional knockout lowers the amount of scar tissue deposited in the wounds (244).

Human M1, M2a, and Mreg macrophages, while morphologically similar, display different surface markers and secrete different cytokines (46). CD163 is a marker of M2 macrophage differentiation that is sometimes classed as an Mreg marker (47, 54). Fibronectin is an unambiguous marker of M2a macrophage differentiation (55). CD206 is sometimes classed as an Mreg marker, and sometimes as an M2a marker (47, 54). CCR7 is a commonly used marker for M1 classical macrophage activation (47). M1 and M2 macrophages also have different secretion profiles, with M1 macrophages secreting higher levels of the cytokine IL-12 compared to M2 macrophages (46). M2 regulatory macrophages secrete increased levels of the anti-inflammatory cytokine IL-10 (46). M2a macrophages secrete intermediate amounts of IL-12 and IL-10, and high amounts of IL-4

(46, 245). Polarized macrophages display a spectrum of markers, and macrophage phenotypes can only be assessed by examining multiple differentiation markers (46).

In this report, we show that trypsin, tryptase and thrombin bias populations of human unpolarized macrophages, M1 macrophages, or M2 regulatory macrophages towards an M2a phenotype, suggesting an additional mechanism whereby mast cells degranulating, and/or blood clotting, releases and/or activates extracellular proteases to induce and/or potentiate wound healing and fibrosis.

Materials and methods

Proteases, PAR agonists, and PAR inhibitors

TPCK-treated bovine trypsin (10,000 BAEE units/mg, Sigma, St. Louis, MO) and human thrombin (1000 NIH units/mg, Sigma) were resuspended following the manufacturer's instructions. Tryptase purified from human mast cells (70 BPVANA units/mg, Fitzgerald, Acton, MA) was mixed with 15 kDa heparin from porcine stomach (Sigma) in a 1:10 molar ratio of tryptase to heparin immediately after thawing (196).

Immunohistochemistry and ELISAs

Human blood was collected from volunteers who gave written consent and with specific approval from the Texas A&M University human subjects Institutional Review Board. PBMC were isolated and cultured as previously described (53) to bias macrophage differentiation towards M1 and M2 phenotypes, with the following modifications. PBMC were cultured with 25 ng/ml MCSF or GMCSF for one week in 10% serum, as previously

described (53), after which the cells were treated with 12.5 ng/ml trypsin, tryptase, or thrombin for two days. Cells were fixed and stained for CCR7 (mouse monoclonal clone 150503, R&D systems, Minneapolis, MN), CD163 (mouse monoclonal clone GH1/61, Biolegend, San Diego, CA), CD206 (mouse monoclonal clone 15-2, Biolegend), and fibronectin (rabbit polyclonal, Sigma), as previously described (195). Fibrocytes and macrophages were counted based on their morphology, as previously described (36). For each donor and each stain, at least 200 macrophages and at least 100 fibrocytes were scored. Conditioned media from PBMC cultured in SFM with or without 12.5 ng/ml protease were analyzed for IL-10, IL-12, and IL-4 using a human IL-12 ELISA kit (Peprotech, Rocky Hill, NJ), a human IL-10 ELISA kit (Biolegend), and a human IL-4 ELISA kit (Peprotech, Rocky Hill, NJ), following the manufacturer's instructions.

Staining intensity measurements

Images of cells were obtained with a Nikon D1X SLR camera (Nikon, Tokyo, Japan) or a 10 MP USB camera (OMAX, Kent, WA) imager on a Nikon diaphot inverted tissue culture microscope (Nikon) with a 10x lens. The image analysis program CellProfiler (200) was used to identify cells in the images as either macrophages or fibrocytes (based on their elongated shape), and measure the relative mean staining intensity of each cell. For each donor and each stain, at least 5 fields of view, comprising about ~200 cells, were analyzed. The CellProfiler pipeline is in the supplemental methods section.

Statistics

Statistics were performed using Prism (Graphpad Software, San Diego, CA). Differences were assessed by two-tailed unpaired and two-tailed paired t-tests, where indicated. Significance was defined by $p<0.05$.

Results

Trypsin, tryptase, and thrombin potentiate the differentiation of monocytes into M2a macrophages

To determine if trypsin, tryptase, or thrombin influence the differentiation of monocytes into macrophages, we co-incubated PBMC and proteases for five days, and examined the expression of CCR7, CD163, CD206 and fibronectin on the macrophages. We used physiological concentrations of proteases that we previously observed to potentiate fibrocyte differentiation (17, 42). CCR7 is a marker for M1 macrophage activation (23). No protease increased CCR7 staining (Figures 1A and S1A). CD163 and CD206 are markers of Mreg and M2a macrophages (23, 34). Tryptase and thrombin increased the percentage of CD163-positive macrophages, and all three proteases increased the percentage of CD206-positive macrophages (Figures 21A, 22B, and 22C). Fibronectin is a marker of M2a macrophage differentiation (35). Each protease significantly increased the percentage of fibronectin-positive macrophages (Figures 21A and 22D). In these assays, each protease also increased the percentage of fibrocytes expressing CD206 (Figures 21B and 22C) and tryptase and thrombin increased the percentage of fibrocytes expressing fibronectin.

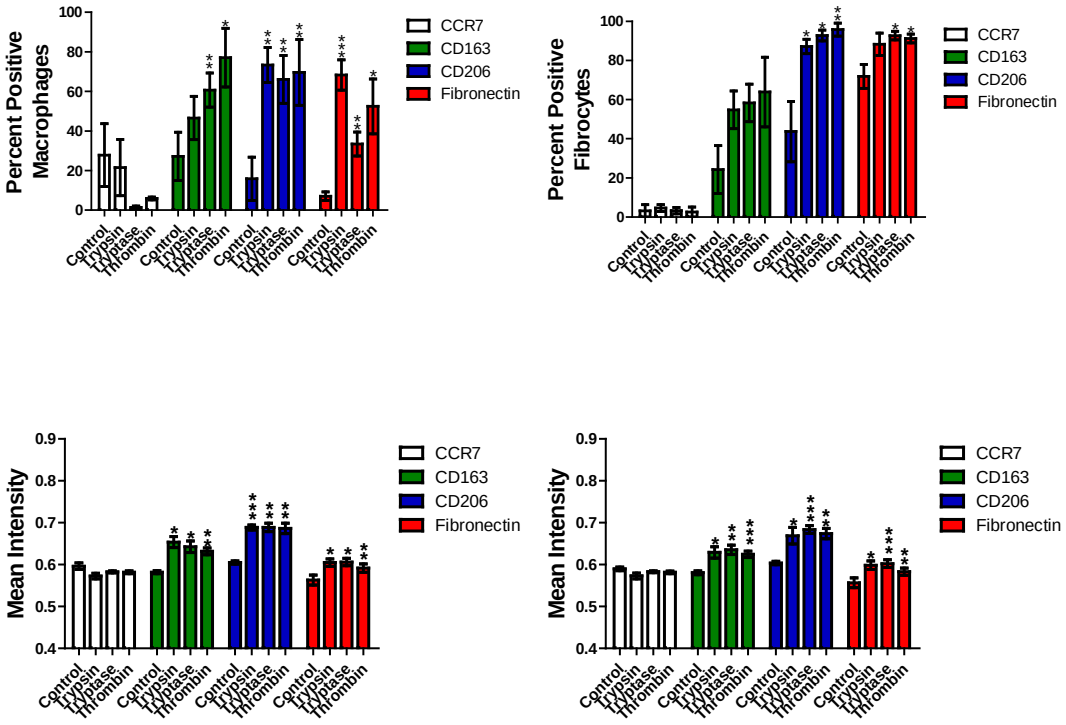

Figure 21. **Trypsin, tryptase, and thrombin bias monocyte differentiation towards an M2a phenotype.**

PBMC were cultured in serum-free media in the presence or absence of trypsin, tryptase, or thrombin. Macrophages (A, C) and fibrocytes (B, D) were counted by morphology from representative fields of view. (A) and (B) were performed by eye, while (C) and (D) show analysis of staining intensity. Cells were stained for the indicated markers. Values are mean ± SEM, n=6. * indicates $p < .05$, ** $p < .01$, and *** $p < .001$ compared to the no-protease control (paired two-tailed t-tests).

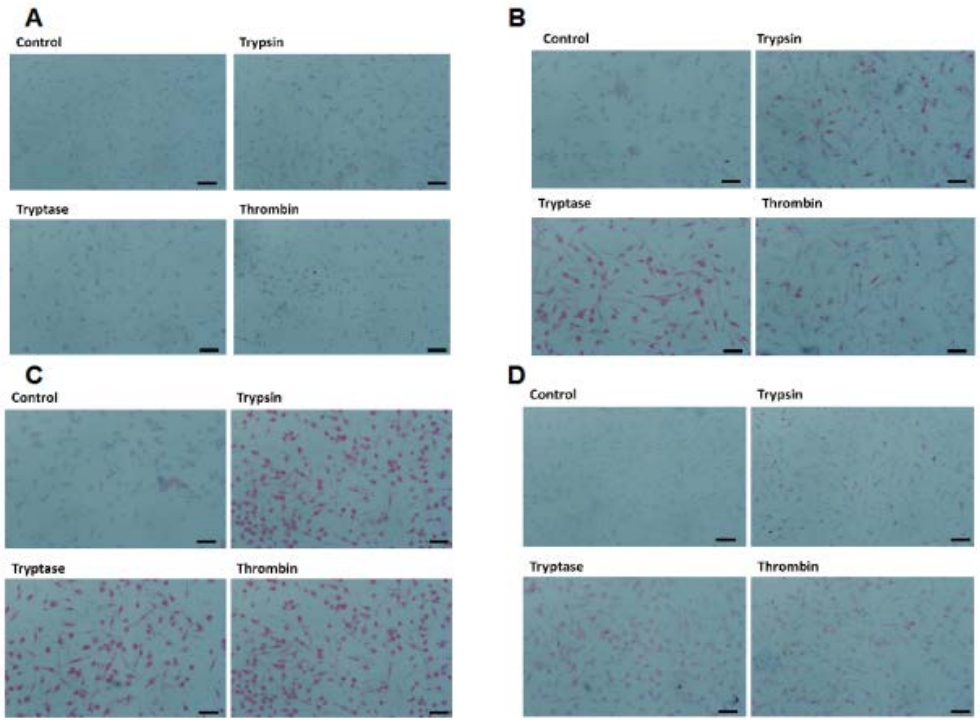

Figure 22. **Images of PBMC cultured with proteases.**
Panels show representative images from slides used for Figure 21, staining for (A) CCR7, (B) CD163, (C) CD206, and (D) fibronectin. Bars are 50 µm.

To determine if protease treatment changed the staining intensity of the macrophage marker immunohistochemistry, stained slides were further analyzed by image analysis that identified cells as macrophages, fibrocytes, or other cells and then measured the mean staining intensity of each cell (Figure 23). As expected, the image analysis indicated that the proteases increased the number of fibrocytes (Figure 24). Trypsin, tryptase, and thrombin did not increase the staining intensity of CCR7, and increased the mean staining intensity of CD163, CD206, and fibronectin on both macrophages and fibrocytes (Figures 21C and D). Together, the data indicate that as determined by staining for M1, M2, and M2a markers, the proteases biased monocyte differentiation towards an M2a phenotype.

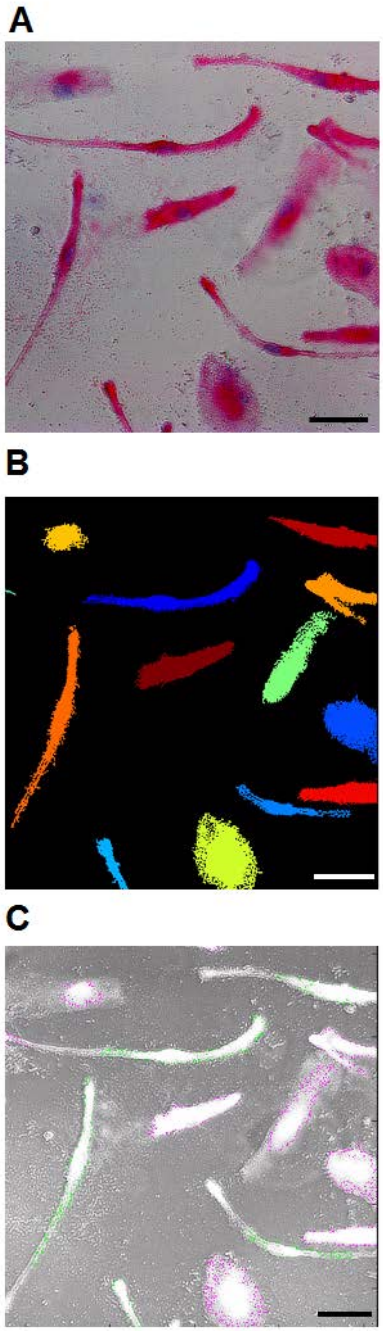

Figure 23. **CellProfiler analysis of PBMC images.**
CellProfiler's pipeline is capable of distinguishing individual cells, separating these cells into macrophages and fibrocytes based on morphology, and recording the intensity of the staining for these cells. (A) A representative image analyzed by CellProfiler. (B) CellProfiler's detected cells. (C) CellProfiler's detected fibrocytes in green, and macrophages in red. Bar is 50 µm.

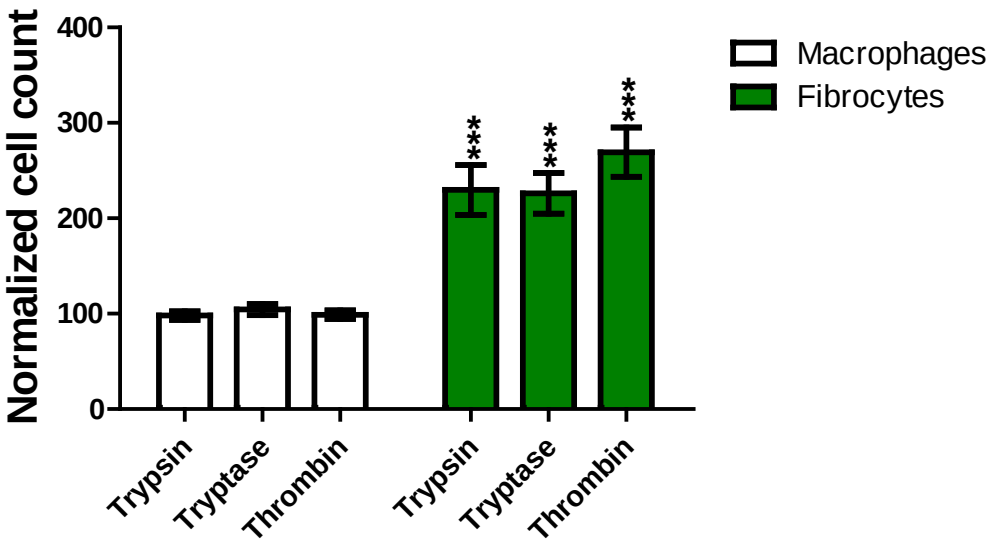

Figure 24. **Proteases increase fibrocyte numbers when added to PBMC.**
Cellprofiler counts of fibrocytes and macrophages from slides used for Figure 21 were normalized as a percent of controls. Values are mean ± SEM, n=6. *** $p < .001$ compared to the no-protease control (paired two-tailed t-tests).

To determine if proteases also affect extracellular cytokine accumulation by cultured macrophages, conditioned media from human PBMC cultured for five days with 12.5 ng/ml of trypsin, tryptase, or thrombin was assayed by ELISA for IL-4, IL-10, and IL-12. Trypsin, but not tryptase or thrombin, cleaves IL-4, IL-10, and IL-12 (ExPASy peptide cutter). Compared to conditioned media from untreated control cells, tryptase increased IL-4 accumulation in PBMC conditioned media (Figure 25A). Thrombin increased both IL-10 and IL-12 (Figure 25B and C). The data thus suggest that tryptase biases monocytes towards an M2a phenotype (high IL-4, moderate IL-10 and IL-12), while thrombin increased both IL-10 and IL-12 in the conditioned media.

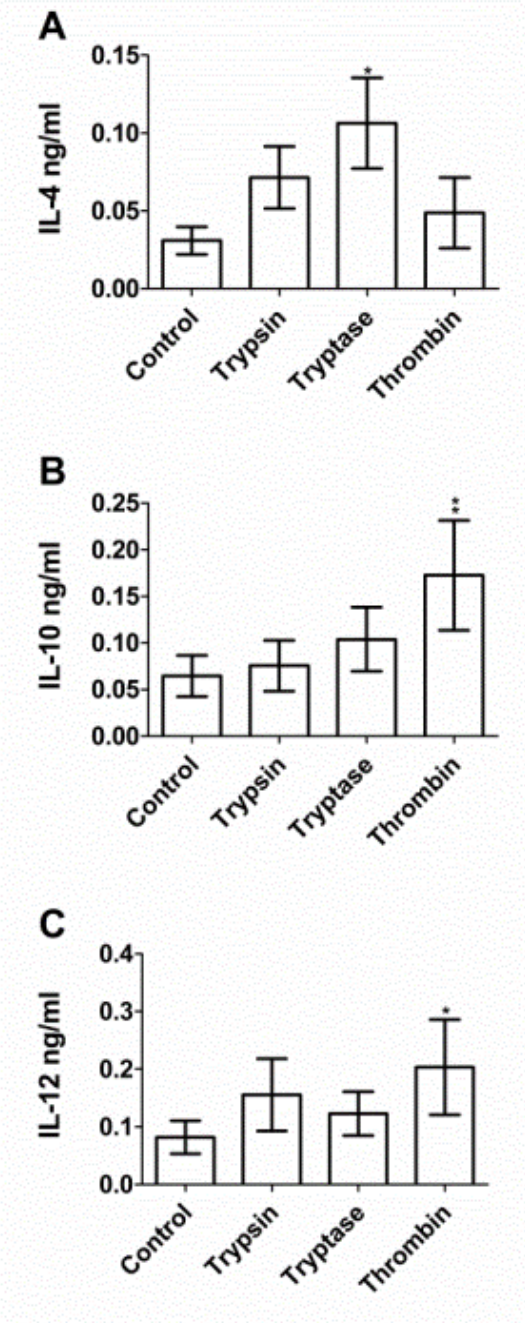

Figure 25. **The effect of proteases on extracellular cytokine accumulation from monocytes.**

PBMC were cultured as in Figure 21, and after 5 days conditioned media were analyzed by ELISA for (A) IL-4, (B) IL-10, and (C) IL-12. Values are mean ± SEM, n=20. * indicates $p < .05$ and ** $p < .01$ compared to the no-protease control (paired two-tailed t-tests).

Trypsin, tryptase, and thrombin potentiate the differentiation of M2 macrophages into M2a macrophages

M2a macrophages can differentiate not only from unpolarized monocytes, but also from other macrophage subsets (247). M2 macrophages are associated with decreased inflammation and increased tissue repair (48, 52). To determine if proteases can potentiate the differentiation of M2a macrophages from M2 macrophages, we biased unpolarized monocytes towards M2 phenotypes, as previously described (53), after which we added proteases to the macrophage population for two days, and stained for macrophage markers. Trypsin, tryptase, and thrombin had no significant effect on the percentage of macrophages staining for the M1 marker CCR7 or the M2 marker CD163, both tryptase and thrombin significantly increased the percentage of CD206-positive macrophages, and all three proteases increased the percentage of fibronectin-positive macrophages (Figures 26A and 27). In this assay, tryptase increased the percentage of fibrocytes that were positive for CD206, and trypsin, tryptase, and thrombin increased the percentage of fibrocytes that were positive for fibronectin (Figures 26B and 27). All three proteases had no significant effect on CCR7 staining intensity, increased the staining intensity of CD163 on macrophages, and tryptase and thrombin increased the staining intensities of CD206 and fibronectin on macrophages (Figure 26C). CellProfiler also detected that the proteases increased the number of fibrocytes when added to the M2-biased PBMC population (Figure 28). All three proteases increased the staining intensity of CD163 on fibrocytes, thrombin increased the CD206 staining intensity, and tryptase and thrombin increased the fibronectin staining intensity (Figure 26D). Together, the data indicate that as determined

by staining for M1, M2, and M2a markers, the proteases biased M2 macrophage polarization towards an M2a phenotype.

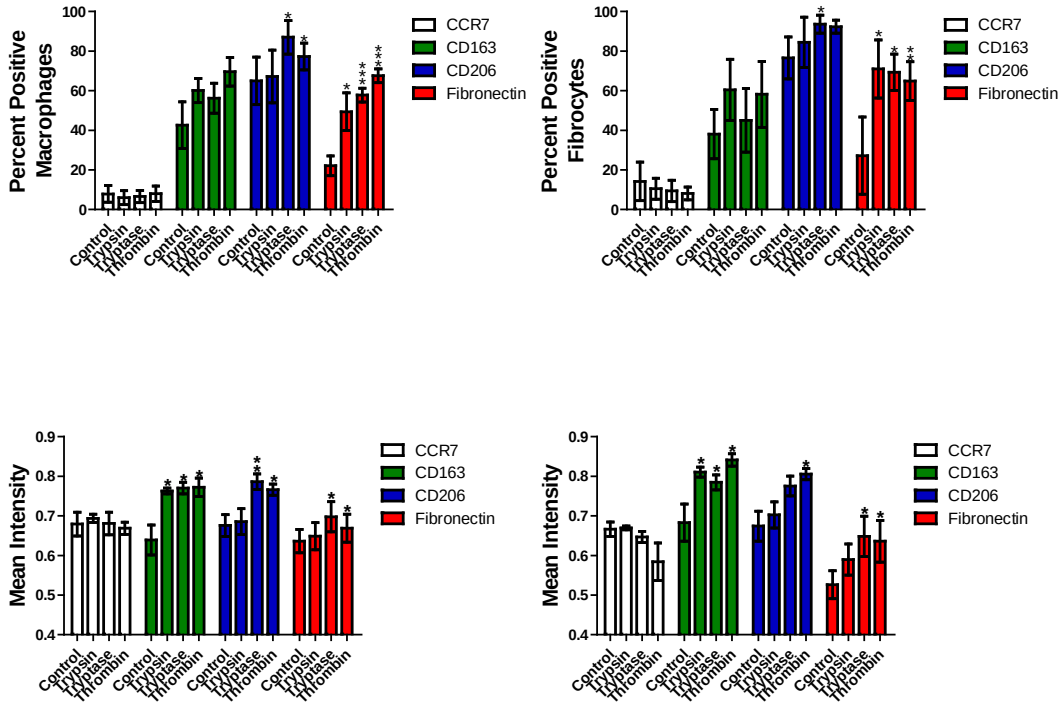

Figure 26. **Trypsin, tryptase, and thrombin bias M2 macrophage differentiation towards an M2a phenotype.**
PBMC were cultured with MCSF for 7 days to generate M2 macrophages, after which the media was removed and proteases were added to the PBMC for 2 days. Macrophages (A, C) and fibrocytes (B, D) were counted by morphology from representative fields of view. (A) and (B) were performed by eye, while (C) and (D) show analysis of staining intensity. Cells were stained for the indicated markers. Values are mean ± SEM, n=6. * indicates $p < .05$, ** $p < .01$, and *** $p < .001$ compared to the no-protease control (paired two-tailed t-tests).

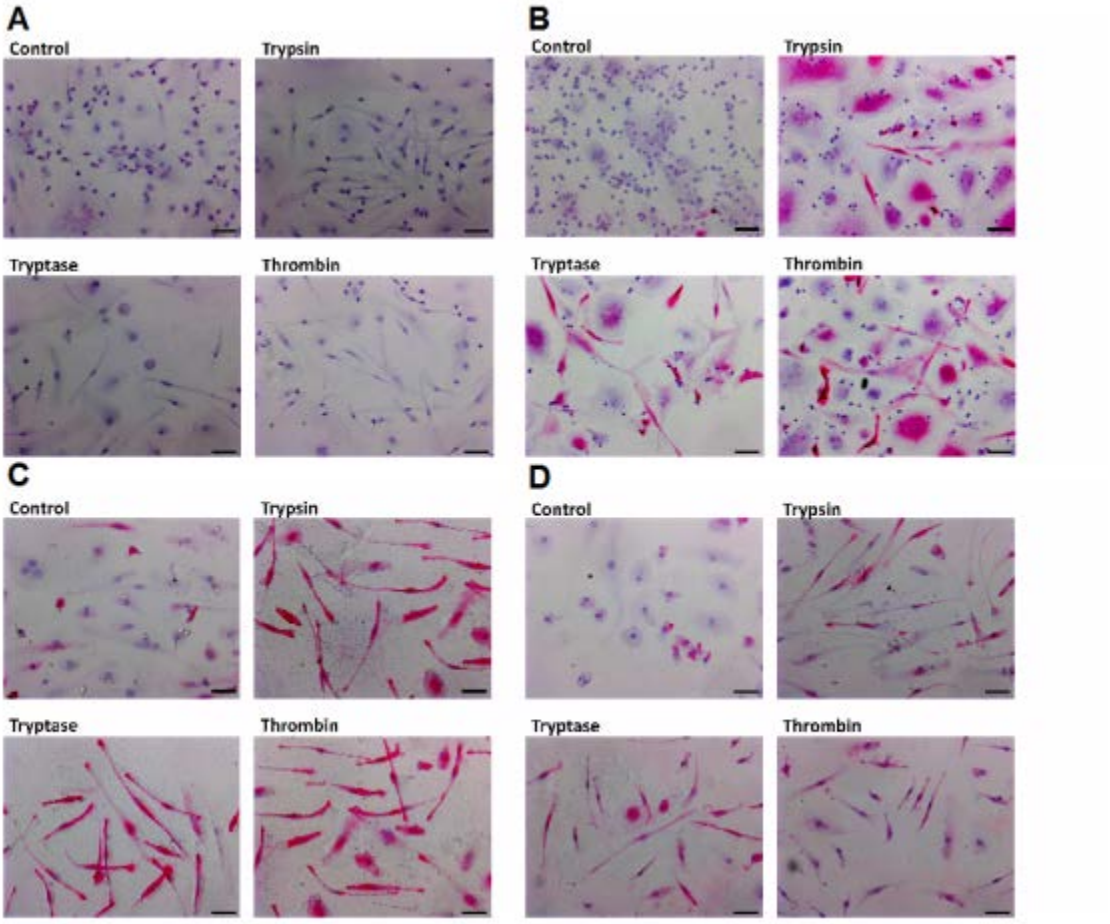

Figure 27. Images of cultures containing M2-biased macrophages subsequently cultured with proteases.

Panels show representative images from slides used for Figure 26, staining for (A) CCR7, (B) CD163, (C) CD206, and (D) fibronectin. Bars are 50 µm.

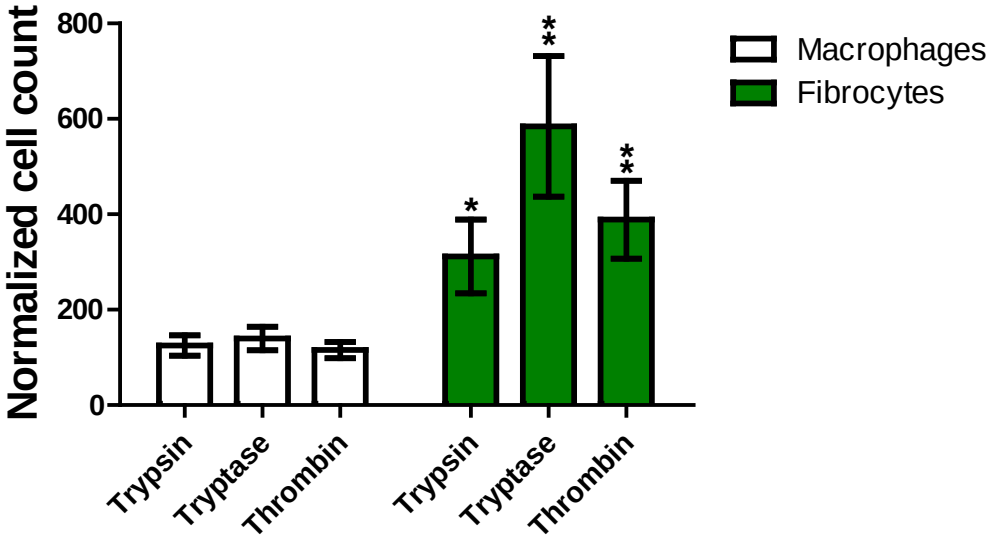

Figure 28. Proteases increase fibrocyte numbers when added to cultures containing M2-biased macrophages.
Cellprofiler counts of fibrocytes and macrophages from slides used for Figure 26 were normalized as a percent of controls. Values are mean ± SEM, n=6. * indicates $p < .05$ and ** $p < .01$ compared to the no-protease control (paired two-tailed t-tests).

To determine if proteases also affect extracellular cytokine accumulation by cultured M2 macrophages, conditioned media from M2 macrophages cultured for two days with trypsin, tryptase, or thrombin was assayed by ELISA for IL-4, IL-10, and IL-12. Thrombin increased IL-4 accumulation (Figure 29A). Trypsin and tryptase decreased IL-10 (Figure 29B). No protease significantly altered IL-12 concentrations (Figure 29C). The data thus suggest that the proteases may bias M2 macrophages towards an M2a phenotype by either decreasing the concentration of the anti-inflammatory cytokine IL-10 or increasing the concentration of the pro-fibrotic cytokine IL-4.

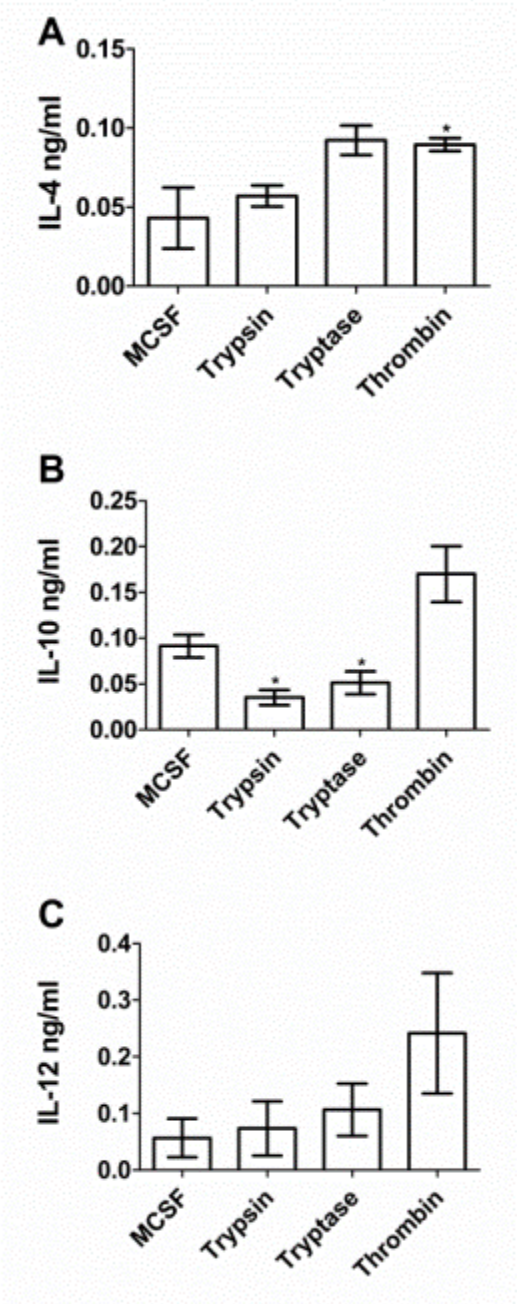

Figure 29. **The effect of proteases on extracellular cytokine accumulation from cultures containing M2-biased macrophages.**
PBMC were cultured as in Figure 26, and after 2 days of protease treatment, conditioned media were analyzed by ELISA for (A) IL-4, (B) IL-10, and (C) IL-12. Values are mean ± SEM, n=6. * indicates $p < .05$ compared to the no-protease control (paired two-tailed t-tests).

Trypsin, tryptase, and thrombin potentiate the differentiation of M1 macrophages into M2a macrophages

M1 macrophages are associated with inflammatory immune responses to pathogens like bacteria and viruses (47). To determine if proteases could bias M1 macrophages towards an M2a phenotype, we biased monocytes towards an M1 phenotype (53), after which we added proteases to the macrophage population for two days, and stained for macrophage markers. None of the proteases significantly affected CCR7 or CD163 staining, but all three increased the percentage of macrophages staining for CD206 and fibronectin, and all three increased fibronectin intensity staining on macrophages (Figures 30A, 30C, and 31). CellProfiler also detected that the proteases increased the number of fibrocytes when added to the M1-biased PBMC population (Figure 32). Each protease increased CD206 and fibronectin staining on fibrocytes, and each protease increased fibronectin intensity staining on fibrocytes (Figures 30B, 30D, and 31). Together, the data indicate that as determined by staining for M1, M2, and M2a markers, the proteases biased M1 macrophage polarization towards an M2a phenotype.

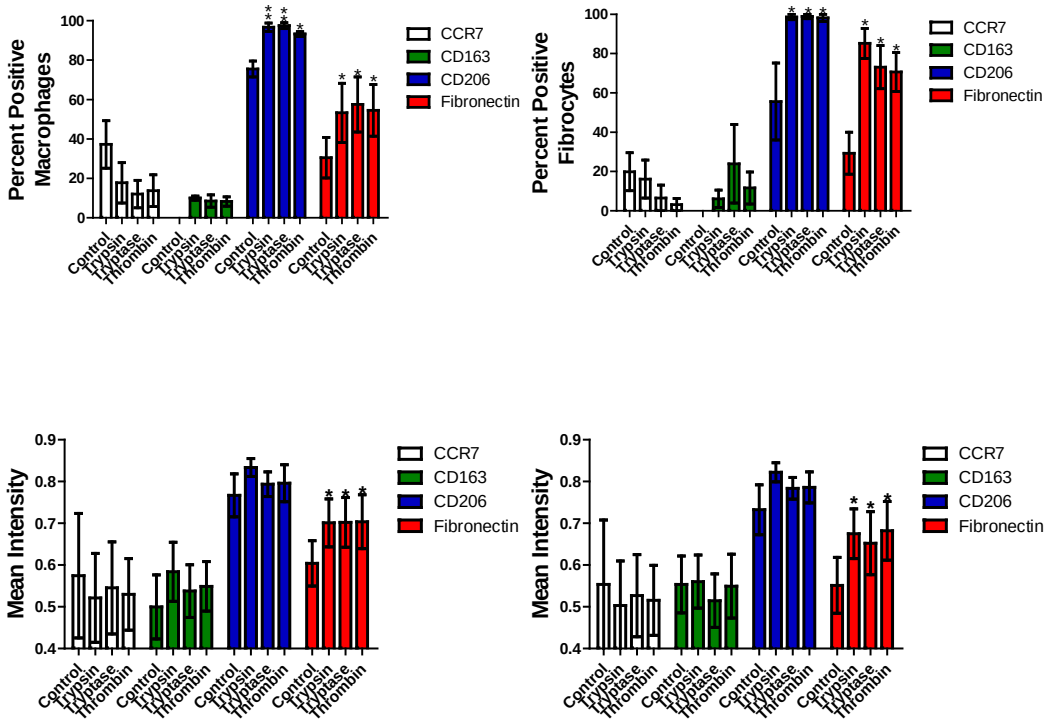

Figure 30. **Trypsin, tryptase, and thrombin bias M1 macrophage differentiation towards an M2a phenotype.**

PBMC were cultured with GMCSF for 7 days to generate M2 macrophages, after which the media was removed and proteases were added to the PBMC for 2 days. Macrophages (A, C) and fibrocytes (B, D) were counted by morphology from representative fields of view. (A) and (B) were performed by eye, while (C) and (D) show analysis of staining intensity. Cells were stained for the indicated markers. Values are mean ± SEM, n=6. * indicates $p < .05$ and ** $p < .01$, compared to the no-protease control (paired two-tailed t-tests).

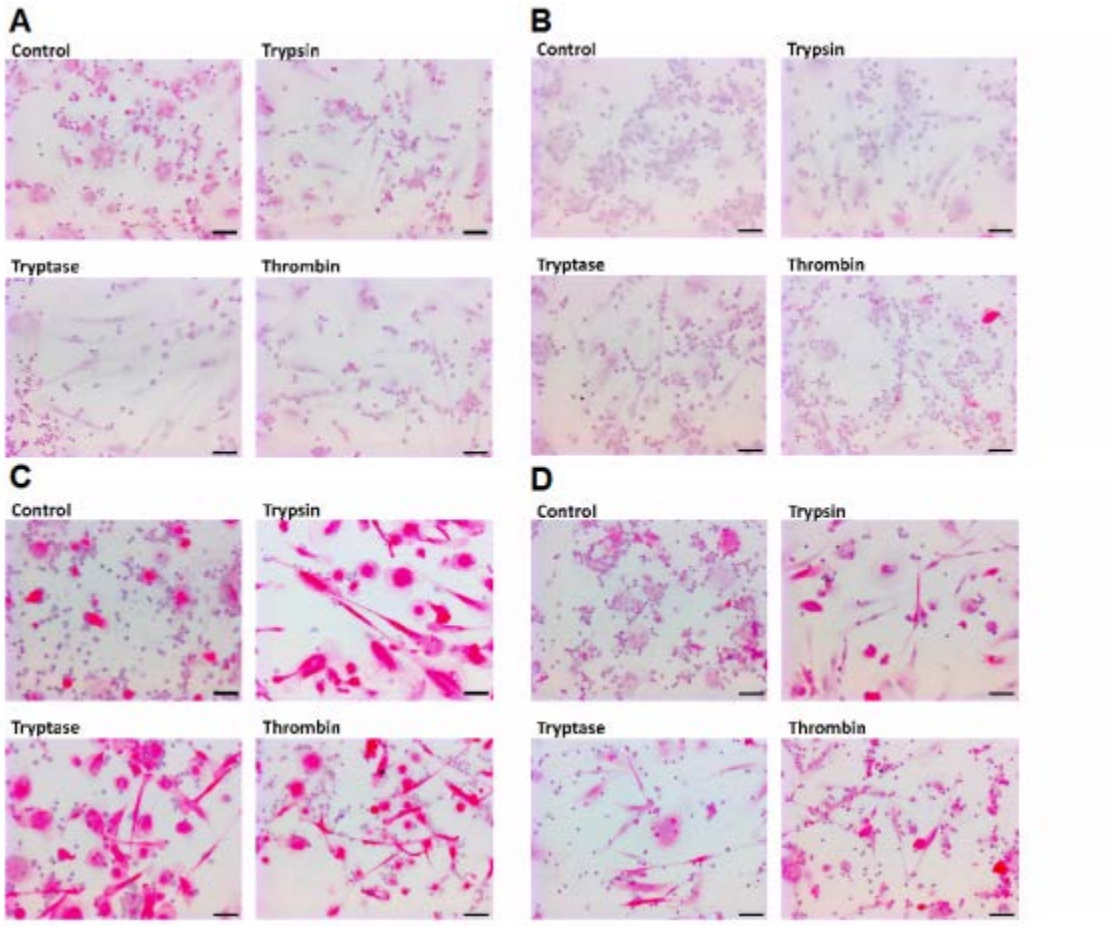

Figure 31. **Images of cultures containing M1-biased macrophages subsequently cultured with proteases.**
Panels show representative images from slides used for Figure 30, staining for (A) CCR7, (B) CD163, (C) CD206, and (D) fibronectin. Bars are 50 µm.

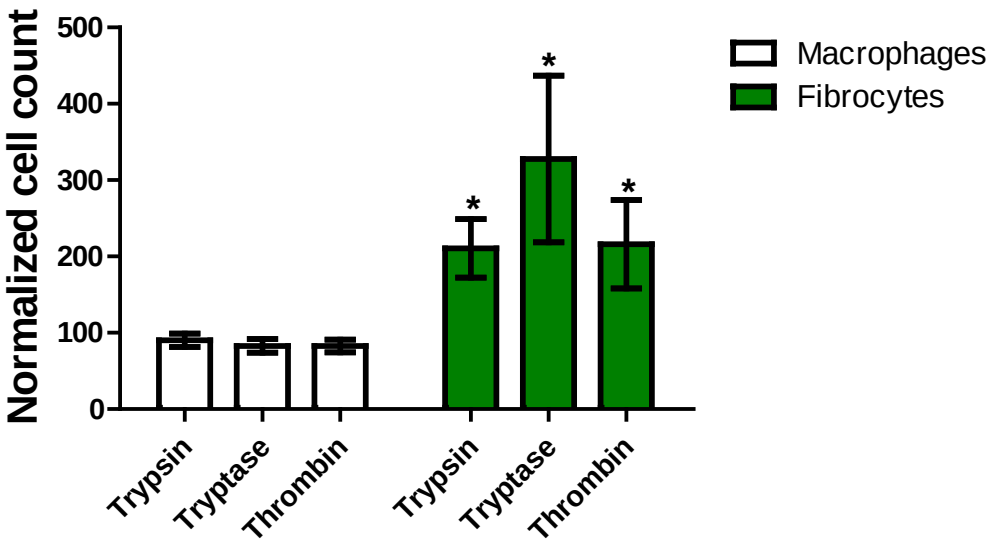

Figure 32. **Proteases increase fibrocyte numbers when added to cultures containing M1-biased macrophages.**
Cellprofiler counts of fibrocytes and macrophages from slides used for Figure 30 were normalized as a percent of controls. Values are mean ± SEM, n=6. * indicates $p < .05$ compared to the no-protease control (paired two-tailed t-tests).

To determine if proteases also affect extracellular cytokine accumulation by cultured M1 macrophages, conditioned media from human M1 macrophages cultured for two days with trypsin, tryptase, or thrombin was assayed by ELISA for IL-4, IL-10, and IL-12. Tryptase increased IL-4 accumulation (Figure 33A), no protease significantly affected IL-10, and all three proteases decreased IL-12 (Figure 33C). The data thus indicate that as determined by cytokine accumulation, tryptase polarizes M1 macrophages towards an M2a phenotype.

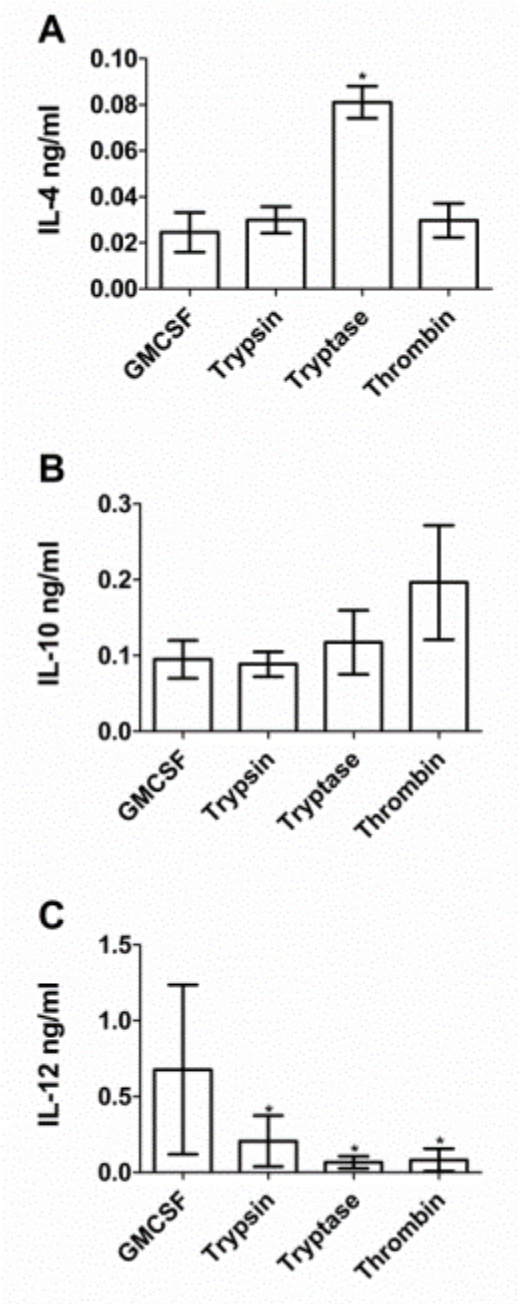

Figure 33. **The effect of proteases on extracellular cytokine accumulation from cultures containing M1-biased macrophages.**
PBMC were cultured as in Figure 30, and after 2 days of protease treatment, conditioned media were analyzed by ELISA for (A) IL-4, (B) IL-10, and (C) IL-12. Values are mean ± SEM, n=6. * indicates $p < .05$ compared to the no-protease control (paired two-tailed t-tests).

Discussion

In this report we show that physiological levels of trypsin, tryptase, and thrombin, in addition to acting as pro-fibrotic signals to fibrocytes (18) and fibroblasts (9, 13-15), appear act as pro-fibrotic signals to macrophages, altering macrophage surface marker expression and the secretion profile towards an M2a phenotype. M2a macrophages are involved in scar tissue formation (25-28).Trypsin, tryptase, and thrombin increased fibronectin staining of macrophages differentiated from monocytes, M1 macrophages, or M2 macrophages. Tryptase increased the extracellular IL-4 accumulation in cultures of both monocytes and M1 macrophages, while trypsin and tryptase lowered both IL-10 and IL-12 accumulation in cultures of M1 and M2 macrophages, respectively.

Physiological levels of tryptase and thrombin (18) bias macrophages and monocytes towards an M2a phenotype suggests that mast cell degranulation or thrombin activation act to polarize M2a macrophages in both wounds or fibrotic lesions. Physiological levels of tryptase and thrombin also potentiate fibrocyte differentiation (18) and increase fibroblast-mediated collagen deposition (9, 13-15). Thus tryptase and thrombin are pro-fibrotic signals to each of fibrocytes, fibroblasts, and macrophages, comprising the vast majority of cells in a scar (25-28, 46, 47).

M2a macrophages secrete increased IL-4. IL-4 potentiates fibrocyte differentiation (48) and collagen secretion by fibroblasts (49). Trypsin, tryptase, and thrombin are directly pro-fibrotic in their signaling to monocyte, macrophages, and fibroblasts, and are indirectly pro-fibrotic by increasing the amount of IL-4 in wounds and fibrotic lesions. To our knowledge, there is no information to suggest IL-4 promotes thrombin activation or

mast cell degranulation, indicating that trypsin, tryptase, thrombin and IL-4 do not constitute a pro-fibrotic vicious cycle.

Mast cell degranulation lowers the number of M2 macrophages in the local environment without increasing CD163 staining, exactly as we observe (50). Activated platelets, which are present during the clotting cascade, and thrombin itself increase IL-10 secretion and decrease IL-12 secretion from macrophages (51, 52). However, fibrin, which also is present during clotting, increases M1 macrophage differentiation, as measured by macrophage inflammatory chemokines (53). While these findings appear contradictory, there is general agreement that macrophages progress from pro-inflammatory (M1) to anti-inflammatory and remodeling (M2 and M2a) phenotypes during wound healing, so macrophage polarization in a wound depends on an interplay of factors, of which thrombin is only one signal (54-56). While thrombin is active early in wound healing, mast cells appear more active in the later stages of wound healing (57), and could provide an additional signal to polarize macrophages to an M2a phenotype as the wound nears resolution.

Here we present data that physiological concentrations proteases bias macrophage differentiation towards an M2a phenotype, further implicating proteases in the development of fibrosis (18). Our results expand protease's pro-fibrotic signaling from fibroblasts and fibrocytes to include macrophages present in scar tissue.

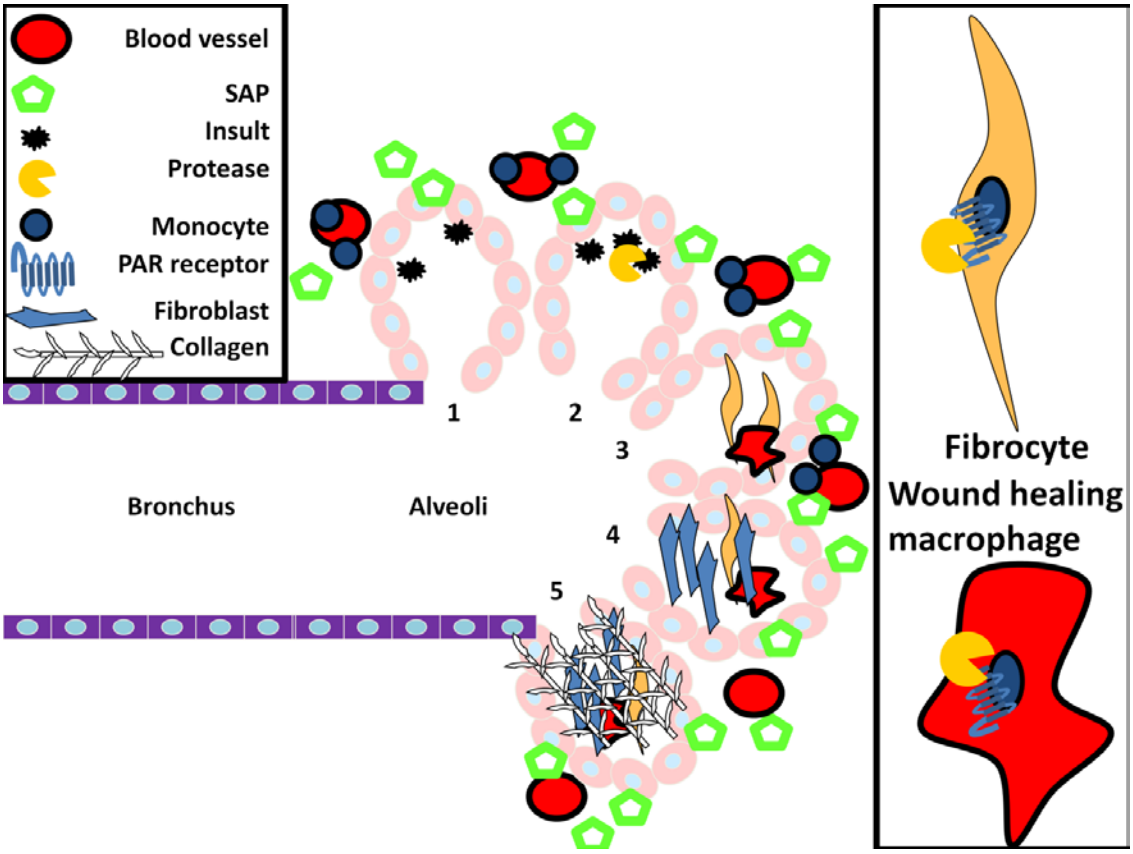

Model 1. Model for protease-induced fibrosis.
This model indicates a progression of pulmonary fibrosis based on the data presented in chapters 2-4 of this thesis. (1) Indicates an alveoli that has suffered an environmental insult, causing inflammation. (2) Indicates the presence of proteases within this inflammation. (3) Indicates the presence of fibrocytes and wound-healing m2a macrophages within the alveoli. These fibrocytes and macrophages have differentiated from the blood monocytes from the capillary near the lung, in the presence of both proteases and SAP. (4) Fibrocytes and wound-healing macrophages induce fibroblast proliferation. (5) Fibrocytes, fibroblasts, and macrophages together secrete collagen and begin to form fibrosis.

CHAPTER V

GALECTIN-3 BINDING PROTEIN SECRETED BY BREAST CANCER CELLS INHIBITS FIBROCYTE DIFFERENTIATION

Summary

To metastasize, tumor cells often need to migrate through a layer of collagen-containing scar tissue which encapsulates the tumor. A key component of scar tissue and fibrosing diseases is the fibrocyte, a monocyte-derived, collagen-secreting pro-fibrotic cell. To test the hypothesis that invasive tumor cells may block the formation of the fibrous sheath, we determined if tumor cells secrete factors that inhibit fibrocyte differentiation. We found that the human metastatic breast cancer cell line MDA-MB 231 secretes a factor that inhibits human fibrocyte differentiation, while less aggressive breast cancer cell lines secrete less of this activity. Purification indicated that Galectin-3 Binding Protein (LGALS3BP) is the active factor. Recombinant LGALS3BP inhibits fibrocyte differentiation, and immunodepletion of LGALS3BP from MDA-MB 231 conditioned media removes the fibrocyte differentiation-inhibiting activity. LGALS3BP inhibits the differentiation of fibrocytes from wild-type mouse spleen cells , but not from SIGN-R1$^{-/-}$ mouse cells, suggesting that CD209/SIGN-R1 is required for the LGALS3BP effect. Galectin-3 and galectin-1, binding partners of LGALS3BP, potentiate fibrocyte differentiation. In breast cancer biopsies, increased levels of tumor cell-associated LGALS3BP were observed in regions of the tumor that were invading the surrounding

stroma. These findings suggest LGALS3BP and galectin-3 as new targets to treat metastatic cancer and fibrosing diseases.

Hypothesis: Types of metastatic cancer secrete anti-fibrotic activity, and conditioned media from these cell lines will inhibit monocyte to fibrocyte differentiation

Introduction

A key component of scar tissue is the fibrocyte, a collagen-producing monocyte-derived cell found in healing wounds and fibrotic lesions. Monocytes are recruited to wounds or fibrotic lesions by chemokines (25, 26), and in response to wound signals such as tryptase released from mast cells, or thrombin activated during blood clotting, differentiate into fibrocytes (27, 28, 239). Monocytes isolated from peripheral blood mononuclear cells differentiate *in vitro* in a defined media into fibrocytes (33). Fibrocytes express collagen and other extracellular matrix proteins, secrete pro-angiogenic factors, and activate nearby fibroblasts to proliferate and secrete collagen (22, 23, 27, 29, 30). Increased fibrocyte differentiation correlates with increased fibrosis in animal models (32, 41). Elevated fibrocyte counts also associate with poor prognosis in human diseases (248).

In response to a foreign object or inflammatory environment, the immune system can initiate a desmoplastic response in which monocytes differentiate into fibrocytes to form a sheath of fibrotic tissue around the foreign object (74-77). In response to some tumors, the immune system also initiates a desmoplastic response, attempting to contain the tumor (4, 9). This desmoplastic sheath is a dynamic, responsive tissue that adjusts to changing conditions in the tumor microenvironment (5, 6).

To metastasize through this desmoplastic tissue, cancer cells must find a way to remove scar tissue or to prevent scar tissue from forming (5-8, 10, 11). As cancer progresses towards metastasis and a more mesenchymal phenotype, it interacts with the immune system in different ways. Some tumors attempt to evade the immune system, and others act to suppress the immune system (98-102).

The MDA-MB-231 cell line was isolated from metastases of a breast cancer patient (103). MDA-MB-231 cells behave aggressively in culture and murine models, displaying a metastatic phenotype that suggests that these cells retain the protein expression profile which allowed them to metastasize through the basement membrane of the original patient (104).

Galectin-3 binding protein (LGALS3BP), previously called Mac-2 binding protein and tumor-associated antigen 90K, is a heavily glycosylated 90 kDa protein (127). LGALS3BP binds to galectins 1, 3, and 7, fibronectin, and collagen IV, V, and VI (127-129). LGALS3BP is a member of the scavenger receptor cysteine-rich domain (SRCR) family of proteins (130). LGALS3BP is ubiquitously expressed in bodily secretions, including milk, tears, semen, and serum, usually 10 µg/ml (131). In patients with aggressive hormone-regulated cancers, including breast cancer, serum LGALS3BP concentration can be an order of magnitude higher than in normal serum (132, 136, 137). In breast milk, LGALS3BP concentration can rise and fall over the same range (approximately 10 µg/ml to 100 µg/ml) depending on the length of time after the pregnancy (131). LGALS3BP is produced mostly by epithelial cells in glands (breast and tear ducts) and cancer cells (especially breast cancer cells) (249).

Higher levels of serum LGALS3BP correlate with worse outcomes in breast cancer patients (136-139), while higher levels of LGALS3BP's binding partner galectin-3 correlate with better outcomes for breast cancer patients (140). LGALS3BP promotes angiogenesis by increasing VEGF signaling and directly signaling endothelial cells (128, 141). Mouse knockouts of LGALS3BP show higher circulating levels of TNF-alpha, IL-

12, and interferon-gamma, suggesting a role of LGALS3BP in regulating the immune system (142).

Galectin-3 is a ~30 kDa protein expressed nearly ubiquitously in human tissues, and can be secreted from cells, associated with membrane bound carbohydrates, or located in the cytoplasm (140, 147-150). Galectin-3 is a biomarker of fibrosing diseases such as heart disease and pulmonary fibrosis (143, 144). As the disease severity increases, serum galectin-3 concentrations increase. Galectin-3 is widely expressed by immune system cells, and promotes the differentiation of monocytes into macrophages (145). Galectin-3 interacts with a number of intercellular and intracellular receptors and ligands, and is theorized to have roles in inflammation, host response to a virus, and wound healing (145, 146, 148).

In this report, we show that MDA-MB 231 cells secrete LGALS3BP, which in turn inhibits fibrocyte differentiation, and that conversely galectin-3 promotes fibrocyte differentiation. LGALS3BP and galectin-3 are new modulators of fibrosis in the tumor microenvironment. Additionally, the effects of LGALS3BP and galectin-3 on fibrocytes show these proteins are active signaling molecules in cancer and fibrosis, respectively, and not passive biomarkers.

Materials and methods

PBMC isolation and culture

Human blood was collected from adult volunteers who gave written consent and with specific approval from the Texas A&M University human subjects Institutional

Review Board. Peripheral blood mononuclear cells (PBMC) were isolated and cultured as previously described (34, 194). Protein-free medium (PFM) was Fibrolife basal medium (Lifeline, Walkersville, MD) supplemented with 10 mM HEPES (Sigma, St. Louis, MO), 1× non-essential amino acids (Sigma), 1 mM sodium pyruvate (Sigma), 2 mM glutamine (Lonza, Basel, Switzerland), 100 U/ml penicillin and 100 μg/ml streptomycin (Lonza). Serum-free media (SFM) was PFM further supplemented with 10 μg/ml recombinant human insulin (Sigma), 5 μg/ml recombinant human transferrin (Sigma), and 550 μg/ml filter-sterilized human albumin (194). PBMC were cultured in SFM with the indicated concentrations of conditioned media, recombinant human galectin-1 and galectin-3 (Peprotech, Rocky Hill, NJ), or recombinant human galectin-3 binding protein (R & D systems, Minneapolis, MN) for five days, after which PBMC were stained, and fibrocytes were counted, as previously counted (194). Adhered cells and macrophages were counted as previously described (194). Human monocytes were purified, tested for purity, and cultured as previously described (194, 195). For immunohistochemistry, PBMC were fixed and stained for CD209 (Biolegend, San Diego, CA) as previously described (195).

Tumor cell lines and conditioned media

MDA-MB 231 (103), MDA-MB 435 (105), and DCIS.com (111) cells were the kind gift of Dr. Weston Porter. HT-29 (112), SW480 (113), DKOB8 (114), and HCT (115) cells were the kind gift of Dr. Robert Chapkin. MCF-7 (110), ADR-RES (116), OVCAR-8 (107, 108), SNU 398 (117), HEP-G2 (118), SW 1088 (119), U87 MG (109), and PANC-1 (120) cells were the kind gift of Dr. Deann Wallis. Mono mac-1 (121) and Mono mac-6

(122) were from the DSMZ (Liebniz Institute: German Collection of Microogranisms and Cell Culture, Braunschwieg, Germany), and U-937 (123), HL-60 (124), THP-1 (125), and HEK-293 (250) cells were from the ATCC (Manassas, VA). The MDA-MB 435 cell line has previously been classed as a breast cancer cell line, but is currently classed as a melanoma cell line (105, 106). Each tumor cell line was tested for mycoplasma contamination using a PCR detection kit (MDBioproducts, St. Paul, MN) following the manufacturer's instructions, and all work was done with cell lines containing undetectable levels of mycoplasma.

Tumor cell lines were grown in DMEM supplemented with 10% fetal calf serum (Genesee Scientific, San Diego, CA) in 75 cm^2 flasks (BD, Franklin Lakes, NJ) until 70% confluent. Adhered cells were washed three times with PBS, and were then incubated with 10 ml protein free media (PFM). After 24 or 48 hours, the conditioned medium was collected and clarified by centrifugation at 300 x g for 10 minutes. Conditioned media from MDA-MB 231 cells was further clarified by centrifugation at 1,000 x g for 10 minutes, followed by clarification at 200,000 x g for 1 hour. The supernatant was then concentrated with a 100 kDa centrifugal filter (EMD Millipore, Billerica, MD), and buffer exchanged with 20 mM sodium phosphate, pH 7.2. Proteins were visualized by silver stain on 4-20% SDS-PAGE gels (Bio-Rad, Hercules, California) and protein concentration was assessed by absorbance at 280 nm (Synergy MX, Biotek, Winooski, VT).

Protein purification and identification

300 ml of MDA-MB 231 CM was clarified by ultracentrifugation, concentrated, and buffer-exchanged as described above, and resuspended in 1 ml. This was loaded on a

5 ml MonoQ anion exchange column on an AKTA chromatography system (GE Healthcare, Piscataway, NJ). The column was washed with 6 ml of 20 mM NaPO4 pH 7.4 buffer (first 6 fractions), and bound proteins were then eluted with a 14 ml gradient of 0 to 0.3 M NaCl in 20 mM NaPO4 pH 7.4, collecting 0.5 ml fractions. Serial doubling dilutions of fractions were then mixed with PBMC, and their effect on fibrocyte differentiation was measured as previously described (36). Trypsin digestion of samples, purification of peptides with Zip tips (EMD Millipore), and mass spectrometry was performed by the University of Utah mass spectrometry core facility, and peptides with MASCOT scores > 40 and mass errors < 3 ppm were used for protein identification.

Flow cytometry

PBMC were placed on an ultra low attachment plate (Corning, Corning, NY) and incubated with MDA-MB 231 conditioned media at the indicated concentrations for the indicated time. These cells were then removed from the plate using ice cold 5 mM EDTA in PBS (Rockland, Limerick, PA) with gentle pipetting. PBMC were collected by centrifugation at 300 x g for 10 minutes, resuspended in 100 µl ice cold PBS, and analyzed for viability using propidium iodide (Sigma) and forward/side scatter via flow cytometry (Accuri-BD, Franklin Lakes, NJ) as previously described (251, 252).

Immunodepletion of conditioned media

For immunodepletion, rabbit polyclonal anti-galectin-3 binding protein (BIOSS, Woburn, MA), mouse monoclonal anti-galectin-3 (Biolegend), mouse IgG isotype control

(Jackson, West Grove, PA) and rabbit polyclonal anti-protein S (Sigma) antibodies were bound to protein G-coated Dynabeads (Invitrogen, Carlsbad, CA) beads following the manufacturer's instructions. Beads complexed with antibodies were mixed 1:10 with conditioned media at 37° C for 2 hours. Beads were then removed from the conditioned media following the manufacturer's instructions.

Sequencing MDA-MB 231 LGALS3BP

Total RNA was isolated from MDA-MB 231 cells using a kit (Omega Biotek, Norcross, GA), and cDNA was generated using a kit (Thermo Scientific, Waltham, MA). LGALS3BP was amplified using Phusion polymerase (New England Biolabs, Ipswich, MA) with primers 5'-AACTCGAGGTCCACACCTGAGTTGG-3' and 5'-AAACTCCTAGTCCACACCTGAGG-3' that encompassed all known or predicted transcript variants (253), and resulted in a single band on a DNA gel. Amplified LGALS3BP was ligated into pCMV and sequenced at Lonestar Labs (Houston, TX), using the primers listed above and internal primers (5'-CGCCCTGGGCTTCTGTGG-3' and 5'-GGTCTATCAGTCCAGACG-3').

Isolation of mouse spleen cells

SIGN-R1 -/- spleens were developed by Andrew McKenzie (254) and were the kind gift of Dr. Jeffrey Ravetch at Rockefeller University. Mouse spleen cells were isolated as previously described (255).

Staining of biopsies

De-identified slides of formalin fixed paraffin-embedded biopsies or surgical specimens from patients with confirmed infiltrative ductal carcinoma of the breast were kindly provided by Dr. Kelly Hunt at The University of Texas M.D. Anderson Cancer Center. Patients signed informed consent prior to the initiation of treatment. The M.D. Anderson Institutional Review Board approved the use of all patient-derived tissues and data. Slides were deparaffinized in xylene and rehydrated through graded ethanols. Antigens were retrieved by incubating sections with Antigen Unmasking Solution H-3300 (Vector Labs, Burlingame, CA) in a steamer for 20 minutes. Slides were then permeabilized by incubating with 0.2% Triton X-100 in PBS for 45 minutes at room temperature. Slides were blocked by incubating with 1% Bovine Serum Albumin in PBS for one hour at room temperature. Slides were then incubated with primary antibody diluted in 0.1% BSA/PBS overnight at 4ºC. Primary antibodies were collagen-I (Rabbit pAb, 1:500, Abcam #ab34710), CD45RO (Mouse mAb, 1:100, Biolegend #304202), LGALS3BP (Rabbit pAb, 1:200, GeneTex #GTX116497), galectin-3 (Rat mAb, 1:200, BioLegend #125401). Secondary antibody in 0.1% BSA/PBS was then added for one hour at room temperature. Secondary antibodies were donkey anti-mouse DyLight 488, donkey anti-rabbit Red X, and goat anti-rat 488 (1:500, Jackson ImmunoResearch). Sections were DAPI stained for 10 minutes and mounted with Dako Fluorescent mounting medium (Dako, Carpinteria, CA). Images were captured with a Olympus BX51 microscope and Olympus DP72 camera (Olympus, Tokyo, JP) and CellSens software (Center Valley, PA).

Statistics

Statistics were performed using Prism (Graphpad Software, San Diego, CA). Differences were assessed by two-tailed t-tests or two-tailed Mann-Whitney tests. Significance was defined as $p<0.05$.

Results

MDA-MB 231 and MDA-MB 435 cells secrete factors that inhibit fibrocyte differentiation

To determine whether factors secreted from tumors might promote or inhibit fibrocyte differentiation, we examined the effect of conditioned media (CM) from a variety of human tumor cell lines on human fibrocyte differentiation. Human PBMC were incubated in the presence or absence of tumor cell line CM, and after 5 days, fibrocytes were counted. In the absence of CM, we observed 81 to 1374 fibrocytes per 10^5 PBMCs from the different donors, similar to what we have previously observed (194). Because of this variability, fibrocyte numbers were thus normalized to CM-free controls. CM from MDA-MB-231 (231) (103) and MDA-MB-435 (435) cells (105) inhibited fibrocyte differentiation in a concentration-dependent manner (Figure 34A and Figure 35A), and this effect was observed for PBMC from all donors tested. The 435 CM did not affect the number of adherent cells after removing weakly adhering cells, and then fixing and staining, while 231 CM slightly inhibited adherent cell number only at 12.5% CM, which is well above the IC50 for fibrocyte inhibition (Figure 34B and Figure 35B). PBMC exposed to 231 CM or 435 CM for 5 days did not have significantly increased cell death

as assessed by propidium iodide staining (Figure 34C and Figure 35C), or decreased total cell number (this includes the weakly adherent cells removed before fixing and staining) as assessed by removing all cells from the assay well and counting by flow cytometry (Figure 34D and Figure 35D). Some concentrations of 231 CM increased total cell numbers (Fig. 34D). This may be due to factors in the conditioned media that promote cell survival and/or cell proliferation.

Fibrocytes differentiate from monocytes (22, 27, 33). Cells in the PBMC population include T-cells, B-cells, monocytes, and NK cells (36). To determine whether the CM effect on fibrocyte differentiation is a direct effect on monocytes, or is mediated by the other cells in a PBMC population, 231 or 435 CM was added to purified human monocytes. 231 CM and 435 CM inhibited fibrocyte differentiation from purified monocytes (Figure 34E and Figure 35E). For the inhibition of fibrocyte differentiation from PBMC, the IC50 of 231 CM was 0.33 ± 0.05% (mean ± SEM, n=37, Hill coefficient 1.06 ± 0.13), and that of 435 CM was 0.45 ± 0.17% (n=7, Hill coefficient 0.73 ± 0.20). When added to monocytes, the 231 and 435 IC50s were 1.2 ± 0.2% (n=5, Hill coefficient 1.08 ± 0.15) and 1.9 ± 0.7% (n=3, Hill coefficient 1.70 ± 0.60), respectively. The difference in IC50s for 231 CM between PBMCs and monocytes was significant with $p < 0.05$ (t test); the difference for 435 CM was not significant. Since purifying monocytes and thus removing other cells from the PBMC population modestly increased the 231 CM IC50, these data suggest that either the monocyte purification procedure modestly reduced the ability of monocytes to respond to the factor(s) in CM that inhibits fibrocyte differentiation, or else the presence of the other cells in the PBMC population somewhat

potentiates the ability of monocytes to respond to the factor(s). In either case, the data indicate that monocytes can respond directly to the factor(s).

In addition to differentiating into fibrocytes, monocytes can also differentiate into macrophages. To determine if the CMs that inhibit fibrocyte differentiation also affect macrophage differentiation from monocytes, we counted the total number of adhered macrophages, as assessed by morphology. 231 CM caused a decrease in macrophage differentiation at 12.5% CM, but did not affect the number of macrophages at lower concentrations which inhibited fibrocyte differentiation, and 435 did not significantly inhibit macrophage differentiation (Figure 34F and Figure 35F). Together, the data indicate that factors in 231 and 435 CM affect monocytes to strongly inhibit fibrocyte differentiation, while having no effect, or a relatively modest effect, on cell death, total cell numbers, numbers of macrophages, and the numbers of adherent cells.

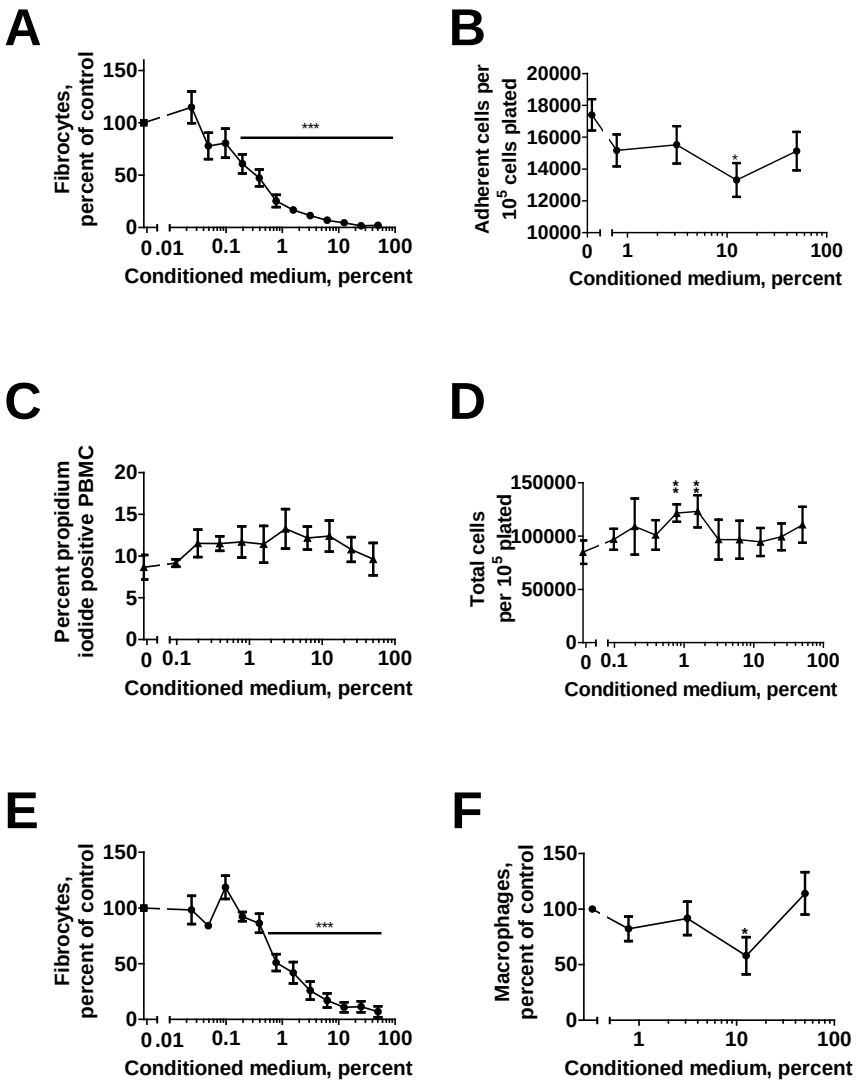

Figure 34. **MDA-MB 231 conditioned media inhibits fibrocyte differentiation.** (A) PBMC were cultured in serum free media in the presence of the indicated concentrations of MDA-MB 231 (231 CM) conditioned media for five days. Fibrocyte counts were normalized for each donor to the SFM control. (B) Counts of total adherent PBMC per five fields of view at the indicated concentrations of 231 CM. (C) Total propidium iodide positive PBMC, and (D) total PBMC, after 5 days at the indicated concentrations of 231 CM, measured by flow cytometry. (E) Total number of fibrocytes from monocytes cultured at the indicated concentrations of 231 CM for 5 days. Monocytes were 16% ± 9% (mean ± SEM, n=3) of the PBMCs and 92% ± 5% in the purified fraction. (F) Total number of macrophages from PBMC cultured at the indicated concentrations of 231 CM for 5 days. Values are mean ± SEM. The absence of error bars indicates that the error was smaller than the plot symbol. (A, B, F) n=38, (C, D, E) n=3. * indicates $p < .05$, ** $p < 0.01$, and *** $p < 0.001$ compared to the control (t-test).

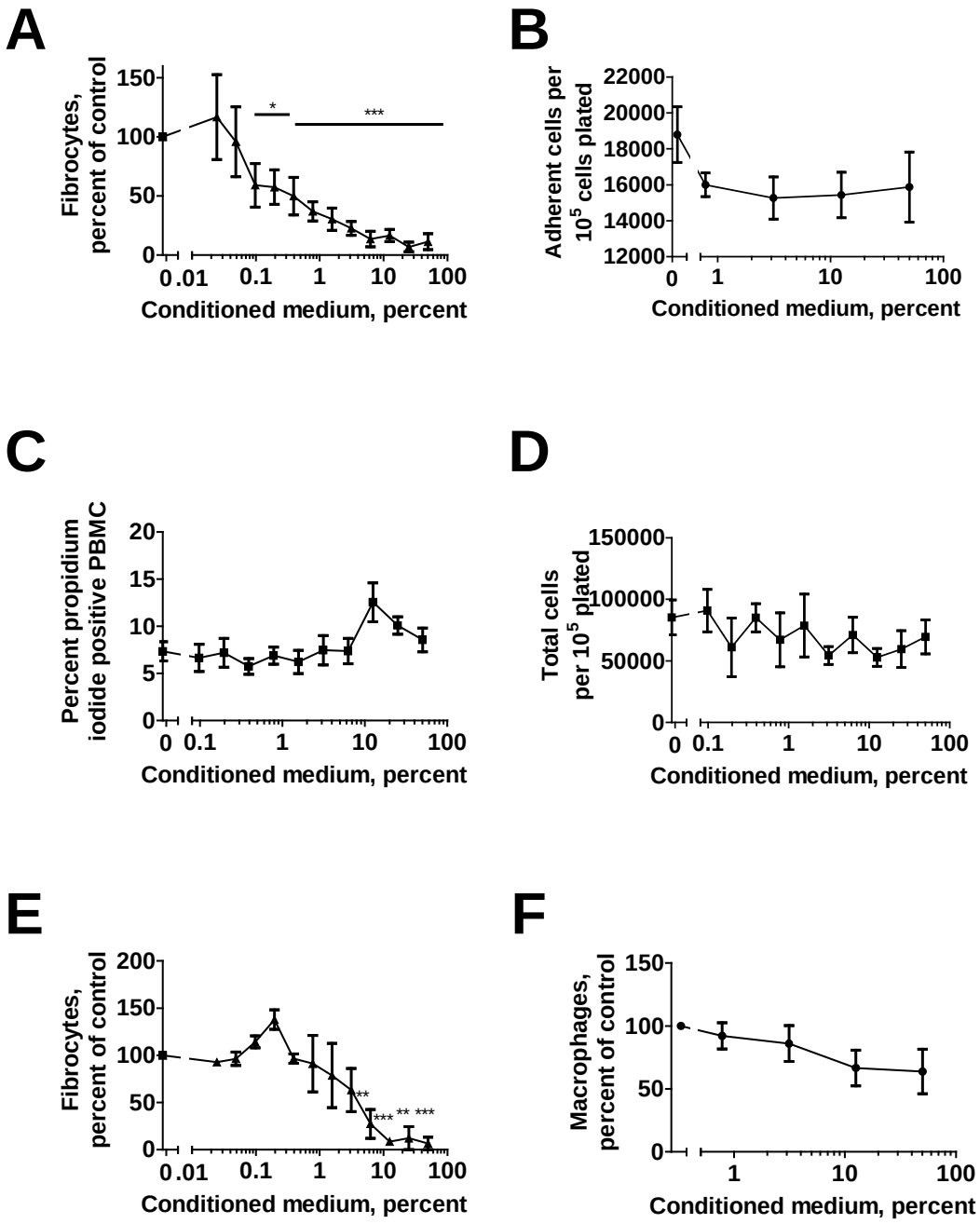

Figure 35. **MDA-MB 435 conditioned media inhibits fibrocyte differentiation.** PBMC were cultured as in Figure 34, except 435 CM was used instead of 231 CM. (A, B, F) n=10, (C, D, E) n=3. * indicates $p < .05$, ** $p < 0.01$, and *** $p < 0.001$ compared to the control (t-test).

Some but not all human cancer cell lines also secrete a fibrocyte inhibitory activity

To determine if other tumor types might secrete factors that inhibit fibrocyte differentiation, we exposed PBMC to conditioned media from cancer cell lines derived from human breast, skin, colon, liver, pancreas, brain, ovary, and leukocyte tissue. We defined units of activity as the inverse of the CM's IC50 for fibrocyte inhibition. Of the cell lines tested, conditioned media from OVCAR-8, U87-mg, MDA-MB 231, MDA-MB 435, MCF-7, and DCIS.com significantly inhibited fibrocyte differentiation (Figure 36). OVCAR-8 is an ovarian cancer cell line derived from a metastatic site (107, 108). U87-mg is derived from a glioblastoma (109). MDA-MB 231 is derived from a breast cancer metastasis (103). MDA-MB 435 has an uncertain origin: originally the cell line was listed as a breast cancer line by the ATCC (105). Currently, the cell line is listed as a melanoma cell line (106). MCF-7 is a breast cancer cell line derived from a pleural effusion (110). DCIS.com is derived from a normal breast tissue cell line (MCF10A) passaged through a mouse, and forms a non-metastatic ductal carcinoma in-situ when injected into mice (111). Each cell line whose CM inhibited fibrocyte differentiation was isolated from hormone secreting tissues (breast, ovarian), with the exception of the U87-mg and MDA-MB 435 cell lines. No colon, liver, pancreatic, or leukemia CM significantly inhibited fibrocyte differentiation (Figure 36A), and 0.4 to 10% SW480 colon cancer CM modestly potentiated fibrocyte differentiation (Figure 36B).

Figure 36. **The effect of conditioned media from other cancer cell lines on fibrocyte differentiation.**
(A) Conditioned media from 20 different cancer cell lines show different levels of potentiation and inhibition for fibrocyte differentiation. Activity Units are the dilution of CM which inhibited fibrocyte differentiation to 50% of the control value. Higher activity units indicate more potent inhibition of fibrocyte differentiation. n=3 for Mono mac-1, Mono mac-6, U937, HL-60, THP-1, DK0B8, HCT (P21+/P53+), HCT (P21-/P53+), HCT (P21+/P53-), HCT (P21-/P53-), HEK-293, K562; n=6 for ADR-RES, OVCAR-8, snU-398, HEP-G2, U-87 MG, PANC-1, SW480, n=7 for DCIS.com, n=10 for MCF-7 and MDA-MB 435, and n=38 for MDA-MB 231. A = cancers derived from breast tissue, B = skin, C = leukocyte, D = colon, E = embryonic kidney, F = ovarian, G = Liver, H = Brain, and I = Pancreas. The absence of error bars indicates that the error was smaller than the plot symbol. # indicates inconsistent inhibition of fibrocyte differentiation (variability of response of PBMC from different donors), * indicates $p < .05$, ** $p < 0.01$, and *** $p < 0.001$ compared to the control (t-test). (B) Conditioned media from SW480 cells potentiated fibrocyte differentiation. Values are mean ± SEM, n=6. * indicates $p < 0.05$, ** $p < 0.01$, and *** $p < 0.001$ compared to the control (t-test).

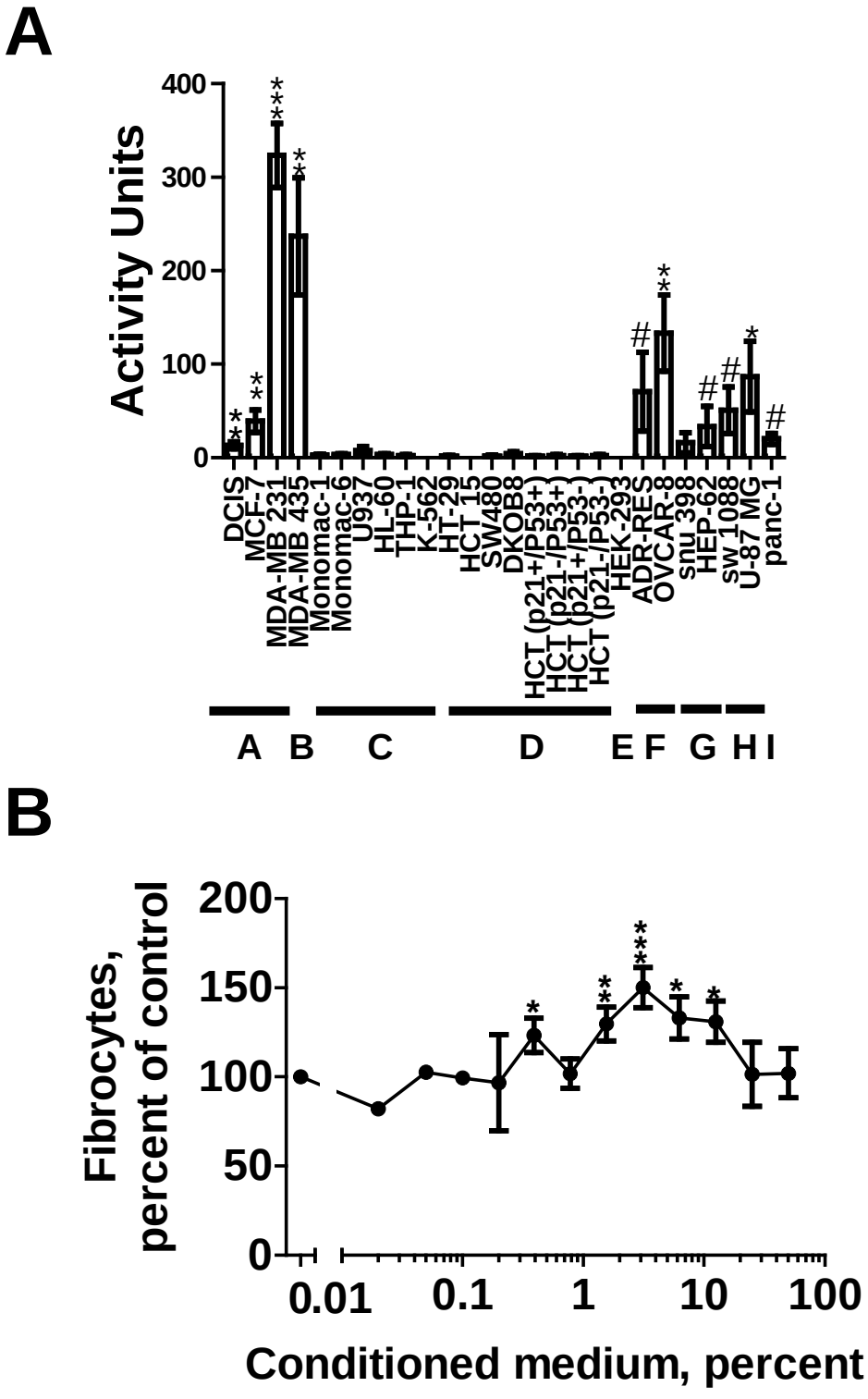
A
Activity Units
400
300
200
100
0
DCIS
MCF-7
MDA-MB 231
MDA-MB 435
Monomac-1
Monomac-6
U937
HL-60
THP-1
K-562
HT-29
HCT 15
SW480
DKOB8
HCT (p21+/P53+)
HCT (p21-/P53+)
HCT (p21+/P53-)
HCT (p21-/P53-)
HEK-293
ADR-RES
OVCAR-8
snu 398
HEP-62
sw1088
U-87 MG
panc-1
A B C D E F G H I
B
Fibrocytes, percent of control
200
150
100
50
0
0.01
0.1
1
10
100
Conditioned medium, percent

The 231 fibrocyte inhibitor is a protein, and can be concentrated and purified

To determine if the fibrocyte inhibition activity in 231 conditioned media is due to a protein, we exposed conditioned media to trypsin, heat, and freeze-thaw cycles. All three treatments strongly decreased the ability of 231 CM to inhibit fibrocyte differentiation (Figure 37). The 231 CM retained ~80% activity after clarification by ultracentrifugation, and was largely retained by a 100 kDa filter (Figure 38A). The components of 231 CM that passed through a 100 kDa filter potentiated fibrocyte differentiation (Figure 39A). This potentiating activity was retained by a 10 kDa filter (Figure 39B). Together, these results suggest that the 231 CM activity which inhibits fibrocyte differentiation is a protein.

To purify the 231 CM fibrocyte differentiation inhibitor, the 100 kDa retentate was fractionated by anion exchange chromatography, and fractions were assayed for activity (Figure 40A). There was little activity in the flow-through, some activity throughout the elution, and a large peak of activity in fractions 27 and 28, corresponding to a NaCl concentration of 375 mM. The IC50 of both of these fractions occurred at a ~4,096-fold dilution, with a Hill coefficient of 4.6 ± 1.7 (mean ± SEM, n=6). Silver-stained gels showed prominent bands at ~85 and ~39 kDa in fraction 27 (Figure 40B). Tryptic fragments of proteins in fraction 27 were analyzed by mass spectrometry. In decreasing order of the number of identified peptides, the identified proteins were human galectin-3 binding protein, desmoplakin, plakoglobin, desmoglein type 1, pentraxin-3 (PTX-3), adult intestinal phosphatase, and dermcidin. However, after purifying peptides with a Ziptip, the only identified peptides corresponded to galectin-3 binding protein (LGALS3BP;

GI:5031863).

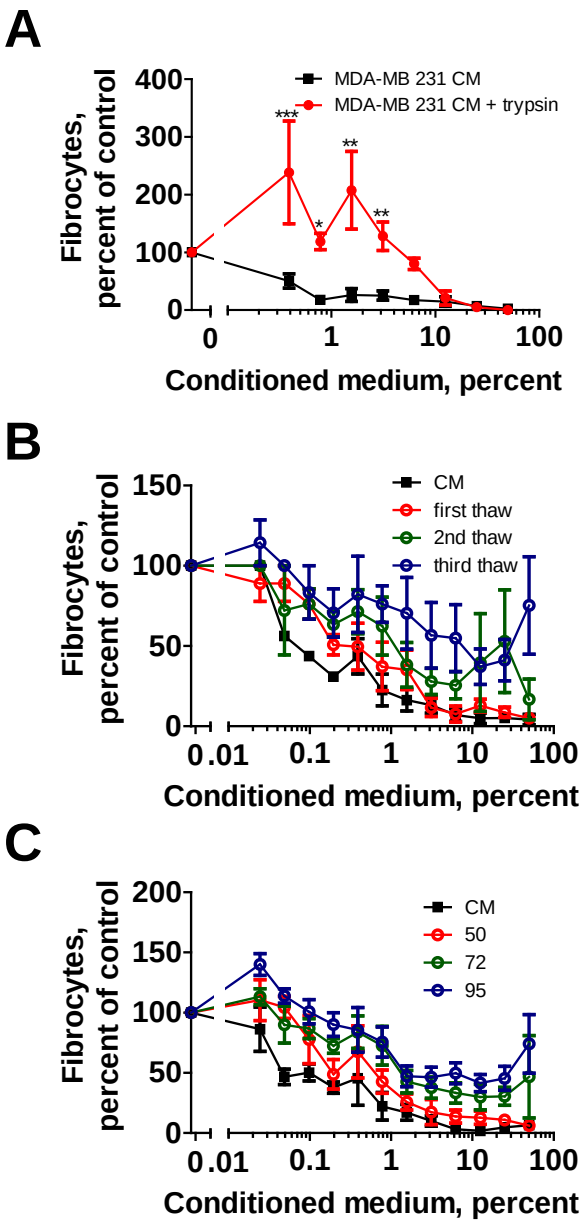

Figure 37. **The fibrocyte inhibitory factor in MDA-MB 231 conditioned media is a protein.**

PBMC were cultured as in Figure 34, with the indicated concentrations of (A) 231 CM or CM digested with trypsin, (B) 231 CM or CM frozen and thawed one, two, or three times, or (C) 231 CM or CM heated to 50, 72, or 95 ˚C. Values are mean ± SEM; the absence of error bars indicates that the error was smaller than the plot symbol. * indicates $p < 0.05$, ** $p < 0.01$, and *** $p < 0.001$ compared to the control (t-test).

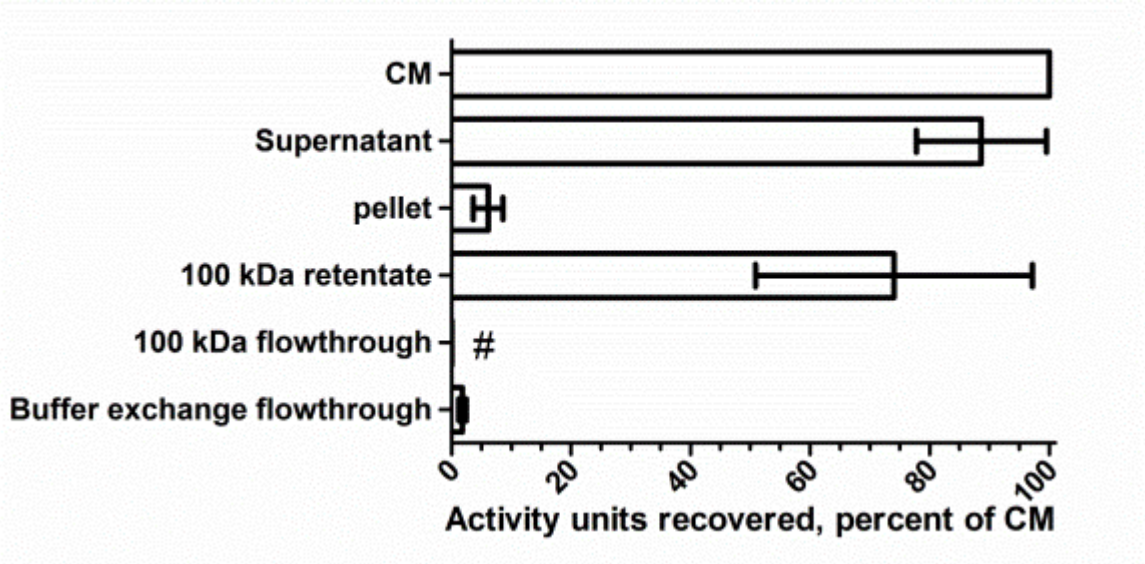

Figure 38. **MDA-MB 231 conditioned media's fibrocyte inhibitory activity is greater than 100 kDa.**
(A) The indicated fractions were assessed for their ability to inhibit fibrocyte differentiation. The activity units were normalized to the value for the CM. Values are mean ± SEM, n=24.

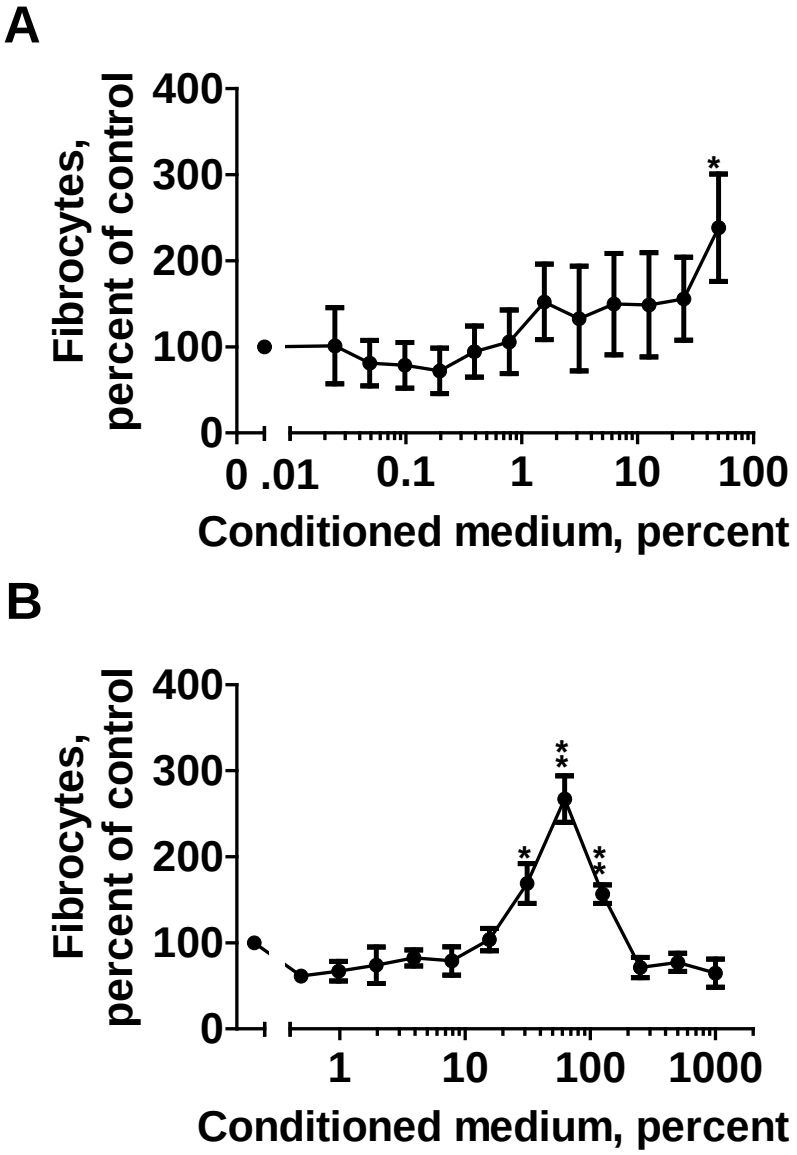

Figure 39. **A component of MDA-MB 231 conditioned media which passes through a 100 kDa filter potentiates fibrocyte differentiation.**
(A) PBMC were cultured as in Figure 34, with the indicated concentrations of 231 CM that flowed through a 100 kDa filter. (B) The material assayed in A was then fractionated and concentrated using a 10 kDa filter, and the material retained by the 10 kDa filter was assayed. Values are mean ± SEM, n = 6; the absence of error bars indicates that the error was smaller than the plot symbol. * indicates $p < 0.05$ and ** $p < 0.01$ compared to the control (t-test).

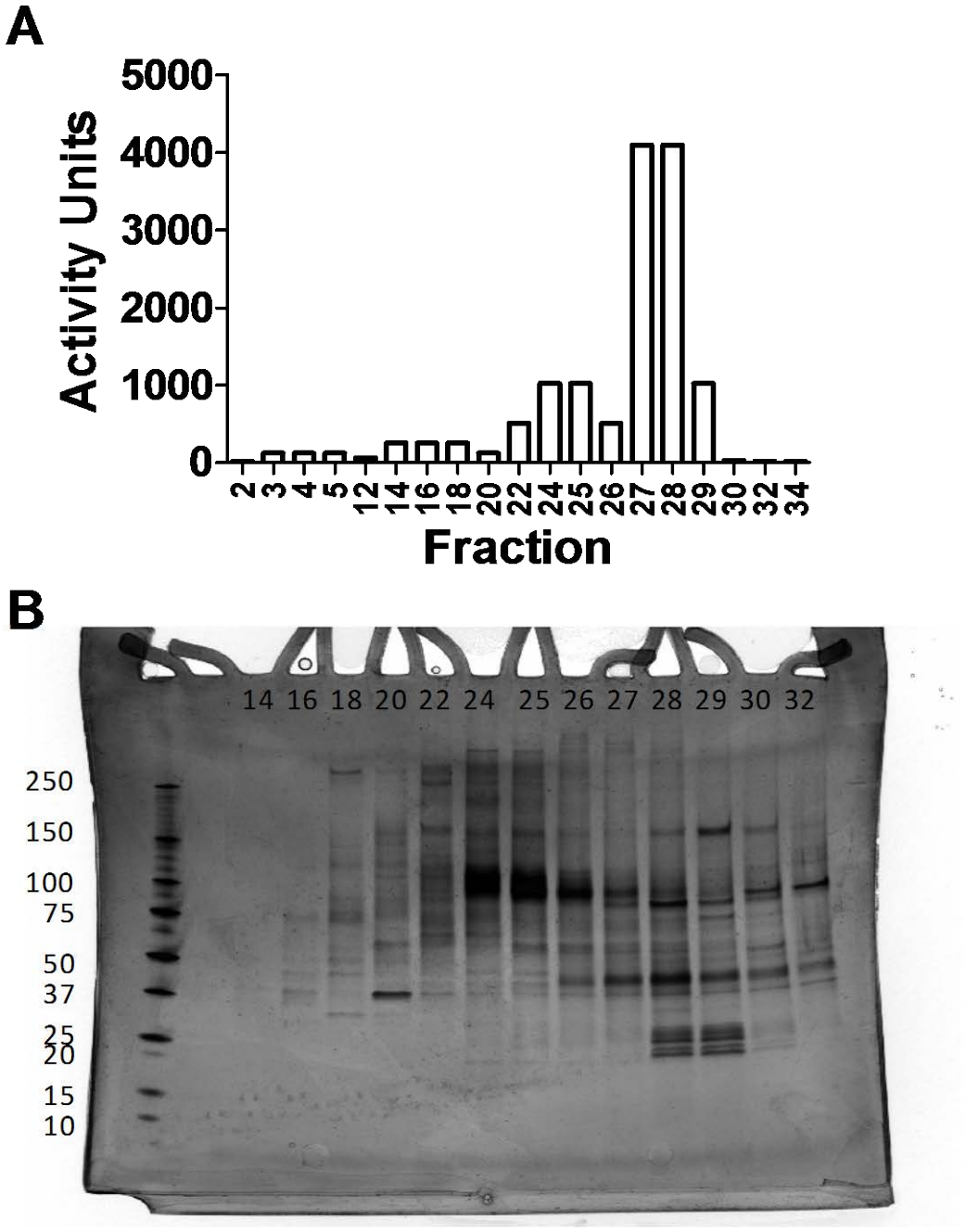

Figure 40. **Anion exchange chromatography of the partially purified factor.** (A) 100 kDa concentrated MDA-MB 231 CM, produced as in Figure 38, was fractionated on an anion exchange column. Fractions were assayed as in Figure 34, and the resulting fibrocyte inhibition was measured by activity units, as in Figure 36. (B) SDS-PAGE gel of the fractions, silver stained.

Immunodepletion of LGALS3BP from CM removes most of the fibrocyte inhibitory activity

To determine if the LGALS3BP detected in CM affects fibrocyte differentiation, we immunodepleted LGALS3BP from 231 and 435 CM. Immunodepletion with a control antibody had little effect on the ability of CM to inhibit fibrocyte differentiation (Figure 41 and 39). Immunodepletion of LGALS3BP from 231 CM (Figure 41) increased the IC50 by 8.6 ± 1.3 fold (mean ± SEM, n=7, $p < 0.001$, t-test). Similarly, immunodepletion of LGALS3BP from 435 CM (Figure 42) increased the IC50 by 21 ± 11 fold (mean ± SEM, n=7, $p < 0.001$, t-test). These results suggest that LGALS3BP is a significant component of the 231 and 435 CM fibrocyte inhibitory activity.

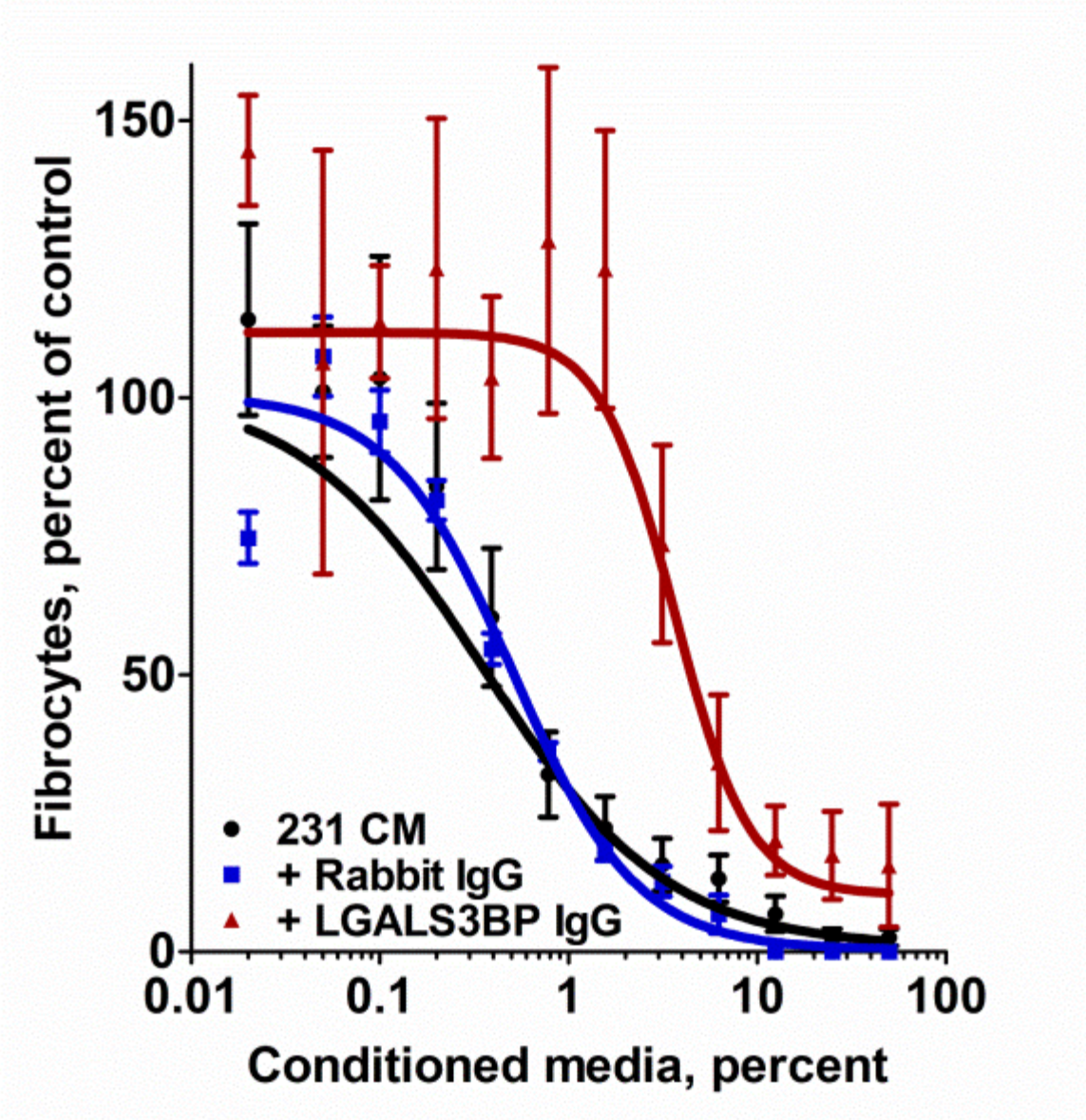

Figure 41. **Immunodepletion of LGALS3BP decreases MDA-MB 231 CM's fibrocyte inhibitory activity.**
MDA-MB 231 CM was immunodepleted with anti-LGALS3BP or isotype control antibodies. Values are mean ± SEM, n=7.

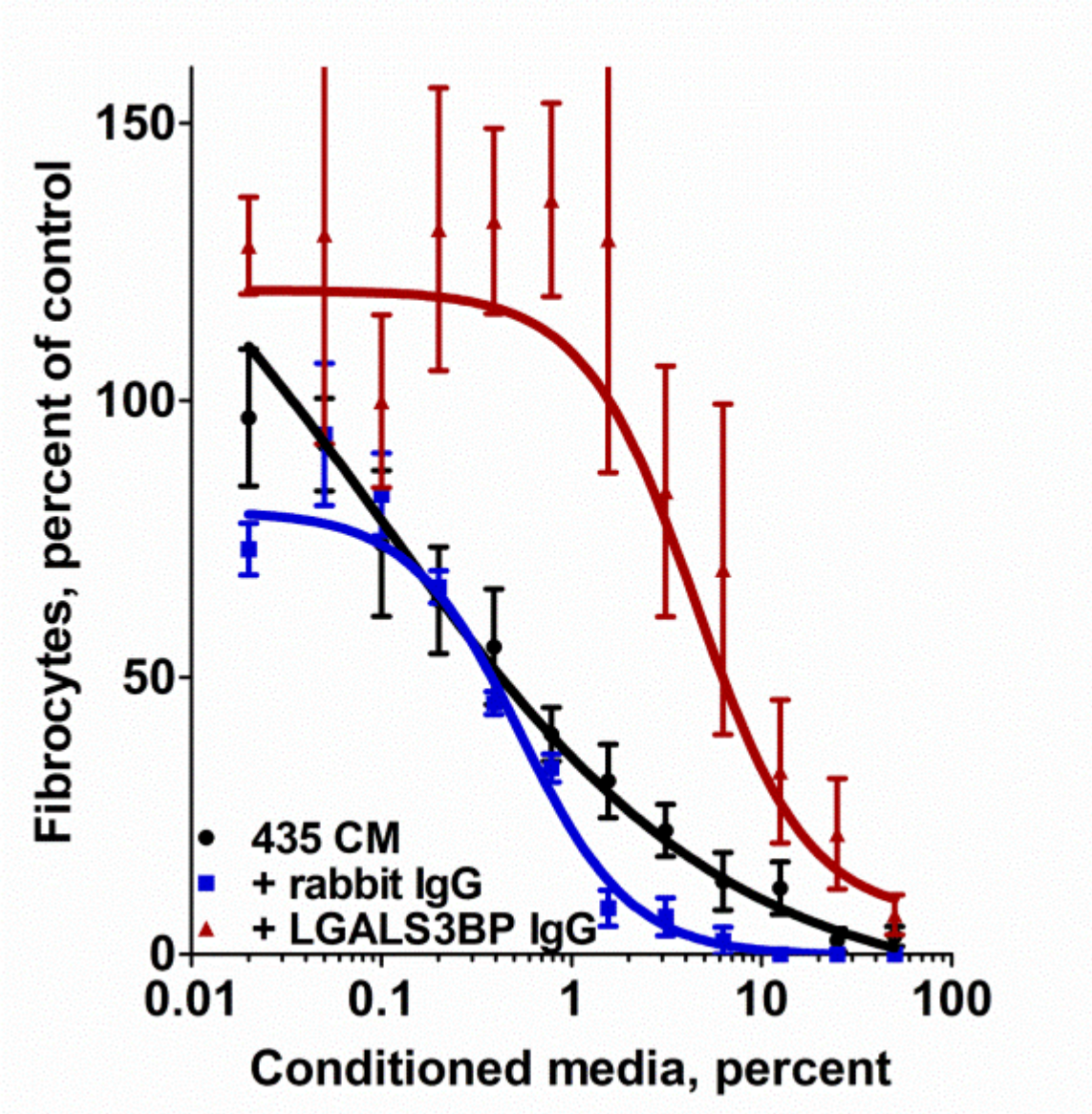

Figure 42. **Immunodepletion of LGALS3BP decreases MDA-MB 435 CM's fibrocyte inhibitory activity.**
MDA-MB 435 CM was immunodepleted with anti-LGALS3BP or isotype control antibodies, and then assessed for the ability to inhibit fibrocyte differentiation as in Figure 34. Values are mean ± SEM, n=7.

Recombinant LGALS3BP inhibits fibrocyte differentiation

To test the hypothesis that LGALS3BP inhibits fibrocyte differentiation, we incubated PBMC with recombinant human LGALS3BP. LGALS3BP significantly

inhibited fibrocyte differentiation with an IC50 of 0.22 ± 0.05 µg/ml (Hill coefficient 6.5 ± 2.2) (Figure 43), but unlike 231 CM (Figure 34A), did not completely inhibit fibrocyte differentiation. Together with the immunodepletion assays, the data indicate that LGALS3BP does inhibit fibrocyte differentiation.

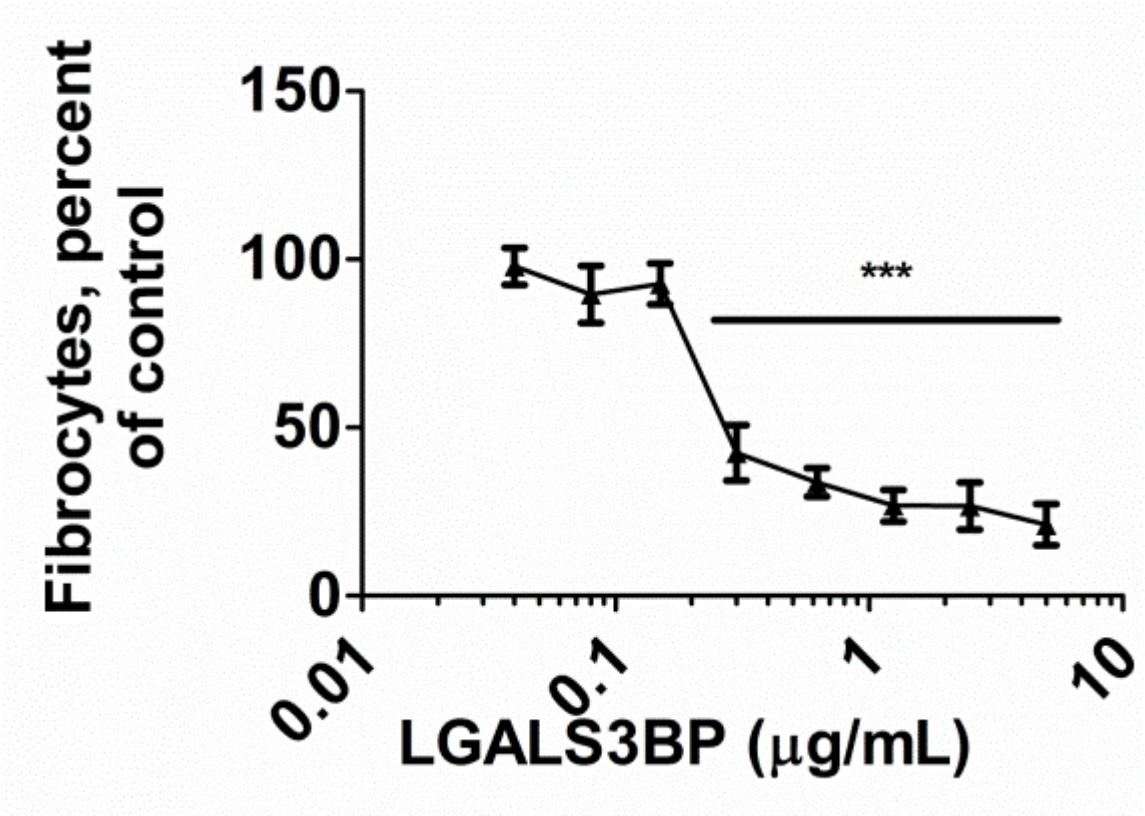

Figure 43. **Recombinant LGALS3BP inhibits fibrocyte differentiation.** Recombinant LGALS3BP was added to PBMC, and fibrocyte differentiation was assessed as in Figure 34. Values are mean ± SEM, n=8. * indicates $p < .05$, ** $p < 0.01$, and *** $p < 0.001$ compared to the control (t-test).

The 231 LGALS3BP mRNA encodes a canonical LGALS3BP

LGALS3BP has an experimentally verified transcript variant, and several predicted transcript variants (253). To determine if MDA-MB 231 cells secreted a truncated or alternatively spliced variant of LGALS3BP, mRNA was isolated from MDA-

MB 231 and converted to cDNA. Using primers which encompass all known or predicted transcript variants (253), *LGALS3BP* cDNA was amplified via PCR and sequenced. The sequence encoded the four LGALS3BP peptides detected by mass spectrometry, and was identical to human *LGALS3BP* from oral squamous carcinoma cells (256), and is identical to the sequence of the recombinant full-length human LGALS3BP (R&D datasheet).

LGALS3BP produced in cancer cells has a higher mass than recombinant LGALS3BP

To determine the concentration of LGALS3BP in CM, western blots of CM and known amounts of recombinant LGALS3BP were stained for LGALS3BP. MDA-MB 231, MDA-MB 435, and OVCAR-8 CMs showed high concentrations of LGALS3BP compared to MCF-7, DCIS.com, and U87-mg CMs (Figure 44). MDA-MB 435, MDA-MB 231, and OVCAR-8 cells accumulated ~1 µg/ml LGALS3BP in their CMs. U87-mg CM had very little LGALS3BP, suggesting that glioma cells may inhibit fibrocyte differentiation by other means. LGALS3BP has a predicted mass of ~60 kDa, but LGALS3BP isolated from the serum of cancer patients has a mass of ~90 kDa (249) and the LGALS3BP we observed in cancer cell CMs has a mass of ~85 kDa. While LGALS3BP in cancer CM appears as a single band, the recombinant LGALS3BP from CHO cells has several bands. R&D Systems is the only manufacturer of recombinant LGALS3BP produced in eukaryotic cells, and they have also observed their product to appear as multiple bands on a gel (personal communication).

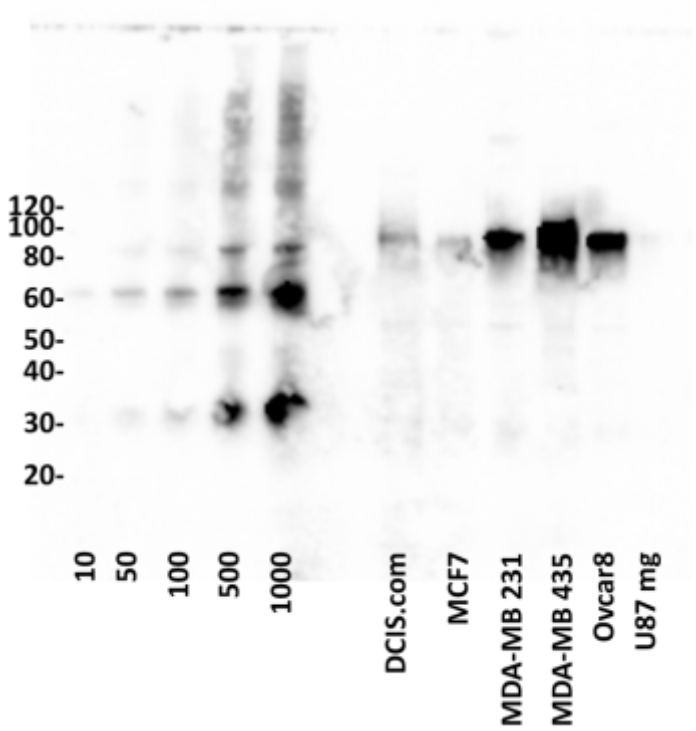

Figure 44. **High concentrations of LGALS3BP are present in 321 and 435 conditioned media.**
Western blot of equal volumes of the indicated concentrations (in ng/ml) of recombinant LGALS3BP and conditioned media from the indicated cell types were stained with anti-LGALS3BP antibodies. Blot image is representative of three separate experiments.

231 and 435 CMs inhibit fibrocyte differentiation using a DC-SIGN-dependent mechanism

The C-type lectin receptor DC-SIGN/CD209 is expressed on monocytes, and is upregulated as monocytes differentiate into dendritic cells (257). IgG is capable of inducing a pro- or anti-inflammatory macrophage phenotype by interacting with monocytes (258). IgG that is glycosylated with N-linked sialic-acid glycans binds DC-SIGN, and causes macrophages to secrete IL-10, reducing inflammation (258, 259). Both

glycosylated IgG and LGALS3BP bind human DC-SIGN (129, 258). To determine if the DC-SIGN receptor might mediate the effect of LGALS3BP on fibrocyte differentiation, we added 231 CM and 435 CM to spleen cells from WT and CD209-/- (SIGN-R1-/-) mice. 231 CM and 435 CM inhibited fibrocyte differentiation from wild type C57BL/6 mouse spleen cells, but potentiated fibrocyte differentiation from CD209 knockout mouse spleen cells (Figure 45) in a similar manner to 231 CM components that passed through a 100 kDa filter (Figure 39). Recombinant LGALS3BP, 231 CM, and 435 CM each upregulated CD209 expression on PBMC as measured by immunohistochemistry (Figure 46).

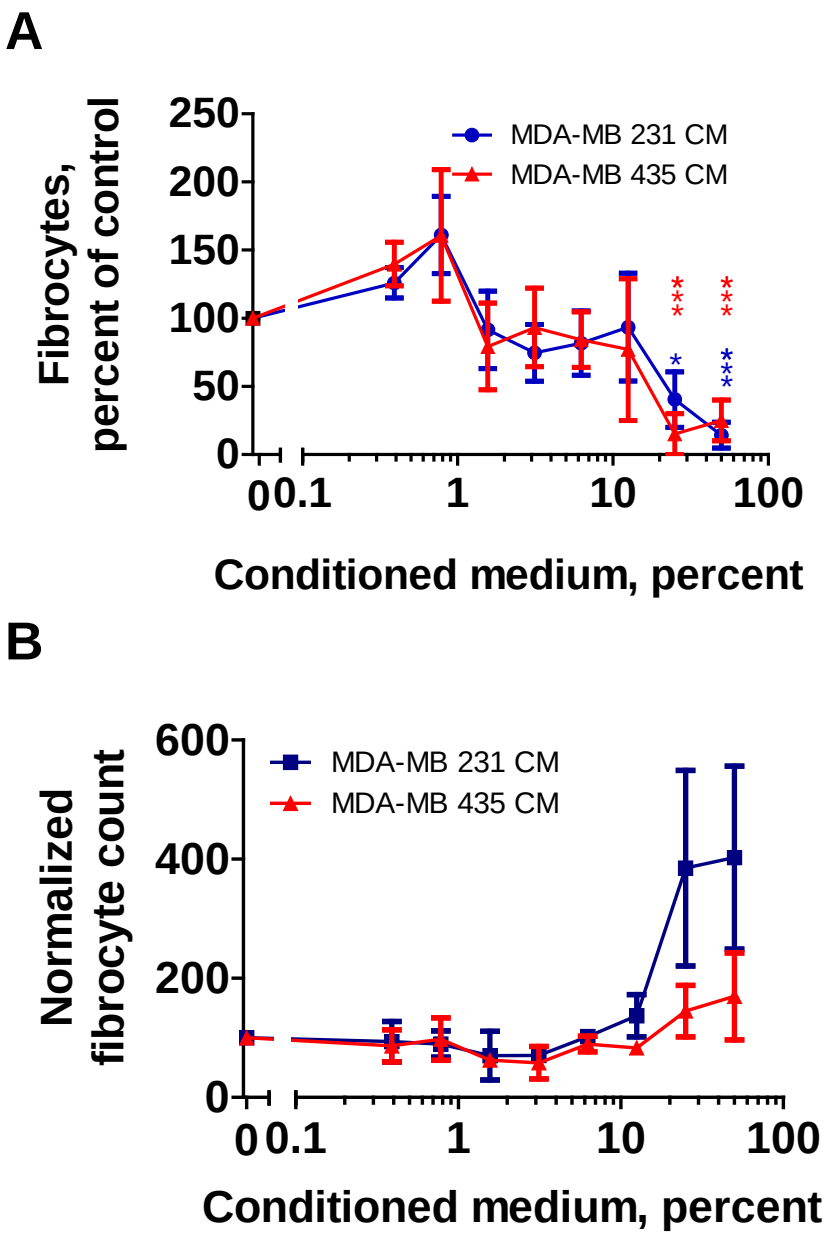

Figure 45. CD209 (SIGN-R1) is needed for the effect of MDA-MB 231 and MDA-MB 435 CM on mouse fibrocyte differentiation.
Cells were isolated from mouse spleens and incubated with the indicated concentrations of CM. Spleen cells from (A) wild-type C57BL/6 and (B) SIGN-R1 -/- knockout mice were incubated with the indicated concentrations of MDA-MB 231 or MDA-MB 435 CM. After 5 days, fibrocytes were counted. Values are mean ± SEM, n=3, * indicates $p < 0.05$ and ** $p < 0.01$ compared to the control (t-test).

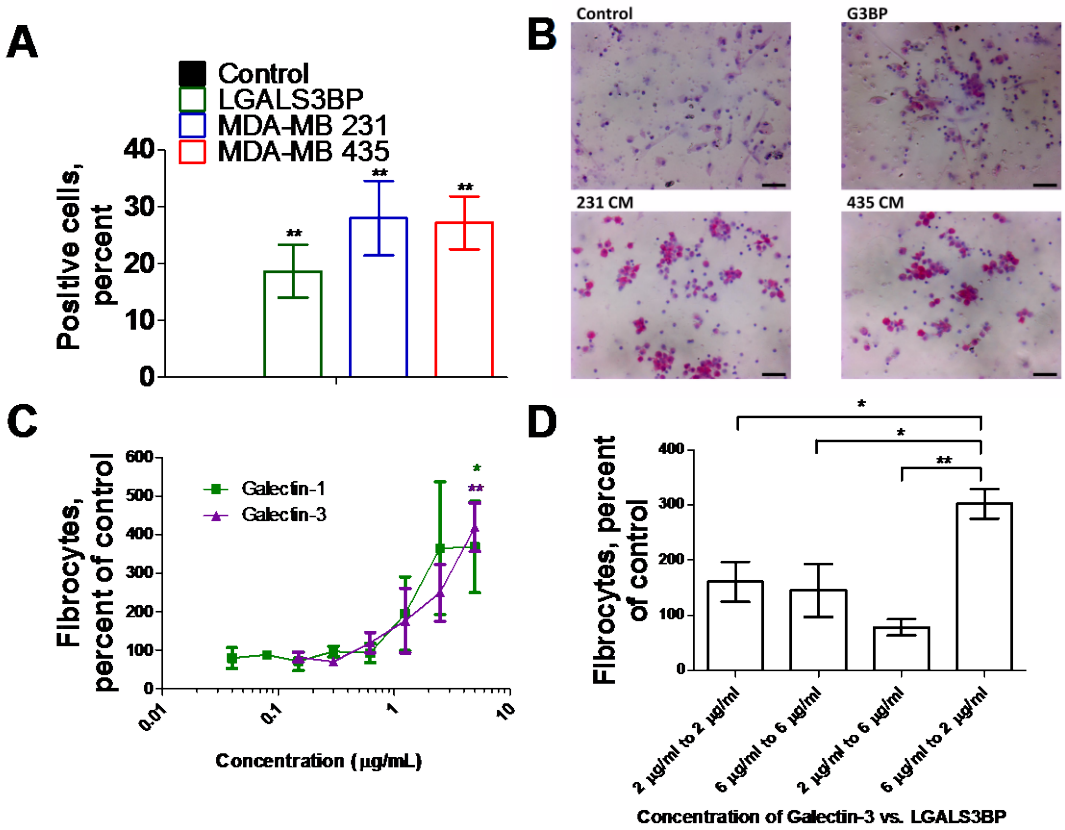

Figure 46. LGALS3BP, 231 CM, and 435 CM increase CD209 staining, and recombinant galectin-3 and galectin-1 potentiate fibrocyte differentiation.
(A) LGALS3BP, 231 CM, and 435 CM increase CD209 staining on PBMC by immunohistochemistry. Values are mean ± SEM, n=4, ** $p < .01$, compared to the SFM control (two-tailed t-test). (B) Panel shows representative images from slides used for (A). Bars are 50 µm. (C) The effects of recombinant galectin-3 and recombinant galectin-1 on human fibrocyte differentiation were assessed as in Figure 34. Values are mean ± SEM, n=8, * indicates $p < 0.05$, ** $p < 0.01$ compared to the control (t-test). (D) The indicated mixtures of galectin-3 and LGALS3BP were assessed for their effects on fibrocyte differentiation, and fibrocyte counts were normalized to serum-free medium controls. Values are mean ± SEM, n=8. * indicates $p < 0.05$ and ** $p < 0.01$ compared to the control (t-test).

Galectin-3 and galectin-1 potentiate fibrocyte differentiation

Galectin-1 and galectin-3 are binding partners for LGALS3BP (249, 260). To determine if galectins -1 and -3 affect fibrocyte differentiation, we incubated PBMC with

recombinant human galectins -1 and -3 (261, 262). Galectin-1 and -3 significantly potentiated fibrocyte differentiation (Figure 46A). To determine how a mixture of galectin-3 and LGALS3BP would influence fibrocyte differentiation, recombinant galectin-3 and LGALS3BP were co-incubated with PBMC. Concentrations of galectin-3 that potentiated fibrocyte differentiation continued to potentiate fibrocyte differentiation when mixed with concentrations of LGALS3BP that inhibited fibrocyte differentiation (Figure 43 and 46). Galectin-3 did not potentiate fibrocyte differentiation when mixed with a 3-fold higher quantity of LGALS3BP (Figure 46B). This suggests that the fibrocyte-potentiating effect of galectin-3 competes with the fibrocyte-inhibiting effect of LGALS3BP.

Increased LGALS3BP expression at the interface between breast cancer and scar tissue

To determine how tumor cells, LGALS3BP, galectin-3, and fibrocytes interact in human tumors, we stained sections of human infiltrative ductal carcinomas for CD45RO, collagen-I, galectin-3, and LGALS3BP. For all biopsies tested, the tumor cells strongly expressed LGALS3BP.

The staining intensity of LGALS3BP increased at the interface of tumor cells and stroma, particularly where tumor cells were invading through layers of collagen-rich stroma (Figure 47). 'X' indicates the tumor, the arrow indicates tumor infiltration into scar tissue, and '*' indicates areas with fibrocytes. Galectin-3 colocalized with the fibrocyte markers CD45RO and collagen-I (Figure 47). These data suggest that in some breast tumors, LGALS3BP expression is increased at the interface between the tumor and desmoplastic tissue, and that fibrocytes are reduced when LGALS3BP expression is increased. Intriguingly, galectin-3, which we observed to potentiate fibrocyte differentiation, colocalized with fibrocytes (Figure 47).

Figure 47. **Breast cancer tumor sections visualized by immunofluorescence show increased LGALS3BP at the edge of tumors.**
Human infiltrative ductal carcinoma tumor specimens were sectioned and stained for CD45RO, collagen WHAT type, LGALS3BP, and galectin-3. Images are (A) Hematoxylin and eosin stain of a representative biopsy section, (B) immunofluorescence for collagen (red) and CD45RO (green), and (C) immunofluorescence for LGALS3BP (red) and galectin-3 (green). Yellow indicates co-localization. The box in (A) indicates area of magnification, 'X' indicates the tumor, the arrow indicates tumor infiltration into scar tissue, and '*' indicates areas with fibrocytes. Bar in A is 200 μm and bars in B and C are 50 μm.

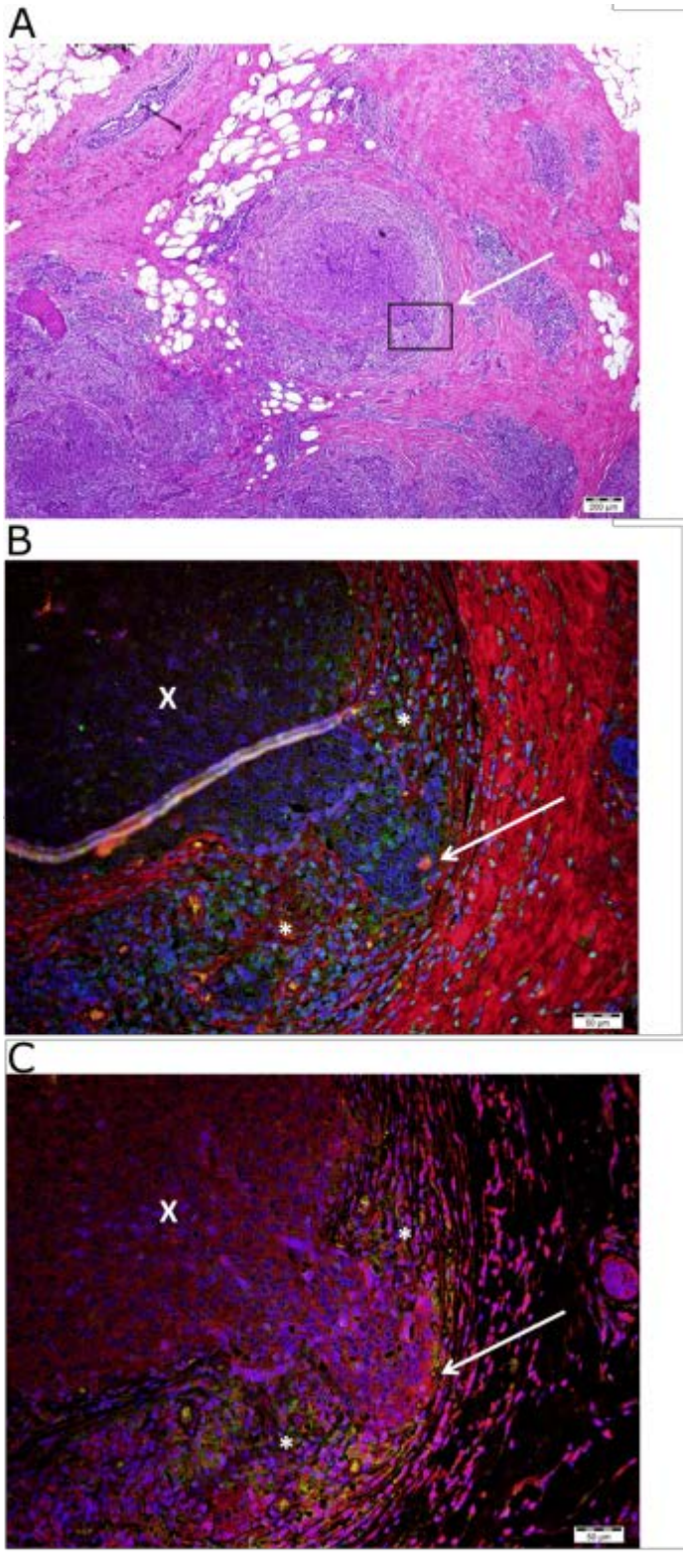
A
B
X
*
*
C
X
*
*

Discussion

In this report, we show that several human tumor cell lines secrete activity that inhibits the differentiation of human monocytes into fibrocytes. For a metastatic breast cell line and a metastatic melanoma cell line, the majority of the activity is LGALS3BP. LGALS3BP produced by cancer cells appears to act through the CD209 receptor to inhibit fibrocyte differentiation. LGALS3BP's binding partner, galectin-3, is upregulated in fibrotic tissue surrounding breast cancer tumors, and promotes fibrocyte differentiation at physiological concentrations. In breast cancer biopsies, LGALS3BP is concentrated at the edge of the tumor in regions with fewer fibrocytes. Taken together, this suggests that LGALS3BP may inhibit fibrocyte differentiation to facilitate metastasis in breast cancer and melanoma.

LGALS3BP (Mac2-BP, Antigen 90K) is a secreted member of the scavenger-receptor cysteine-rich (SRCR) family of proteins (249). LGALS3BP binds to galectins -1 and -3 (263), both collagen and fibronectin (264), and increases cell adhesion (260). Mouse knockouts of LGALS3BP show higher circulating levels of TNF-alpha, IL-12, and IFN-γ, suggesting multiple roles in regulating the immune system (151).

MCF-7 and DCIS.com cells, which are derived from non-metastatic breast cancers (110, 111), accumulate relatively low extracellular levels of LGALS3BP, while MDA-MB 231 cells, which are derived from a metastatic breast cancer (103), accumulate high extracellular levels of LGALS3BP (265-271). Patients with metastatic breast cancer tend to have abnormally high serum levels of LGALS3BP (139, 249). MDA-MB 435 accumulates high concentrations of extracellular LGALS3BP compared to other cancer

cell lines (272), and patients with metastatic melanoma have higher serum LGALS3BP than patients with benign skin cancer (126). In patients with breast cancer (273, 274), ovarian cancer (275-278), or melanoma (279-281), serum LGALS3BP concentrations increase during the progression to metastasis (137, 282). An intriguing possibility is that LGALS3BP may play a role in metastasis by inhibiting fibrocyte differentiation.

The Hill coefficient of recombinant LGALS3BP for fibrocyte inhibition is 6.5, but 231 and 435 CM have Hill coefficients close to 1. Fractions of 231 CM containing LGALS3BP have a Hill coefficient of 4.6. Both 231 CM and 435 CM contain a factor (or factors) that potentiate fibrocyte differentiation (Figure 39), suggesting that perhaps LGALS3BP competes with these factors to produce a Hill coefficient of ~1. Recombinant LGALS3BP, 231 CM, and 435 CM all increase CD209 staining on monocytes, suggesting that LGALS3BP may cooperatively bind to monocytes by increasing CD209 expression.

LGALS3BP secreted from MDA-MB 231 cells has a higher apparent mass than recombinant LGALS3BP produced in CHO cells, despite the two having an identical primary structure. Since LGALS3BP is glycosylated (129), this suggests that the LGALS3BPs from the two cell lines have different glycosylations and/or other posttranslational modifications. MDA-MB 231 and 435 secrete ~1 µg/ml of LGALS3BP into conditioned media, and 231 and 435 CM have an IC50 for fibrocyte differentiation of ~0.3% (Figures 34 and 35). Taken together, these results indicate that the IC50 for LGALS3BP should be ~0.3% x 1 µg/ml = ~3 ng/ml. Recombinant LGALS3BP's IC50 for fibrocyte inhibition was 300 ng/ml. This then suggests that glycosylation and/or posttranslational modification of LGALS3BP may affect its ability to inhibit fibrocyte

differentiation. In agreement with this, LGALS3BP produced by cancer cells has at least a fourfold higher affinity for CD209 (DCSIGN) receptors than LGALS3BP produced by non-cancer cells (129). The CD209 receptor, which we found to be necessary for the ability of LGALS3BP to inhibit fibrocyte differentiation, is activated by posttranslational glycosylations (258). A reasonable possibility is thus that the posttranslational glycosylations of LGALS3BP produced in CHO and MDA-MB 231 cells have different affinities for CD209, resulting in the observed differences in IC50's.

Galectin-3 is expressed by monocytes and macrophages (283). Serum galectin-3 is upregulated in heart disease and other fibrosing diseases (284), and inhibitors of galectin-3 are currently in clinical trials for the treatment of fibrosing diseases (285, 286). While serum galectin-3 is 100-900 ng/ml (261), we observed potentiation of fibrocyte differentiation at 2.5 to 5 μg/ml. Similar concentrations of galectin-3 are necessary to induce changes in other cells (262), suggesting that either the effects of galectin-3 we and others observed in tissue culture are not physiological, or that extracellular concentrations of galectin-3 in some tissues may be much higher than in the serum.

If galectin-3 levels in a tissue are high enough to potentiate fibrocyte differentiation, this would suggest that high levels of galectin-3 could potentiate fibrosis in part by potentiating fibrocyte differentiation. Since we observed that galectin-1 also

potentiates fibrocyte differentiation, high levels of galectin-1 may similarly potentiate fibrosis.

Together, this work elucidates a signal and receptor used by metastatic tumor cells to block a response of the innate immune system. An intriguing possibility is that blocking LGALS3BP may decrease the ability of tumor cells to inhibit the desmoplastic response and metastasize. Conversely, LGALS3BP might be useful to decrease fibrocyte differentiation and thus decrease fibrosis. Since galectin-3 and galectin-1 potentiate fibrocyte differentiation, these proteins might be useful to inhibit metastasis, although with the danger that they might promote fibrosis.

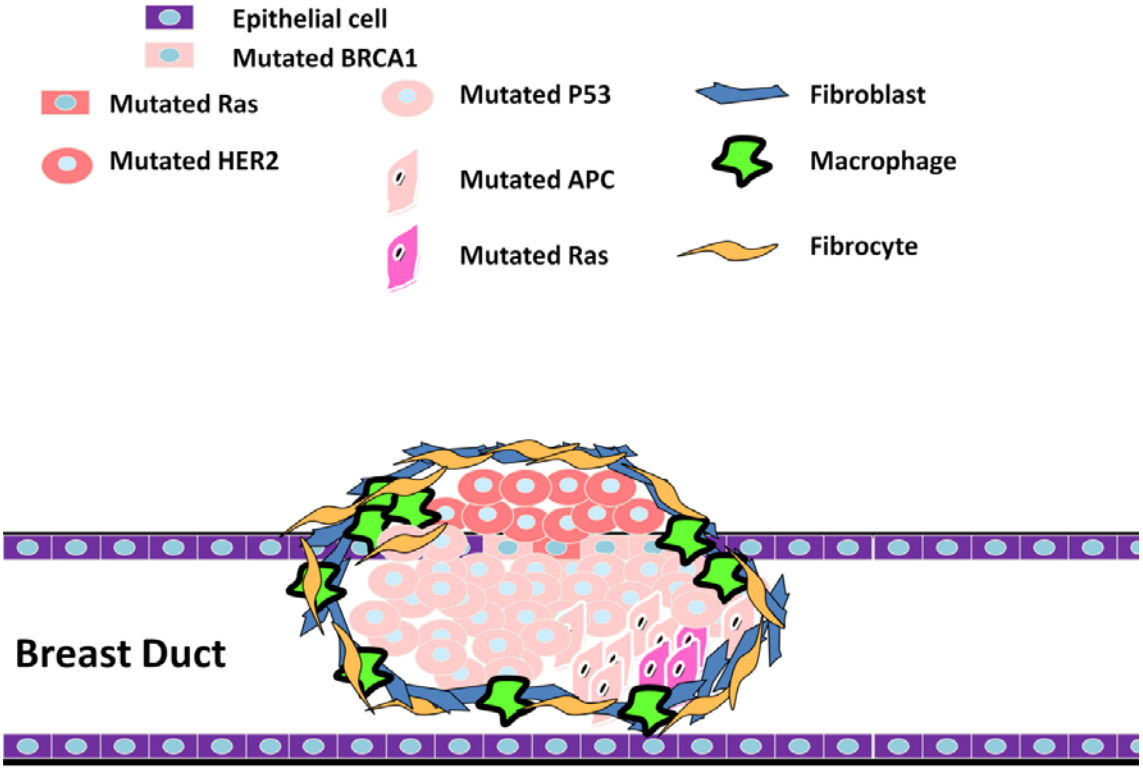

Model 2. Model of breast cancer surrounded by fibrotic sheath.
This model of pre-metastatic breast cancer shows a heterogeneous tumor composed of epithelial duct cells that have undergone different mutations. This tumor has been identified by the immune system, and quarantined behind a fibrotic sheath composed of fibroblasts, fibrocytes, and inflammatory macrophages, together comprising scar tissue.

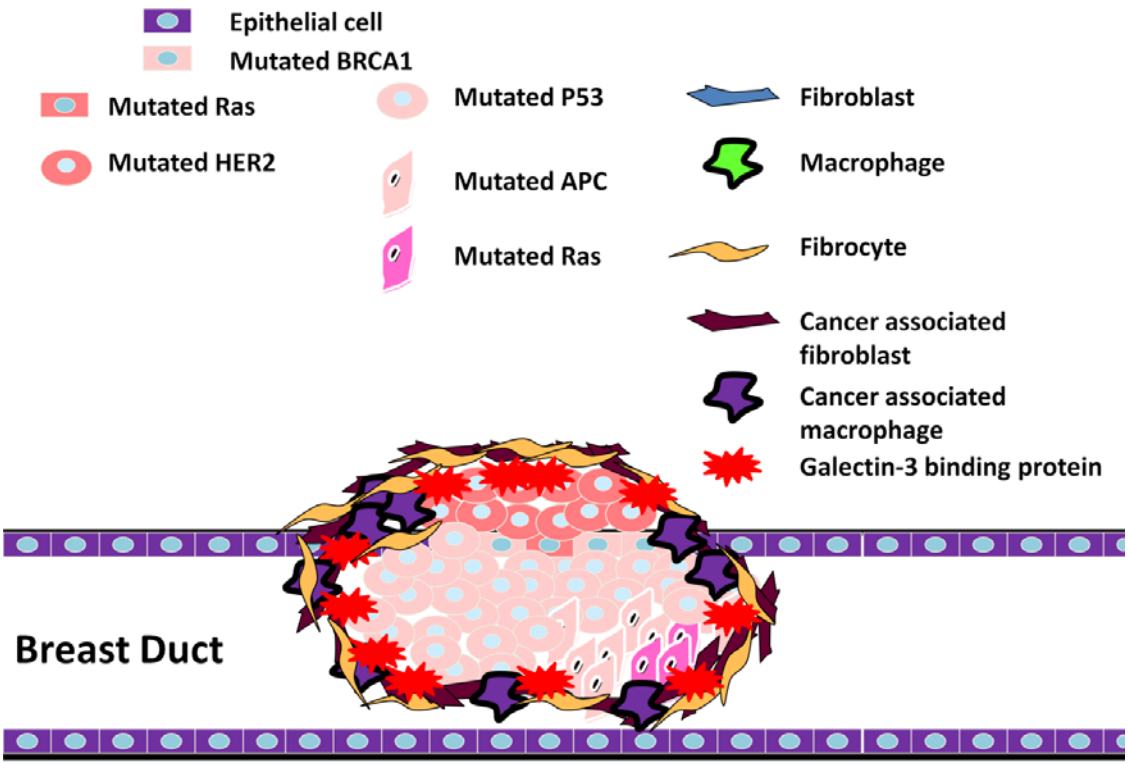

Model 3. Model of fibrotic sheath around breast cancer becoming co-opted or suppressed by tumor.
The pre-metastatic breast cancer has converted the fibroblasts and inflammatory macrophages into cancer associated fibroblasts and anti-inflammatory macrophages, both of which act as myeloid derived suppressor cells (MDSC). Increased secretion of galectin03 binding protein at the tumor edge inhibits fibrocyte differentiation as well, further weakening the scar tissue.

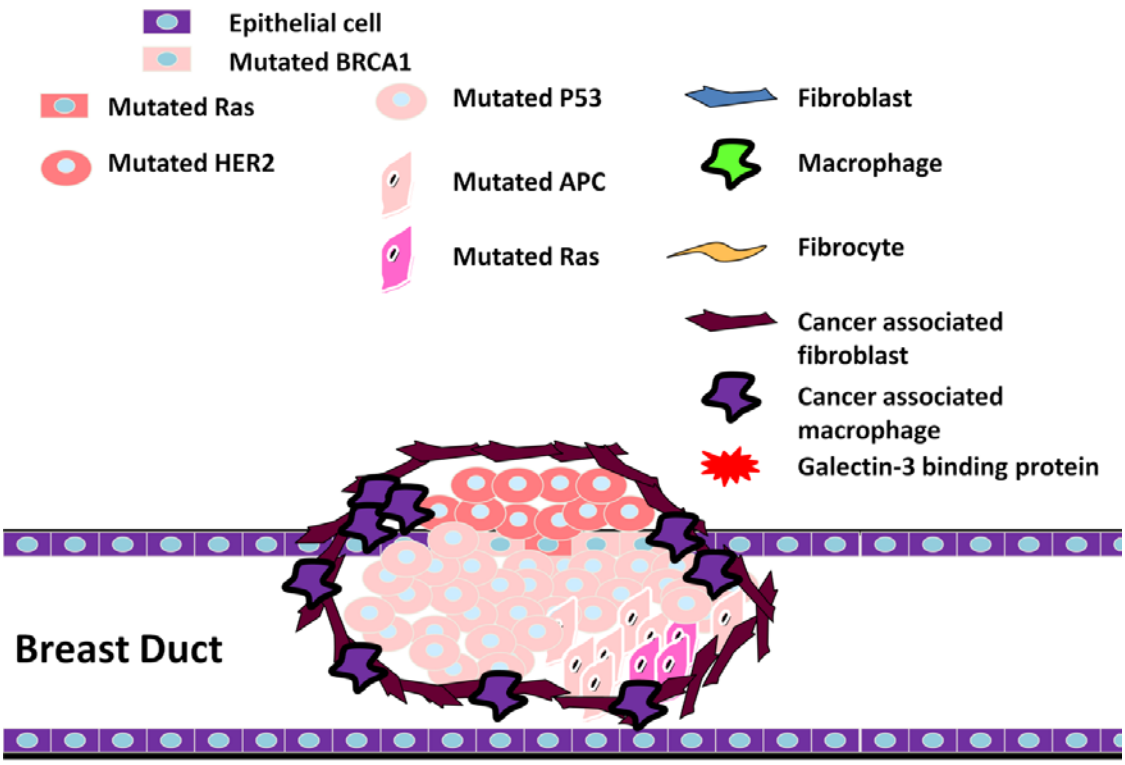

Model 4. Model of breast cancer metastasis through fibrotic sheath.
With fibrocytes inhibited, and fibroblasts and macrophages co-opted, then cancer cells are free to metastasize to neighboring or distant tissues.

CHAPTER VI

CONCLUSIONS AND FUTURE DIRECTIONS

Conclusions

Fibrosing diseases are involved in 45% of deaths in the US, and there are currently few FDA approved treatments for these diseases (20, 21). Chronic wounds affect more than 6.5 million US patients per year, and annually cost more than $25 billion to treat (17). Cancer is diagnosed in 1.5 million Americans annually, is involved in 25% of US deaths, and has an economic cost of $216 billion annually (1, 2). Metastases are responsible for the majority of cancer caused deaths (3). In some cases, the innate immune system can recognize and encapsulate tumors in a sheath of desmoplastic scar tissue (4). Thus, there is compelling reason to study scar tissue, and develop treatments to inhibit or promote scar tissue, as treatments for each of fibrosing diseases, wound healing, and cancer.

Scar tissue is a heterogeneous mixture of fibroblasts, fibrocytes, and macrophages, each of which are differentially regulated by inflammatory proteases (287). Monocyte-derived fibrocytes are found in scars (287), wound healing environments (22, 27, 28) and at tissue near a tumor edge (7, 8, 11). Increased fibrocyte formation correlates with increased scar tissue formation (185) and faster wound healing (32).

Tryptase, thrombin, PAR-1 signaling, and PAR-2 signaling have been implicated in the development of fibrosis through their effects on fibroblasts (61, 67, 68, 73, 80, 87-89, 215). Both PAR-1 and -2 have been implicated in liver fibrosis in mice (216, 217), and both PAR-1 knockout mice and PAR-2 knockout mice are less susceptible to both induced

heart disease and inflammation (218-220). Intratracheal administration of trypsin, tryptase, and thrombin cause inflammation, and inhibition of tryptase and thrombin attenuate this inflammation (63, 66, 82, 84). Inhibitors of tryptase (221-223) and thrombin (224), and antagonists of both PAR-1 (225) and PAR-2 (226) are patented for the treatment of fibrosis. Both tryptase (227) and thrombin (228) inhibitors are currently in clinical trials for the treatment of fibrosis. However, while PAR-1 and PAR-2 antagonists have been suggested as therapeutics (229, 230), neither is currently in clinical trials. PAR-1 and PAR-2 thus mediate both fibroblast proliferation and fibrocyte differentiation, two major components of scar tissue (195, 231-233). Our work thus strongly supports and expands the idea that tryptase, thrombin, PAR-1 signaling, and PAR-2 signaling potentiate wound healing and fibrosis.

The mechanism that triggers the exuberant deposition of scar tissue in fibrotic disease is an unresolved question. We have shown that tryptase and thrombin potentiate fibrocyte differentiation and collagen production, and that this potentiation occurs even in the presence of levels of serum or SAP that completely inhibit fibrocyte differentiation. Tryptase and thrombin potentiation appears to act directly on monocytes, and is mediated by PAR-2 and PAR-1, respectively. Tryptase and thrombin potentiate fibrocyte differentiation at biologically relevant concentrations and exposure times.

Trypsin, tryptase, and thrombin also bias monocyte and macrophage differentiation towards a pro-fibrotic M2a phenotype. These proteases change the expression of markers on macrophages, and change the secretion profile of macrophages. Trypsin, tryptase, and thrombin increase fibronectin staining of macrophages and

fibrocytes, whether the population of cells differentiated from unpolarized, M1, or M2 macrophages. Tryptase increases IL-4 concentration in both unpolarized and M1 macrophages, while trypsin and tryptase lower both IL-10 and IL-12 concentration from M2 and M1 macrophages, respectively. Additionally, both PAR-1 agonist and PAR-2 agonist increase the concentration of IL-4, IL-10, and IL-12 from unpolarized macrophages. When combined, the data indicate that these proteases bias monocyte differentiation towards M2a macrophages and fibrocytes, each of which is a pro-fibrotic and inflammatory cell. Not all proteases are pro-fibrotic, as pepsin and chymotrypsin do not activate PAR-1 or PAR-2 (212-214), and do not potentiate fibrocyte differentiation (194). These results suggest a triggering mechanism for fibrocyte-mediated wound healing and fibrotic lesions, where thrombin from clotting blood or tryptase from a sufficient amount of mast cell degranulation override SAP inhibition and initiate fibrocyte differentiation.

Activation of PAR-1 and PAR-2 seem to independently effect macrophage differentiation. Trypsin, tryptase, and PAR-2 agonist activation of PAR-2 on macrophages produced higher quantities of IL-4 and lower levels of IL-10 regardless of previous M-CSF or GM-CSF exposure. Thrombin and PAR-1 agonist activation of PAR-1 produced lower levels of IL-4 and higher levels of IL-10 regardless of previous M-CSF or GM-CSF exposure. These data suggest that activation of PAR-1 or PAR-2 triggers a slightly different fibrotic response in macrophages.

That tryptase and thrombin compete with SAP suggests that the PAR-1 or PAR-2 pathway is capable of potentiating fibrocyte differentiation in the presence of SAP.

Trypsin potentiates fibrocyte differentiation in the presence of SAP after a brief exposure (Figure 20), but not over the course of a 5-day differentiation (Figure 15). Tryptase and thrombin potentiated fibrocyte differentiation under all time-course, SAP, and serum conditions. Tryptase and trypsin appear to signal through the same receptor (73). Whether our results imply that different PAR-2 isoforms exist, or that PAR-2 can differentiate between trypsin and tryptase signaling, is unclear.

Systemic mastocytosis involves the degranulation of mast cells throughout the body (234), and is associated with serious local—and moderate systemic—fibrosis (235, 236). Mast cell degranulation causes the release of tryptase. Serum tryptase in healthy patients is ~2 ng/ml, while mastocytosis patients have 20 to 100 ng/ml (237, 238). Our observation that 4 to 56 ng/ml tryptase potentiates fibrocyte differentiation suggests that the fibrosis seen in mastocytosis patients may be due to tryptase inducing fibrocyte differentiation.

Fibrocytes and scar tissue are also involved in cancer metastasis. Tumors are composed not primarily of cancer cells but rather of associated cells which provide scaffolding on which the cancer cells grow. These myeloid derived suppressor cells promote angiogenesis and assist with metastasis by chaperoning cancer cells through the bloodstream (288, 289). Signals in the tumor microenvironment suppress macrophage activity or direct macrophages and fibrocytes to aid the tumor rather than to hinder it.

As tumors progress, cancer cells undergo additional mutations, and progressively lose control over cell-cycle regulation and basic cellular control functions (91). These mutations can change multiple aspects of the tumor's biology, including the milieu of

signals in the tumor microenvironment (290-294). These protein expression changes have the effect of changing the tumor cell from a more epithelial phenotype (terminally differentiated cells which display tissue specific markers) to a more mesenchymal phenotype (stem-like progenitor cells which lack tissue specific markers) (92, 93). The tumor itself may break and expand into adjacent tissues or into the surrounding blood vessels (5). Thus, metastasis changes the protein expression profile of the cancer cells, the tumor, and of the surrounding stromal cells (295). These stromal cells include macrophages, fibrocytes, and fibroblasts, which can be essential for tumor maintenance, signaling, and metastasis (296-299). LGALS3BP concentration is upregulated in the serum of patients with metastatic breast cancer and melanoma.

MDA-MB 231 secretes more LGALS3BP compared to MCF-7 and DCIS.com cell lines (265-271), and MDA-MB 435 has high levels of LGALS3BP (272). The MDA-MB 435 cell line has previously been classified as both a breast cancer cell line, but is currently considered a melanoma cell line (105, 106). Breast cancer (273, 274), ovarian cancer (275-278), and melanoma (279-281) each secrete increasing amounts of LGALS3BP during the progression to metastasis (137, 282). Mouse knockouts of LGALS3BP show higher circulating levels of TNF-alpha, IL-12, and interferon-gamma, suggesting a definite role in regulating the immune system (151).

LGALS3BP produced by cancer cells is differentially glycosylated due to genetic changes affecting the endoplasmic reticulum of cancer cells, and due to the altered biochemistry and metabolic environment within cancer cells (129). LGALS3BP produced by cancer cells has a greater affinity for CD209 (DCSIGN) receptors (129). While cancer

conditioned media containing LGALS3BP inhibits fibrocyte differentiation in mouse spleen cells, the same media does not inhibit fibrocyte differentiation from CD209 -/- spleen cells. LGALS3BP secreted by MDA-MB 231 breast cancer cells is not alternatively spliced or prematurely truncated. While cancer conditioned media potently inhibits fibrocyte differentiation, and immunodepleting LGALS3BP abrogates this inhibition, recombinant LGALS3BP produced in CHO cells inhibits fibrocyte differentiation to a smaller degree.

While fibrocytes appear to inhibit carcinoma metastasis, fibrocyte-like cells can act as myeloid derived suppressor cells (MDSC) in Ewing's sarcoma, increasing metastasis (300). Further, LGALS3BP is a negative indicator of survival in carcinomas, but is a positive indicator of survival in Ewing's sarcoma (301). There role of LGALS3BP and fibrocytes in cancer metastasis is far from settled.

Galectin-3 is a widely expressed protein secreted by epithelial cells. Galectin-3 is an upregulated bio-marker in heart disease specifically and in other fibrosing diseases generally (284). While Galectin-3 concentration in the blood is 100-900 ng/ml (261), we observed fibrocyte differentiation at 2.5 to 5 μg/ml. Similar concentrations of galectin-3 are necessary to induce changes in other cells, suggesting that local concentrations of galectin-3 may be much higher in order to potentiate fibrocyte differentiation in tumor stroma desmoplasia (262).

Galectin-3 knockout mice have decreased granulocyte number, increased susceptibility to *S. pneumonaie* infection, and lack macrophage activation and chemotaxis under stimulation by IL-4 and IL-13, and have fewer atherosclerotic lesions of the heart

(151). Additionally, knockout mice have lower numbers of leukocytes and monocytes after thioglycollate broth administration than do control mice (151).

In this dissertation, I have demonstrated that the CM from cancer cell lines is capable of preferentially inhibiting fibrocyte differentiation. Metastatic cancer lines tend to inhibit fibrocyte differentiation more than benign cancer cell lines. LGALS3BP is upregulated in metastatic cancers (including breast cancers and melanomas) and is the factor that inhibits fibrocyte differentiation in the CM of MDA-MB 231 breast cancer cells and MDA-MB 435 melanoma cells. Physiological concentrations of LGALS3BP inhibit fibrocyte differentiation, and physiological concentrations of galectin-3 potentiate fibrocyte differentiation. Additionally, LGALS3BP is upregulated at the interface between breast tumors and scar tissue, and LGALS3BP concentration is highest at portions where the fewest fibrocytes are present.

I have also demonstrated that physiological concentrations of proteases potentiate fibrocyte differentiation through the PAR-1 and PAR-2 receptors. Trypsin, tryptase, and thrombin compete with SAP and human serum to potentiate fibrocyte differentiation. Additionally, trypsin, tryptase and thrombin potentiate fibrocyte differentiation over physiological time ranges. These proteases are upregulated in both wound healing and fibrosing diseases.

Fibrosing diseases are involved in 45% of deaths in the United States. Cancer is involved in 25% of deaths in the United States. Even healthy individuals regularly need to heal wounds, and treatment of wounds costs the United States about $25 billion annually. This dissertation approaches these diseases by using LGALS3BP, produced by

metastatic cancers, as a possible treatment for fibrosing diseases. More specifically, this dissertation analyzes the effect of LGALS3BP, which is upregulated in cancer, and proteases, which are upregulated in fibrosis and wound healing, on the innate immune system in humans and mice. Future work will expand the knowledge about the mechanisms of LGALS3BP fibrocyte inhibition and protease-induced fibrocyte potentiation, with the ultimate goal of developing treatments for metastatic cancers and fibrosing diseases.

Future Directions

Several interesting avenues remain to be explored for both the role of fibrocytes and cancer and the role of proteases in scar tissue formation.

One future project idea would be to determine which glycosylated amino acids on LGALS3BP are necessary to inhibit fibrocyte differentiation, and determine whether these amino acids are only glycosylated in cancer cells. It is unknown how LGALS3BP acquires altered glycosylations within the cancer cell. Does the altered chemistry and metabolism within cancer cells change LGALS3BP's glycosylations, or do cancer cells attach different glycosylations to LGALS3BP through mutations in the ER, or both? Additionally, linking specific mutations in cancer metabolism or ER function to these changes in LGALS3BP metabolism could provide a new biomarker for metastatic potential in cancer patients. Alternatively, if the metabolic environment inside the cancer cell is responsible for the glycosylation changes to LGALS3BP, that too would constitute a novel mechanism for the treatment of cancer.

Recombinant LGALS3BP is a difficult protein to produce, both in our labs and in other labs (Private communication, R&D Systems). However, recombinant production of LGALS3BP would allow us to analyze differentially glycosylated LGALS3BP, and how these glycosylated residues interact with CD209, or other receptors with which LGALS3BP might interact.

Another possible project would be to analyze whether LGALS3BP knockout mice are deficient in metastasis, or whether galectin-3 knockout mice are resistant to fibrosis. Both LGALS3BP and galectin-3 mediate fibrocyte differentiation, and using a

different model organism would help explain how fibrocytes, LGALS3BP, and galectin-3 operate in a disease model of cancer and fibrosis.

LGALS3BP, or molecules with mimic LGALS3BP, could be useful therapeutics for fibrosing diseases or metastatic cancers. Since LGALS3BP is upregulated by metastatic cancers, and increased concentrations of LGALS3BP are associated with decreased 5-year survival, then LGALS3BP is an obvious target for antibody therapy in patients with cancer. Similarly, LGALS3BP could be a potential therapeutic for fibrosing diseases, for which there currently are few FDA treatments. (20, 21) Even if the use of LGALS3BP directly does not lead to a useful treatment for either fibrosing diseases or cancer, understanding of this new element of immune evasion would be an important step in basic immunology.

MDA-MB 231, MDA-MB 435, and SW480 cell lines secrete factors into their conditioned media that potentiate fibrocyte differentiation. Both SW480 CM and unknown protein(s) in 231 and 435 CM potentiate fibrocyte differentiation through an unknown mechanism. An unknown factor secreted by the U87-MG brain cancer cell line appears to have a mild inhibitory effect on fibrocyte differentiation. While it is certain that the potentiating factor in SW480, MDA-MB 231, and MDA-MB 435 is a protein, it appears resistant to heat treatment.

We have shown that 231 CM, 435 CM, and LGALS3BP inhibit fibrocyte differentiation. If monocytes are not differentiating into fibrocytes, what type of cells are they differentiating into? Monocytes are components of the innate immune system, but what about the effect 231 CM, 435 CM, or LGALS3BP has on the adaptive immune

system? Does cancer modulate the markers for macrophages or dendritic cells in tumors? Does cancer CM modulate T-cell proliferation or secretion profiles?

Another possible project would be to research the PAR signal transduction cascade. While inhibitors of proteases and PAR are already patented, the specific signaling cascade that promotes fibrocyte differentiation within the cell is largely unknown. Modulators of this pathway could be used a potential therapeutics, and could be a patentable invention.

REFERENCES

1. Howlader N, N. A., Krapcho M, Neyman N, Aminou R, Waldron W, Altekruse SF, Kosary CL, Ruhl J, Tatalovich Z, Cho H, Mariotto A, Eisner MP, Lewis DR, Chen HS, Feuer EJ, Cronin KA, Edwards BK. 2011. SEER Cancer Statistics Review, 1975-2008, National Cancer Institute. Bethesda, MD.

2. Siegel, R., D. Naishadham, and A. Jemal. 2013. Cancer statistics, 2013. *CA: a cancer journal for clinicians* 63: 11-30.

3. Jemal, A., R. Siegel, E. Ward, Y. Hao, J. Xu, and M. J. Thun. 2009. Cancer statistics, 2009. *CA: a cancer journal for clinicians* 59: 225-249.

4. Schedin, P., and A. Elias. 2004. Multistep tumorigenesis and the microenvironment. *Breast Cancer Res* 6: 93-101.

5. Kim, B. G., H. J. An, S. Kang, Y. P. Choi, M. Q. Gao, H. Park, and N. H. Cho. 2011. Laminin-332-rich tumor microenvironment for tumor invasion in the interface zone of breast cancer. *Am J Pathol* 178: 373-381.

6. Coulson-Thomas, V. J., Y. M. Coulson-Thomas, T. F. Gesteira, C. A. de Paula, A. M. Mader, J. Waisberg, M. A. Pinhal, A. Friedl, L. Toma, and H. B. Nader. 2011. Colorectal cancer desmoplastic reaction up-regulates collagen synthesis and restricts cancer cell invasion. *Cell Tissue Res*.

7. Walker, R. A. 2001. The complexities of breast cancer desmoplasia. *Breast Cancer Res* 3: 143-145.

8. Coulson-Thomas, V. J., Y. M. Coulson-Thomas, T. F. Gesteira, C. A. de Paula, A. M. Mader, J. Waisberg, M. A. Pinhal, A. Friedl, L. Toma, and H. B. Nader. 2011.

Colorectal cancer desmoplastic reaction up-regulates collagen synthesis and restricts cancer cell invasion. *Cell Tissue Res* 346: 223-236.

9. Bellini, A., and S. Mattoli. 2007. The role of the fibrocyte, a bone marrow-derived mesenchymal progenitor, in reactive and reparative fibroses. *Lab Invest* 87: 858-870.

10. Cichon, M. A., A. C. Degnim, D. W. Visscher, and D. C. Radisky. 2010. Microenvironmental influences that drive progression from benign breast disease to invasive breast cancer. *J Mammary Gland Biol Neoplasia* 15: 389-397.

11. Shao, Z. M., M. Nguyen, and S. H. Barsky. 2000. Human breast carcinoma desmoplasia is PDGF initiated. *Oncogene* 19: 4337-4345.

12. Drew, P., J. Posnett, and L. Rusling. 2007. The cost of wound care for a local population in England. *Int Wound J* 4: 149-155.

13. Hurd, T., and J. Posnett. 2009. Point prevalence of wounds in a sample of acute hospitals in Canada. *Int Wound J* 6: 287-293.

14. Vowden, K. R., and P. Vowden. 2009. The prevalence, management and outcome for acute wounds identified in a wound care survey within one English health care district. *J Tissue Viability* 18: 7-12.

15. Vowden, K. R., and P. Vowden. 2009. A survey of wound care provision within one English health care district. *J Tissue Viability* 18: 2-6.

16. Srinivasaiah, N., H. Dugdall, S. Barrett, and P. J. Drew. 2007. A point prevalence survey of wounds in north-east England. *J Wound Care* 16: 413-416, 418-419.

17. Sen, C. K., G. M. Gordillo, S. Roy, R. Kirsner, L. Lambert, T. K. Hunt, F. Gottrup, G. C. Gurtner, and M. T. Longaker. 2009. Human skin wounds: a major and snowballing threat to public health and the economy. *Wound Repair Regen* 17: 763-771.

18. Guo, S., and L. A. Dipietro. 2010. Factors affecting wound healing. *J Dent Res* 89: 219-229.

19. Sakai, N., T. Wada, H. Yokoyama, M. Lipp, S. Ueha, K. Matsushima, and S. Kaneko. 2006. Secondary lymphoid tissue chemokine (SLC/CCL21)/CCR7 signaling regulates fibrocytes in renal fibrosis. *Proc Natl Acad Sci U S A* 103: 14098-14103.

20. Wynn, T. A. 2004. Fibrotic disease and the T(H)1/T(H)2 paradigm. *Nat Rev Immunol* 4: 583-594.

21. Spagnolo, P. 2015. Novel treatments for idiopathic pulmonary fibrosis. *The American journal of medicine*.

22. Reilkoff, R. A., R. Bucala, and E. L. Herzog. 2011. Fibrocytes: emerging effector cells in chronic inflammation. *Nat Rev Immunol* 11: 427-435.

23. Strieter, R. M., E. C. Keeley, M. D. Burdick, and B. Mehrad. 2009. The role of circulating mesenchymal progenitor cells, fibrocytes, in promoting pulmonary fibrosis. *Trans Am Clin Climatol Assoc* 120: 49-59.

24. Paget, J. 1853. *Lectures on Surgical Pathology Delivered at the Royal College of Surgeons of England*. Wilson and Ogilvy, London.

25. Hamilton, J. A. 2008. Colony-stimulating factors in inflammation and autoimmunity. *Nat Rev Immunol* 8: 533-544.

26. Murray, P. J., and T. A. Wynn. 2011. Protective and pathogenic functions of macrophage subsets. *Nat Rev Immunol* 11: 723-737.

27. Abe, R., S. C. Donnelly, T. Peng, R. Bucala, and C. N. Metz. 2001. Peripheral blood fibrocytes: differentiation pathway and migration to wound sites. *J Immunol* 166: 7556-7562.

28. Bucala, R., L. A. Spiegel, J. Chesney, M. Hogan, and A. Cerami. 1994. Circulating fibrocytes define a new leukocyte subpopulation that mediates tissue repair. *Mol Med* 1: 71-81.

29. Moeller, A., S. E. Gilpin, K. Ask, G. Cox, D. Cook, J. Gauldie, P. J. Margetts, L. Farkas, J. Dobranowski, C. Boylan, P. M. O'Byrne, R. M. Strieter, and M. Kolb. 2009. Circulating fibrocytes are an indicator of poor prognosis in idiopathic pulmonary fibrosis. *Am J Respir Crit Care Med* 179: 588-594.

30. Quan, T. E., S. E. Cowper, and R. Bucala. 2006. The role of circulating fibrocytes in fibrosis. *Curr Rheumatol Rep* 8: 145-150.

31. Yang, L., P. G. Scott, C. Dodd, A. Medina, H. Jiao, H. A. Shankowsky, A. Ghahary, and E. E. Tredget. 2005. Identification of fibrocytes in postburn hypertrophic scar. *Wound Repair Regen* 13: 398-404.

32. Naik-Mathuria, B., D. Pilling, J. R. Crawford, A. N. Gay, C. W. Smith, R. H. Gomer, and O. O. Olutoye. 2008. Serum amyloid P inhibits dermal wound healing. *Wound Repair Regen* 16: 266-273.

33. Pilling, D., V. Vakil, and R. H. Gomer. 2009. Improved serum-free culture conditions for the differentiation of human and murine fibrocytes. *J Immunol Methods* 351: 62-70.

34. Cox, N., D. Pilling, and R. H. Gomer. 2012. NaCl Potentiates Human Fibrocyte Differentiation. *PLoS One* 7: e45674.

35. Maharjan, A. S., D. Pilling, and R. H. Gomer. 2011. High and low molecular weight hyaluronic acid differentially regulate human fibrocyte differentiation. *PLoS One* 6: e26078.

36. Pilling, D., C. D. Buckley, M. Salmon, and R. H. Gomer. 2003. Inhibition of fibrocyte differentiation by serum amyloid P. *Journal of immunology* 171: 5537-5546.

37. Shao, D. D., R. Suresh, V. Vakil, R. H. Gomer, and D. Pilling. 2008. Pivotal Advance: Th-1 cytokines inhibit, and Th-2 cytokines promote fibrocyte differentiation. *J Leukoc Biol* 83: 1323-1333.

38. Nelson, S. R., G. A. Tennent, D. Sethi, P. E. Gower, F. W. Ballardie, S. Amatayakul-Chantler, and M. B. Pepys. 1991. Serum amyloid P component in chronic renal failure and dialysis. *Clinica chimica acta; international journal of clinical chemistry* 200: 191-199.

39. Crawford, J. R., D. Pilling, and R. H. Gomer. 2012. FcgammaRI mediates serum amyloid P inhibition of fibrocyte differentiation. *J Leukoc Biol* 92: 699-711.

40. Jager, P. L., B. P. Hazenberg, E. J. Franssen, P. C. Limburg, M. H. van Rijswijk, and D. A. Piers. 1998. Kinetic studies with iodine-123-labeled serum amyloid P component in patients with systemic AA and AL amyloidosis and assessment of clinical

value. *Journal of nuclear medicine : official publication, Society of Nuclear Medicine* 39: 699-706.

41. Pilling, D., D. Roife, M. Wang, S. D. Ronkainen, J. R. Crawford, E. L. Travis, and R. H. Gomer. 2007. Reduction of bleomycin-induced pulmonary fibrosis by serum amyloid P. *J Immunol* 179: 4035-4044.

42. Gomer, R. H., D. Pilling, L. M. Kauvar, S. Ellsworth, S. D. Ronkainen, D. Roife, and S. C. Davis. 2009. A serum amyloid P-binding hydrogel speeds healing of partial thickness wounds in pigs. *Wound Repair Regen* 17: 397-404.

43. Moreira, A. P., K. A. Cavassani, R. Hullinger, R. S. Rosada, D. J. Fong, L. Murray, D. P. Hesson, and C. M. Hogaboam. 2010. Serum amyloid P attenuates M2 macrophage activation and protects against fungal spore-induced allergic airway disease. *The Journal of allergy and clinical immunology* 126: 712-721 e717.

44. Murray, L. A., R. Rosada, A. P. Moreira, A. Joshi, M. S. Kramer, D. P. Hesson, R. L. Argentieri, S. Mathai, M. Gulati, E. L. Herzog, and C. M. Hogaboam. 2010. Serum amyloid P therapeutically attenuates murine bleomycin-induced pulmonary fibrosis via its effects on macrophages. *PLoS One* 5: e9683.

45. Murray, L. A., Q. Chen, M. S. Kramer, D. P. Hesson, R. L. Argentieri, X. Peng, M. Gulati, R. J. Homer, T. Russell, N. van Rooijen, J. A. Elias, C. M. Hogaboam, and E. L. Herzog. 2011. TGF-beta driven lung fibrosis is macrophage dependent and blocked by Serum amyloid P. *Int J Biochem Cell Biol* 43: 154-162.

46. Mosser, D. M., and J. P. Edwards. 2008. Exploring the full spectrum of macrophage activation. *Nat Rev Immunol* 8: 958-969.

47. Mantovani, A., A. Sica, S. Sozzani, P. Allavena, A. Vecchi, and M. Locati. 2004. The chemokine system in diverse forms of macrophage activation and polarization. *Trends in immunology* 25: 677-686.

48. Geissmann, F., S. Gordon, D. A. Hume, A. M. Mowat, and G. J. Randolph. 2010. Unravelling mononuclear phagocyte heterogeneity. *Nat Rev Immunol* 10: 453-460.

49. Kharraz, Y., J. Guerra, C. J. Mann, A. L. Serrano, and P. Munoz-Canoves. 2013. Macrophage plasticity and the role of inflammation in skeletal muscle repair. *Mediators of inflammation* 2013: 491497.

50. Mann, C. J., E. Perdiguero, Y. Kharraz, S. Aguilar, P. Pessina, A. L. Serrano, and P. Munoz-Canoves. 2011. Aberrant repair and fibrosis development in skeletal muscle. *Skeletal muscle* 1: 21.

51. Ferrante, C. J., and S. J. Leibovich. 2012. Regulation of Macrophage Polarization and Wound Healing. *Advances in wound care* 1: 10-16.

52. Novak, M. L., and T. J. Koh. 2013. Macrophage phenotypes during tissue repair. *J Leukoc Biol* 93: 875-881.

53. Jaguin, M., N. Houlbert, O. Fardel, and V. Lecureur. 2013. Polarization profiles of human M-CSF-generated macrophages and comparison of M1-markers in classically activated macrophages from GM-CSF and M-CSF origin. *Cellular immunology* 281: 51-61.

54. Lolmede, K., L. Campana, M. Vezzoli, L. Bosurgi, R. Tonlorenzi, E. Clementi, M. E. Bianchi, G. Cossu, A. A. Manfredi, S. Brunelli, and P. Rovere-Querini. 2009. Inflammatory and alternatively activated human macrophages attract vessel-associated

stem cells, relying on separate HMGB1- and MMP-9-dependent pathways. *J Leukoc Biol* 85: 779-787.

55. David, S., and A. Kroner. 2011. Repertoire of microglial and macrophage responses after spinal cord injury. *Nature reviews. Neuroscience* 12: 388-399.

56. Rodriguez, J., N. Gupta, R. D. Smith, and P. A. Pevzner. 2008. Does trypsin cut before proline? *J Proteome Res* 7: 300-305.

57. Appel, W. 1986. Chymotrypsin: molecular and catalytic properties. *Clin Biochem* 19: 317-322.

58. Dunn, B. M. 2001. Overview of pepsin-like aspartic peptidases. *Curr Protoc Protein Sci* Chapter 21: Unit 21 23.

59. Drapeau, G. R. 1976. Protease from Staphyloccus aureus. *Methods Enzymol* 45: 469-475.

60. Drapeau, G. R. 1977. Cleavage at glutamic acid with staphylococcal protease. *Methods Enzymol* 47: 189-191.

61. Duitman, J., R. R. Ruela-de-Sousa, K. Shi, O. J. De Boer, K. S. Borensztajn, S. Florquin, M. P. Peppelenbosch, and C. A. Spek. 2014. Protease activated receptor-1 deficiency diminishes bleomycin-induced skin fibrosis. *Mol Med*.

62. Undas, A., K. Brummel, J. Musial, K. G. Mann, and A. Szczeklik. 2001. Blood coagulation at the site of microvascular injury: effects of low-dose aspirin. *Blood* 98: 2423-2431.

63. Moffatt, J. D., R. Lever, and C. P. Page. 2004. Effects of inhaled thrombin receptor agonists in mice. *Br J Pharmacol* 143: 269-275.

64. Scotton, C. J., M. A. Krupiczojc, M. Konigshoff, P. F. Mercer, Y. C. Lee, N. Kaminski, J. Morser, J. M. Post, T. M. Maher, A. G. Nicholson, J. D. Moffatt, G. J. Laurent, C. K. Derian, O. Eickelberg, and R. C. Chambers. 2009. Increased local expression of coagulation factor X contributes to the fibrotic response in human and murine lung injury. *J Clin Invest* 119: 2550-2563.

65. Howell, D. C., N. R. Goldsack, R. P. Marshall, R. J. McAnulty, R. Starke, G. Purdy, G. J. Laurent, and R. C. Chambers. 2001. Direct thrombin inhibition reduces lung collagen, accumulation, and connective tissue growth factor mRNA levels in bleomycin-induced pulmonary fibrosis. *The American journal of pathology* 159: 1383-1395.

66. Bogatkevich, G. S., A. Ludwicka-Bradley, P. J. Nietert, T. Akter, J. van Ryn, and R. M. Silver. 2011. Antiinflammatory and antifibrotic effects of the oral direct thrombin inhibitor dabigatran etexilate in a murine model of interstitial lung disease. *Arthritis Rheum* 63: 1416-1425.

67. Vu, T. K., D. T. Hung, V. I. Wheaton, and S. R. Coughlin. 1991. Molecular cloning of a functional thrombin receptor reveals a novel proteolytic mechanism of receptor activation. *Cell* 64: 1057-1068.

68. Coughlin, S. R. 1999. How the protease thrombin talks to cells. *Proc Natl Acad Sci U S A* 96: 11023-11027.

69. Lopez-Pedrera, C., M. A. Aguirre, P. Buendia, N. Barbarroja, P. Ruiz-Limon, E. Collantes-Estevez, F. Velasco, M. Khamashta, and M. J. Cuadrado. 2010. Differential expression of protease-activated receptors in monocytes from patients with primary antiphospholipid syndrome. *Arthritis Rheum* 62: 869-877.

70. Gallwitz, M., M. Enoksson, M. Thorpe, and L. Hellman. 2012. The extended cleavage specificity of human thrombin. *PLoS One* 7: e31756.

71. Hermes, B., I. Feldmann-Boddeker, P. Welker, B. Algermissen, M. U. Steckelings, J. Grabbe, and B. M. Henz. 2000. Altered expression of mast cell chymase and tryptase and of c-Kit in human cutaneous scar tissue. *The Journal of investigative dermatology* 114: 51-55.

72. Pesci, A., M. Majori, M. L. Piccoli, A. Casalini, A. Curti, D. Franchini, and M. Gabrielli. 1996. Mast cells in bronchiolitis obliterans organizing pneumonia. Mast cell hyperplasia and evidence for extracellular release of tryptase. *Chest* 110: 383-391.

73. Wygrecka, M., B. K. Dahal, D. Kosanovic, F. Petersen, B. Taborski, S. von Gerlach, M. Didiasova, D. Zakrzewicz, K. T. Preissner, R. T. Schermuly, and P. Markart. 2013. Mast cells and fibroblasts work in concert to aggravate pulmonary fibrosis: role of transmembrane SCF and the PAR-2/PKC-alpha/Raf-1/p44/42 signaling pathway. *The American journal of pathology* 182: 2094-2108.

74. Andrade, Z. A. 2009. Schistosomiasis and liver fibrosis. *Parasite immunology* 31: 656-663.

75. Boros, D. L. 1989. Immunopathology of Schistosoma mansoni infection. *Clinical microbiology reviews* 2: 250-269.

76. Wahl, S. M., M. Frazier-Jessen, W. W. Jin, J. B. Kopp, A. Sher, and A. W. Cheever. 1997. Cytokine regulation of schistosome-induced granuloma and fibrosis. *Kidney international* 51: 1370-1375.

77. Wyler, D. J., S. M. Wahl, and L. M. Wahl. 1978. Hepatic fibrosis in schistosomiasis: egg granulomas secrete fibroblast stimulating factor in vitro. *Science* 202: 438-440.

78. Eklund, A., M. van Hage-Hamsten, C. M. Skold, and S. G. Johansson. 1993. Elevated levels of tryptase in bronchoalveolar lavage fluid from patients with sarcoidosis. *Sarcoidosis* 10: 12-17.

79. Walls, A. F., A. R. Bennett, R. C. Godfrey, S. T. Holgate, and M. K. Church. 1991. Mast cell tryptase and histamine concentrations in bronchoalveolar lavage fluid from patients with interstitial lung disease. *Clinical science* 81: 183-188.

80. Andersson, C. K., A. Andersson-Sjoland, M. Mori, O. Hallgren, A. Pardo, L. Eriksson, L. Bjermer, C. G. Lofdahl, M. Selman, G. Westergren-Thorsson, and J. S. Erjefalt. 2011. Activated MCTC mast cells infiltrate diseased lung areas in cystic fibrosis and idiopathic pulmonary fibrosis. *Respiratory research* 12: 139.

81. Molino, M., E. S. Barnathan, R. Numerof, J. Clark, M. Dreyer, A. Cumashi, J. A. Hoxie, N. Schechter, M. Woolkalis, and L. F. Brass. 1997. Interactions of mast cell tryptase with thrombin receptors and PAR-2. *J Biol Chem* 272: 4043-4049.

82. Huang, C., G. T. De Sanctis, P. J. O'Brien, J. P. Mizgerd, D. S. Friend, J. M. Drazen, L. F. Brass, and R. L. Stevens. 2001. Evaluation of the substrate specificity of human mast cell tryptase beta I and demonstration of its importance in bacterial infections of the lung. *J Biol Chem* 276: 26276-26284.

83. Oh, S. W., C. I. Pae, D. K. Lee, F. Jones, G. K. Chiang, H. O. Kim, S. H. Moon, B. Cao, C. Ogbu, K. W. Jeong, G. Kozu, H. Nakanishi, M. Kahn, E. Y. Chi, and W. R.

Henderson, Jr. 2002. Tryptase inhibition blocks airway inflammation in a mouse asthma model. *J Immunol* 168: 1992-2000.

84. Krishna, M. T., A. Chauhan, L. Little, K. Sampson, R. Hawksworth, T. Mant, R. Djukanovic, T. Lee, and S. Holgate. 2001. Inhibition of mast cell tryptase by inhaled APC 366 attenuates allergen-induced late-phase airway obstruction in asthma. *The Journal of allergy and clinical immunology* 107: 1039-1045.

85. Saw, S., S. L. Kale, and N. Arora. 2012. Serine protease inhibitor attenuates ovalbumin induced inflammation in mouse model of allergic airway disease. *PLoS One* 7: e41107.

86. McLarty, J. L., G. C. Melendez, G. L. Brower, J. S. Janicki, and S. P. Levick. 2011. Tryptase/Protease-activated receptor 2 interactions induce selective mitogen-activated protein kinase signaling and collagen synthesis by cardiac fibroblasts. *Hypertension* 58: 264-270.

87. Chambers, R. C., K. Dabbagh, R. J. McAnulty, A. J. Gray, O. P. Blanc-Brude, and G. J. Laurent. 1998. Thrombin stimulates fibroblast procollagen production via proteolytic activation of protease-activated receptor 1. *The Biochemical journal* 333 (Pt 1): 121-127.

88. Dawes, K. E., A. J. Gray, and G. J. Laurent. 1993. Thrombin stimulates fibroblast chemotaxis and replication. *European journal of cell biology* 61: 126-130.

89. Pilcher, B. K., D. W. Kim, D. H. Carney, and J. J. Tomasek. 1994. Thrombin stimulates fibroblast-mediated collagen lattice contraction by its proteolytically activated receptor. *Experimental cell research* 211: 368-373.

90. Rennstam, K., and I. Hedenfalk. 2006. High-throughput genomic technology in research and clinical management of breast cancer. Molecular signatures of progression from benign epithelium to metastatic breast cancer. *Breast Cancer Res* 8: 213.

91. Vogelstein, B., and K. W. Kinzler. 1993. The multistep nature of cancer. *Trends in genetics : TIG* 9: 138-141.

92. Willipinski-Stapelfeldt, B., S. Riethdorf, V. Assmann, U. Woelfle, T. Rau, G. Sauter, J. Heukeshoven, and K. Pantel. 2005. Changes in cytoskeletal protein composition indicative of an epithelial-mesenchymal transition in human micrometastatic and primary breast carcinoma cells. *Clin Cancer Res* 11: 8006-8014.

93. Dubois-Marshall, S., J. S. Thomas, D. Faratian, D. J. Harrison, and E. Katz. 2011. Two possible mechanisms of epithelial to mesenchymal transition in invasive ductal breast cancer. *Clin Exp Metastasis*.

94. Hanahan, D., and R. A. Weinberg. 2011. Hallmarks of cancer: the next generation. *Cell* 144: 646-674.

95. Yilmaz, M., G. Christofori, and F. Lehembre. 2007. Distinct mechanisms of tumor invasion and metastasis. *Trends Mol Med* 13: 535-541.

96. Lai, T. C., H. C. Chou, Y. W. Chen, T. R. Lee, H. T. Chan, H. H. Shen, W. T. Lee, S. T. Lin, Y. C. Lu, C. L. Wu, and H. L. Chan. 2010. Secretomic and proteomic analysis of potential breast cancer markers by two-dimensional differential gel electrophoresis. *J Proteome Res* 9: 1302-1322.

97. Kalluri, R., and R. A. Weinberg. 2009. The basics of epithelial-mesenchymal transition. *J Clin Invest* 119: 1420-1428.

98. Finn, O. J. 2012. Immuno-oncology: understanding the function and dysfunction of the immune system in cancer. *Annals of oncology : official journal of the European Society for Medical Oncology / ESMO* 23 Suppl 8: viii6-9.

99. Gajewski, T. F., H. Schreiber, and Y. X. Fu. 2013. Innate and adaptive immune cells in the tumor microenvironment. *Nature immunology* 14: 1014-1022.

100. Solito, S., L. Pinton, V. Damuzzo, and S. Mandruzzato. 2012. Highlights on molecular mechanisms of MDSC-mediated immune suppression: paving the way for new working hypotheses. *Immunological investigations* 41: 722-737.

101. Biragyn, A., and D. L. Longo. 2012. Neoplastic "Black Ops": cancer's subversive tactics in overcoming host defenses. *Seminars in cancer biology* 22: 50-59.

102. Lakshmi Narendra, B., K. Eshvendar Reddy, S. Shantikumar, and S. Ramakrishna. 2013. Immune system: a double-edged sword in cancer. *Inflammation research : official journal of the European Histamine Research Society ... [et al.]* 62: 823-834.

103. Cailleau, R., R. Young, M. Olive, and W. J. Reeves, Jr. 1974. Breast tumor cell lines from pleural effusions. *Journal of the National Cancer Institute* 53: 661-674.

104. Abdelkarim, M., N. Vintonenko, A. Starzec, A. Robles, J. Aubert, M. L. Martin, S. Mourah, M. P. Podgorniak, S. Rodrigues-Ferreira, C. Nahmias, P. O. Couraud, C. Doliger, O. Sainte-Catherine, N. Peyri, L. Chen, J. Mariau, M. Etienne, G. Y. Perret, M. Crepin, J. L. Poyet, A. M. Khatib, and M. Di Benedetto. 2011. Invading basement membrane matrix is sufficient for MDA-MB-231 breast cancer cells to develop a stable in vivo metastatic phenotype. *PLoS One* 6: e23334.

105. Cailleau, R., M. Olive, and Q. V. Cruciger. 1978. Long-term human breast carcinoma cell lines of metastatic origin: preliminary characterization. *In vitro* 14: 911-915.

106. Rae, J. M., C. J. Creighton, J. M. Meck, B. R. Haddad, and M. D. Johnson. 2007. MDA-MB-435 cells are derived from M14 melanoma cells--a loss for breast cancer, but a boon for melanoma research. *Breast Cancer Res Treat* 104: 13-19.

107. Hamilton, T. C., R. C. Young, W. M. McKoy, K. R. Grotzinger, J. A. Green, E. W. Chu, J. Whang-Peng, A. M. Rogan, W. R. Green, and R. F. Ozols. 1983. Characterization of a human ovarian carcinoma cell line (NIH:OVCAR-3) with androgen and estrogen receptors. *Cancer Res* 43: 5379-5389.

108. Hamilton, T. C., R. C. Young, and R. F. Ozols. 1984. Experimental model systems of ovarian cancer: applications to the design and evaluation of new treatment approaches. *Seminars in oncology* 11: 285-298.

109. Ponten, J., and E. H. Macintyre. 1968. Long term culture of normal and neoplastic human glia. *Acta pathologica et microbiologica Scandinavica* 74: 465-486.

110. Soule, H. D., J. Vazguez, A. Long, S. Albert, and M. Brennan. 1973. A human cell line from a pleural effusion derived from a breast carcinoma. *Journal of the National Cancer Institute* 51: 1409-1416.

111. Miller, F. R., S. J. Santner, L. Tait, and P. J. Dawson. 2000. MCF10DCIS.com xenograft model of human comedo ductal carcinoma in situ. *Journal of the National Cancer Institute* 92: 1185-1186.

112. von Kleist, S., E. Chany, P. Burtin, M. King, and J. Fogh. 1975. Immunohistology of the antigenic pattern of a continuous cell line from a human colon tumor. *Journal of the National Cancer Institute* 55: 555-560.

113. Leibovitz, A., J. C. Stinson, W. B. McCombs, 3rd, C. E. McCoy, K. C. Mazur, and N. D. Mabry. 1976. Classification of human colorectal adenocarcinoma cell lines. *Cancer Res* 36: 4562-4569.

114. Shirasawa, S., M. Furuse, N. Yokoyama, and T. Sasazuki. 1993. Altered growth of human colon cancer cell lines disrupted at activated Ki-ras. *Science* 260: 85-88.

115. Dexter, D. L., J. A. Barbosa, and P. Calabresi. 1979. N,N-dimethylformamide-induced alteration of cell culture characteristics and loss of tumorigenicity in cultured human colon carcinoma cells. *Cancer Res* 39: 1020-1025.

116. Scudiero, D. A., A. Monks, and E. A. Sausville. 1998. Cell line designation change: multidrug-resistant cell line in the NCI anticancer screen. *Journal of the National Cancer Institute* 90: 862.

117. Park, J. G., J. H. Lee, M. S. Kang, K. J. Park, Y. M. Jeon, H. J. Lee, H. S. Kwon, H. S. Park, K. S. Yeo, K. U. Lee, and et al. 1995. Characterization of cell lines established from human hepatocellular carcinoma. *Int J Cancer* 62: 276-282.

118. Aden, D. P., A. Fogel, S. Plotkin, I. Damjanov, and B. B. Knowles. 1979. Controlled synthesis of HBsAg in a differentiated human liver carcinoma-derived cell line. *Nature* 282: 615-616.

119. Fogh, J., J. M. Fogh, and T. Orfeo. 1977. One hundred and twenty-seven cultured human tumor cell lines producing tumors in nude mice. *Journal of the National Cancer Institute* 59: 221-226.

120. Lieber, M., J. Mazzetta, W. Nelson-Rees, M. Kaplan, and G. Todaro. 1975. Establishment of a continuous tumor-cell line (panc-1) from a human carcinoma of the exocrine pancreas. *Int J Cancer* 15: 741-747.

121. Steube, K. G., D. Teepe, C. Meyer, M. Zaborski, and H. G. Drexler. 1997. A model system in haematology and immunology: the human monocytic cell line MONO-MAC-1. *Leukemia research* 21: 327-335.

122. Ziegler-Heitbrock, H. W., E. Thiel, A. Futterer, V. Herzog, A. Wirtz, and G. Riethmuller. 1988. Establishment of a human cell line (Mono Mac 6) with characteristics of mature monocytes. *Int J Cancer* 41: 456-461.

123. Sundstrom, C., and K. Nilsson. 1976. Establishment and characterization of a human histiocytic lymphoma cell line (U-937). *Int J Cancer* 17: 565-577.

124. Collins, S. J., R. C. Gallo, and R. E. Gallagher. 1977. Continuous growth and differentiation of human myeloid leukaemic cells in suspension culture. *Nature* 270: 347-349.

125. Tsuchiya, S., M. Yamabe, Y. Yamaguchi, Y. Kobayashi, T. Konno, and K. Tada. 1980. Establishment and characterization of a human acute monocytic leukemia cell line (THP-1). *Int J Cancer* 26: 171-176.

126. Cesinaro, A. M., C. Natoli, A. Grassadonia, N. Tinari, S. Iacobelli, and G. P. Trentini. 2002. Expression of the 90K tumor-associated protein in benign and malignant melanocytic lesions. *The Journal of investigative dermatology* 119: 187-190.

127. Koths, K., E. Taylor, R. Halenbeck, C. Casipit, and A. Wang. 1993. Cloning and characterization of a human Mac-2-binding protein, a new member of the superfamily defined by the macrophage scavenger receptor cysteine-rich domain. *The Journal of biological chemistry* 268: 14245-14249.

128. Ullrich, A., I. Sures, M. D'Egidio, B. Jallal, T. J. Powell, R. Herbst, A. Dreps, M. Azam, M. Rubinstein, C. Natoli, and et al. 1994. The secreted tumor-associated antigen 90K is a potent immune stimulator. *J Biol Chem* 269: 18401-18407.

129. Nonaka, M., B. Y. Ma, H. Imaeda, K. Kawabe, N. Kawasaki, K. Hodohara, N. Kawasaki, A. Andoh, Y. Fujiyama, and T. Kawasaki. 2011. Dendritic cell-specific intercellular adhesion molecule 3-grabbing non-integrin (DC-SIGN) recognizes a novel ligand, Mac-2-binding protein, characteristically expressed on human colorectal carcinomas. *J Biol Chem* 286: 22403-22413.

130. Resnick, D., A. Pearson, and M. Krieger. 1994. The SRCR superfamily: a family reminiscent of the Ig superfamily. *Trends in biochemical sciences* 19: 5-8.

131. D'Ostilio, N., G. Sabatino, C. Natoli, A. Ullrich, and S. Iacobelli. 1996. 90K (Mac-2 BP) in human milk. *Clinical and experimental immunology* 104: 543-546.

132. Iacobelli, S., E. Arno, A. D'Orazio, and G. Coletti. 1986. Detection of antigens recognized by a novel monoclonal antibody in tissue and serum from patients with breast cancer. *Cancer research* 46: 3005-3010.

133. Natoli, C., S. Iacobelli, and F. Ghinelli. 1991. Unusually high level of a tumor-associated antigen in the serum of human immunodeficiency virus-seropositive individuals. *The Journal of infectious diseases* 164: 616-617.

134. Iacobelli, S., C. Natoli, M. D'Egidio, E. Tamburrini, A. Antinori, and L. Ortona. 1991. Lipoprotein 90K in human immunodeficiency virus-infected patients: a further serologic marker of progression. *The Journal of infectious diseases* 164: 819.

135. Fornarini, B., S. Iacobelli, N. Tinari, C. Natoli, M. De Martino, and G. Sabatino. 1999. Human milk 90K (Mac-2 BP): possible protective effects against acute respiratory infections. *Clinical and experimental immunology* 115: 91-94.

136. Wang, Y., X. Ao, H. Vuong, M. Konanur, F. R. Miller, S. Goodison, and D. M. Lubman. 2008. Membrane glycoproteins associated with breast tumor cell progression identified by a lectin affinity approach. *J Proteome Res* 7: 4313-4325.

137. Mbeunkui, F., B. J. Metge, L. A. Shevde, and L. K. Pannell. 2007. Identification of differentially secreted biomarkers using LC-MS/MS in isogenic cell lines representing a progression of breast cancer. *J Proteome Res* 6: 2993-3002.

138. Tinari, N., R. Lattanzio, P. Querzoli, C. Natoli, A. Grassadonia, S. Alberti, M. Hubalek, D. Reimer, I. Nenci, P. Bruzzi, M. Piantelli, S. Iacobelli, and B.-O. Consorzio Interuniversitario Nazionale per la. 2009. High expression of 90K (Mac-2 BP) is associated with poor survival in node-negative breast cancer patients not receiving adjuvant systemic therapies. *International journal of cancer. Journal international du cancer* 124: 333-338.

139. Iacobelli, S., P. Sismondi, M. Giai, M. D'Egidio, N. Tinari, C. Amatetti, P. Di Stefano, and C. Natoli. 1994. Prognostic value of a novel circulating serum 90K antigen in breast cancer. *Br J Cancer* 69: 172-176.

140. Hughes, R. C. 1999. Secretion of the galectin family of mammalian carbohydrate-binding proteins. *Biochimica et biophysica acta* 1473: 172-185.

141. Piccolo, E., N. Tinari, D. Semeraro, S. Traini, I. Fichera, A. Cumashi, R. La Sorda, F. Spinella, A. Bagnato, R. Lattanzio, M. D'Egidio, A. Di Risio, P. Stampolidis, M. Piantelli, C. Natoli, A. Ullrich, and S. Iacobelli. 2013. LGALS3BP, lectin galactoside-binding soluble 3 binding protein, induces vascular endothelial growth factor in human breast cancer cells and promotes angiogenesis. *Journal of molecular medicine* 91: 83-94.

142. Trahey, M., and I. L. Weissman. 1999. Cyclophilin C-associated protein: a normal secreted glycoprotein that down-modulates endotoxin and proinflammatory responses in vivo. *Proc Natl Acad Sci U S A* 96: 3006-3011.

143. Gruson, D., and G. Ko. 2012. Galectins testing: new promises for the diagnosis and risk stratification of chronic diseases? *Clinical biochemistry* 45: 719-726.

144. McCullough, P. A., A. Olobatoke, and T. E. Vanhecke. 2011. Galectin-3: a novel blood test for the evaluation and management of patients with heart failure. *Reviews in cardiovascular medicine* 12: 200-210.

145. Sundblad, V., D. O. Croci, and G. A. Rabinovich. 2011. Regulated expression of galectin-3, a multifunctional glycan-binding protein, in haematopoietic and non-haematopoietic tissues. *Histology and histopathology* 26: 247-265.

146. Krzeslak, A., and A. Lipinska. 2004. Galectin-3 as a multifunctional protein. *Cellular & molecular biology letters* 9: 305-328.

147. Moutsatsos, I. K., M. Wade, M. Schindler, and J. L. Wang. 1987. Endogenous lectins from cultured cells: nuclear localization of carbohydrate-binding protein 35 in proliferating 3T3 fibroblasts. *Proceedings of the National Academy of Sciences of the United States of America* 84: 6452-6456.

148. Hughes, R. C. 1997. The galectin family of mammalian carbohydrate-binding molecules. *Biochemical Society transactions* 25: 1194-1198.

149. Xu, X. C., A. K. el-Naggar, and R. Lotan. 1995. Differential expression of galectin-1 and galectin-3 in thyroid tumors. Potential diagnostic implications. *The American journal of pathology* 147: 815-822.

150. Coli, A., G. Bigotti, F. Zucchetti, F. Negro, and G. Massi. 2002. Galectin-3, a marker of well-differentiated thyroid carcinoma, is expressed in thyroid nodules with cytological atypia. *Histopathology* 40: 80-87.

151. Blake, J. A., C. J. Bult, J. T. Eppig, J. A. Kadin, J. E. Richardson, and G. Mouse Genome Database. 2014. The Mouse Genome Database: integration of and access to knowledge about the laboratory mouse. *Nucleic Acids Res* 42: D810-817.

152. Collins, N. 2001. The difference between albumin and prealbumin. *Adv Skin Wound Care* 14: 235-236.

153. Iizaka, S., H. Sanada, Y. Matsui, M. Furue, T. Tachibana, T. Nakayama, J. Sugama, K. Furuta, M. Tachi, K. Tokunaga, and Y. Miyachi. 2011. Serum albumin level

is a limited nutritional marker for predicting wound healing in patients with pressure ulcer: two multicenter prospective cohort studies. *Clin Nutr* 30: 738-745.

154. Anthony, D., L. Rafter, T. Reynolds, and M. Aljezawi. 2011. An evaluation of serum albumin and the sub-scores of the Waterlow score in pressure ulcer risk assessment. *J Tissue Viability* 20: 89-99.

155. Williams, D. F., N. A. Stotts, and K. Nelson. 2000. Patients with existing pressure ulcers admitted to acute care. *J Wound Ostomy Continence Nurs* 27: 216-226.

156. James, T. J., M. A. Hughes, G. W. Cherry, and R. P. Taylor. 2000. Simple biochemical markers to assess chronic wounds. *Wound Repair Regen* 8: 264-269.

157. Elzer, K. L., D. A. Heitzman, M. I. Chernin, and J. F. Novak. 2008. Differential effects of serine proteases on the migration of normal and tumor cells: implications for tumor microenvironment. *Integr Cancer Ther* 7: 282-294.

158. Hirahara, F., Y. Miyagi, E. Miyagi, H. Yasumitsu, N. Koshikawa, Y. Nagashima, H. Kitamura, H. Minaguchi, M. Umeda, and K. Miyazaki. 1995. Trypsinogen expression in human ovarian carcinomas. *Int J Cancer* 63: 176-181.

159. Koivunen, E., O. Saksela, O. Itkonen, S. Osman, M. L. Huhtala, and U. H. Stenman. 1991. Human colon carcinoma, fibrosarcoma and leukemia cell lines produce tumor-associated trypsinogen. *Int J Cancer* 47: 592-596.

160. Miyata, S., N. Koshikawa, S. Higashi, Y. Miyagi, Y. Nagashima, S. Yanoma, Y. Kato, H. Yasumitsu, and K. Miyazaki. 1999. Expression of trypsin in human cancer cell lines and cancer tissues and its tight binding to soluble form of Alzheimer amyloid precursor protein in culture. *J Biochem* 125: 1067-1076.

161. Ohta, T., T. Terada, T. Nagakawa, H. Tajima, H. Itoh, L. Fonseca, and I. Miyazaki. 1994. Pancreatic trypsinogen and cathepsin B in human pancreatic carcinomas and associated metastatic lesions. *Br J Cancer* 69: 152-156.

162. Soreide, K., E. A. Janssen, H. Korner, and J. P. Baak. 2006. Trypsin in colorectal cancer: molecular biological mechanisms of proliferation, invasion, and metastasis. *J Pathol* 209: 147-156.

163. Fields, R. C., J. G. Schoenecker, J. P. Hart, M. R. Hoffman, S. V. Pizzo, and J. H. Lawson. 2003. Protease-activated receptor-2 signaling triggers dendritic cell development. *The American journal of pathology* 162: 1817-1822.

164. Toth, J., E. Siklodi, P. Medveczky, K. Gallatz, P. Nemeth, L. Szilagyi, L. Graf, and M. Palkovits. 2007. Regional distribution of human trypsinogen 4 in human brain at mRNA and protein level. *Neurochemical research* 32: 1423-1433.

165. Wang, Y., W. Luo, and G. Reiser. 2008. Trypsin and trypsin-like proteases in the brain: proteolysis and cellular functions. *Cellular and molecular life sciences : CMLS* 65: 237-252.

166. Paju, A., and U. H. Stenman. 2006. Biochemistry and clinical role of trypsinogens and pancreatic secretory trypsin inhibitor. *Critical reviews in clinical laboratory sciences* 43: 103-142.

167. Cocks, T. M., B. Fong, J. M. Chow, G. P. Anderson, A. G. Frauman, R. G. Goldie, P. J. Henry, M. J. Carr, J. R. Hamilton, and J. D. Moffatt. 1999. A protective role for protease-activated receptors in the airways. *Nature* 398: 156-160.

168. Fujimoto, D., Y. Hirono, T. Goi, K. Katayama, K. Hirose, and A. Yamaguchi. 2006. Expression of protease activated receptor-2 (PAR-2) in gastric cancer. *J Surg Oncol* 93: 139-144.

169. Hansen, K. K., K. Oikonomopoulou, Y. Li, and M. D. Hollenberg. 2008. Proteinases, proteinase-activated receptors (PARs) and the pathophysiology of cancer and diseases of the cardiovascular, musculoskeletal, nervous and gastrointestinal systems. *Naunyn Schmiedebergs Arch Pharmacol* 377: 377-392.

170. Suen, J. Y., B. Gardiner, S. Grimmond, and D. P. Fairlie. 2010. Profiling gene expression induced by protease-activated receptor 2 (PAR2) activation in human kidney cells. *PLoS One* 5: e13809.

171. Martin, G. J. 1961. Wound healing composition. In *United States Patent Office*. The National Drug Company., United States.

172. Anigstein, L. 1959. Wound healing agent obtained from blood and method of preparation. In *United States Patent Office*, United States.

173. Fortney, D. Z. 1996. Compositions containing protease produced by vibrio and method of use in debridement and wound healing. In *United States Patent Office*. W.R. Grace and Company, United States.

174. Pritchard, D. I. 2011. Treatment of wounds. In *United States Patent Office*. U. S. P. Office, ed, United States.

175. Cetrulo, G. I. 1953. Use of trypsin intravenously in a gunshot wound. *J Am Med Assoc* 152: 605-606.

176. Carson, S. N., C. Wiggins, K. Overall, and J. Herbert. 2003. Using a castor oil-balsam of Peru-trypsin ointment to assist in healing skin graft donor sites. *Ostomy Wound Manage* 49: 60-64.

177. Beitz, J. M. 2005. Heparin-induced thrombocytopenia syndrome bullous lesions treated with trypsin-balsam of peru-castor oil ointment: a case study. *Ostomy Wound Manage* 51: 52-54, 56-58.

178. Russell, T. M., E. L. Herzog, and R. Bucala. 2012. Flow cytometric identification of fibrocytes in scleroderma lung disease. *Methods Mol Biol* 900: 327-346.

179. Pilling, D., N. M. Tucker, and R. H. Gomer. 2006. Aggregated IgG inhibits the differentiation of human fibrocytes. *J Leukoc Biol* 79: 1242-1251.

180. Rothmeier, A. S., and W. Ruf. 2012. Protease-activated receptor 2 signaling in inflammation. *Semin Immunopathol* 34: 133-149.

181. Hortin, G. L., D. Sviridov, and N. L. Anderson. 2008. High-abundance polypeptides of the human plasma proteome comprising the top 4 logs of polypeptide abundance. *Clin Chem* 54: 1608-1616.

182. Green, N. M. 1953. Competition among trypsin inhibitors. *J Biol Chem* 205: 535-551.

183. Bundy, H. F., and J. W. Mehl. 1958. Trypsin inhibitors of human serum. I. Standardization, mechanism of reaction, and normal values. *J Clin Invest* 37: 947-955.

184. Bundy, H. F., and J. W. Mehl. 1959. Trypsin inhibitors of human serum. II. Isolation of the alpha 1-inhibitor and its partial characterization. *J Biol Chem* 234: 1124-1128.

185. Moore, B. B., L. Murray, A. Das, C. A. Wilke, A. B. Herrygers, and G. B. Toews. 2006. The role of CCL12 in the recruitment of fibrocytes and lung fibrosis. *American journal of respiratory cell and molecular biology* 35: 175-181.

186. MacNaughton, W. K. 2005. Epithelial effects of proteinase-activated receptors in the gastrointestinal tract. *Mem Inst Oswaldo Cruz* 100 Suppl 1: 211-215.

187. Mall, M., T. Gonska, J. Thomas, S. Hirtz, R. Schreiber, and K. Kunzelmann. 2002. Activation of ion secretion via proteinase-activated receptor-2 in human colon. *Am J Physiol Gastrointest Liver Physiol* 282: G200-210.

188. Ramachandran, R., and M. D. Hollenberg. 2008. Proteinases and signalling: pathophysiological and therapeutic implications via PARs and more. *Br J Pharmacol* 153 Suppl 1: S263-282.

189. Vergnolle, N. 2004. Modulation of visceral pain and inflammation by protease-activated receptors. *Br J Pharmacol* 141: 1264-1274.

190. Li, W., D. M. Danilenko, S. Bunting, R. Ganesan, S. Sa, R. Ferrando, T. D. Wu, G. A. Kolumam, W. Ouyang, and D. Kirchhofer. 2009. The serine protease marapsin is expressed in stratified squamous epithelia and is up-regulated in the hyperproliferative epidermis of psoriasis and regenerating wounds. *J Biol Chem* 284: 218-228.

191. Borgono, C. A., I. P. Michael, and E. P. Diamandis. 2004. Human tissue kallikreins: physiologic roles and applications in cancer. *Molecular cancer research : MCR* 2: 257-280.

192. Yamamoto, H., S. Iku, Y. Adachi, A. Imsumran, H. Taniguchi, K. Nosho, Y. Min, S. Horiuchi, M. Yoshida, F. Itoh, and K. Imai. 2003. Association of trypsin

expression with tumour progression and matrilysin expression in human colorectal cancer. *J Pathol* 199: 176-184.

193. Nakamura, K., A. Hongo, J. Kodama, F. Abarzua, Y. Nasu, H. Kumon, and Y. Hiramatsu. 2009. Expression of matriptase and clinical outcome of human endometrial cancer. *Anticancer research* 29: 1685-1690.

194. White, M. J., M. Glenn, and R. H. Gomer. 2013. Trypsin potentiates human fibrocyte differentiation. *PLoS One* 8: e70795.

195. Pilling, D., T. Fan, D. Huang, B. Kaul, and R. H. Gomer. 2009. Identification of markers that distinguish monocyte-derived fibrocytes from monocytes, macrophages, and fibroblasts. *PLoS One* 4: e7475.

196. Schwartz, L. B., and T. R. Bradford. 1986. Regulation of tryptase from human lung mast cells by heparin. Stabilization of the active tetramer. *J Biol Chem* 261: 7372-7379.

197. Ahn, H. S., C. Foster, G. Boykow, A. Stamford, M. Manna, and M. Graziano. 2000. Inhibition of cellular action of thrombin by N3-cyclopropyl-7-[[4-(1-methylethyl)phenyl]methyl]-7H-pyrrolo[3, 2-f]quinazoline-1,3-diamine (SCH 79797), a nonpeptide thrombin receptor antagonist. *Biochemical pharmacology* 60: 1425-1434.

198. Chackalamannil, S., Y. Wang, W. J. Greenlee, Z. Hu, Y. Xia, H. S. Ahn, G. Boykow, Y. Hsieh, J. Palamanda, J. Agans-Fantuzzi, S. Kurowski, M. Graziano, and M. Chintala. 2008. Discovery of a novel, orally active himbacine-based thrombin receptor antagonist (SCH 530348) with potent antiplatelet activity. *Journal of medicinal chemistry* 51: 3061-3064.

199. Maharjan, A. S., D. Roife, D. Brazill, and R. H. Gomer. 2013. Serum amyloid P inhibits granulocyte adhesion. *Fibrogenesis Tissue Repair* 6: 2.

200. Kamentsky, L., T. R. Jones, A. Fraser, M. A. Bray, D. J. Logan, K. L. Madden, V. Ljosa, C. Rueden, K. W. Eliceiri, and A. E. Carpenter. 2011. Improved structure, function and compatibility for CellProfiler: modular high-throughput image analysis software. *Bioinformatics* 27: 1179-1180.

201. Huttunen, M., and I. T. Harvima. 2005. Mast cell tryptase and chymase in chronic leg ulcers: chymase is potentially destructive to epithelium and is controlled by proteinase inhibitors. *The British journal of dermatology* 152: 1149-1160.

202. Harvima, I. T., R. J. Harvima, T. O. Eloranta, and J. E. Fraki. 1988. The allosteric effect of salt on human mast cell tryptase. *Biochimica et biophysica acta* 956: 133-139.

203. Iizaka, S., H. Sanada, G. Nakagami, R. Sekine, H. Koyanagi, C. Konya, and J. Sugama. 2010. Estimation of protein loss from wound fluid in older patients with severe pressure ulcers. *Nutrition* 26: 890-895.

204. Laiho, K. 2004. Albumin as a marker of plasma transudation in experimental skin lesions. *International journal of legal medicine* 118: 282-288.

205. Ossovskaya, V. S., and N. W. Bunnett. 2004. Protease-activated receptors: contribution to physiology and disease. *Physiological reviews* 84: 579-621.

206. Hoekstra, W. J., B. L. Hulshizer, D. F. McComsey, P. Andrade-Gordon, J. A. Kauffman, M. F. Addo, D. Oksenberg, R. M. Scarborough, and B. E. Maryanoff. 1998.

Thrombin receptor (PAR-1) antagonists. Heterocycle-based peptidomimetics of the SFLLR agonist motif. *Bioorganic & medicinal chemistry letters* 8: 1649-1654.

207. Kanke, T., H. Ishiwata, M. Kabeya, M. Saka, T. Doi, Y. Hattori, A. Kawabata, and R. Plevin. 2005. Binding of a highly potent protease-activated receptor-2 (PAR2) activating peptide, [3H]2-furoyl-LIGRL-NH2, to human PAR2. *Br J Pharmacol* 145: 255-263.

208. Vassallo, R. R., Jr., T. Kieber-Emmons, K. Cichowski, and L. F. Brass. 1992. Structure-function relationships in the activation of platelet thrombin receptors by receptor-derived peptides. *J Biol Chem* 267: 6081-6085.

209. Gardell, L. R., J. N. Ma, J. G. Seitzberg, A. E. Knapp, H. H. Schiffer, A. Tabatabaei, C. N. Davis, M. Owens, B. Clemons, K. K. Wong, B. Lund, N. R. Nash, Y. Gao, J. Lameh, K. Schmelzer, R. Olsson, and E. S. Burstein. 2008. Identification and characterization of novel small-molecule protease-activated receptor 2 agonists. *The Journal of pharmacology and experimental therapeutics* 327: 799-808.

210. Ishida, Y., T. Kondo, T. Takayasu, Y. Iwakura, and N. Mukaida. 2004. The essential involvement of cross-talk between IFN-gamma and TGF-beta in the skin wound-healing process. *J Immunol* 172: 1848-1855.

211. Shigehara, K., N. Shijubo, M. Ohmichi, R. Takahashi, S. Kon, H. Okamura, M. Kurimoto, Y. Hiraga, T. Tatsuno, S. Abe, and N. Sato. 2001. IL-12 and IL-18 are increased and stimulate IFN-gamma production in sarcoid lungs. *J Immunol* 166: 642-649.

212. Kawao, N., Y. Sakaguchi, A. Tagome, R. Kuroda, S. Nishida, K. Irimajiri, H. Nishikawa, K. Kawai, M. D. Hollenberg, and A. Kawabata. 2002. Protease-activated receptor-2 (PAR-2) in the rat gastric mucosa: immunolocalization and facilitation of pepsin/pepsinogen secretion. *Br J Pharmacol* 135: 1292-1296.

213. Altrogge, L. M., and D. Monard. 2000. An assay for high-sensitivity detection of thrombin activity and determination of proteases activating or inactivating protease-activated receptors. *Analytical biochemistry* 277: 33-45.

214. Dong, Y., C. Q. Zeng, J. M. Ball, M. K. Estes, and A. P. Morris. 1997. The rotavirus enterotoxin NSP4 mobilizes intracellular calcium in human intestinal cells by stimulating phospholipase C-mediated inositol 1,4,5-trisphosphate production. *Proc Natl Acad Sci U S A* 94: 3960-3965.

215. Scheel, G., B. Rahfoth, J. Franke, and P. Grau. 1991. Acceleration of wound healing by local application of fibronectin. *Archives of orthopaedic and trauma surgery* 110: 284-287.

216. Kallis, Y. N., C. J. Scotton, A. C. Mackinnon, R. D. Goldin, N. A. Wright, J. P. Iredale, R. C. Chambers, and S. J. Forbes. 2014. Proteinase activated receptor 1 mediated fibrosis in a mouse model of liver injury: a role for bone marrow derived macrophages. *PLoS One* 9: e86241.

217. Knight, V., J. Tchongue, D. Lourensz, P. Tipping, and W. Sievert. 2012. Protease-activated receptor 2 promotes experimental liver fibrosis in mice and activates human hepatic stellate cells. *Hepatology* 55: 879-887.

218. Lindner, J. R., M. L. Kahn, S. R. Coughlin, G. R. Sambrano, E. Schauble, D. Bernstein, D. Foy, A. Hafezi-Moghadam, and K. Ley. 2000. Delayed onset of inflammation in protease-activated receptor-2-deficient mice. *J Immunol* 165: 6504-6510.

219. Damiano, B. P., W. M. Cheung, R. J. Santulli, W. P. Fung-Leung, K. Ngo, R. D. Ye, A. L. Darrow, C. K. Derian, L. de Garavilla, and P. Andrade-Gordon. 1999. Cardiovascular responses mediated by protease-activated receptor-2 (PAR-2) and thrombin receptor (PAR-1) are distinguished in mice deficient in PAR-2 or PAR-1. *The Journal of pharmacology and experimental therapeutics* 288: 671-678.

220. Pawlinski, R., M. Tencati, C. R. Hampton, T. Shishido, T. A. Bullard, L. M. Casey, P. Andrade-Gordon, M. Kotzsch, D. Spring, T. Luther, J. Abe, T. H. Pohlman, E. D. Verrier, B. C. Blaxall, and N. Mackman. 2007. Protease-activated receptor-1 contributes to cardiac remodeling and hypertrophy. *Circulation* 116: 2298-2306.

221. Randall S. Alberte, W. P. R., Jr. 2010. Tryptase enzyme inhibiting aminopyridines. In *United States Patent Office*. U. States, ed, United States.

222. Hiroshi Kido, H. N. 2002. Tryptase inhibitor and novel guanidino derivatives. U. S. P. Office, ed, United States.

223. Yong Mi Choi-Sledeski, G. L., Patrick Wai-Kwok. 2012. Tropinone benzylamines as beta-tryptase inhibitors. U. S. P. Office, ed, United States.

224. Joanne Van Ryn, P. G.-C., Flavio Solca. 2014. Combination therapy in treatment of cancer and fibrotic diseases. In *United States Patent Office.* U. States, ed.

225. Steve Cohen, M. N. 2008. Antagonists of protease activated receptor-1 (par1). In *United States Patent Office.* . U. S. P. Office, ed, United States.

226. Joe William Boyd, P. M., Michael Higginbottom, Iain Simpson, David Mark Mountford, Edward Daniel Savory. 2012. PROTEASE ACTIVATED RECEPTOR 2 (PAR2) ANTAGONISTS U. S. P. Office, ed, United States.

227. Cairns, J. A. 2005. Inhibitors of mast cell tryptase beta as therapeutics for the treatment of asthma and inflammatory disorders. *Pulmonary pharmacology & therapeutics* 18: 55-66.

228. Utah, U. o. 2013. Dabigatran's Effect on Changes in Atrial Fibrosis in Patients With Atrial Fibrillation (DEPAF).

229. Lohman, R. J., A. J. Cotterell, G. D. Barry, L. Liu, J. Y. Suen, D. A. Vesey, and D. P. Fairlie. 2012. An antagonist of human protease activated receptor-2 attenuates PAR2 signaling, macrophage activation, mast cell degranulation, and collagen-induced arthritis in rats. *FASEB journal : official publication of the Federation of American Societies for Experimental Biology* 26: 2877-2887.

230. Datta, A., C. J. Scotton, and R. C. Chambers. 2011. Novel therapeutic approaches for pulmonary fibrosis. *Br J Pharmacol* 163: 141-172.

231. Haudek, S. B., J. Cheng, J. Du, Y. Wang, J. Hermosillo-Rodriguez, J. Trial, G. E. Taffet, and M. L. Entman. 2010. Monocytic fibroblast precursors mediate fibrosis in angiotensin-II-induced cardiac hypertrophy. *Journal of molecular and cellular cardiology* 49: 499-507.

232. Kong, P., P. Christia, and N. G. Frangogiannis. 2014. The pathogenesis of cardiac fibrosis. *Cellular and molecular life sciences : CMLS* 71: 549-574.

233. Mollmann, H., H. M. Nef, S. Kostin, C. von Kalle, I. Pilz, M. Weber, J. Schaper, C. W. Hamm, and A. Elsasser. 2006. Bone marrow-derived cells contribute to infarct remodelling. *Cardiovascular research* 71: 661-671.

234. Akin, C., and D. D. Metcalfe. 2004. Systemic mastocytosis. *Annual review of medicine* 55: 419-432.

235. Chiu, A., N. M. Nanaji, M. Czader, G. Gheorghe, D. M. Knowles, A. Chadburn, and A. Orazi. 2009. The stromal composition of mast cell aggregates in systemic mastocytosis. *Mod Pathol* 22: 857-865.

236. Li, C. Y., and J. Y. Baek. 2002. Mastocytosis and fibrosis: role of cytokines. *International archives of allergy and immunology* 127: 123-126.

237. Schwartz, L. B., K. Sakai, T. R. Bradford, S. Ren, B. Zweiman, A. S. Worobec, and D. D. Metcalfe. 1995. The alpha form of human tryptase is the predominant type present in blood at baseline in normal subjects and is elevated in those with systemic mastocytosis. *J Clin Invest* 96: 2702-2710.

238. Matito, A., J. M. Morgado, I. Alvarez-Twose, L. Sanchez-Munoz, C. E. Pedreira, M. Jara-Acevedo, C. Teodosio, P. Sanchez-Lopez, E. Fernandez-Nunez, R. Moreno-Borque, A. Garcia-Montero, A. Orfao, and L. Escribano. 2013. Serum tryptase monitoring in indolent systemic mastocytosis: association with disease features and patient outcome. *PLoS One* 8: e76116.

239. White, M. J., Galvis-Carvajal, E. D., Gomer, R. H. 2014. A brief exposure to tryptase or thrombin potentiates fibrocyte differentiation in the presence of serum or SAP. *Journal of Immunology*.

240. Weidenbusch, M., and H. J. Anders. 2012. Tissue microenvironments define and get reinforced by macrophage phenotypes in homeostasis or during inflammation, repair and fibrosis. *Journal of innate immunity* 4: 463-477.

241. Mahdavian Delavary, B., W. M. van der Veer, M. van Egmond, F. B. Niessen, and R. H. Beelen. 2011. Macrophages in skin injury and repair. *Immunobiology* 216: 753-762.

242. Gratchev, A., P. Guillot, N. Hakiy, O. Politz, C. E. Orfanos, K. Schledzewski, and S. Goerdt. 2001. Alternatively activated macrophages differentially express fibronectin and its splice variants and the extracellular matrix protein betaIG-H3. *Scandinavian journal of immunology* 53: 386-392.

243. Leibovich, S. J., and R. Ross. 1975. The role of the macrophage in wound repair. A study with hydrocortisone and antimacrophage serum. *The American journal of pathology* 78: 71-100.

244. Lucas, T., A. Waisman, R. Ranjan, J. Roes, T. Krieg, W. Muller, A. Roers, and S. A. Eming. 2010. Differential roles of macrophages in diverse phases of skin repair. *J Immunol* 184: 3964-3977.

245. Lech, M., and H. J. Anders. 2013. Macrophages and fibrosis: How resident and infiltrating mononuclear phagocytes orchestrate all phases of tissue injury and repair. *Biochimica et biophysica acta* 1832: 989-997.

246. White, M. J., E. Galvis-Carvajal, and R. H. Gomer. 2014. A Brief Exposure to Tryptase or Thrombin Potentiates Fibrocyte Differentiation in the Presence of Serum or Serum Amyloid P. *J Immunol*.

247. Stout, R. D., C. Jiang, B. Matta, I. Tietzel, S. K. Watkins, and J. Suttles. 2005. Macrophages sequentially change their functional phenotype in response to changes in microenvironmental influences. *J Immunol* 175: 342-349.

248. Herzog, E. L., and R. Bucala. 2010. Fibrocytes in health and disease. *Experimental hematology* 38: 548-556.

249. Grassadonia, A., N. Tinari, I. Iurisci, E. Piccolo, A. Cumashi, P. Innominato, M. D'Egidio, C. Natoli, M. Piantelli, and S. Iacobelli. 2004. 90K (Mac-2 BP) and galectins in tumor progression and metastasis. *Glycoconjugate journal* 19: 551-556.

250. Graham, F. L., J. Smiley, W. C. Russell, and R. Nairn. 1977. Characteristics of a human cell line transformed by DNA from human adenovirus type 5. *The Journal of general virology* 36: 59-74.

251. Buckley, C. D., D. Pilling, N. V. Henriquez, G. Parsonage, K. Threlfall, D. Scheel-Toellner, D. L. Simmons, A. N. Akbar, J. M. Lord, and M. Salmon. 1999. RGD peptides induce apoptosis by direct caspase-3 activation. *Nature* 397: 534-539.

252. Salmon, M., D. Scheel-Toellner, A. P. Huissoon, D. Pilling, N. Shamsadeen, H. Hyde, A. D. D'Angeac, P. A. Bacon, P. Emery, and A. N. Akbar. 1997. Inhibition of T cell apoptosis in the rheumatoid synovium. *J Clin Invest* 99: 439-446.

253. UniProt, C. 2014. Activities at the Universal Protein Resource (UniProt). *Nucleic Acids Res* 42: D191-198.

254. Lanoue, A., M. R. Clatworthy, P. Smith, S. Green, M. J. Townsend, H. E. Jolin, K. G. Smith, P. G. Fallon, and A. N. McKenzie. 2004. SIGN-R1 contributes to protection against lethal pneumococcal infection in mice. *The Journal of experimental medicine* 200: 1383-1393.

255. Crawford, J. R., D. Pilling, and R. H. Gomer. 2010. Improved serum-free culture conditions for spleen-derived murine fibrocytes. *J Immunol Methods* 363: 9-20.

256. Endo, H., T. Muramatsu, M. Furuta, N. Uzawa, A. Pimkhaokham, T. Amagasa, J. Inazawa, and K. Kozaki. 2013. Potential of tumor-suppressive miR-596 targeting LGALS3BP as a therapeutic agent in oral cancer. *Carcinogenesis* 34: 560-569.

257. Bullwinkel, J., A. Ludemann, J. Debarry, and P. B. Singh. 2011. Epigenotype switching at the CD14 and CD209 genes during differentiation of human monocytes to dendritic cells. *Epigenetics : official journal of the DNA Methylation Society* 6: 45-51.

258. Anthony, R. M., F. Wermeling, M. C. Karlsson, and J. V. Ravetch. 2008. Identification of a receptor required for the anti-inflammatory activity of IVIG. *Proc Natl Acad Sci U S A* 105: 19571-19578.

259. Anthony, R. M., and J. V. Ravetch. 2010. A novel role for the IgG Fc glycan: the anti-inflammatory activity of sialylated IgG Fcs. *Journal of clinical immunology* 30 Suppl 1: S9-14.

260. Inohara, H., S. Akahani, K. Koths, and A. Raz. 1996. Interactions between galectin-3 and Mac-2-binding protein mediate cell-cell adhesion. *Cancer Res* 56: 4530-4534.

261. Iurisci, I., N. Tinari, C. Natoli, D. Angelucci, E. Cianchetti, and S. Iacobelli. 2000. Concentrations of galectin-3 in the sera of normal controls and cancer patients. *Clinical cancer research : an official journal of the American Association for Cancer Research* 6: 1389-1393.

262. Kohatsu, L., D. K. Hsu, A. G. Jegalian, F. T. Liu, and L. G. Baum. 2006. Galectin-3 induces death of Candida species expressing specific beta-1,2-linked mannans. *J Immunol* 177: 4718-4726.

263. Iurisci, I., A. Cumashi, A. A. Sherman, Y. E. Tsvetkov, N. Tinari, E. Piccolo, M. D'Egidio, V. Adamo, C. Natoli, G. A. Rabinovich, S. Iacobelli, N. E. Nifantiev, and B.-O. Consorzio Interuniversitario Nazionale Per la. 2009. Synthetic inhibitors of galectin-1 and -3 selectively modulate homotypic cell aggregation and tumor cell apoptosis. *Anticancer research* 29: 403-410.

264. Sasaki, T., C. Brakebusch, J. Engel, and R. Timpl. 1998. Mac-2 binding protein is a cell-adhesive protein of the extracellular matrix which self-assembles into ring-like structures and binds beta1 integrins, collagens and fibronectin. *The EMBO journal* 17: 1606-1613.

265. Whelan, S. A., J. He, M. Lu, P. Souda, R. E. Saxton, K. F. Faull, J. P. Whitelegge, and H. R. Chang. 2012. Mass spectrometry (LC-MS/MS) identified proteomic biosignatures of breast cancer in proximal fluid. *J Proteome Res* 11: 5034-5045.

266. Lawlor, K., A. Nazarian, L. Lacomis, P. Tempst, and J. Villanueva. 2009. Pathway-based biomarker search by high-throughput proteomics profiling of secretomes. *J Proteome Res* 8: 1489-1503.

267. Kulasingam, V., and E. P. Diamandis. 2008. Tissue culture-based breast cancer biomarker discovery platform. *Int J Cancer* 123: 2007-2012.

268. Pavlou, M. P., and E. P. Diamandis. 2010. The cancer cell secretome: a good source for discovering biomarkers? *Journal of proteomics* 73: 1896-1906.

269. Colzani, M., P. Waridel, J. Laurent, E. Faes, C. Ruegg, and M. Quadroni. 2009. Metabolic labeling and protein linearization technology allow the study of proteins secreted by cultured cells in serum-containing media. *J Proteome Res* 8: 4779-4788.

270. Palazzolo, G., N. N. Albanese, D. I. C. G, D. Gygax, M. L. Vittorelli, and I. Pucci-Minafra. 2012. Proteomic analysis of exosome-like vesicles derived from breast cancer cells. *Anticancer research* 32: 847-860.

271. Zhang, Y., X. Tang, L. Yao, K. Chen, W. Jia, X. Hu, and L. X. Xu. 2012. Lectin capture strategy for effective analysis of cell secretome. *Proteomics* 12: 32-36.

272. Ross, D. T., U. Scherf, M. B. Eisen, C. M. Perou, C. Rees, P. Spellman, V. Iyer, S. S. Jeffrey, M. Van de Rijn, M. Waltham, A. Pergamenschikov, J. C. Lee, D. Lashkari, D. Shalon, T. G. Myers, J. N. Weinstein, D. Botstein, and P. O. Brown. 2000. Systematic variation in gene expression patterns in human cancer cell lines. *Nature genetics* 24: 227-235.

273. He, J., S. A. Whelan, M. Lu, D. Shen, D. U. Chung, R. E. Saxton, K. F. Faull, J. P. Whitelegge, and H. R. Chang. 2011. Proteomic-based biosignatures in breast cancer

classification and prediction of therapeutic response. *International journal of proteomics* 2011: 896476.

274. Kostianets, O., S. Antoniuk, V. Filonenko, and R. Kiyamova. 2012. Immunohistochemical analysis of medullary breast carcinoma autoantigens in different histological types of breast carcinomas. *Diagnostic pathology* 7: 161.

275. Lee, J. H., X. Zhang, B. K. Shin, E. S. Lee, and I. Kim. 2009. Mac-2 binding protein and galectin-3 expression in mucinous tumours of the ovary: an annealing control primer system and immunohistochemical study. *Pathology* 41: 229-233.

276. Iacobelli, S., I. Bucci, M. D'Egidio, C. Giuliani, C. Natoli, N. Tinari, M. Rubistein, and J. Schlessinger. 1993. Purification and characterization of a 90 kDa protein released from human tumors and tumor cell lines. *FEBS letters* 319: 59-65.

277. Scambia, G., P. B. Panici, G. Baiocchi, L. Perrone, S. Iacobelli, and S. Mancuso. 1988. Measurement of a monoclonal-antibody-defined antigen (90K) in the sera of patients with ovarian cancer. *Anticancer research* 8: 761-764.

278. Gortzak-Uzan, L., A. Ignatchenko, A. I. Evangelou, M. Agochiya, K. A. Brown, P. St Onge, I. Kireeva, G. Schmitt-Ulms, T. J. Brown, J. Murphy, B. Rosen, P. Shaw, I. Jurisica, and T. Kislinger. 2008. A proteome resource of ovarian cancer ascites: integrated proteomic and bioinformatic analyses to identify putative biomarkers. *J Proteome Res* 7: 339-351.

279. Inohara, H., and A. Raz. 1994. Identification of human melanoma cellular and secreted ligands for galectin-3. *Biochemical and biophysical research communications* 201: 1366-1375.

280. Traini, S., E. Piccolo, N. Tinari, C. Rossi, R. La Sorda, F. Spinella, A. Bagnato, R. Lattanzio, M. D'Egidio, A. Di Risio, F. Tomao, A. Grassadonia, M. Piantelli, C. Natoli, and S. Iacobelli. 2014. Inhibition of tumor growth and angiogenesis by SP-2, an anti-lectin, galactoside-binding soluble 3 binding protein (LGALS3BP) antibody. *Molecular cancer therapeutics* 13: 916-925.

281. Morandi, F., M. V. Corrias, I. Levreri, P. Scaruffi, L. Raffaghello, B. Carlini, P. Bocca, I. Prigione, S. Stigliani, L. Amoroso, S. Ferrone, and V. Pistoia. 2011. Serum levels of cytoplasmic melanoma-associated antigen at diagnosis may predict clinical relapse in neuroblastoma patients. *Cancer immunology, immunotherapy : CII* 60: 1485-1495.

282. Chen, S. T., T. L. Pan, H. F. Juan, T. Y. Chen, Y. S. Lin, and C. M. Huang. 2008. Breast tumor microenvironment: proteomics highlights the treatments targeting secretome. *J Proteome Res* 7: 1379-1387.

283. Liu, F. T., D. K. Hsu, R. I. Zuberi, I. Kuwabara, E. Y. Chi, and W. R. Henderson, Jr. 1995. Expression and function of galectin-3, a beta-galactoside-binding lectin, in human monocytes and macrophages. *The American journal of pathology* 147: 1016-1028.

284. Grandin, E. W., P. Jarolim, S. A. Murphy, L. Ritterova, C. P. Cannon, E. Braunwald, and D. A. Morrow. 2012. Galectin-3 and the development of heart failure after acute coronary syndrome: pilot experience from PROVE IT-TIMI 22. *Clin Chem* 58: 267-273.

285. Traber, P. G., and E. Zomer. 2013. Therapy of experimental NASH and fibrosis with galectin inhibitors. *PLoS One* 8: e83481.

286. Traber, P. G., H. Chou, E. Zomer, F. Hong, A. Klyosov, M. I. Fiel, and S. L. Friedman. 2013. Regression of fibrosis and reversal of cirrhosis in rats by galectin inhibitors in thioacetamide-induced liver disease. *PLoS One* 8: e75361.

287. Blakaj, A., and R. Bucala. 2012. Fibrocytes in health and disease. *Fibrogenesis Tissue Repair* 5: S6.

288. Lisanti, M. P., U. E. Martinez-Outschoorn, B. Chiavarina, S. Pavlides, D. Whitaker-Menezes, A. Tsirigos, A. Witkiewicz, Z. Lin, R. Balliet, A. Howell, and F. Sotgia. 2010. Understanding the "lethal" drivers of tumor-stroma co-evolution: emerging role(s) for hypoxia, oxidative stress and autophagy/mitophagy in the tumor micro-environment. *Cancer Biol Ther* 10: 537-542.

289. Mishra, P., D. Banerjee, and A. Ben-Baruch. 2011. Chemokines at the crossroads of tumor-fibroblast interactions that promote malignancy. *J Leukoc Biol* 89: 31-39.

290. Weber, C. E., and P. C. Kuo. 2011. The tumor microenvironment. *Surg Oncol*.

291. Mbeunkui, F., and D. J. Johann, Jr. 2009. Cancer and the tumor microenvironment: a review of an essential relationship. *Cancer Chemother Pharmacol* 63: 571-582.

292. Anderson, A. R., A. M. Weaver, P. T. Cummings, and V. Quaranta. 2006. Tumor morphology and phenotypic evolution driven by selective pressure from the microenvironment. *Cell* 127: 905-915.

293. Bianchi, G., G. Borgonovo, V. Pistoia, and L. Raffaghello. 2011. Immunosuppressive cells and tumour microenvironment: focus on mesenchymal stem cells and myeloid derived suppressor cells. *Histol Histopathol* 26: 941-951.

294. Mantovani, A., P. Allavena, A. Sica, and F. Balkwill. 2008. Cancer-related inflammation. *Nature* 454: 436-444.

295. Kong, C., C. Wang, L. Wang, M. Ma, C. Niu, X. Sun, J. Du, Z. Dong, S. Zhu, J. Lu, and B. Huang. 2011. NEDD9 is a positive regulator of epithelial-mesenchymal transition and promotes invasion in aggressive breast cancer. *PLoS One* 6: e22666.

296. Rasanen, K., and A. Vaheri. 2010. Activation of fibroblasts in cancer stroma. *Exp Cell Res* 316: 2713-2722.

297. Franco, O. E., A. K. Shaw, D. W. Strand, and S. W. Hayward. 2010. Cancer associated fibroblasts in cancer pathogenesis. *Semin Cell Dev Biol* 21: 33-39.

298. Bhowmick, N. A., E. G. Neilson, and H. L. Moses. 2004. Stromal fibroblasts in cancer initiation and progression. *Nature* 432: 332-337.

299. Lorusso, G., and C. Ruegg. 2008. The tumor microenvironment and its contribution to tumor evolution toward metastasis. *Histochem Cell Biol* 130: 1091-1103.

300. Zhang, H., I. Maric, M. J. DiPrima, J. Khan, R. J. Orentas, R. N. Kaplan, and C. L. Mackall. 2013. Fibrocytes represent a novel MDSC subset circulating in patients with metastatic cancer. *Blood* 122: 1105-1113.

301. Zambelli, D., M. Zuntini, F. Nardi, M. C. Manara, M. Serra, L. Landuzzi, P. L. Lollini, S. Ferrari, M. Alberghini, A. Llombart-Bosch, E. Piccolo, S. Iacobelli, P. Picci, and K. Scotlandi. 2010. Biological indicators of prognosis in Ewing's sarcoma: an

emerging role for lectin galactoside-binding soluble 3 binding protein (LGALS3BP). *Int J Cancer* 126: 41-52.

302. Goldberg, B., E. H. Epstein, Jr., and C. J. Sherr. 1972. Precursors of collagen secreted by cultured human fibroblasts. *Proc Natl Acad Sci U S A* 69: 3655-3659.

303. Iqbal, S. A., G. P. Sidgwick, and A. Bayat. 2012. Identification of fibrocytes from mesenchymal stem cells in keloid tissue: a potential source of abnormal fibroblasts in keloid scarring. *Archives of dermatological research* 304: 665-671.

304. Darby, I. A., and T. D. Hewitson. 2007. Fibroblast differentiation in wound healing and fibrosis. *International review of cytology* 257: 143-179.

305. Wessel, D., and U. I. Flugge. 1984. A method for the quantitative recovery of protein in dilute solution in the presence of detergents and lipids. *Analytical biochemistry* 138: 141-143.

306. Murray, L. A., M. S. Kramer, D. P. Hesson, B. A. Watkins, E. G. Fey, R. L. Argentieri, F. Shaheen, D. A. Knight, and S. T. Sonis. 2010. Serum amyloid P ameliorates radiation-induced oral mucositis and fibrosis. *Fibrogenesis Tissue Repair* 3: 11.

307. Gamer, L. W., J. Nove, and V. Rosen. 2003. Return of the chalones. *Developmental cell* 4: 143-144.

308. Bouvy, N. D., R. L. Marquet, J. Jeekel, and H. J. Bonjer. 1997. Laparoscopic surgery is associated with less tumour growth stimulation than conventional surgery: an experimental study. *The British journal of surgery* 84: 358-361.

309. Demicheli, R., M. W. Retsky, W. J. Hrushesky, M. Baum, and I. D. Gukas. 2008. The effects of surgery on tumor growth: a century of investigations. *Annals of oncology : official journal of the European Society for Medical Oncology / ESMO* 19: 1821-1828.

310. Crowley, N. J., and H. F. Seigler. 1992. Relationship between disease-free interval and survival in patients with recurrent melanoma. *Archives of surgery* 127: 1303-1308.

311. Demicheli, R., A. Abbattista, R. Miceli, P. Valagussa, and G. Bonadonna. 1996. Time distribution of the recurrence risk for breast cancer patients undergoing mastectomy: further support about the concept of tumor dormancy. *Breast Cancer Res Treat* 41: 177-185.

312. Goodison, S., K. Kawai, J. Hihara, P. Jiang, M. Yang, V. Urquidi, R. M. Hoffman, and D. Tarin. 2003. Prolonged dormancy and site-specific growth potential of cancer cells spontaneously disseminated from nonmetastatic breast tumors as revealed by labeling with green fluorescent protein. *Clinical cancer research : an official journal of the American Association for Cancer Research* 9: 3808-3814.

313. GO Gey, W. C., MT Kubicek. 1952. Tissue culture studies of the proliferative capacity of cervical carcinoma and normal epithelium. *Cancer Research* 12: 264–265.

314. Hodis, E., I. R. Watson, G. V. Kryukov, S. T. Arold, M. Imielinski, J. P. Theurillat, E. Nickerson, D. Auclair, L. Li, C. Place, D. Dicara, A. H. Ramos, M. S. Lawrence, K. Cibulskis, A. Sivachenko, D. Voet, G. Saksena, N. Stransky, R. C. Onofrio, W. Winckler, K. Ardlie, N. Wagle, J. Wargo, K. Chong, D. L. Morton, K. Stemke-Hale, G. Chen, M. Noble, M. Meyerson, J. E. Ladbury, M. A. Davies, J. E.

Gershenwald, S. N. Wagner, D. S. Hoon, D. Schadendorf, E. S. Lander, S. B. Gabriel, G. Getz, L. A. Garraway, and L. Chin. 2012. A landscape of driver mutations in melanoma. *Cell* 150: 251-263.

315. Cai, Z., J. F. Chiu, and Q. Y. He. 2004. Application of proteomics in the study of tumor metastasis. *Genomics, proteomics & bioinformatics* 2: 152-166.

316. Geiger, T., S. F. Madden, W. M. Gallagher, J. Cox, and M. Mann. 2012. Proteomic portrait of human breast cancer progression identifies novel prognostic markers. *Cancer Res* 72: 2428-2439.

317. Agathocleous, M., and W. A. Harris. 2013. Metabolism in physiological cell proliferation and differentiation. *Trends in cell biology* 23: 484-492.

318. Wen, H., J. P. Ting, and L. A. O'Neill. 2012. A role for the NLRP3 inflammasome in metabolic diseases--did Warburg miss inflammation? *Nature immunology* 13: 352-357.

319. Kratz, M., B. R. Coats, K. B. Hisert, D. Hagman, V. Mutskov, E. Peris, K. Q. Schoenfelt, J. N. Kuzma, I. Larson, P. S. Billing, R. W. Landerholm, M. Crouthamel, D. Gozal, S. Hwang, P. K. Singh, and L. Becker. 2014. Metabolic dysfunction drives a mechanistically distinct proinflammatory phenotype in adipose tissue macrophages. *Cell metabolism* 20: 614-625.

320. Vander Heiden, M. G., L. C. Cantley, and C. B. Thompson. 2009. Understanding the Warburg effect: the metabolic requirements of cell proliferation. *Science* 324: 1029-1033.

321. Dandapani, M., and D. G. Hardie. 2013. AMPK: opposing the metabolic changes in both tumour cells and inflammatory cells? *Biochemical Society transactions* 41: 687-693.

322. Marroquin, L. D., J. Hynes, J. A. Dykens, J. D. Jamieson, and Y. Will. 2007. Circumventing the Crabtree effect: replacing media glucose with galactose increases susceptibility of HepG2 cells to mitochondrial toxicants. *Toxicological sciences : an official journal of the Society of Toxicology* 97: 539-547.

323. Vaupel, P., F. Kallinowski, and P. Okunieff. 1989. Blood flow, oxygen and nutrient supply, and metabolic microenvironment of human tumors: a review. *Cancer Res* 49: 6449-6465.

324. Palmer, B. F., and D. J. Clegg. 2014. Oxygen sensing and metabolic homeostasis. *Molecular and cellular endocrinology* 397: 51-58.

325. Martinez-Outschoorn, U., F. Sotgia, and M. P. Lisanti. 2014. Tumor microenvironment and metabolic synergy in breast cancers: critical importance of mitochondrial fuels and function. *Seminars in oncology* 41: 195-216.

326. Sen, C. K. 2009. Wound healing essentials: let there be oxygen. *Wound Repair Regen* 17: 1-18.

327. Zheng, J., F. Song, S. L. Lu, and X. Q. Wang. 2014. Dynamic hypoxia in scar tissue during human hypertrophic scar progression. *Dermatologic surgery : official publication for American Society for Dermatologic Surgery [et al.]* 40: 511-518.

328. Bucala, R. 2007. *Fibrocytes : new insights into tissue repair and systemic fribrosis*. World Scientific, Hackensack, NJ.

329. Pilling, D., Z. Zheng, V. Vakil, and R. H. Gomer. 2014. Fibroblasts secrete Slit2 to inhibit fibrocyte differentiation and fibrosis. *Proc Natl Acad Sci U S A* 111: 18291-18296.

APPENDIX A

SAP DOES NOT INFLUENCE DERMAL OR LUNG FIBROBLAST PROLIFERATION OR PROTEOME AS MEASURED BY 2D GEL ELECTROPHORESIS

Introduction

Wound healing and fibrosis are major medical concerns. Approximately 1 in 250 people will require medical treatment for a wound in a given year (15). Fibrosing diseases—including heart disease, pulmonary fibrosis, kidney fibrosis, and liver cirrhosis—are associated with 45% of deaths in the United States (20). In fibrosing diseases, scar tissue buildup in and on organs reduces their function (20). Fibrosing diseases can reduce the quality of life or the length of life for patients.

Monocytes are a type of immune system cell involved in wound healing and fibrosis. Monocytes are circulating cells that are recruited to wounds and sites of tissue injury by chemokines (25, 26). Monocytes enter the wound and differentiate into a number of monocyte-derived cell types, one of which is the fibrocyte (27, 28). Fibrocytes are fibroblast-like monocyte-derived cells which are CD45 positive, and express collagen (27). Fibrocytes are involved in forming collagen scars in both wound healing and fibrosis (29, 30).

Fibroblasts are a tissue resident cell which divide more quickly and secrete more collagen in a wound or site of tissue injury (302).

Wound healing and fibrosis are major medical concerns tied together by the process of scar tissue formation (303). In scar tissue formation, fibroblasts and fibrocytes secrete collagen to form scar tissue (304).

Serum amyloid P (SAP) is a protein which inhibits the differentiation of monocytes to fibrocytes (36). SAP slows wound healing when added to wounds, and removing SAP from wounds speeds wound healing (32). SAP's affect on fibroblasts is unknown. Here we investigate whether SAP has a direct affect on two different types of fibroblasts from adult tissues, dermal fibroblasts and lung fibroblasts.

Materials and Methods

Fibroblasts

Normal adult lung fibroblasts (Lonza, Basel, Switzerland) and normal adult dermal fibroblasts (Lonza) were cultured in growth medium (RPMI supplemented to 10% with U.S. origin fetal bovine serum (FBS) (Genessee scientific, San Diego, CA) and 100 U/ml penicillin (Lonza) and 100 μg/ml streptomycin (Lonza) and 2mM glutamine (Lonza)). At approximately 40% confluency the growth media was removed, cells were gently washed three times with 1x PBS while still adhered to the plate, and protein free media (PFM) (Composed of Fibrolife basal media (Lifeline Cell Technology, Walkersville, MD) supplemented with 10 mM HEPES (Sigma, St. Louis, MO), 1× non-essential amino acids (Sigma), 1 mM sodium pyruvate (Sigma), 2 mM glutamine (Lonza), 100 U/ml penicillin and 100 μg/ml streptomycin (Lonza)) was added to the cells, and where indicated was supplemented with 10 μg/ml of Serum Amyloid P (SAP) (EMD Millipore, Billerica, MD)

or 10 µg/ml bovine serum albumin (BSA) (Sigma). Fibroblasts were allowed to remain in PFM for the indicated time, and either counted by hemocytometer, lysed, or fixed and stained for immunofluorescence.

Phase contrast

Fibroblasts were photographed at 24 and 48 hours after the addition of PFM or PFM supplemented with 10 µg/ml SAP (EMD Millipore) in 24 well tissue culture treated plates (BD biosciences, San Jose, CA) using a Nikon diaphot inverted tissue culture microscope (Nikon, Tokyo, Japan) and a Nikon D1X SLR camera (Nikon).

SAP purification

SAP was purified as previously described (36), with the following modifications. Human serum from blood donors was mixed 1:1 with PBS. This serum was mixed with gentle rolling in a 10:1 ratio with SP sepharose beads (GE healthcare, Piscataway, NJ) in 20 mM Tris, 140 mM NaCl, 2 mM $CaCl_2$ pH 8.0 buffer and eluted as previously described (36). SAP purification was checked by silver stain on an SDS-PAGE gel and concentration was assessed by absorbance at 280 nm.

PBMC SAP assays

SAP (calbiochem), SAP (kind gift of Promedior biosciences), and purified SAP from human serum were tested to ensure that they inhibited monocyte to fibrocyte

differentiation as previously described (33). PBMC were acquired, stained, and counted as previously described (34).

Proliferation assay

SAP was depleted from serum as previously described (36) with the following modifications. Undiluted sterile filtered non-blood type specific human serum, tested negative for hepatitis A and B and HIV I and II (Lonza) was mixed with SP sepharose beads (GE healthcare) in 20 mM Tris, 140 mM NaCl, 2 mM $CaCl_2$ pH 8.0 buffer. A serum control was mixed solely with buffer. Beads were removed by five minutes of centrifugation at 200 x g. Human serum (Lonza) was also supplemented with 30 μg/ml of recombinant SAP (kind gift of Promedior) or purified native SAP.

Fibroblasts growing in RPMI (supplemented to 10% with FBS (Genessee scientific) and 100 U/ml penicillin (Lonza) and 100 μg/ml streptomycin (Lonza) and 2mM glutamine (Lonza)) were washed twice with 1x PBS trypsinized with 1x porcine trypsin (Sigma). These fibroblasts were mixed with growth medium and centrifuged at 300 x g twice, before being incubated on ice and counted using a hemocytometer.

3,000 cells were placed in each well of a 24-well plate with 1 ml of growth medium supplemented with 10% human serum or Fibrolife supplemented with fibroblast growth additives (Lifeline), where indicated. Fibroblasts were trypsinized and counted on a hemocytometer every 24 hours for the following nine days.

In the two day PFM proliferation assays, growth media was removed from cells around 40% confluency. After three washed with 1x PBS, PFM or PFM supplemented with SAP was added to fibroblasts. All other details are identical to those above.

One dimensional gels

After two days in protein free media (PFM) or PFM supplemented with SAP (EMD Millipore)to 10 µg/ml, fibroblasts were lysed with 6x SDS sample buffer with 2-mercaptoethanol. At the same time, fibroblast conditioned media was mixed with 6x SDS sample buffer with 2-mercaptoethanol. Samples were heated to 95 degrees for 10 minutes and then loaded onto a 4-20% SDS-PAGE reducing gel (Bio-Rad, Hercules, California) at 130V for 50 minutes. Gels were silver stained and imaged.

Two dimensional gels

Fibroblasts in a 6-well plate (BD Falcon) were washed three times with 1x PBS and placed in PFM or PFM supplemented with BSA (Sigma) or SAP (Calbiochem) to 10 µg/ml. After 48 hours fibroblasts were lysed with 400 ul 2% (w/v) CHAPS buffer and removed from the plate with a rubber policeman. Cell lysate was centrifuged at 18,000 x g in 4 degrees for 20 minutes, and the bottom 100 ul of lysate was discarded. Approximately 35 µg of protein from the cell lysates were concentrated by precipitation with methanol/chloroform (305).

For lung fibroblasts, approximately 12 µg of protein was dissolved in 1 ml IEF buffer containing 8.5 M urea, 4% CHAPS, 100 mM DTT, 18mM Destreak, and 10 ul carrier ampholytes (Calbiochem). 125 ul of buffer was used to resuspend the protein and actively rehydrate an immobilized pH gradient IPG dry strips (Bio-Rad, pH 4-7, 7 cm) for 12 hours at room temperature and 50V. The proteins were focused using a Protean IEF cell (Bio-Rad) using a four step program: 15 minutes at 250V, 2 hour linear gradient to 4000V, a hold at 4000 V until 16,000 VH was reached, and finally a 500 V hold. After focusing, the IPG strips were equilibrated in a solution containing 6M urea, 75 mM Tris, 30% (v/v) glycerol, 2% SDS (w/v), 0.002% (w/v) Bromophenol blue and 10 mg/ml DTT for 15 minutes at room temperature. The strips were transferred to a second equilibration buffer (same composition as the first buffer) replacing DTT with Iodoacetamide (25 mg/ml). The strips were then transferred to the top of a top of a 12% polyacrylamide slab gel (Bio-Rad) and anchored in place with low melting temperature agarose (0.5%). The proteins were separated until the dye reached the bottom of the gel. Following this, the gels were fixed and stained as by a silverquest stain kit (Invitrogen, Grand Island, NY), following the manufacturer's instructions.

For the dermal fibroblasts, the 2d gels were run using the same protocol with the following adjustments. The proteins were dissolved in a solution containing 7M Urea, 2M Thiourea, 4% CHAPS, 18mM Destreak, 0.5% Pharmalyte (pH3-10) and used to rehydrate immobilized pH gradient IPG dry strips (GE Healthcare, Piscataway, pH 3-10NL, 13 cm) overnight at room temperature. The proteins were focused according to manufacturer's recommendations on an IPGPhor (GE Healthcare) using a four step program (1 hour at

500 volts, 1 hour at 1000 volts, 2.5 hour gradient to 8000 volts and hold there to reach a total of 25,000 volt-hours). The strips were then transferred to the top of a 12% polyacrylamide slab gel (Laemmli) and anchored in place with low melting temperature agarose (0.5%). A small paper tab saturated with molecular weight markers (BioRad, 161-0317) was aligned beside the strip. The proteins were separated at 40 mAmps per gel until the dye front reached the bottom of the gel.

Immunofluorescence

PFM (or PFM supplemented to 10 µg/ml with SAP or BSA) was removed from fibroblasts on 8-well EZ slides (EMD Millipore) after the amount of time indicated (24, 48, or 72 hours) and the adhered cells were washed twice in 1x PBS. Fibroblasts were then fixed in freshly prepared 4% paraformaldehyde (Electron microscopy science, Hartfield, PA) for 10 minutes. Fibroblasts were then permeabilized with 0.1% triton (w/v, Fisher) in 1x PBS. Wells were gently washed with 1x PBS/tween (0.05% w/v) twice, and were allowed to sit for 10 minutes in PBS/tween three times.

Rabbit polyclonal antibody against EDF-1's N-terminal region (Aviva systems biology, San Diego, CA) was added at 5 µg/ml in 4% BSA/PBS (w/v, Sigma) for 2 hours after blocking the fibroblasts for 1 hour in 4% BSA/PBS. Cells were washed as above, and 2.5 µg/ml biotinylated donkey anti-rabbit IgG secondary antibody (Jackson immunoresearch, West Grove, PA) was added in 4% BSA/PBS. Cells were washed as above. A streptavidin / alexafluor conjugate at 2 µg/ml was added in 4% BSA/PBS. Cells were washed as above, and a coverslip was mounted on the slide with vectashield

mounting media, with DAPI (Vector, Burlingame, CA). Slides were imaged on an IX70 inverted microscope (Olympus, Center Valley, PA) and a coolsnap HQ2 camera (Actimetrics, Wilmette, IL).

Immunofluorescence for vimentin and hsp90b1 was performed as above, with the following changes. Monoclonal mouse anti-hsp90b1, V9 clone (Sigma) was added to cells at 1 µg/ml in 1x PBS with no blocking, and rabbit polyclonal anti-hsp90b1 (Genetex, Irvine, CA) was added to cells at 5 µg/ml in 1x PBS with no blocking. 2 µg/ml Alexafluor 488 goat anti-mouse or Alexafluor 488 goat anti-rabbit (Molecular probes, Eugene, OR) were added to the cells in 1x PBS. Slides were mounted as above, and imaged on a microphot-fx fluorescent microscope (Nikon) with a Nikon D1X SLR camera (Nikon).

Results

SAP, a pentameric protein found at approximately 30 µg/ml in human blood, inhibits the differentiation of monocytes to into fibroblast-like cells called fibrocytes. SAP also slows wound healing when added to a wound, and the absence of SAP speeds wound healing. We wanted to examine the effect of SAP on another type of wound healing cell found ubiquitously in wounds, the fibroblast. Fibroblasts in wounds proliferate and secrete more collagen.

Fibroblast morphology does not change after exposure to SAP

To determine if Serum Amyloid P (SAP) had any effect on the morphology of fibroblasts, SAP was added to protein-free culture media for both adult lung and adult dermal fibroblasts. The addition of SAP at a biological concentration of 10 µg/ml for 24 or 48 hours did not result in any morphological changes to the fibroblasts when compared to the control cells (Figure 48 A-B).

Fibroblast secretome does not appear to change under SAP stimulation, but proteome analysis reveals potential differences

To determine if Serum Amyloid P (SAP) might have subtler effects on either the proteome or secretome of fibroblasts, SAP was added to fibroblasts for 48 hours. The control cells were lysed by the addition of 2x sds sample buffer and electrophoresed on an SDS-PAGE gel. Conditioned media from SAP treated and control fibroblasts was also analyzed via gel. Close examination of the band patterns revealed no differences between SAP treated and control cells (Figure 49).

Fibroblasts were also analyzed by two-dimensional gel electrophoresis on two different gel apparatus platforms to determine if SAP treatment changed the proteome of either adult lung or adult dermal fibroblasts. Two dimensional gels were run for fibroblasts treated with no protein, SAP, and bovine serum albumin (BSA) at 10 µg/ml. The 2d gels were closely analyzed using flicker software for spots that moved or changed in intensity, indicating proteins that changed in size, isoelectric point (PI), concentration, or in which post-translational modifications were adorning the protein. Very few regions of difference were present between the gels of cells not treated with protein or treated with SAP or BSA.

Gel spots were excised and identified by mass spectrometry, and spots that were identified as SAP or BSA breakdown products were excluded. In the adult lung fibroblasts, endothelial differentiation factor 1 (EDF-1) was identified as a candidate protein to be downregulated by SAP (Figure 50). In the adult dermal fibroblasts, both vimentin and hsp90b1 were identified as candidate proteins to be downregulated by SAP (Figure 50).

Immunofluorescence does not show an increase in EDF-1, HSP90B1, and Vimentin staining intensity under SAP stimulation

To further analyze these potential protein hits, fluorescent antibody staining was used to visualize these proteins within the cell. Fluorescent staining of each of EDF-1 at 24, 48, and 72 hours revealed no large scale differences in protein intensity or localization with the cell after SAP treatment when compared to the control adult lung cells (Figure 51). For adult dermal cells, staining for both vimentin and HSP90b1 revealed no differences in intensity or cellular localization (Figure 51). These results suggest that SAP does not affect the proteome of lung or dermal fibroblasts under these experimental conditions.

SAP does not increase fibroblast proliferation

Previous wound healing research demonstrated that fibroblasts proliferate in a wound as part of the healing process. Previous research has also suggested the SAP does not affect fibroblast proliferation after short term exposure (306). To test whether SAP influences fibroblast proliferation during a long term exposure, SAP was added to both

human and dermal fibroblasts in a defined protein media. All SAP used during this paper was additionally tested on PBMC to ensure that the SAP was biologically active and inhibited the differentiation of monocytes to fibrocytes (Figure 52).

To test SAP's affect on fibroblasts in a longer proliferation assay, adult dermal and lung fibroblasts were grown in the presence of human serum containing different concentrations of SAP. SAP was depleted from (Figure 53) and added to human serum. Both adult dermal and adult lung fibroblasts were allowed to proliferate for 9 days in serum containing different quantities of SAP. Counts of these fibroblasts revealed no significant differences between SAP treated and control cell proliferation (Figures 54 and 55). Culturing fibroblasts in a defined, serum-free media supplemented with 30 and 60 μg/ml SAP also revealed no changes in proliferation (Figures 56 and 57).

Taken together, these results suggest the SAP does not have an effect on the morphology, proteome, secretome, or proliferation of adult dermal or lung fibroblasts when measured using these assays. These results suggest that SAP's potent activity in inhibiting wound healing does not act through fibroblasts directly, and instead acts solely through fibrocytes, acts indirectly on fibroblasts, or acts on fibroblasts when mixed with other wound healing cytokines.

Discussion

SAP inhibits the differentiation of monocytes to fibrocytes, and slows wound healing when added to a wound. SAP's affect on fibroblasts in a wound environment is unknown. We analyzed SAP's affect on fibroblasts by examining adult lung and dermal fibroblast's morphology, secretomes, proteomes, and proliferation by a series of visual inspections, gel analysis, and proliferation assays. In each case, SAP treatment of fibroblasts at biological concentrations did not yield differences in our assays.

These results suggest that in a wound, SAP either exerts its activity on fibrocytes or exerts its activity on fibroblasts only when activated by secondary signals.

Figures

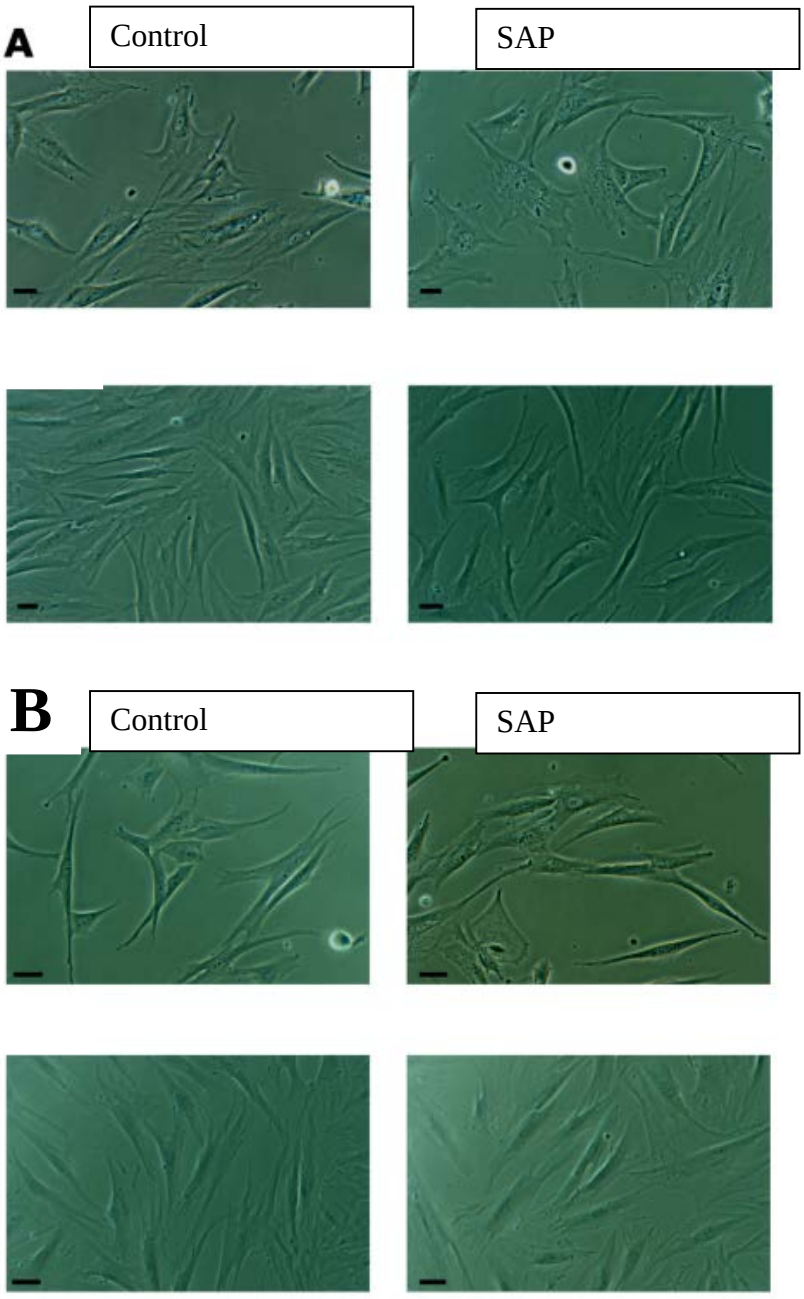

Figure 48. Fibroblasts under SAP stimulation show no morphological differences. (A) Lung fibroblasts and (B) dermal fibroblasts exposed to 10 µg/ml SAP for two days show no obvious morphological differences when compared to SAP-free controls. Images are representative of six separate replicates for both lung and dermal fibroblasts. Bar is 30 microns.

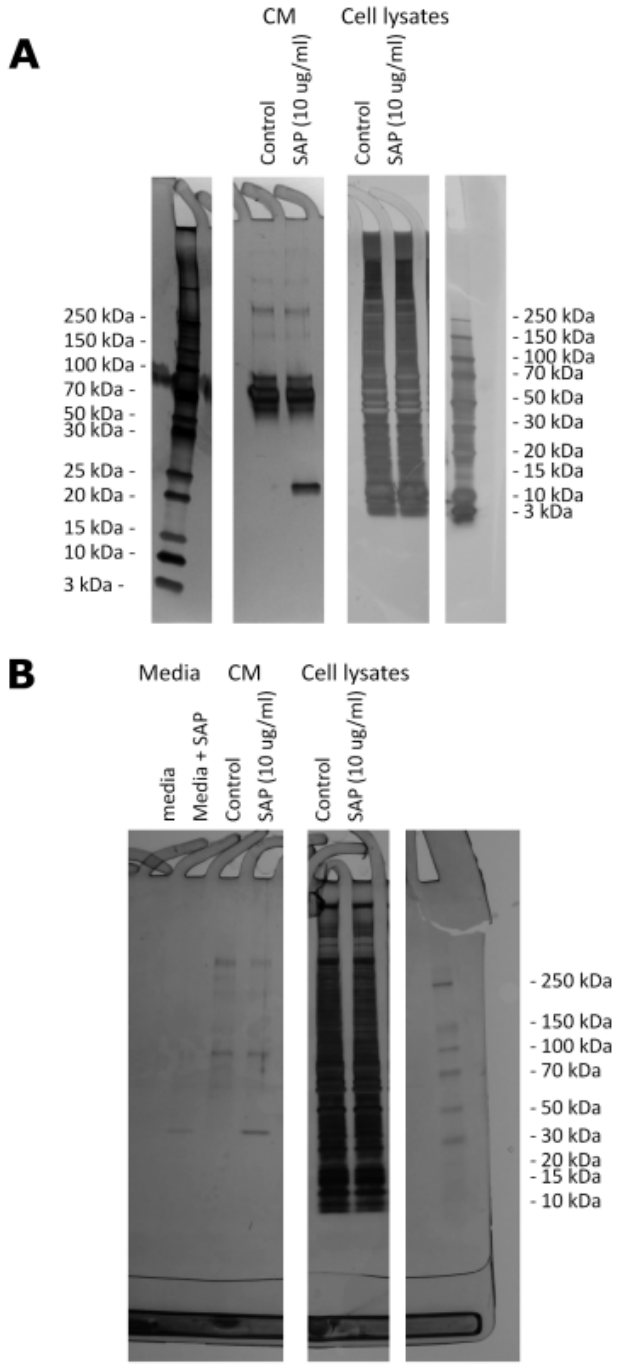

Figure 49. SAP stimulation causes no obvious change to fibroblast conditioned media or proteome when silver stained on an SDS-page gel.

Band patterns from SAP stimulated (A) lung and (B) dermal fibroblasts and conditioned media on a silver stained SDS-page gel do not appear different when compared to band patterns from SAP-free fibroblasts and conditioned media. SAP was added to both dermal and lung fibroblasts at 10 µg/ml for 48 hours.

Figure 50. Two dimensional gel analysis reveals candidate proteins differences in SAP treated fibroblast proteomes.
After 48 hour 10 µg/ml SAP stimulation, lung and dermal fibroblasts proteomes were separated by 2-D gel electrophoresis. A comparison of gels from (A) SAP-free controls and (B) SAP-treated samples in protein-free media or 10 µg/ml BSA, followed by mass spectrometry, revealed EDF-1 in lung fibroblasts and HSP-90b1 and vimentin in dermal fibroblasts as proteins potentially up or down-regulated by SAP.

pH 3 pH 7

A

Lung Fibroblasts

pH 3 pH 7

B

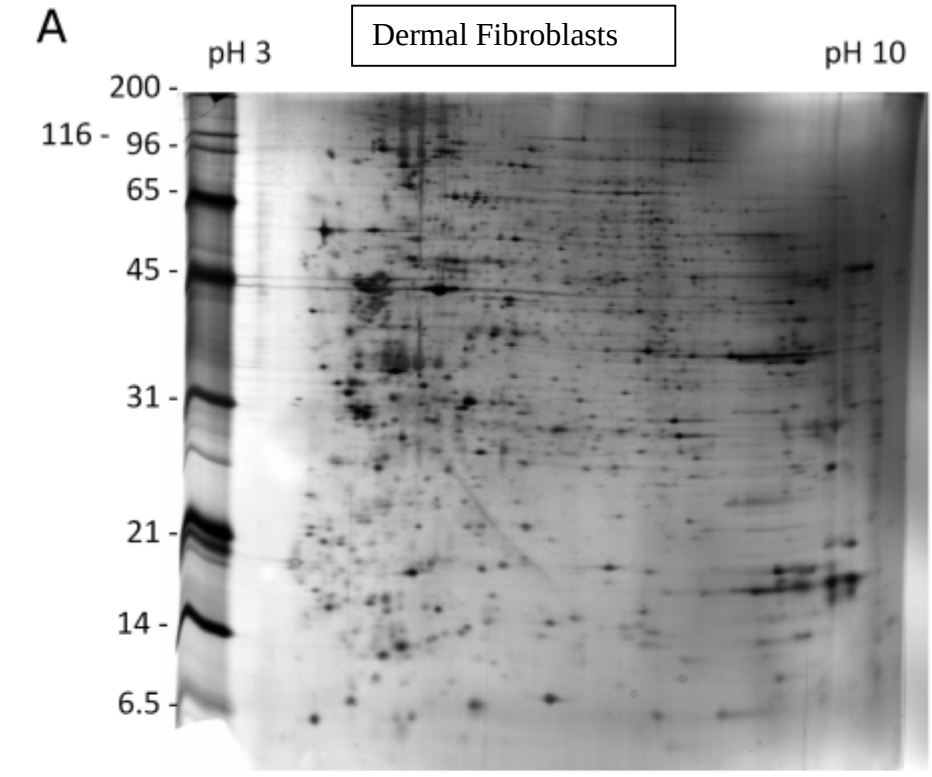
A
Dermal Fibroblasts
pH 3
pH 10
200 -
116 -
96 -
65 -
45 -
31 -
21 -
14 -
6.5 -

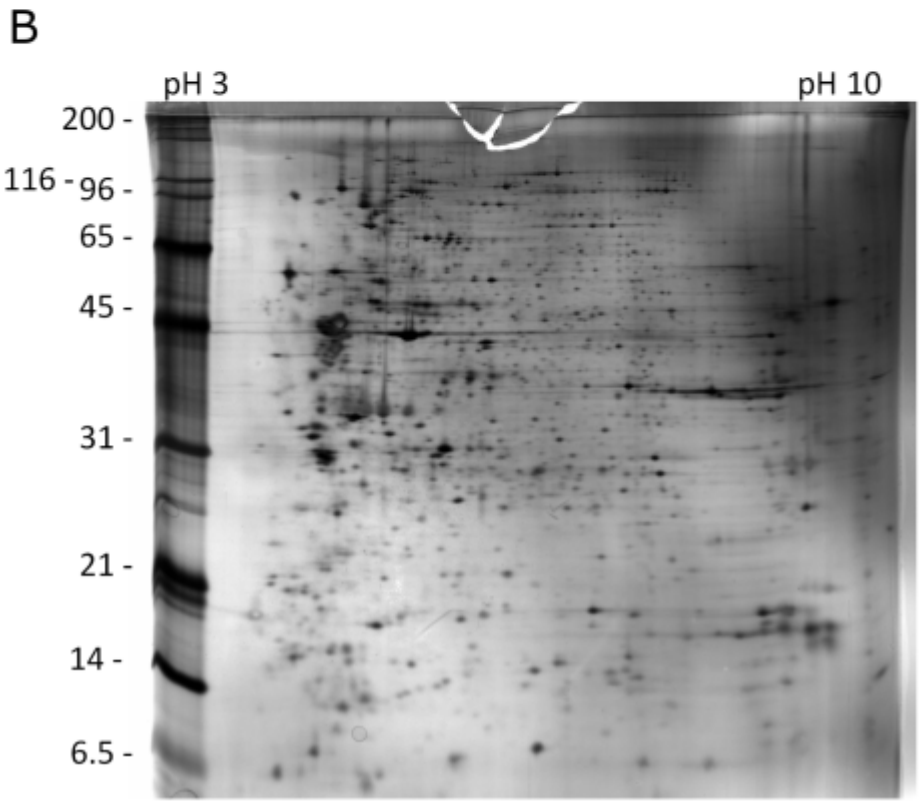
B
pH 3
pH 10
200 -
116 -
96 -
65 -
45 -
31 -
21 -
14 -
6.5 -

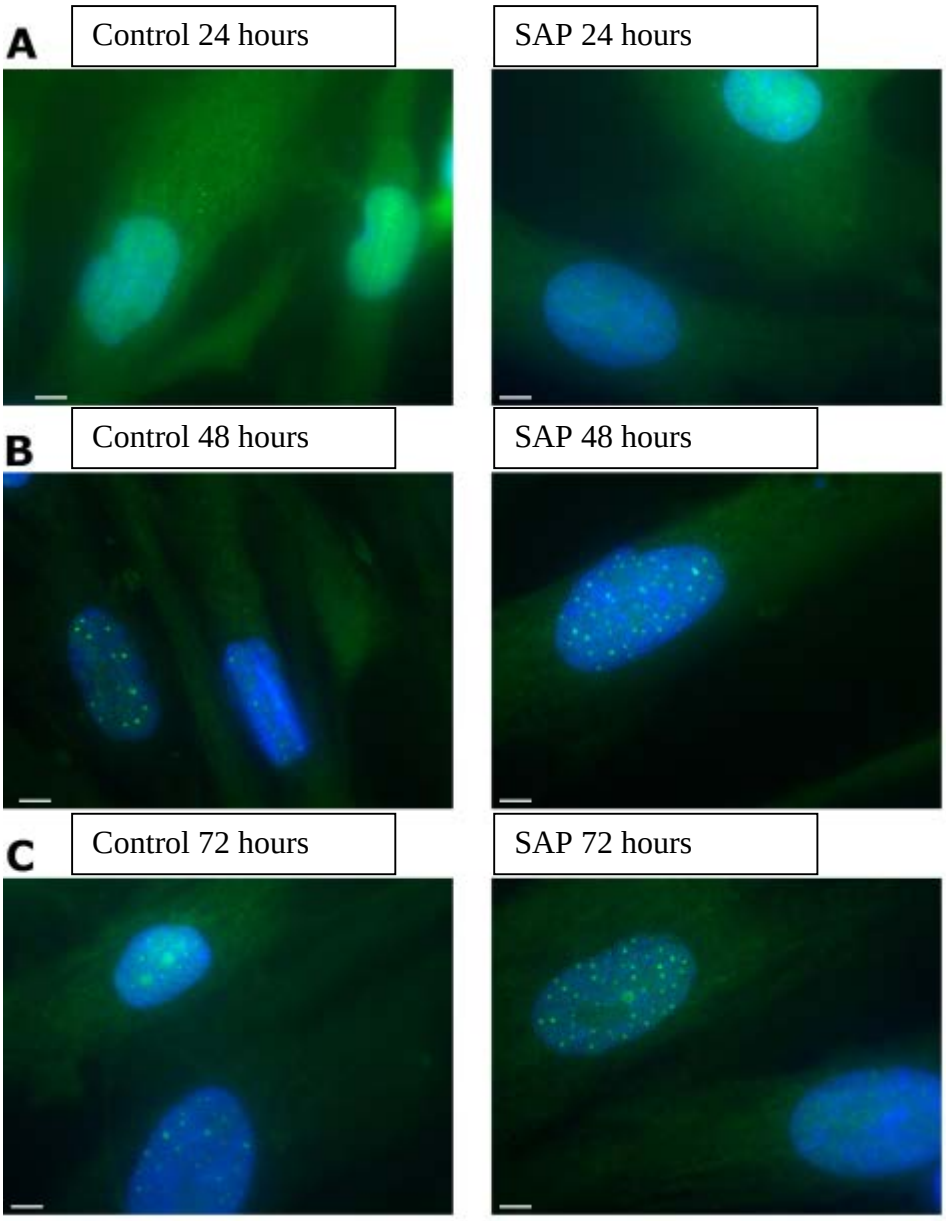
A
Control 24 hours
SAP 24 hours
B
Control 48 hours
SAP 48 hours
C
Control 72 hours
SAP 72 hours

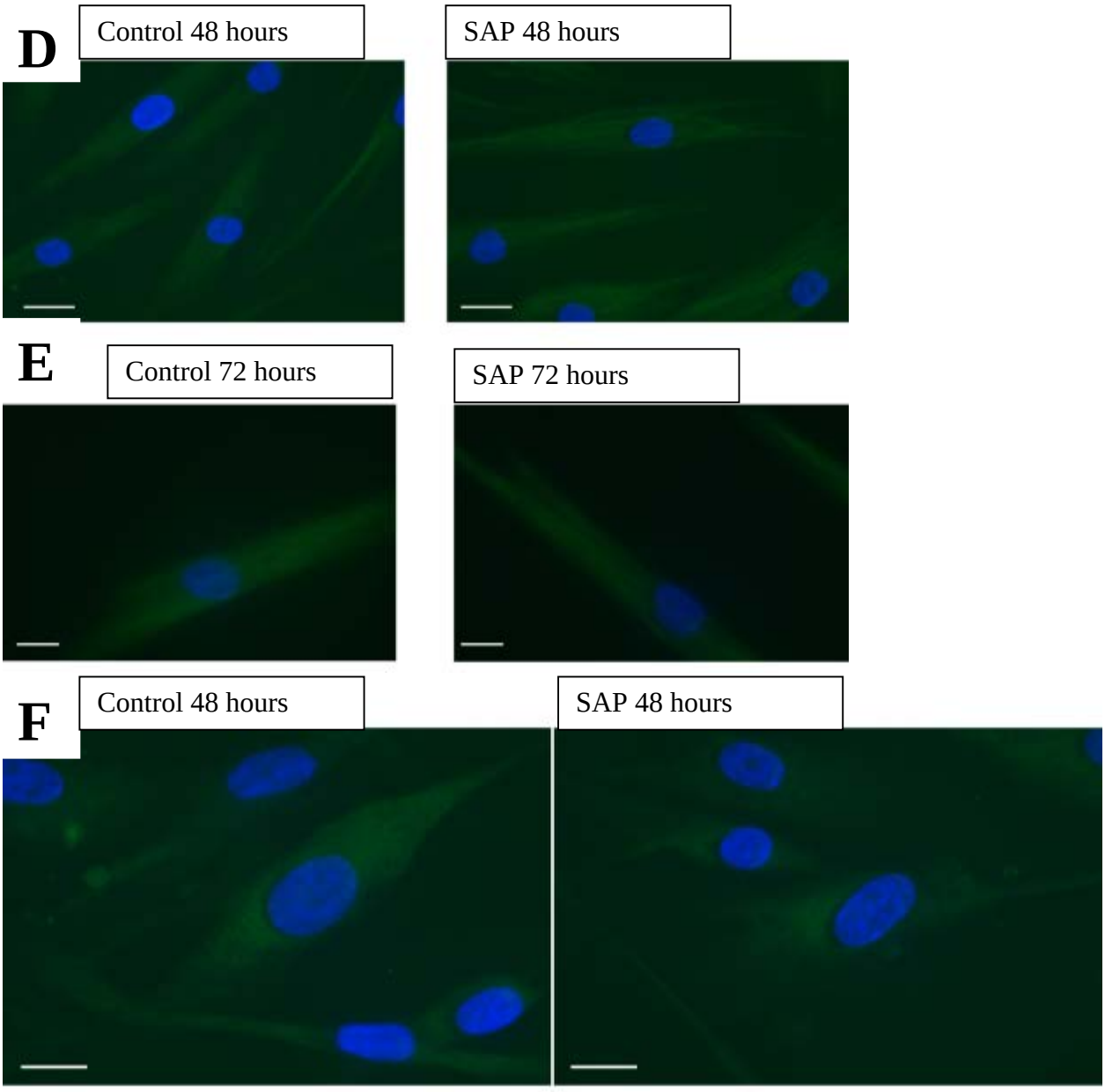

Figure 51. Immunofluorescence for vimentin, HSP-90b and EDF-1 reveal no obvious differences between fibroblasts exposed to SAP.
Immunofluorescence of fibroblasts treated with 10 µg/ml SAP or BSA reveals no significant differences for either (A-C) EDF-1, (D-E) vimentin, or (F) HSP-90b1. Bar = 30 microns.

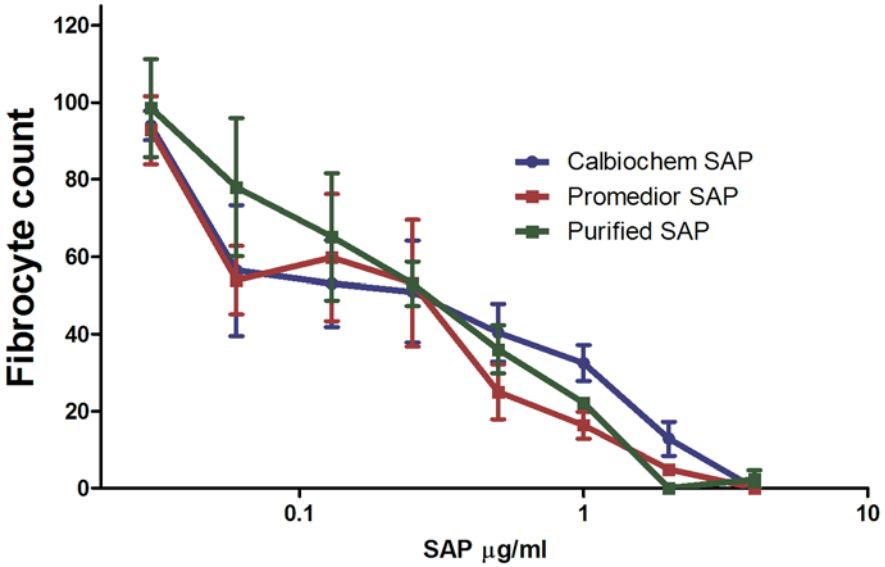

Figure 52. SAP inhibits monocyte to fibrocyte differentiation.
SAP, as previously described, inhibits the differentiation of monocytes to fibrocytes. Mean ± SEM, n=3.

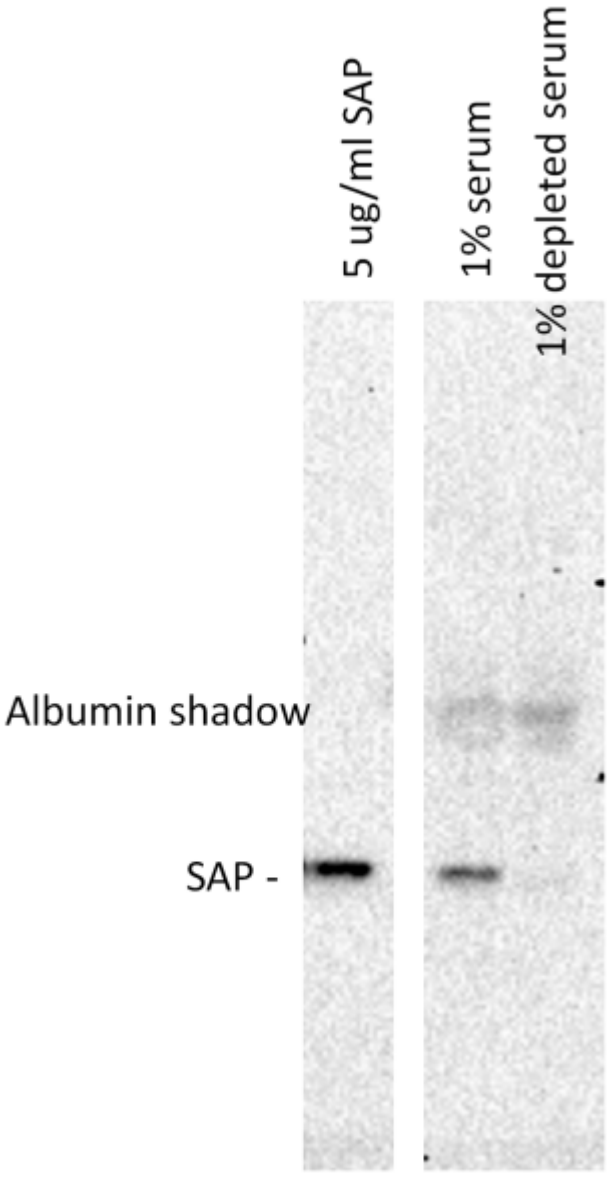

Figure 53. SAP is depleted from human serum.
Human serum was depleted of SAP, and was run a 4-20% SDS-page gel. Western blots were probed with anti-SAP antibody.

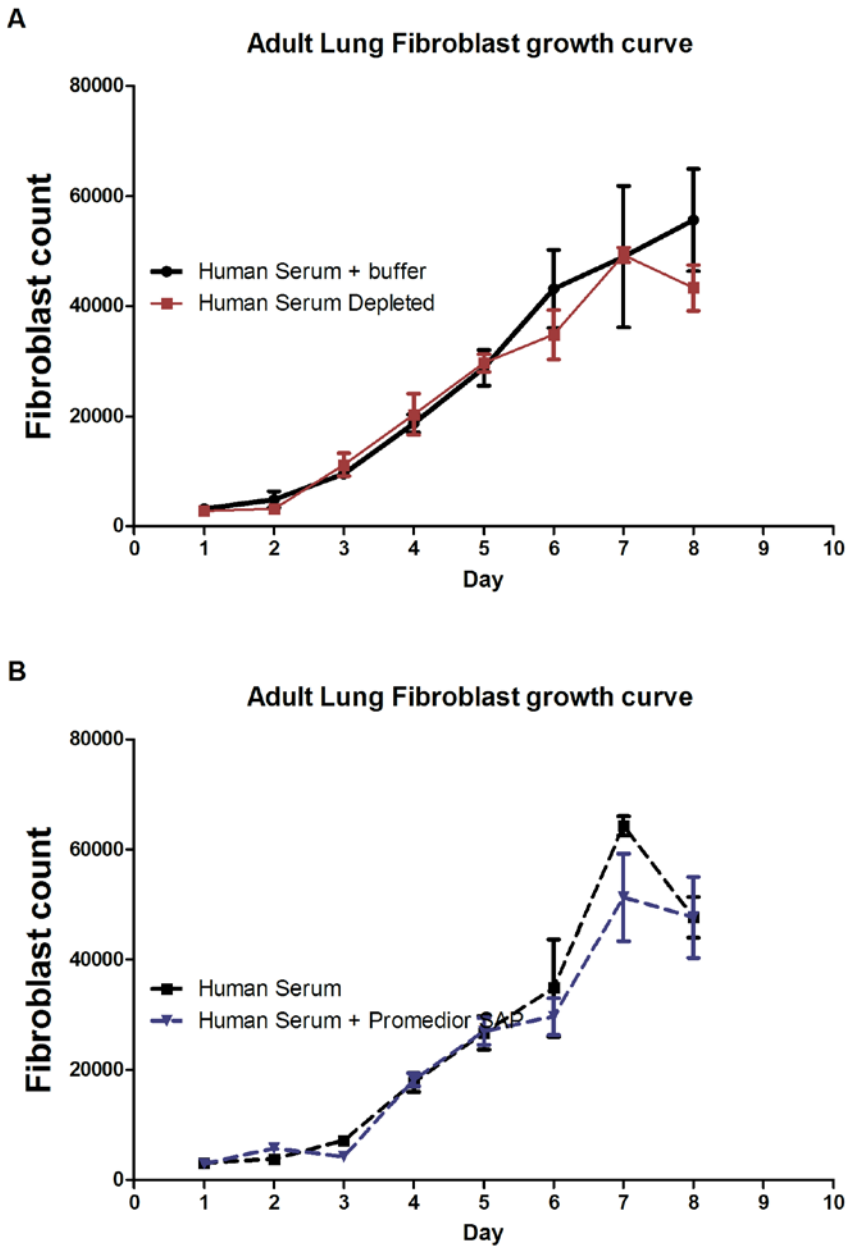

Figure 54. Lung fibroblast proliferation is not significantly affected by SAP concentration in human serum.
Human serum was depleted of SAP and supplemented with 10, 30, or 60 µg/ml SAP. This serum was used to supplement RPMI to 10% total concentration (v/v). Fibroblasts grown in 10% serum which had been depleted or supplemented with SAP showed no significant changes in proliferation over 1-8 days when proliferation was measured by resuspending fibroblasts and counting them on a hemocytometer. Mean ± SEM, n=4.

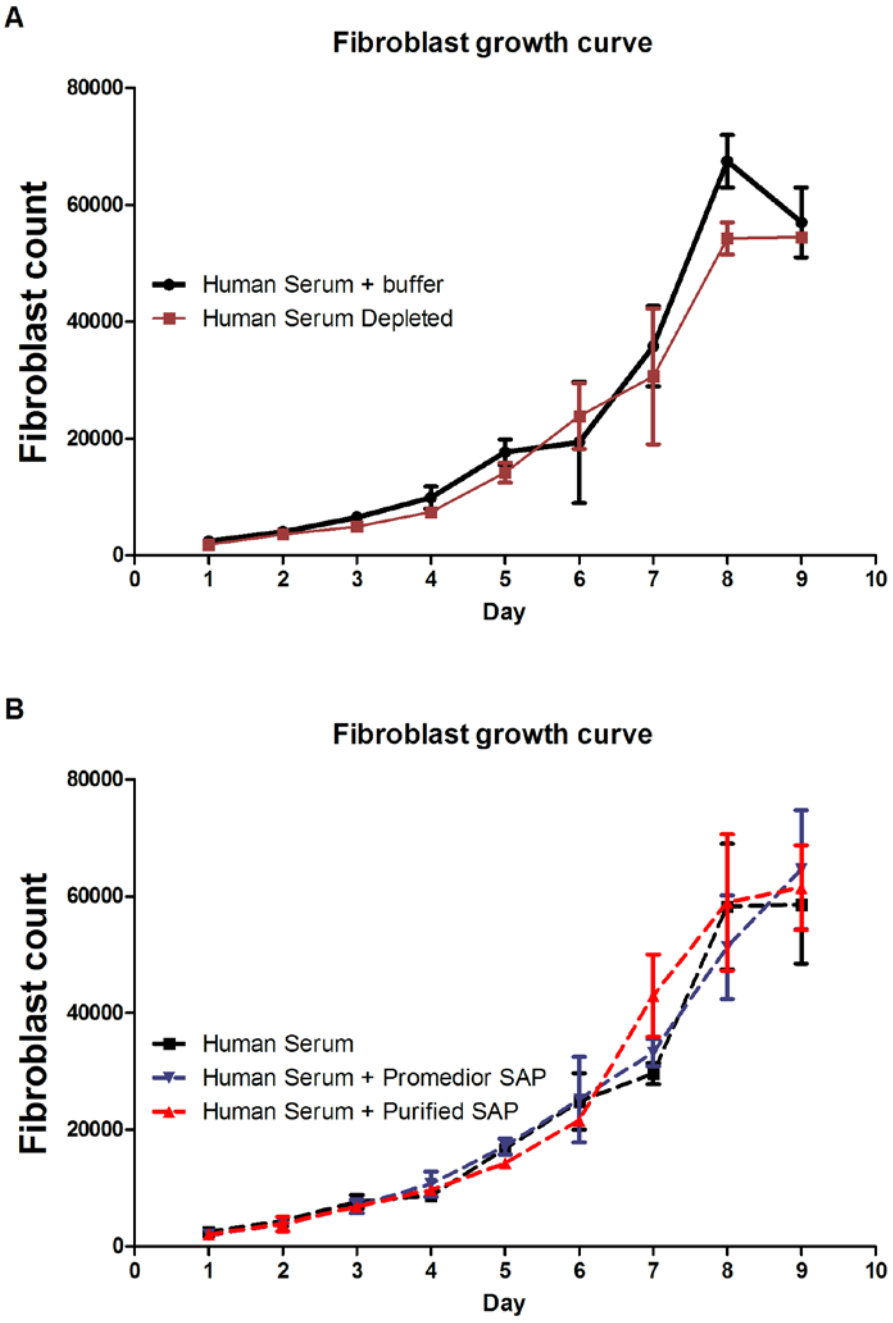

Figure 55. Dermal fibroblast proliferation is not significantly affected by SAP concentration in serum.
Dermal fibroblasts were allowed to proliferate and were counted as in figure 7. Mean ± SEM, n=4.

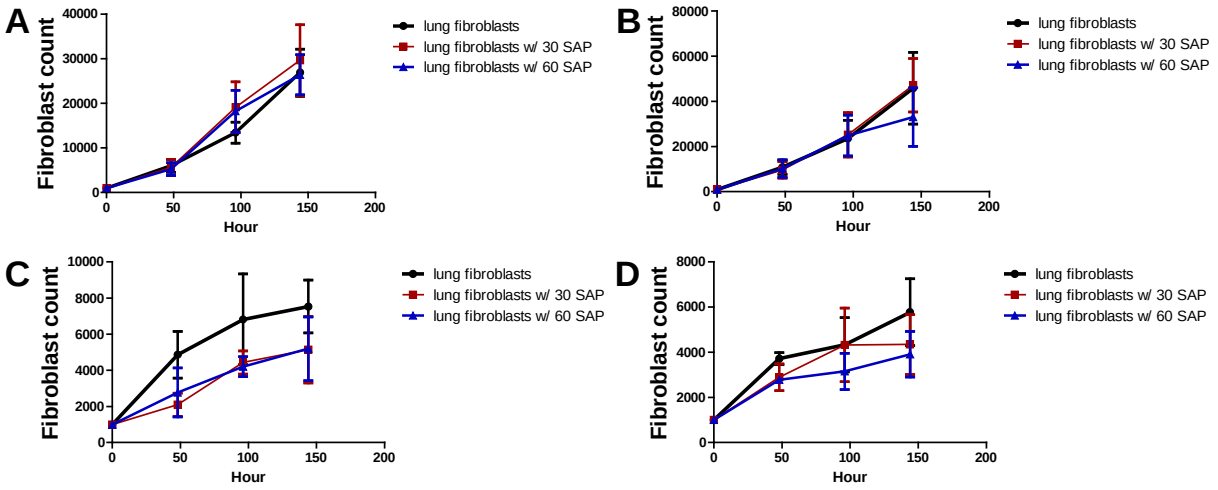

Figure 56. Lung fibroblasts proliferation in serum-free media is not affected by SAP concentration.

Lung fibroblasts were grown in (A-B) serum-free media containing fibroblast growth factors or fetal calf serum (C-D) and supplemented with 30 or 60 µg/ml SAP. Media was supplemented with TGF-beta where indicated (B, D). Fibroblasts were counted every 48 hours.

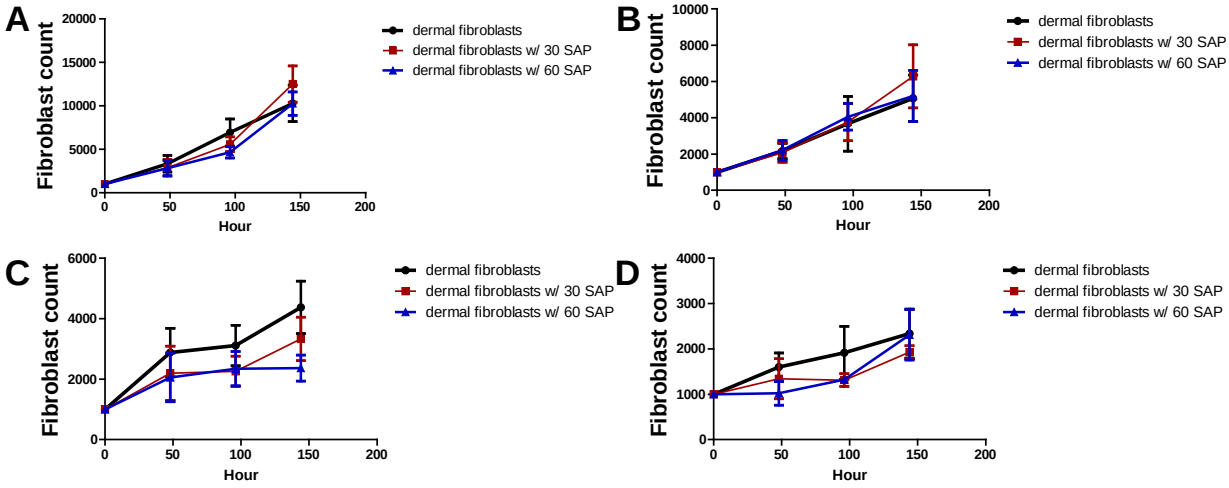

Figure 57. Dermal fibroblasts proliferation in serum-free media is not affected by SAP concentration.

Dermal fibroblasts were grown in (A-B) serum-free media containing fibroblast growth factors or fetal calf serum (C-D) and supplemented with 30 or 60 µg/ml SAP. Media was supplemented with TGF-beta where indicated (B, D). Fibroblasts were counted every 48 hours.

APPENDIX B

MCF-7 CONDITIONED MEDIA SLOWS THE PROLIFERATION OF MDA-MB 231 AND MDA-MB 435 CELLS

Introduction

How tissues regulate their size is an important and fundamental problem in biology. Very little is known about the mechanism(s) that tissues use to regulate their size. While tissue size regulation is an important problem in human biology, population size regulation is an important problem for single celled organisms, such as bacteria or amoebas (307). The size of tissues and the density of single-celled organisms are both products of the total number of cells present, and the proliferation of those cells (307). Secreted molecules which slow proliferation in the cell population are called chalones (307). To date, the only chalone that has been identified to regulate the size of a tissue in humans is myostatin for muscle tissue (307).

While cancer is not a normal human tissue, there is some evidence that cancer regulates the overall number of cancer cells in the body. Sometimes, after a tumor is removed by surgery, cancer cells in distant metastases will proliferate and increase in size (308, 309). The surgery-induced metastasis growth occurs in both melanoma (310) and breast cancer (311, 312). That removing a large number of cancer cells from the body (in the form of the primary tumor) can cause a proliferation increase in remaining cancer cells suggests that cancer may regulate the total number of cancer cells in the body. Because these metastases are in distant tissues from the primary tumor, it also makes sense that this

hypothetical factor would have to be a soluble, secreted factor that travels through the bloodstream or the lymphatic system.

We wanted to determine if secreted factors from cancer could slow the growth of either that same cancer, or other cancers.

Materials and methods

Cell lines

HEK-293 (250) cells (from the ATCC, Manassas, VA), normal adult lung fibroblasts (Lonza, Basel, Switzerland), normal adult dermal fibroblasts (Lonza), MCF-7 (110) (Kind gift of Dr. Deanne Wallis), MDA-MB 231 (103) and MDA-MB 435 (105) and DCIS.com (111) and HELA cells (313) (kind gifts of Dr. Weston Porter) were cultured in growth medium (DMEM supplemented to 5% with U.S. origin fetal bovine serum (FBS) (Genessee scientific, San Diego, CA) and 100 U/ml penicillin (Lonza) and 100 μg/ml streptomycin (Lonza) and 2mM glutamine (Lonza)).

Each tumor cell line was tested for mycoplasma contamination using a PCR detection kit (MDBioproducts, St. Paul, MN) following the manufacturer's instructions, and all work was done with cell lines containing undetectable levels of mycoplasma.

Chalone proliferation experiments

Each experiment was broken into two stages. In the 1st stage, cells were used to generate conditioned media. For the 1st stage, all cells to be used for generating conditioned media were grown to ~80% confluency, and their media was removed and

replaced with protein-free media (PFM) (Composed of Fibrolife basal media (Lifeline Cell Technology, Walkersville, MD) supplemented with 10 mM HEPES (Sigma, St. Louis, MO), 1× non-essential amino acids (Sigma), 1 mM sodium pyruvate (Sigma), 2 mM glutamine (Lonza), 100 U/ml penicillin and 100 μg/ml streptomycin (Lonza)). The cells were allowed to condition this protein-free media for 48 hours, after which the media was removed from the cells and centrifuged at 1000 x g for 10 minutes to pellet any cells.

In the 2nd stage, this conditioned media was placed on a different set of cells, which were then measured for proliferation. This conditioned media was added to 2nd stage cells at the ratios indicated with DMEM, supplemented with FCS to 5%, as described above.

2nd stage cells were allowed to grow for the indicated length of time, then counted.

Cell counting

The 2nd stage cells were then imaged by an InCell 2000 microscope (GE Healthcare) and then counted by the image analysis program CellProfiler (200). Using either a 4x or a 10x lens, most of the surface area of a 96-well plate's well was imaged, and these non-overlapping images were counted by different CellProfiler pipelines optimized to recognize the various morphologies of each of the indicated cell types. The CellProfiler pipelines are in the supplemental methods section.

Purification of CM

Conditioned media from MCF-7 cells was concentrated using a 10 kDa filter, and buffer exchanged using 20 mM sodium phosphate buffer. This was loaded on a 5 ml MonoQ anion exchange column on an AKTA chromatography system (GE Healthcare, Piscataway, NJ). The column was washed with 6 ml of 20 mM NaPO4 pH 7.4 buffer (first 6 fractions), and bound proteins were then eluted with a 14 ml gradient of 0 to 0.3 M NaCl in 20 mM NaPO4 pH 7.4, collecting 0.5 ml fractions. Serial doubling dilutions of fractions were then mixed with MDA-MB 231 breast cancer cells for 72 hours, after which the cells were counted as above.

Results

How tissues regulate their size is, for the most part, unknown. Secreted factors that regulate population size in cells are known as chalones. A chalone, myostatin, regulates the overall size of a muscle (307). However, no similar chalone has been identified in any other human tissue (307).

After a tumor is removed by surgery, distant metastases will sometimes increase in size due to proliferation of metastatic cancer cells (308, 309). Primary tumors visible to surgeons contain many more cancer cells than metastases. That metastatic cancer cells increase their proliferation rate following the removal of many cancer cells suggests that certain cancers may regulate the total number of cells in a manner similar to a normal tissue.

To determine if cancer cells secrete a factor that inhibits their own proliferation, we used cell lines to condition media (CM), and then placed that media onto cells of the

same type that were used to generate the CM. CM from normal adult lung fibroblasts, normal adult dermal fibroblasts, DCIS.com non-metastatic breast cancer cells, MCF-7 non-metastatic breast cancer cells, MDA-MB 231 metastatic breast cancer cells, and MDA-MB 435 metastatic melanoma cells failed to slow the proliferation of the same type of cell at a 10% concentration of CM (Figure 58). DCIS.com CM slowed the proliferation of DCIS.com cells at a 50% concentration of CM, and a 100% concentration of CM from MDA-MB 231 cells slowed the proliferation of MDA-MB 231 cells. However, the concentrations of secreted factors in 50% and 100% CM would be unlikely to be reached in the bloodstream of a patient, and thus would be unlikely candidates for factors that could inhibit the proliferation of distant metastases in a cancer patient's body. At 50% and 100% concentrations of CM, nutrient deprivation and waste product accumulation could also slow the proliferation of cells.

To determine if lower concentrations of CM could inhibit the proliferation cells, we took CM from 1st stage, CM-generating cells and added it to different types of 2nd stage, CM recipient cells, and measured the proliferation of these 2nd stage cells. CM from fibroblasts and DCIS.com cells failed to slow the proliferation of the metastatic cell lines MDA-MB 231 and MDA-MB 435 (Data not shown). However, MCF-7 CM at low concentrations slowed the proliferation of both MDA-MB 231 and MDA-MB 435 cells, even at low concentrations of CM (Figure 59). This effect was specific to MDA-MB 231 and MDA-MB 435 cells, as MCF-7 CM did not slow the growth of adult lung fibroblasts, adult dermal fibroblasts, HEK-293 cells, DCIS.com cells, MCF-7 cells, or HELA cells derived from cervical cancer (Figure 59). These results suggest that the non-metastatic

breast cancer cells may secrete a factor that, at relatively low concentrations of CM is capable of slowing the growth of metastatic breast and melanoma cells.

To see if the proliferation inhibiting factor in MCF-7 CM could be purified, CM was concentrated using a 10 kDa filter and placed on an anion exchange column. The fractions eluted from the column were then tested to see if they inhibited the growth of MDA-MB 231 cells. Fraction #16 inhibited the growth of MDA-MB 231 cells at 50% and 10% concentrations, but failed to do so at the 25% concentration (Figure 60).

Taken together, these results suggest that a secreted factor greater than 10 kDa from the non-metastatic breast cancer cell line MCF-7 CM modestly and preferentially inhibits the proliferation of metastatic breast and melanoma cells.

Discussion

Surgical removal of a primary tumor can sometimes lead to an increase in the proliferation of metastatic cells and the size of metastases (308, 309). This increase in size suggests that cancer cells may regulate their total population size within a human body by using a secreted, soluble factor, or chalone (307). Conditioned media from non-metastatic breast cancer cells can slow the proliferation of metastatic breast cancer and metastatic melanoma cells.

“Mutational load” is a measurement of the total number of mutations in a cell. The mutational load of metastatic cells tends to be higher than of non-metastatic cells (314). These mutations lead to metastatic cancer cells that have a different metabolic environment and proteome than either normal tissue cells or non-metastatic cancer cells

(315, 316). That metastatic cancer cells have different proteomes suggests that metastatic cancer cells could respond differently to a chalone than either healthy tissue cells or non-metastatic cells, and provide some basis for the specificity of MCF-7 CM in slowing only the growth of MDA-MB 231 and MDA-MB 435 cells.

Figures

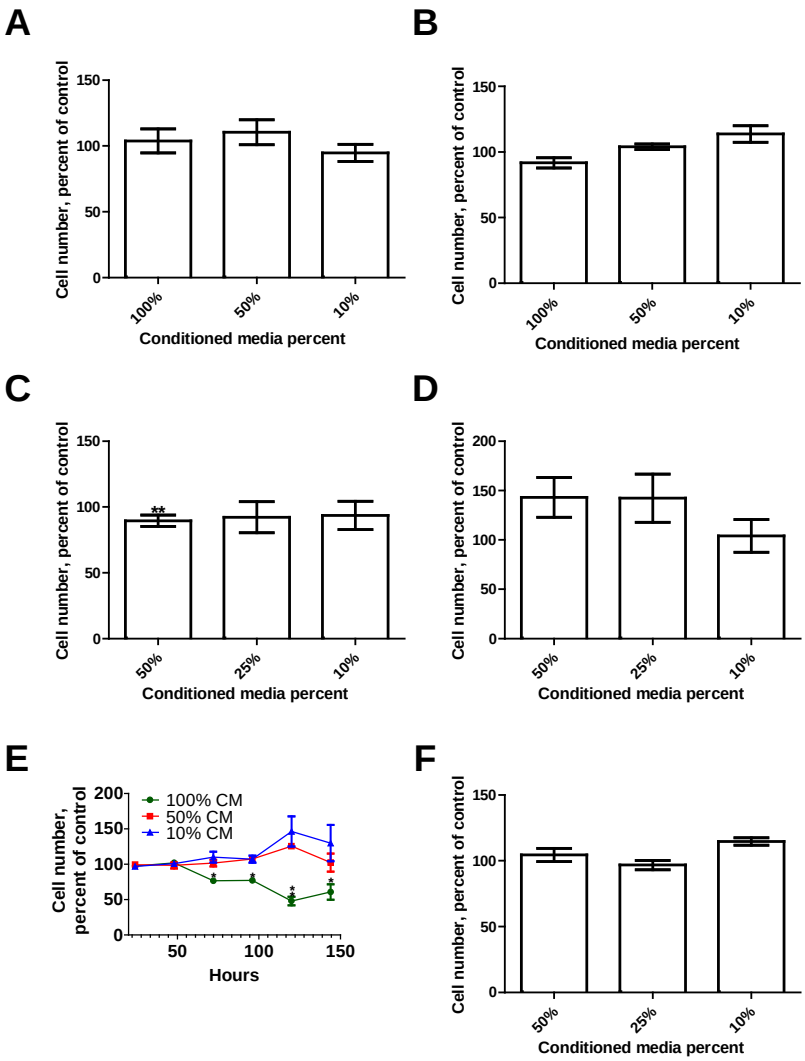

Figure 58. Conditioned media from adult dermal fibroblasts, adult lung fibroblasts, DCIS.com cells, MCF-7 cells, MDA-MB 231 cells, and MDA-MB 435 cells does not inhibit the proliferation of same type of cell used to generate the conditioned media at low concentrations of conditioned media.

Conditioned media from (A) adult dermal fibroblasts, (B) adult lung fibroblasts, (C) DCIS.com cells, (D) MCF-7 cells, (E) MDA-MB 231 cells, and (F) MDA-MB 435 cells does not inhibit the proliferation of same type of cell used to generate the conditioned media, at concentrations of conditioned media below 25% over 72 hours. 50% DCIS.com CM (C) slows the proliferation of DCIS.com, and MDA-MB 231 CM only slows MDA-MB 231 proliferation at a 100% concentration. Values are mean ± SEM, n=3. * indicates $p < .05$ and ** indicates $p < .01$ compared to the CM-free control by a t-test.

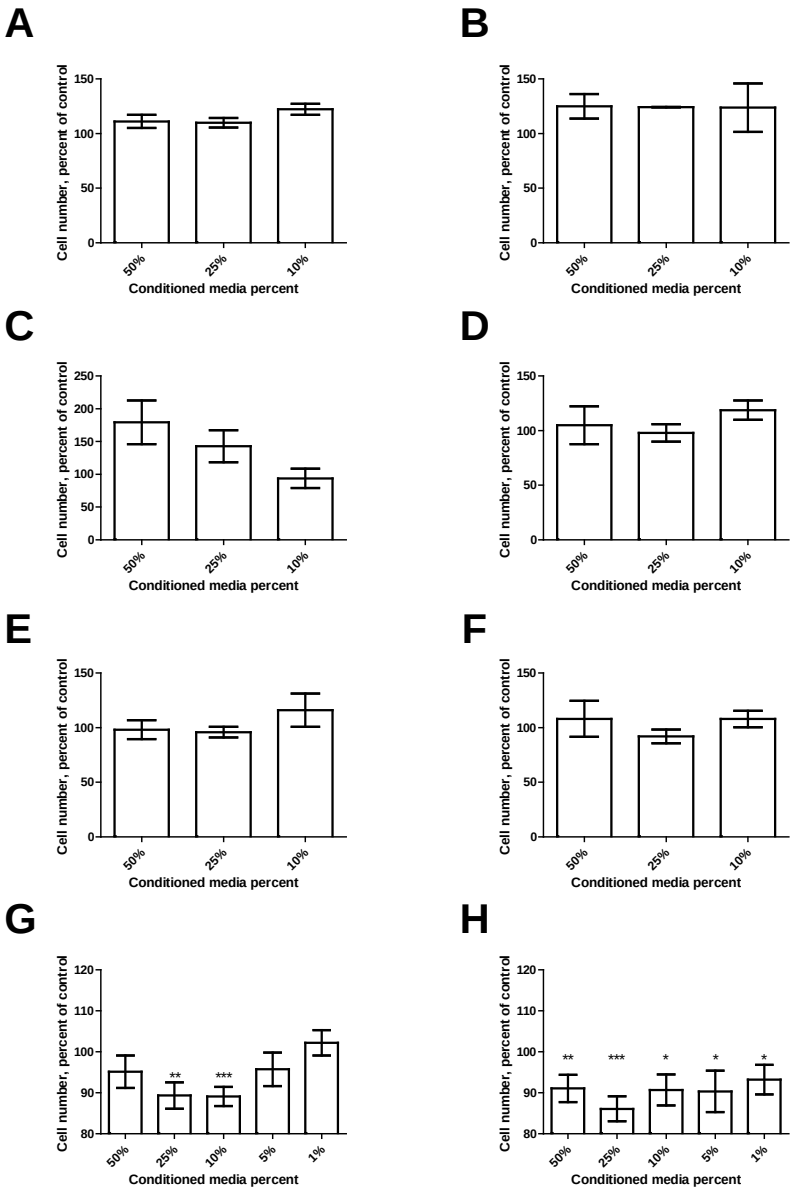

Figure 59. Conditioned media from MCF-7 cells slows the proliferation of MDA-MB 231 and MDA-MB 435 cells.

Conditioned media from MCF-7 cells does not slow the proliferation of (A) HEK-293 cells, (B) HELA cells, (C) adult dermal fibroblasts, (D) adult lung fibroblasts, (E) DCIS.com cells, or (F) MCF-7 cells at any concentration. Conditioned media from MCF-7 cells slows the proliferation of (G) MDA-MB 231 and (H) MDA-MB 435 cells, even at low concentrations. Values are mean ± SEM, n=6. * indicates $p < 0.5$, ** indicates $p < .01$, and *** indicates $p < 0.001$ compared to the CM-free control by a t-test.

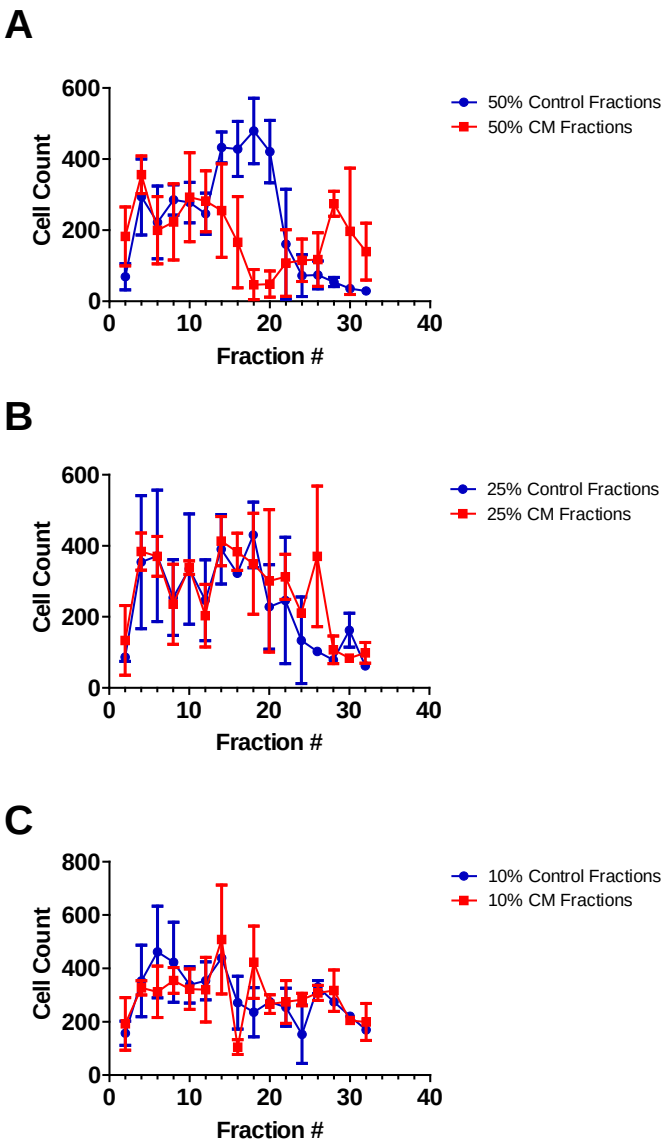

Figure 60. Conditioned media from MCF-7 cells, concentrated and eluted from an anion-exchange column, inhibits MDA-MB 231 proliferation.
Conditioned media from MCF-7 cells, concentrated using a 10 kDa size filter, and eluted from an anion-exchange column results in a fraction 16 that inhibits MDA-MB 231 proliferation at (A) 50% and (C) 10% concentrations, but not at (B) 25% concentrations. Values are mean ± SEM, n=2

APPENDIX C

THE INTERNAL METABOLIC PATHWAYS OF MONOCYTES, METASTATIC BREAST CANCER AND METASTATIC MELANOMA CAN INHIBIT OR PROMOTE FIBROCYTE DIFFERENTIATION

Introduction

The metabolism of a cell is an essential component of a cell's phenotype (317). A cell's metabolism is determined not only by the internal pathways used to generate energy, but also by the extracellular environment of the cell. In the human body, many different metabolic environments exist, which differ by their levels of oxygen, their pH, and the presence of different levels and types of sugars. In the tumor microenvironment, low oxygen content leads to increased glycolysis, which lowers both glucose levels and pH through the secretion of lactic acid. Similar metabolic environments exist in areas of inflammation, like wounds and scar tissue (318).

Monocytes are an immune system cell that differentiates into both macrophages and fibrocytes. Monocytes, macrophages and fibrocytes are found in the bloodstream, healing wounds, scar tissue, and in the tumor microenvironment. While some research has been done on the metabolic pathways used by different types of macrophages (318, 319), very little is known about the metabolic pathways necessary for fibrocyte differentiation.

Within a cell, sugars can be processed by different metabolic pathways. In the presence of oxygen, human cells can process sugars by aerobic pathways like oxidative phosphorylation, producing CO2 as a byproduct. In anaerobic environments, or when

presented with glucose-like sugars, cells can use the glycolysis pathway, which results in the creation of 3-carbon waste products that can be excreted via fermentation or used as materials for growth within the cell.

Cancer cells preferentially use glycolysis to produce energy, even in the presence of oxygen, a pattern termed “Warburg metabolism,” after Otto Warburg (320). Certain immune system cells, including macrophages, are capable of using Warburg metabolism in low oxygen environments, including areas of inflammation (318, 319, 321). Galactose is a 6-carbon sugar that differs in the position of the hydroxyl group on the 4’ carbon. When fed galactose instead of glucose, human cells increase their oxygen consumption and preferentially use oxidative phosphorylation rather than glycolysis to metabolize the galactose (322).

Here we show that restricting monocytes to oxidative phosphorylation lowers fibrocyte differentiation and lowers the ability of fibrocyte potentiators to increase fibrocyte differentiation. Low oxygen environments lower fibrocyte differentiation, but also appear to increase the effect of fibrocyte potentiators and decrease the effect of fibrocyte inhibitors. It seems that glycolysis is the preferred energy metabolism pathway of fibrocytes, which fits well with the presence of fibrocytes in healing wounds and poorly vascularized scars.

Materials and methods

Sugar media

Sugar-free DMEM (Sigma, St. Louis, MO) was supplemented with 10 mM HEPES (Sigma), 1× non-essential amino acids (Sigma), 1 mM sodium pyruvate (Sigma), 100 U/ml penicillin (Lonza), 100 μg/ml streptomycin (Lonza), 2mM glutamine (Lonza), and to 4,500 μg/ml of glucose or galactose (Sigma).

Cell culture

MDA-MB 231 breast cancer cells, MDA-MB 435 melanoma cells, and adult dermal fibroblasts (Lonza) were cultured in regular DMEM was supplemented to 5% with U.S. origin fetal bovine serum (FBS) (Genessee scientific, San Diego, CA) and 100 U/ml penicillin (Lonza) and 100 μg/ml streptomycin (Lonza) and 2mM glutamine (Lonza).

Conditioned media (CM)

Media was conditioned by addition to cells for 48 hours, after which the CM was removed, clarified by centrifugation for 10 minutes at 1000 x G, and added to PBMC at the indicated concentrations.

PBMC culture

PBMC were acquired and cultured, stained, and counted as previously described (239).

Anoxic environment

PBMC were cultured in a 0% oxygen incubator for 5 days in the indicated conditions.

Results

The metabolic environment of a cell largely determines that cell's phenotype (317). Several different metabolic environments exist in the human body, comprised of variations in amount of oxygen, pH, and amount of sugar present (323). Several different metabolic pathways exist within the cell to generate energy, including pathways that make use of oxygen, or different types of sugars (324). The environment that surrounds a tumor, also known as the cancer microenvironment, has a relatively low pH due to the lactic acid produced by anaerobic respiration, as a result of the largely anoxic environment (325). Similar environments can be found in healing wounds and other sites of inflammation (326). Additionally, it has been argued that poorly vascularized scar tissue also represents an anoxic and more acidic environment (327). In each of these environments, fibrocytes can differentiate and help to form scar tissue.

Galactose supplemented media restricts fibrocyte differentiation

The sugars present in the extracellular environment of the cell can determine which metabolic pathways that cell is capable of using. Glucose can be metabolized by aerobic respiration in the presence of oxygen, and by glycolysis in the presence or absence of oxygen. Galactose is preferentially metabolized through aerobic metabolism in the presence of oxygen (318, 322). To determine if fibrocytes were capable of differentiating

when restricted to different metabolic pathways, we incubated PBMC with media containing 4500 µg/ml of either glucose or galactose. Monocytes differentiate into fibrocytes with peak efficiency around ~4500 µg/ml of glucose (328), and that lowering the glucose concentration leads progressively to fewer and eventually to no fibrocytes. PBMC in media supplemented with galactose formed significantly fewer fibrocytes than in media supplemented with glucose (Figure 61A). Interestingly, PBMC supplemented with galactose were also resistant to fibrocyte potentiation by trypsin, while in media supplemented with glucose, trypsin potentiated fibrocyte differentiation as previously observed (239) (Figure 61A). Media supplemented with galactose also lowered fibrocyte differentiation and trypsin-induced fibrocyte potentiation from purified monocyte populations (Figure 61B). Galactose itself does not inhibit fibrocyte differentiation, and PBMC differentiated into fibrocytes in media supplemented with 2250 µg/ml glucose and 2250 µg/ml galactose (Figure 61C). These results indicate that monocytes differentiate into fibrocytes significantly more readily when they are using the glycolysis pathway, when compared to using the oxidative phosphorylation to obtain ATP from galactose.

Galactose supplemented media restricts cancer conditioned media from inhibiting fibrocyte differentiation

Conditioned media from metastatic breast cells, metastatic melanoma cells, and fibroblasts potently inhibits fibrocyte differentiation, while conditioned media from non-metastatic breast cancer cells does not inhibit fibrocyte differentiation to the same degree. Galectin-3 binding protein (LGALS3BP) is the primary active factor that inhibits fibrocyte

differentiation in metastatic breast and melanoma conditioned media. SLIT-2 is the active factor that inhibits fibrocyte differentiation in fibroblast conditioned media (329).

To determine whether cancer cells and fibroblasts secrete fibrocyte-inhibitory activity when using either glycolysis or oxidative phosphorylation to produce ATP, we cultured MDA-MB 231, MDA-MB 435, and adult dermal fibroblasts with media supplemented with galactose or glucose. Fibroblasts secreted potent fibrocyte inhibitory active into media supplemented with either glucose or galactose. MDA-MB 231 metastatic breast cancer and MDA-MB 435 metastatic melanoma cell lines each secreted significantly less fibrocyte inhibitory activity into galactose-supplemented media when compared to glucose-supplemented media (Figure 62).

Anoxic culture conditions also restrict fibrocyte differentiation

To determine if different concentrations of oxygen influence fibrocyte differentiation, we cultured PBMC in 21% and 0% oxygen. PBMC incubated in 21% oxygen formed significantly more fibrocytes (Figure 63A). In oxygen-free environments, cells cannot use oxidative phosphorylation and are restricted to glycolysis. In this environment, it appears that fibrocytes are also less likely to form.

PBMC cultured in anoxic conditions are less responsive to SAP's and MDA-MB 231 CM's fibrocyte inhibition

To determine if PBMC cultured in hypoxic conditions respond differently to factors that inhibit or promote fibrocyte differentiation, we cultured PBMC in 21% and 0% oxygen with fibrocyte potentiators lumican and NaCl, and fibrocyte inhibitors SLIT-2, SAP, and MDA-MB 231 CM. While fewer fibrocytes formed in the anoxic environments (Figure 63A), each of NaCl and lumican potentiated slightly more fibrocytes when compared to the number of fibrocytes in the anoxic control (Figure 63). Similarly, SLIT-2, SAP, and BC CM each inhibited fibrocyte differentiation with slightly less potency (Figure 63).

Discussion

Cell phenotype is largely a product of cell metabolism (317). Cell metabolism is partially a product of internal catabolic processes, and is partially product of the extracellular environment. The role that metabolism plays in monocyte biology is especially interesting, because monocytes can differentiate into heterogeneous cell types with different internal metabolic processes, including macrophages and fibrocytes (318, 319, 321). Monocytes also exist in a variety of extracellular environments, from healing wounds to fibrotic scars to tumors.

Here we show that both internal and extracellular metabolic processes effect fibrocyte differentiation. Monocytes are less likely to differentiate into fibrocytes if they are deprived of the glycolysis pathway. Similarly, monocytes are less likely to become fibrocytes if restricted exclusively to glycolysis in a 0% oxygen environment. Fibrocyte inhibitors are less able to inhibit fibrocytes in a 0% oxygen environment, and fibrocyte

potentiators appear slightly more effective at potentiating fibrocytes in a 0% oxygen environment, suggesting that monocytes restricted to glycolysis are less susceptible to inhibition and more susceptible to potentiation.

Cancer's Warburg metabolism has been well documented, and forcing MDA-MB 231 and MDA-MB 435 cells to use oxidative phosphorylation lowers the fibrocyte inhibition of their CM. This is not a universal effect, as fibroblasts do not suffer a loss of fibrocyte inhibitory activity when forced to use oxidative phosphorylation.

Taken together, these results suggest that the metabolic environment within a monocyte and in the extracellular environment of the monocyte can greatly influence the differentiation of that monocyte not only into macrophages, but also into fibrocytes.

Figures

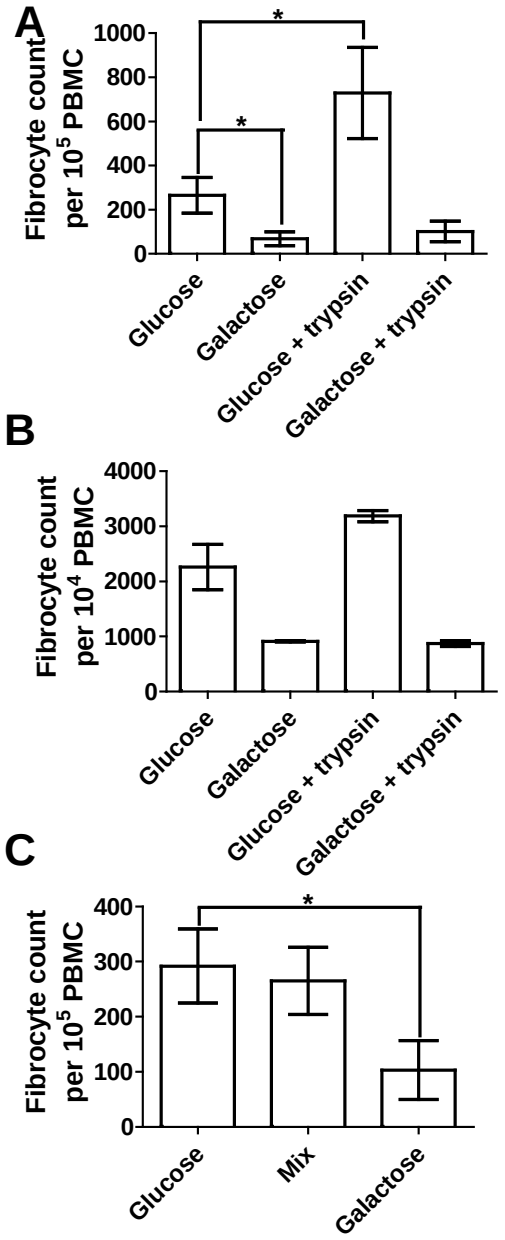

Figure 61. Glycolysis is essential for fibrocyte differentiation.
(A) PBMC were cultured with media containing glucose or galactose and 50 ng/ml trypsin. (B) Monocytes were cultured with media containing glucose or galactose and 50 ng/ml trypsin. (C) PBMC were cultured in media containing equal parts glucose and galactose. Values are mean ± SEM, n=8 for (A), n=2 for (B), and n=4 for (C). * indicates $p < 0.5$ by a t-test.

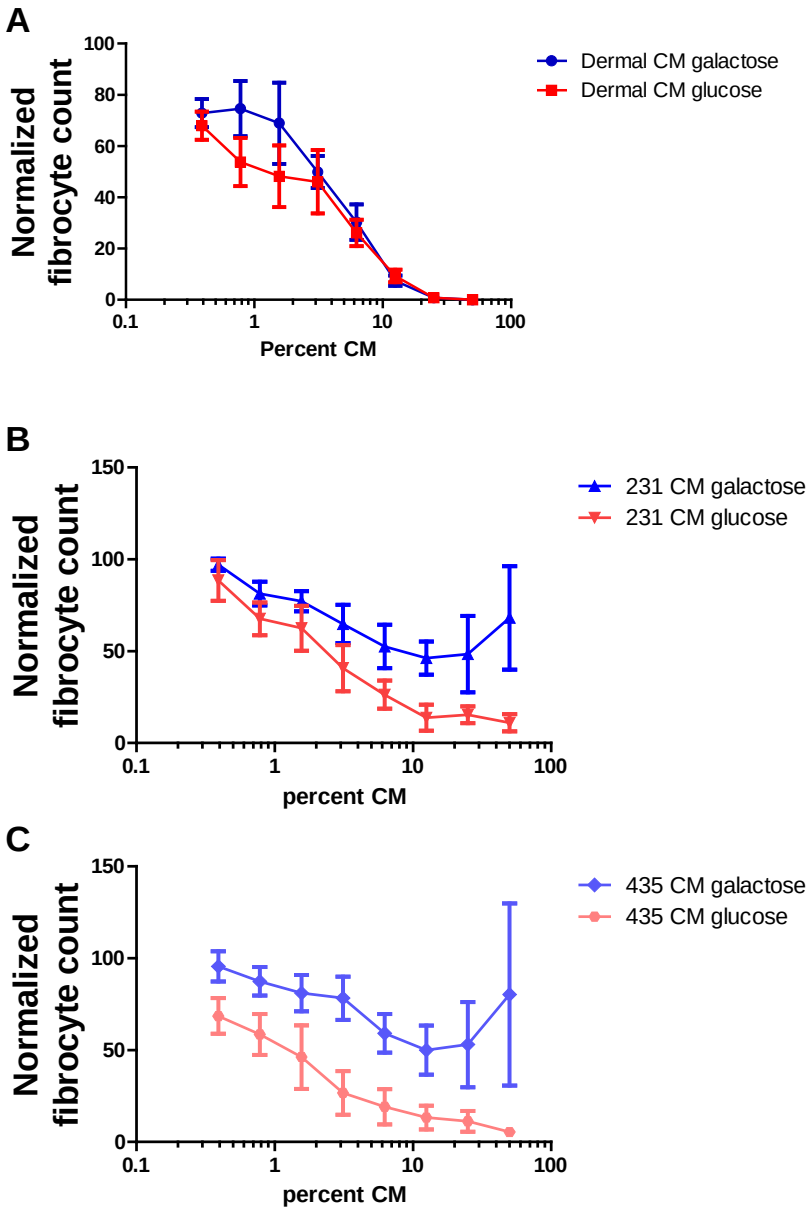

Figure 62. MDA-MB 231 and MDA-MB 435 secrete less fibrocyte inhibitory activity when restricted to oxidative phosphorylation.
(A) Adult dermal fibroblasts, (B) MDA-MB 231 cells, and (C) MDA-MB 435 cells were cultured in media containing glucose or galactose. This media was then placed on fibrocytes, which were cultured and counted as in Figure 1. Values are mean ± SEM, n=6. * indicates $p < 0.5$, ** indicates $p < .01$, and *** indicates $p < 0.001$ compared to the CM-free control by a t-test.

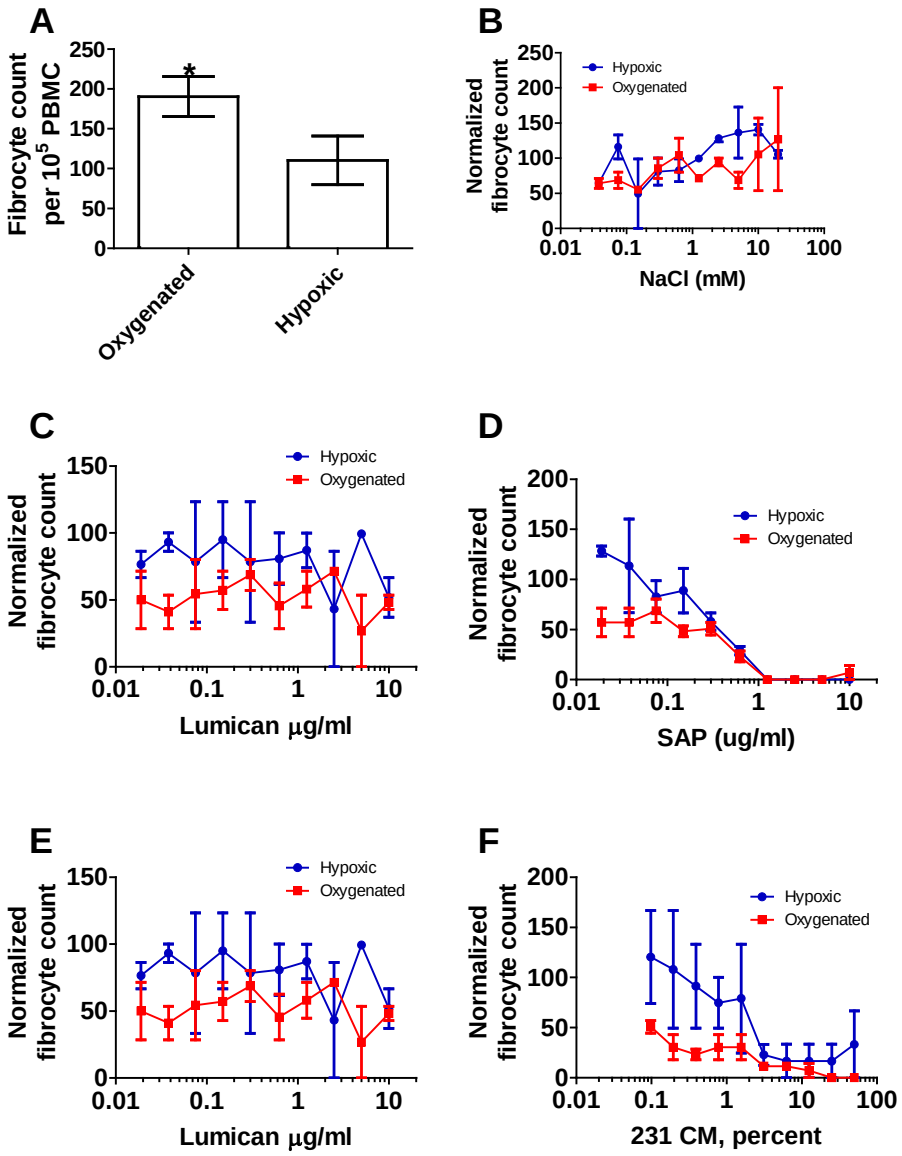

Figure 63. PBMC cultured in anoxic conditions are slightly less susceptible to fibrocyte inhibition.

(A) PBMC were cultured in environments containing either 21% oxygen or 0% oxygen with the indicated concentrations (B) NaCl, (C) lumican, (D) SLIT-2, (E) SAP, and (F) MDA-MB 231 conditioned media. Values are mean ± SEM, n=6. * indicates $p < 0.5$, ** indicates $p < .01$, and *** indicates $p < 0.001$ compared to the control by a t-test.

APPENDIX D

MDA-MB 435 CM, MDA-MB 231 CM, AND LGALS3BP POLARIZE MACROPHAGES TOWARDS AN M2 PHENOTYPE

Introduction

Metastatic breast cancer conditioned media (CM) and metastatic melanoma CM inhibit monocyte-to-fibrocyte differentiation. The active factor in this inhibition is galectin-3 binding protein (LGALS3BP), which also inhibits fibrocyte differentiation. Monocytes also differentiate into macrophages. Macrophages have several distinct phenotypes which are morphologically similar. M1 macrophages are pro-inflammatory and are found in response to infection (47, 48). M2 macrophages are anti-inflammatory and are often found in cancer microenvironments acting as myeloid derived suppressor cells (MDSC) (46). M2a macrophages are associated with scar tissue formation (49-52).

M1 macrophages secrete low levels of IL-10 and high levels of IL-12 (46). M2 macrophages secrete high levels of IL-10 and low levels of IL-12 (46). M2 macrophages also express CD163, CD172, CD206, and CD169 (46). M2a macrophages secrete moderate amounts of IL-10 and IL-12, but high amounts of IL-4, and are produce fibronectin (46).

Materials and methods

Cell culture

Cancer cell lines were cultured and CM was generated as previously described (Chapter V).

PBMC culture

PBMC were cultured as previously described (Chapter IV). After 7 days, PBMC were stained for macrophage markers as previously described (Chapter IV). CD172 (Biolegend) and CD169 (Biolegend) were used at 5 µg/ml.

ELISA

ELISA was performed as previously described (Chapter IV).

Results

Metastatic breast and melanoma conditioned media (CM) inhibits monocyte-to-fibrocyte differentiation (Chapter V). LGALS3BP, the active ingredient in MDA-MB 231 and MDA-MB 435 CM, also inhibits monocyte's differentiation into fibrocytes. We wanted to find out if MDA-MB 231 CM, MDA-MB 435 CM, or LGALS3BP biased monocyte differentiation to macrophages. Macrophages have a morphologically similar but phenotypically distinct subtypes, including M1, M2, and M2a macrophages, involved in inflammation, anti-inflammatory, and wound healing processes, respectively (46). M1,

M2, and M2a macrophages display different surface markers and secrete different proteins (46).

To determine if cancer CM or LGALS3BP biased macrophage differentiation, we added MDA-MB 231 CM, MDA-MB 435 CM, or LGALS3BP to PBMC and stained the resulting macrophage populations for M2 and M2a macrophage markers. 231 CM, 435 CM, and LGALS3BP did not significantly increase fibronectin or CD163 staining, but significantly increased CD206 staining (Figure 64). 231 CM increased CD172 staining, and both 231 and 435 CM increased CD169 staining (Figure 64). These results suggest that cancer CM and LGALS3BP bias macrophages towards an M2, or anti-inflammatory, phenotype.

To determine if cancer CM affected the secretion profile of macrophages, we added cancer CM to PBMC, then probed the PBMC CM by ELISA for IL-10 and IL-12. IL-10 is an anti-inflammatory cytokine, and IL-12 is a pro-inflammatory cytokine. Interestingly, 231 CM, 435 CM, and OVCAR-8 CM inhibited fibrocyte differentiation, contained large quantities of LGALS3BP, and yet lowered IL-10 concentration (Figure 65). MCF-7, SW-1088, and PANC-1 increased IL-12 secretion (Figure 65).

Discussion

MDA-MB 231 CM, MDA-MB 435 CM, and LGALS3BP inhibit fibrocyte differentiation from monocytes. The effect of MDA-MB 231 CM, MDA-MB 435 CM, and LGALS3BP on monocyte to macrophage differentiation is unclear. While surface markers on macrophages suggest that MDA-MB 231 CM, MDA-MB 435 CM, and

LGALS3BP bias macrophages towards an M2 phenotype, the secretion profile of macrophages exposed to MDA-MB 231 CM or MDA-MB 435 CM is low in anti-inflammatory IL-10. More experiments are necessary to break this deadlock.

Figures

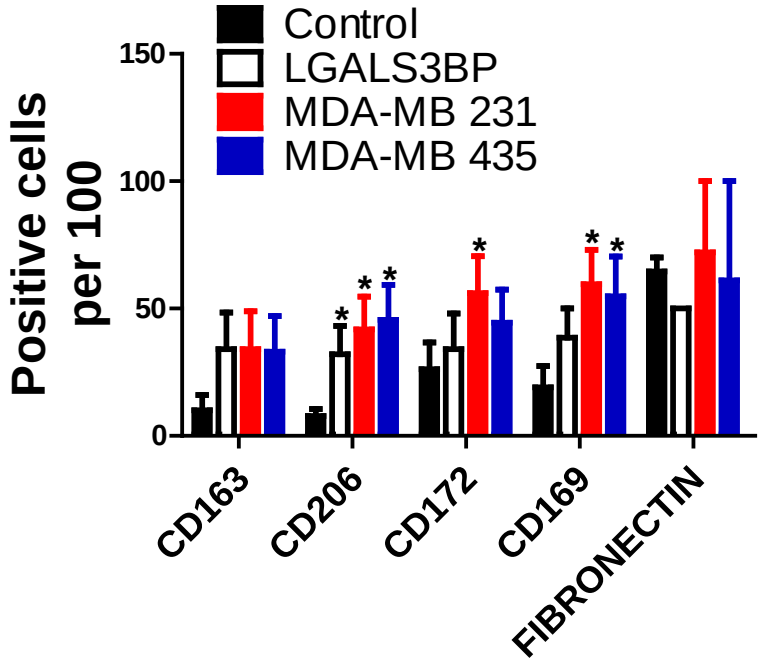

Figure 64. MDA-MB 231 CM, MDA-MB 435 CM, and LGALS3BP bias macrophages towards an M2 phenotype.
MDA-MB 231 CM, MDA-MB 435 CM, and LGALS3BP were added to PBMC. After 7 days, PBMC were stained for CD163, CD172, CD206, CD169, and fibronectin. Values are mean ± SEM, n=4. * indicates $p < 0.5$ compared to the control by a t-test.

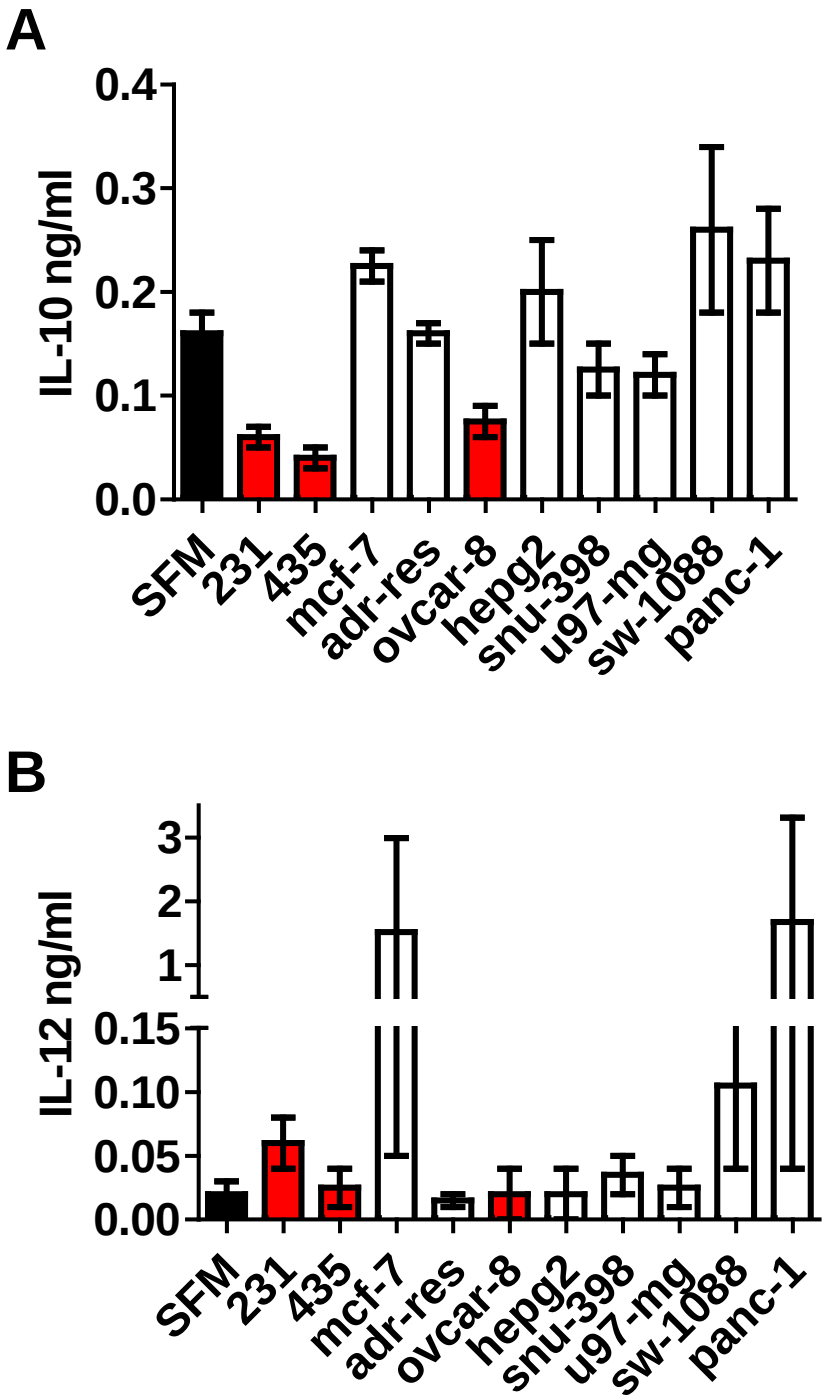

Figure 65. MDA-MB 231 CM and MDA-MB 435 CM lower IL-10 secretion from macrophages.

Cancer CM was added to PBMC as in figure 1, after which PBMC CM was analyzed by ELISA for (A) IL-10 and (B) IL-12. Values are mean ± SEM, n=2.

APPENDIX E

CO-CULTURE OF FIBROBLASTS AND PBMC RECAPITULATES FIBROSIS *IN VITRO*

Introduction

Fibrosing diseases are involved in 45% of deaths in the US (20). Chronic, non-healing wounds affect more than 6.5 million US patients per year, which is approximately 2% of the population, and cost more than $25 billion to treat (17). Both healing wounds and fibrosing diseases involve the formation of scar tissue, and scar tissue forms through interactions between fibroblasts and immune system cells like macrophages and fibrocytes (287). Recapitulating the interactions between fibroblasts and fibrocytes *in-vitro* has been a major goal of the fibrosis community.

Materials and methods

PBMC culture

PBMC were cultured as previously described (194).

Fibroblast culture

Adult dermal fibroblasts (Lonza) were cultured in growth medium (DMEM supplemented to 5% with U.S. origin fetal bovine serum (FBS) (Genessee scientific, San Diego, CA) and 100 U/ml penicillin (Lonza) and 100 μg/ml streptomycin (Lonza) and 2mM glutamine (Lonza)).

Co-culture

800 fibroblasts and 50,000 PBMC were cultured for five days in SFM ((Composed of Fibrolife basal media (Lifeline Cell Technology, Walkersville, MD) supplemented with 10 mM HEPES (Sigma, St. Louis, MO), 1× non-essential amino acids (Sigma), 1 mM sodium pyruvate (Sigma), 2 mM glutamine (Lonza), ITS-3 (Sigma) 100 U/ml penicillin and 100 μg/ml streptomycin (Lonza)). on a tissue culture treated into a 96-well plate well (BD Falcon). Conditioned media was saved after the 5-days for ELISA.

ELISA

Conditioned media from PBMC cultured in SFM with or without cytokines was centrifuged at 1000 x g for 10 minutes to pellet cell debris. Capture antibody against collagen-1 (Mouse, Sigma C2456) was diluted 1:10,000 in PBS and left on immunosorp plate (Nunc) overnight. Plates were then washed 4x with PBS (0.05% tween) and blocked with 2% BSA for 1 hour. Plates were then washed 4x with PBS (0.05% tween) and CM was added to each well for 2 hours. Plates were then washed 4x with PBS (0.05% tween) and incubated with detection antibody against collagen-1 (Rabbit, Abcam 34710) diluted 1:10,000 in PBS for 1 hr. Plates were then washed 4x with PBS (0.05% tween) and incubated with donkey anti-rabbit HRP (Jackson) diluted 1:5000 in PBS for 30 minutes. Plates were then washed 4x with PBS (0.05% tween) and the reaction was quantified with TMB, quenched with 1 N HCl, and read via spectrophotometry at 450 and 570 nm.

Cell-based ELISA

Cell-based ELISA was performed as above, with the following adjustments. No capture antibody was necessary, and standard 96 well plates (BD Falcon) were used. Cells were fixed with 95% ethanol for 15 minutes. Detection antibody was anti-collagen 6 (Rabbit, Novus biologicals).

Aniline-blue staining

Aniline blue staining was performed via a kit, following the manufacturer's instructions (Sigma). Wells were analyzed by spectrophotometry at 455 and 505 nm.

Results

Fibrosing diseases are involved in 45% of deaths in the US (20). Fibrosis is defined by interactions between fibroblasts and immune system cells like macrophages and fibrocytes, which together form scar tissue inappropriately in organs (287). Recapitulating this interaction between fibroblasts and fibrocytes *in vitro* is a major goal of the fibrosis research community.

We have developed an in vitro method of co-culturing fibroblasts and PBMC that displays increased collagen when stained with either collagen-1 or -6 antibodies or aniline blue staining (Figures 66 and 67). Co-culture also increases the amount of collagen-1 secreted by fibroblasts and macrophages, as measured by ELISA (Figure 68). Both the

measurements of secreted and deposited collagen—and aniline blue staining—are sensitive to the signaling molecules in the culture media.

Discussion

Fibrosing diseases and chronic, non-healing wounds are serious medical problems. Scar tissue is the cause of fibrosing diseases, and is the key to healing chronic wounds. Here we have recapitulated some of the interactions between fibrocytes and fibroblasts that form scar tissue.

Figures

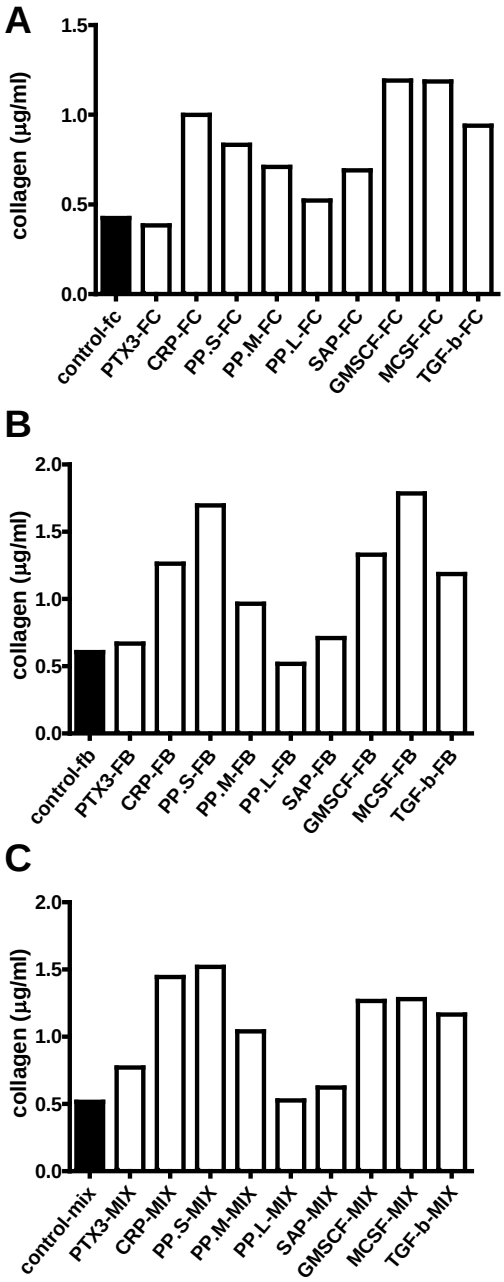

Figure 66. Co-cultured fibroblasts and PBMC increase in collagen deposition.
(A) PBMC, (B) fibroblasts, and (C) the co-culture of fibroblasts and PBMC shows different levels of collagen staining from a cell-based ELISA depending on whether a cytokine is present or absent. n=1.

A

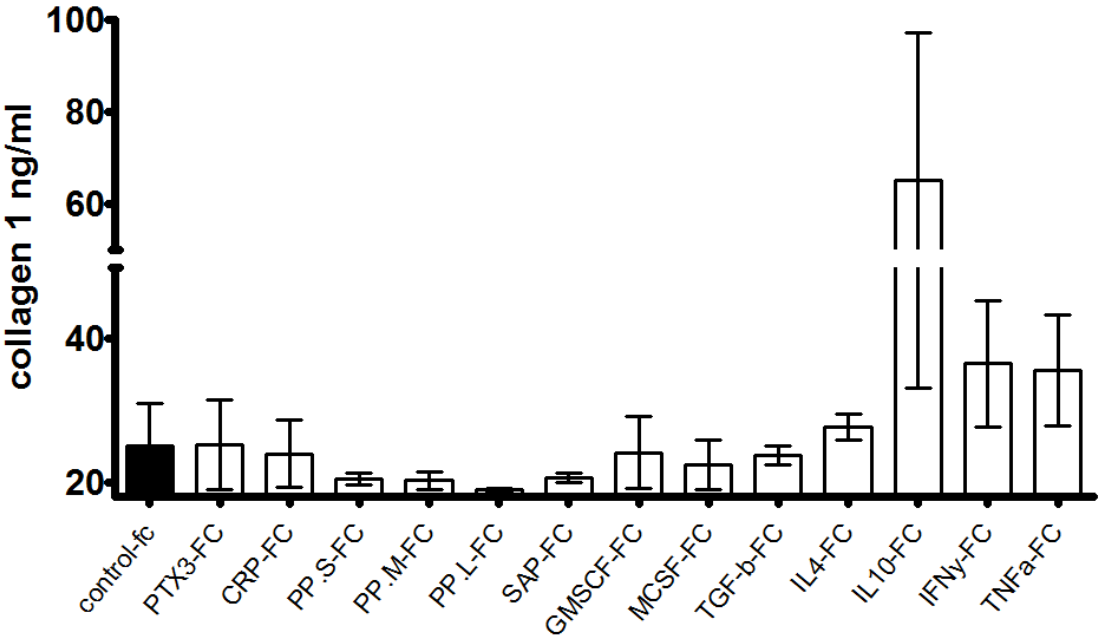
collagen 1 ng/ml
100
80
60
40
20
control-fc
PTX3-FC
CRP-FC
PP.S-FC
PP.M-FC
PP.L-FC
SAP-FC
GMSCF-FC
MCSF-FC
TGF-b-FC
IL4-FC
IL10-FC
IFNy-FC
TNFa-FC

B

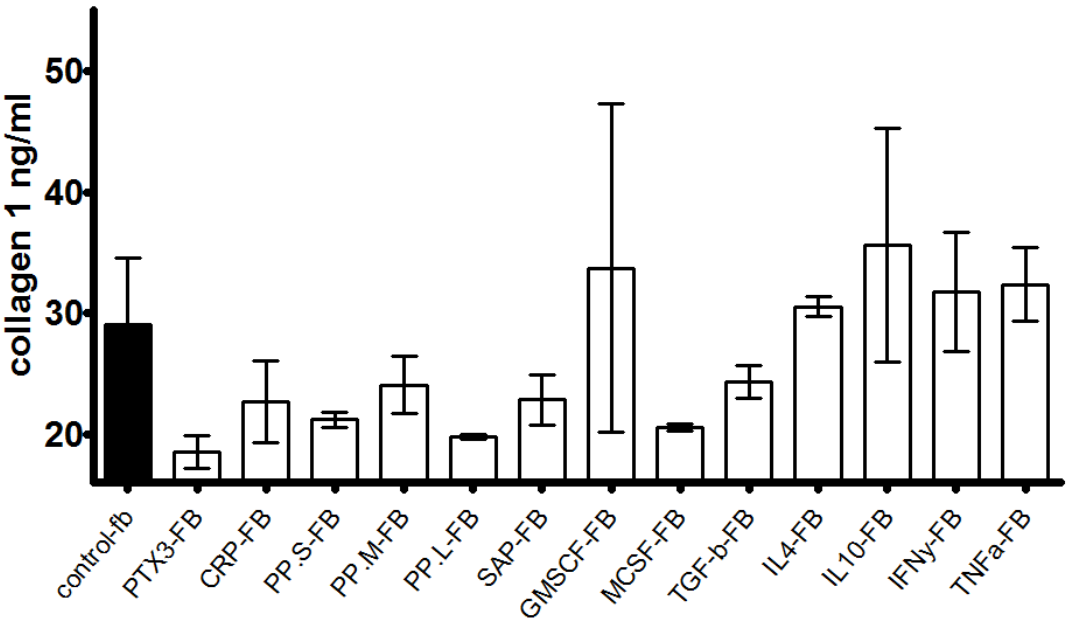
collagen 1 ng/ml
50
40
30
20
control-fb
PTX3-FB
CRP-FB
PP.S-FB
PP.M-FB
PP.L-FB
SAP-FB
GMSCF-FB
MCSF-FB
TGF-b-FB
IL4-FB
IL10-FB
IFNy-FB
TNFa-FB

C

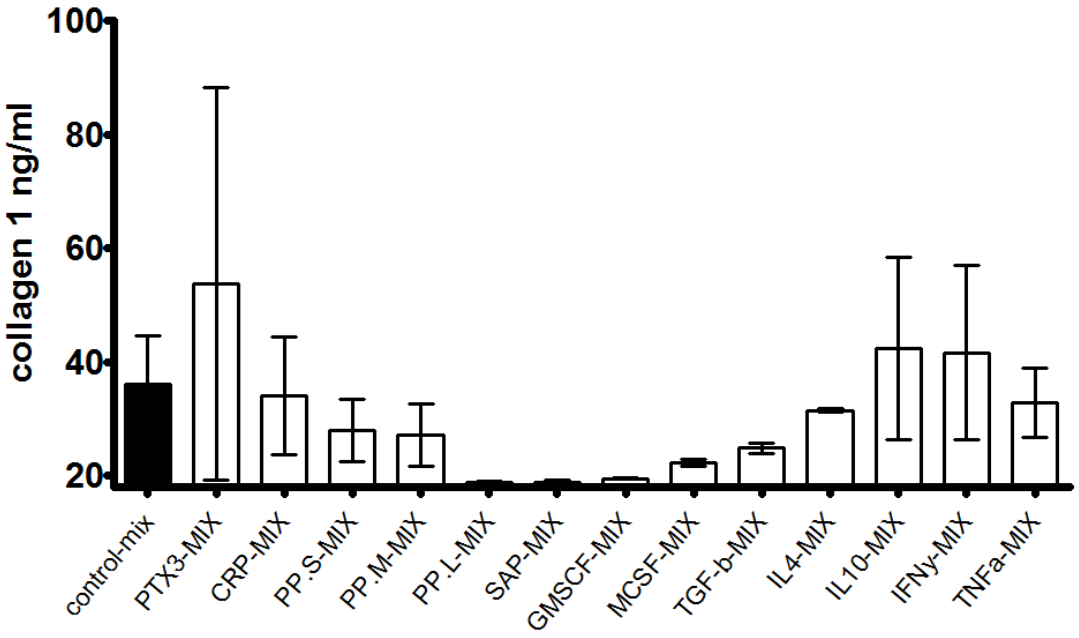

Figure 67. Co-cultured fibroblasts and PBMC increase in collagen deposition. (A) PBMC, (B) fibroblasts, and (C) the co-culture of fibroblasts and PBMC shows different levels of collagen from aniline blue staining depending on whether a cytokine is present or absent. n=2.

pH 3

pH 7

A

Lung Fibroblasts

pH 3

pH 7

B